Regulation of Membrane Fusion by Tlg2p & Vps45p through the Endosomal System of *Saccharomyces Cerevisiae*

A thesis submitted to the
FACULTY OF BIOMEDICAL AND LIFE SCIENCES

For the degree of
DOCTOR OF PHILOSOPHY

By

Chris MacDonald

Division of Molecular & Cellular Biology
Faculty of Biomedical & Life Sciences
University of Glasgow
September 2009

Abstract

SNARE proteins are essential components of the machinery that facilitates membrane fusion in eukaryotic cells. SNARE proteins are subject to multiple levels of regulation, one of which is imbedded in the syntaxin (Qa-SNARE) molecule. It has been demonstrated that some syntaxins adopt a closed conformation, whereby an autonomously folded N terminal domain (the Habc domain) forms intramolecular contacts with the SNARE domain; this conformation precludes complex assembly. The Sec1p / Munc18 (SM) family are a conserved group of proteins that regulate membrane fusion through interactions with their cognate syntaxins. Formulation of unifying hypotheses describing how SM proteins function has been problematic, primarily due to the multiple modes of interaction that have been characterised for different members of this family binding to their cognate SNARE proteins.

The yeast SM protein Vps45p regulates membrane fusion through the *trans*-Golgi / late endosomal system, and interacts directly with the syntaxin (Tlg2p) and the v-SNARE (Snc2p) proteins. Vps45p also binds to the assembled SNARE complex of Tlg2p, Vti1p, Tlg1p and Snc2p. In this thesis I demonstrate that the Habc domain of Tlg2p has an inhibitory effect on SNARE complex formation. This is an important finding, as whether or not Tlg2p adopts a closed conformation has hitherto been controversial. Furthermore, I have demonstrated that the inhibitory effect of the Habc domain on complex formation can be alleviated by Vps45p *in vitro*.

In addition to investigating the functional significance of Vps45p's interaction(s) with Tlg2p, I have also investigated binding of the SM protein to the v-SNARE Snc2p. I have demonstrated that the affinity of Vps45p for Snc2p is weaker than either of the modes of interaction characterised between Vps45p and Tlg2p. Finally, I have developed an *in vitro* fusion assay to enable us to dissect the functional significance of the various interactions that Vps45p displays with its cognate SNARE proteins.

Table of contents

List of tables

List of Figures

Acknowledgments

Firstly, I would like to thank my supervisor, Dr. Nia Bryant, for all her guidance and support throughout the course of this project; and for her helpful comments on this manuscript.

Also, I am grateful to the BBSRC for the funding which allowed me to pursue this project.

I would like to thank all members of Lab 241, both past and present, for their various contributions and helpful comments throughout the project. In particular, thanks to Dr. Fiona Brandie and Dr. Lindsay Carpp for their patience and help when I first joined the lab. Thanks also to Dr. Scott Shanks, who carried out the work for Figure 3.10, and for generally being my first port of call when I have a yeasty or molecular biology problem.

Thanks also to Dr. Mary Munson & Dr. Mel Furgason for making my time at UMass so productive and enjoyable.

A special thanks to my family (Mum, Dad & R. bomb) for their continual support in all my endeavours.

Lastly, I would like to thank Fi for putting up with me over this period; and for her unending love and encouragement, for which I am immeasurably indebted.

Declaration

I declare that the work described in this thesis has been carried out by me unless otherwise cited or acknowledged. It is entirely of my own composition and has not, in whole or in part, been submitted for any other degree.

Chris MacDonald

September 2009

Abbreviations

(v / v)	Volume to volume ratio
(w / v)	Weight to volume ratio
~	Approximately
3-AT	3-aminotriazole
5-FOA	5-fluororotic acid
AD	Activating domain
ALP	Alkaline phosphatase
APS	Ammonium persulfate
Avl	Avalanche (syntaxin)
BD	Binding domain
bp	Basepair
BSA	Bovine serum albumin
C. elegans	*Caenorhabditis elegans*
$CaCl_2$	Calcium chloride
CMC	Critical micelle concentration
CPY	Carboxypeptidase Y
CVT	Cytoplasm to vacuole
D. melanogaster	*Drosophila melanogaster*
DLS	Dynamic light scattering
DNA	Deoxyribonucleic acid
DNaseI	Deoxyribonuclease I
dNTP	Deoxynucleoside (5')-triphosphate
DOPS	1,2-dioleoylphosphatidylserine
DPPE	1,2-dipalmitoyl phosphatidylethanolamine
DTT	Dithiothreitol
E. coli	*Escherichia coli*
ECL	Enhanced chemiluminescence
EDTA	Ethylenediaminetetraacetic acid
EM	Electron microscopy
EMSA	Electrophoretic mobility shift assay
EPR	Electron paramagnetic resonance
EtBr	Ethidium bromide
FP	Fluorescence polarisation
FPLC	Fast protein liquid chromatography

g	Gravitational force
GARP	Golgi associated retrograde protein
GDP	Guanosine triphosphate
GFP	Green fluorescent protein
GST	Glutathione *S* transferase
GTP	Guanosine diphosphate
HA	Hemagglutinin
HCl	Hydrochloric acid
HEPES	2-[4-(2-Hydroxyethyl)-1-piperazine] ethanesulfonic acid
HOPS	Homotypic fusion and vacuole protein sorting
HRP	Horseradish peroxidase
IgG	Immunoglobulin G
IPTG	Isopropyl-β-D-thiogalactopyranoside
ITC	Isothermal titration calorimetry
K_2HPO_4	Di-potassium hydrogen orthophosphate
Kb	kilo basepair
KCl	Potassium chloride
KH_2PO_4	Potassium dihydrogen orthophosphate
KOH	Potassium hydroxide
L. pealei	*Loligo pealei*
Large TAg	Large T antigen (from SV40)
LiTE-Sorb	Lithium acetate Tris EDTA Sorbital
LSB	Laemmli sample buffer
M. musculus	*Mus musculus*
Mg	Magnesium
$MgCl_2$	Magnesium chloride
$MgSO_4$	Magnesium sulphate
MWCO	Molecular weight cut off
Na_2HPO_4	Di-sodium hydrogen orthophosphate
NaCl	Sodium chloride
NBD	(N-(7-nitro-2,1,3-benzoxadizol-4-yl)
NSF	N-ethylmaleimide sensitive factor
NTA	Ni^{2+}- nitrilotriacetic acid
Nycodenz	((5-[*N*-(2,3-dihydroxypropyl)acetamido]-2,4,6-triiodo-*N,N'*-bis(2,3-dihydroxypropyl) isophthalamide))
^oC	Degrees celsius

OD_{600}	Optical density at 600 nm
OG	N-octyl-β-d-glucopyranoisde
PBS	Phosphate buffered saline
PBS-T	Phosphate buffered saline Tween-20
PCR	Polymerase chain reaction
PDB	Protein data bank
Pfu	*Pyrococcus furiosus*
PMSF	Phenylmethylsulfonyl fluoride
POPC	1-palmitoyl-2-oleoyl phosphatidylcholine
psi	Pounds per square inch
R. norvegicus	*Rattus norvegicus*
Rhodamine	(N-(lissamine rhodamine B sulfonyl)
rpm	Rotations per minute
S. cerevisiae	*Saccharomyces cerevisiae*
SAP	Shrimp alkaline phosphatase
SD	Synthetic yeast dropout media
SDM	Site directed mutagenesis
SDS	Sodium dodecyl sulphate
SDS-PAGE	Sodium dodecyl sulphate polyacrylamide gel electrophoresis
SNAP	Soluble NSF attachment protein
SNARE	SNAP receptor
SPR	Surface plasmon resonance
Sx	Syntaxin
TAE	Tris acetate EDTA
TCEP	Tris (2-carboxyethyl) phosphine
TEMED	N, N, N’, N’ - tetramethylenediamine
t-SNARE	Target SNARE
v-SNARE	vesicle SNARE
X-gal	X-Gal (5-bromo-4-chloro-3-indolyl-β-D-galacto-pyranoside)
YPD	Yeast extract peptone dextrose

Chapter I

Introduction

1.1 Cellular trafficking in eukaryotic cells

Eukaryotic cells are compartmentalised into distinct organelles, contained within the plasma membrane. Each organelle has a particular environment, which is circumscribed by an intracellular membrane boundary. Groundbreaking work, using the pancreatic exocrine cell as a model, demonstrated that newly synthesised proteins destined to be secreted, pass through a series of organelles *en route* to the plasma membrane (Palade, 1975). Protein containing vesicles at the periphery of each compartment were observed, leading to the hypothesis that protein was "shuttled" between compartments in membrane bound vesicles (Palade, 1975). The non-disruptive transportation of essential molecules between these isolated organelles is extremely important, and each trafficking event has to be tightly regulated both temporally and spatially to ensure specificity (Bonifacino and Glick, 2004). Transport vesicles containing cargo bud from the donor membrane, travel through the cell to a target membrane where they initially tether, then dock, before fusion of the opposing phospholipid bilayers allows release of the cargo (Pfeffer, 1999). This allows trafficking of molecules into and out of the cell, as well as between intracellular compartments. In addition to cellular transport, the regulated movement of lipid membranes maintains organelle integrity. The myriad biological transport steps found in eukaryotes vary dramatically in the manners by which they are controlled and regulated. Despite this, the basic machinery underpinning these trafficking events is thought to be conserved in all systems (Chen and Scheller, 2001).

1.2 Membrane fusion

The fusion of biological membranes in close apposition does not happen spontaneously, energy is required to overcome the natural physical barriers of the fusion event. At long range the membranes are subject to electrostatic and Van der Waals forces; more importantly, at closer ranges (1 - 2.5 nm), membranes experience a strong repulsive "hydration" force, resulting from the energy required to dehydrate the lipid polar heads (Rand, 1981). A wide range of scientific approaches have been used to understand how fusion of opposing lipid bilayers is actually achieved. Studies of enveloped viruses proved to be an excellent model for membrane fusion (Patzer et al., 1979, White et al., 1983). Investigations into various viral mechanisms have greatly enhanced our understanding of

membrane fusion (White et al., 1983). One such example is the involvement of the influenza virus protein hemagglutinin (HA), which is anchored to the viral membrane and facilitates fusion with the host cell membrane (White et al., 1982a, White et al., 1982b). The crystal structure of HA revealed it has a coiled-coil region extending from the membrane (Wilson et al., 1981). The membrane fusion potential of HA is activated by low pH, which results in a conformational change from this native structure, which involves the extrusion of an N terminal fusion peptide and the alignment of a much extended α-helical region (Bullough et al., 1994, Chen et al., 1995). Structural similarities between the low-pH (fusion competent) form of HA and equivalent regions of other viral membrane fusion proteins suggests that they may share a common mechanism (Harrison, 2008). The protein machinery responsible for membrane fusion of trafficking intermediates and organelles in the cell also contain domains which adopt an energy favourable conformation (an increase in α-helical content), before fusion (Bentz and Mittal, 2000). This suggests that the protein folding events in the domains involved with membrane fusion, in these different systems, provide the energy to overcome the repulsive forces of the opposing membranes (Sollner, 2004).

These viral studies were the basis for a fusion pore model which allows direct fusion of two membranes (Chernomordik and Kozlov, 2005). A more defined model, termed hemi-fusion, better explains the energy requirements of the fusion event (Chernomordik and Kozlov, 2003, Chernomordik and Kozlov, 2005). In this model, the initially contacting outer membrane leaflets merge to form a fusion intermediate (hemifusion), this first bilayer fusion stalk relieves the hydration force (Zimmerberg et al., 1993), before expanding into a diaphragm, which then breaks to form a fusion pore and allows the inner membrane leaflets to mix (Chernomordik and Kozlov, 2008). The hemifusion model is outlined in Figure 1.1. There are still many unanswered questions as to how fusion is triggered and executed, and this ultimately depends on complex involvement of both the proteins and lipids responsible.

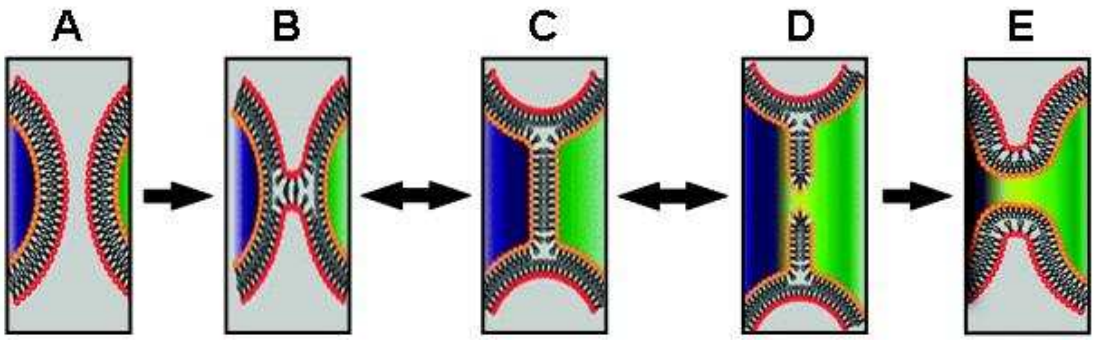

Figure 1.1 Schematic model of membrane fusion via hemifusion intermediate

(A) Membranes of two opposing phospholipid bilayers are shown in close apposition. *(B)* The proximal leaflets (red) from each membrane merge to form a stalk. *(C)* The stalk expands, *(D)* and then ruptures to allow the distal membrane leaflets (orange) to merge. This allows content mixing of the two, previously distinct, aqueous compartments (blue and green). *(E)* Fusion is complete and a single, continuous phospholipid bilayer encloses the mixed contents. Adapted from (McNew, 2008).

1.3 SNARE proteins

The cytosolic proteins *N*-ethylmaleimide sensitive factor (NSF) and soluble NSF attachment protein (SNAP) were originally identified by Rothman and colleagues as essential components of the cellular transport machinery (Clary et al., 1990, Glick and Rothman, 1987). They proposed NSF and SNAP to be part of a membrane bound multisubunit complex required to promote fusion. Subsequently, using recombinant NSF and SNAP on an affinity column, SNAP receptor (SNARE) proteins were isolated from a bovine brain detergent (Sollner et al., 1993b). The isolated SNARE proteins were further analysed and micro-sequenced, each protein sequence was identified by sequence homology with known proteins associated with the synapse (Sollner et al., 1993b). Syntaxin 1a (Sx1a) was identified as a homologue of the 35 kDa synaptotagmin interacting protein from rat brain homogenates (Bennett et al., 1992). Synaptosome associated protein of 25 kDa (SNAP-25), was identified by homology to murine SNAP-25 (Oyler et al., 1989). Finally, synaptobrevin-2 was identified by homology to the previously

characterised bovine brain synaptic vesicle protein, synaptobrevin (Sudhof et al., 1989). Sx1a (containing one SNARE motif) and SNAP-25 (containing 2 SNARE motifs) on the target membrane were thought to form a stable complex with synaptobrevin (containing one SNARE motif) on the vesicle membrane. The association of these proteins was presumed to facilitate membrane fusion (Sollner et al., 1993a). A schematic diagram of the neuronal SNAREs is shown in Figure 1.2.

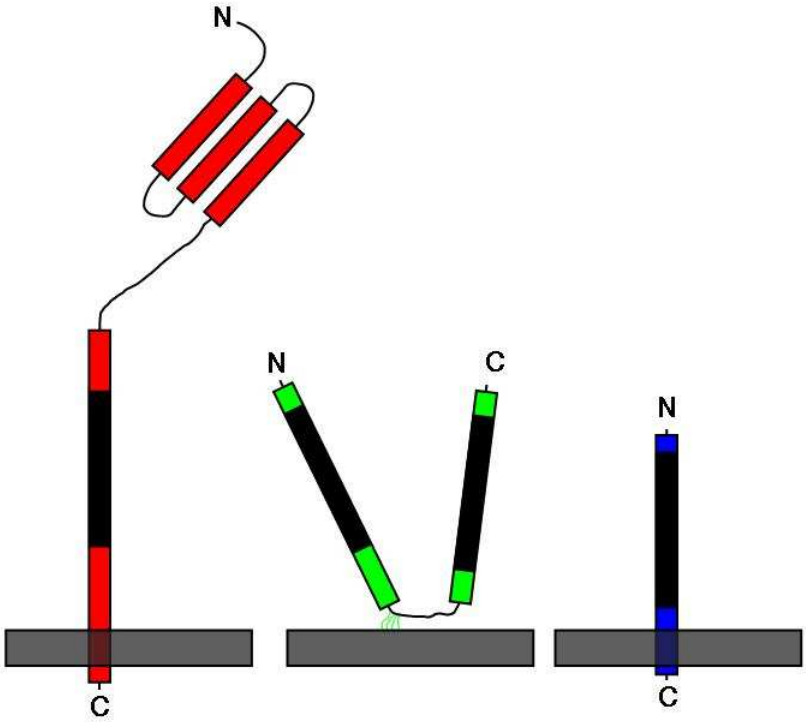

Figure 1.2 The neuronal SNARE proteins

Schematic representation of the neuronal SNARE proteins localised to their respective membranes, SNARE domains are shown in black. Sx1a (red) is anchored to the target membrane by a C terminal transmembrane domain and also contains an autonomously folded N terminal domain. SNAP-25 (green) contains two SNARE motifs, and is anchored to the target membrane by palmitoylation of cysteine residues in the linker region between the two motifs. Synaptobrevin (blue) is anchored to the vesicle membrane by a C terminal transmembrane domain.

1.4 The SNARE hypothesis

The isolation of SNARE proteins from bovine neuronal tissue (Sollner et al., 1993b) led to lucrative avenues of investigation in the membrane fusion field. The SNARE hypothesis was then proposed, in which specific target (t-SNARE) and vesicle (v-SNARE) proteins exist on opposing membranes and form an energy favourable complex which facilitates fusion of the membranes (Rothman, 1994, Sollner et al., 1993b). The yeast homologues of Sx1a, Sed5p and Pep12p, known to be important for vesicle trafficking at the ER-Golgi (Hardwick and Pelham, 1992) and the Golgi-vacuole (Preston et al., 1991) steps respectively, led Rothman and colleagues to propose that a family of SNARE proteins confer specificity to these trafficking events based on their intracellular location (Rothman, 1994, Sollner et al., 1993b). Figure 1.3 outlines the SNARE hypothesis. Homologues of the originally identified neuronal SNARE proteins have subsequently been identified in a range or organisms (Bock et al., 2001, Weimbs et al., 1997). All members of the SNARE protein family have a defining SNARE motif, which is highly conserved throughout evolution (Bennett and Scheller, 1993), and is involved in forming a complex with cognate SNARE partners to facilitate membrane fusion.

The SNARE hypothesis was an appealing concept as it encompassed the two main difficulties experienced in proposing a theory to explain membrane fusion: 1) the specificity required to allow these events to occur in a controlled and regulated manner, which could be conferred through specific SNARE protein family members at each cellular location; 2) the energy requirements of merging opposing phospholipid bilayers, which can be obtained through the formation of a stable complex between SNARE proteins on opposing membranes.

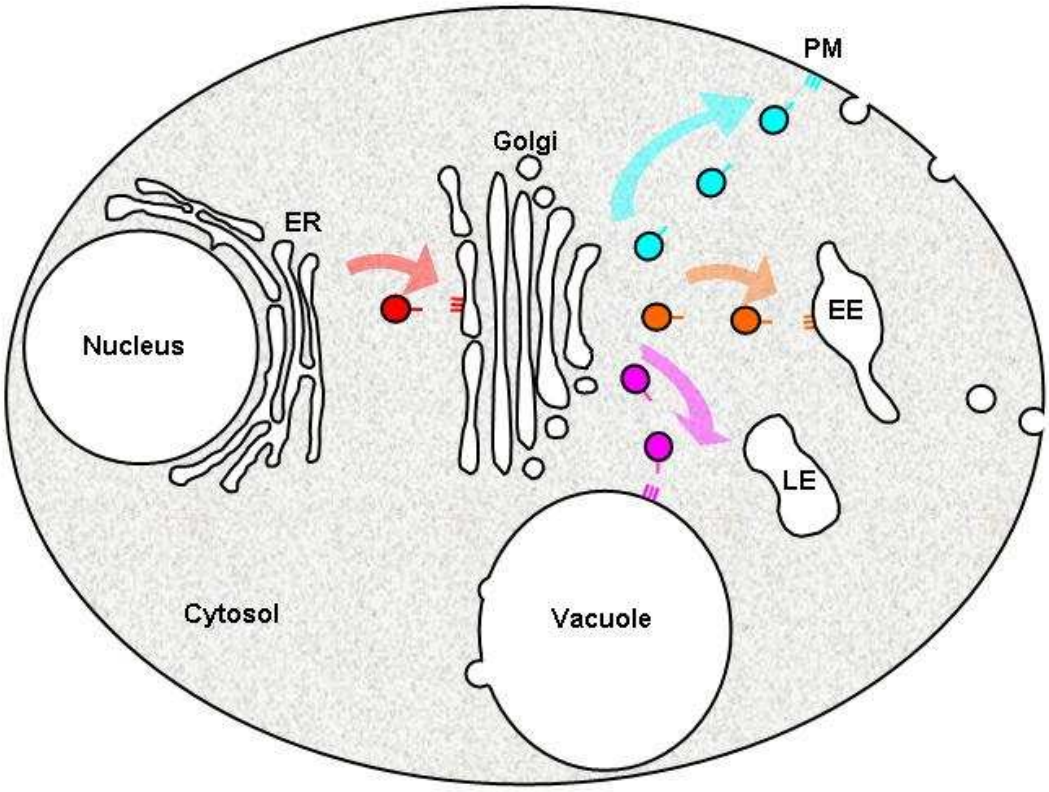

Figure 1.3 The SNARE hypothesis

The SNARE hypothesis predicts that the specificity of membrane fusion is conferred by the SNARE proteins localised to particular membranes. For example, vesicles trafficking from the ER to the Golgi (red arrow) will contain a v-SNARE (red) that will interact specifically with a t-SNARE complex at the *cis*-Golgi. This energy favourable complex will facilitate the fusion of the ER derived vesicle with the membrane of the *cis*-Golgi. The red v-SNARE will not be able to interact with other t-SNARE complexes associated with other transport steps. Three trafficking pathways of vesicles derived from the *trans*-Golgi membrane are also represented: to the plasma membrane (turquoise); to the late endosome (orange); and to the vacuole (pink). Each pathway has its own complement of specific SNARE proteins that facilitate fusion at each target membrane.

1.4.1 SNARE-SNARE protein interactions

The observation that Sx1a can bind directly with the v-SNARE synaptobrevin was in agreement with the SNARE hypothesis (Rothman, 1994, Sollner et al., 1993b). However, the affinity of the interaction is relatively weak (Calakos et al., 1994). Further investigations were pursued to better understand the interactions between individual SNAREs and the complex they form. Glutathione *S* transferase (GST) pull down experiments using recombinant proteins demonstrated that Sx1a binds to SNAP-25, and this binary complex has a greater affinity for synaptobrevin than either of the individual proteins (Hayashi et al., 1994). This study also revealed that Sx1a, SNAP-25 and synaptobrevin form a stochiometric complex that is resistant to the denaturing agent sodium dodecyl sulphate (SDS) (Hayashi et al., 1994). This detergent resistance indicates that the interactions are extremely stable, a contention that was later supported by studies showing that the Sx1a-SNAP-25 complex and the ternary complex involving synaptobrevin protect the SNARE proteins from protease digestion by trypsin, in contrast to the individual SNARE proteins which are susceptible to digestion (Poirier et al., 1998a).

Studies using circular dichroism spectrophotometry were subsequently used to gain further insight into the SNARE complex. This technique was used to ascertain the α-helical content of monomeric SNAREs, which are largely unstructured with the exception of Sx1a (Fasshauer et al., 1997a, Fasshauer et al., 1997b; discussed in more detail in section 1.3.4). It was later shown that formation of the complex between Sx1a and SNAP-25 precedes binding to synaptobrevin (Fasshauer and Margittai, 2004). The binding of Sx1a to SNAP-25 results in a modest increase in α-helical content (Fasshauer et al., 1997a), but the formation of a stochiometric 1:1:1 complex with synaptobrevin results in greatly enhanced α-helicity, beyond the theoretical sum of the individual components alone (Canaves and Montal, 1998, Fasshauer et al., 1997b), corresponding to major conformational changes in the SNARE proteins. Collectively, these data suggested that the energy requirements for membrane fusion may be attained when these largely unstructured SNARE proteins form a stable complex. Biophysical investigations of the homologous SNARE proteins responsible for exocytosis in yeast, Sso1p, Sec9p and Snc2p, have shown that these structural and energetic properties are conserved throughout evolution (Rice et al., 1997).

1.4.2 SNARE complex structure

The crystal structure at 2.4 Å of the neuronal SNARE complex showed that the 4 individual alpha helical SNARE motifs contributed by Sx1a, SNAP-25 and synaptobrevin align in parallel to form a bundle of ~12 nm in length (Sutton et al., 1998). These structural observations were confirmed by spin labelling electron paramagnetic resonance (EPR) spectroscopy, which showed that the individual SNARE domains of the neuronal t-SNAREs align in parallel (Poirier et al., 1998b). The coiled-coil structure of the SNARE complex is generated from the heptad repeat pattern of hydrophobic residues within the SNARE domain of each protein, in layers of interacting amino acid residue side-chains (Sutton et al., 1998). A schematic representation of the layered structure of the neuronal SNARE complex is depicted in Figure 1.4. The crystal structure at 1.9 Å of the mammalian endosomal SNARE complex, comprised of Sx7, Sx8, Vti1b and VAMP8, revealed a helix alignment and layered structure comparable to the neuronal complex (Antonin et al., 2002b). There is limited sequence homology between the SNARE proteins of these two complexes, but their similar structure suggests the superhelical bundle structure is conserved throughout SNARE complexes (Antonin et al., 2002b). This has been corroborated by crystallography studies of the SNAREs responsible for exocytosis in yeast (Protein data bank (PDB) accession number: 3B5N; Strop et al., 2008) and squid (PDB accession number: 1L4A; Bracher et al., 2002), and the complex responsible for homotypic fusion of mammalian early endosomes (PDB accession number: 2NPS; Zwilling et al., 2007); all of which have similar overall structures to that of the neuronal complex.

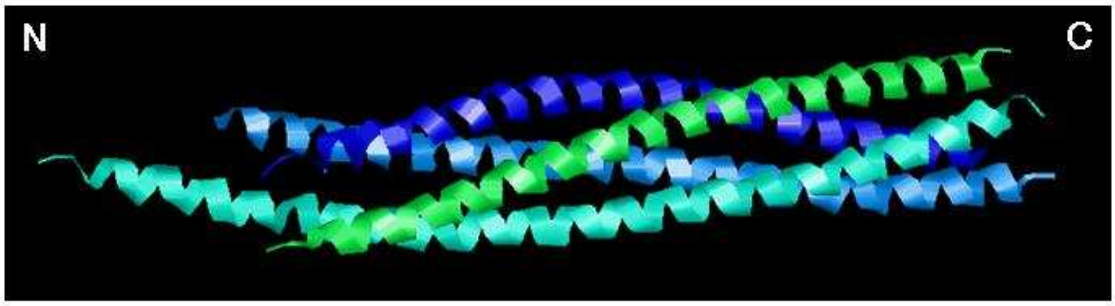

Figure 1.4 Orientation and organisation of the core SNARE complex

(A) Ribbon backbone representation of neuronal SNARE protein core complex. α-helical SNARE domains from Sx1a (green), SNAP-25 N terminus (turquoise), SNAP-25 C terminus (light blue) and VAMP2 (dark blue) align in parallel. Crystal structure data (Sutton et al., 1998) was obtained from the PDB; accession code: 1SFC.and modelled using RasMol software.

Interestingly, analysis of recombinant Sx1a and synaptobrevin containing their distal C terminal regions, including the transmembrane domains, revealed that these residues increased the stability of the complex, and like the SNARE motifs, were resistant to protease digestion (Poirier et al., 1998a). More recently, X-ray crystallography studies have been carried out on the neuronal SNARE complex using versions of Sx1a and synaptobrevin that contain these carboxy-terminal linker and transmembrane domain residues, and have shown that these additional regions are also structured (PDB accession number: 3HD7; Stein et al., 2009). In addition to this, it has been shown that increasing the length of the carboxy-terminal linker regions results in a reduced rate of fusion, suggesting the distance between the membranes and the SNARE proteins is important for fusion (McNew et al., 1999). These data taken together support a model whereby the structured organisation of SNARE proteins in complex extends into the membranes, increasing the energy produced upon complex formation, to overcome the repulsive forces of the opposing phospholipid bilayers.

1.4.3 SNARE classification

SNARE proteins were originally classified as either v- or t- SNAREs depending on whether they were localised to the trafficking vesicle or target membrane respectively. This proved inappropriate under circumstances such as homotypic fusion where vesicle and target membranes are functionally and structurally the same (Wickner, 2002). Sequence alignment and modelling techniques were used to demonstrate that the structure of the neuronal SNARE complex is conserved throughout evolution (Fasshauer et al., 1998). A reclassification of SNARE proteins based on the amino acid contributed by each SNARE motif at the central ionic layer was devised. Q-SNAREs, such as Sx1a and SNAP-25, contribute a glutamine residue (Fasshauer et al., 1998). These SNARE proteins were further classified based on sequence homology into Qa-SNAREs (homologues of Sx1a), Qb-SNAREs (homologues of the N terminal SNAP-25 domain) and Qc-SNARES (homologues of the C terminal SNAP-25 domain) (Bock et al., 2001). R-SNAREs, such as synaptobrevin, contribute an arginine residue (Fasshauer et al., 1998). The importance of this ionic zero layer is highlighted by sequence analysis data from a wide range of homologues, that revealed this residue is the most highly conserved in SNARE proteins (Weimbs et al., 1998). This reassigned nomenclature appears to be the rule of thumb for SNARE proteins, but sequence alignment studies also revealed that 2 yeast proteins: the yeast v-SNARE Sft1p involved with retrograde Golgi traffic (Banfield et al., 1995) and the yeast t-SNARE Bet1p involved with ER to Golgi traffic (Newman et al., 1992) contain an aspartic acid (D) and a serine (S) respectively in this central ionic location (Weimbs et al., 1997). Another exception was revealed from the crystal structure of the mammalian endosomal t-SNARE Vti1p in complex with its cognate partners, which also contributes an aspartic acid (D) to this position instead of a glutamine (Q) (Zwilling et al., 2007). Further investigation of SNARE complexes may reveal whether the replacement of these general components of the ionic layer has any functional relevance.

1.4.4 Syntaxin (Qa-SNARE) family

Sx1a was initially identified as a plasma membrane associated protein in neuronal rat tissue (Inoue et al., 1992). Sx1a was subsequently identified as a SNAP binding protein (Bennett et al., 1992), and a component of the neuronal SNARE complex (Sollner et al., 1993b). There are 15 genes in mammals that encode syntaxins localised to various

compartments within the cell, with some additional alternatively spliced isoforms existing for several syntaxin proteins (Teng et al., 2001). There are only 7 syntaxins encoded in the yeast genome, which are also localised to specific membranes within the cell (Pelham, 2001). Aside from the SNARE domain common to all syntaxins, almost all have a region of hydrophobic residues at the C terminus (Bock et al., 2001, Weimbs et al., 1997); this transmembrane domain allows the protein to anchor to the membrane. Sx11, identified as a Sx1a homologue by sequence alignment analysis (Advani et al., 1998, Tang et al., 1998), appears to be the only exception to this rule so far; it contains a cysteine rich region instead of a typical C terminal transmembrane domain (Tang et al., 1998), and is incorporated into the membrane after posttranslational palmitoylation of this cysteine rich domain (Prekeris et al., 2000).

Another characteristic of some syntaxin family members is that they contain an additional N terminal structured domain, which was originally identified, and has subsequently been characterised, using NMR studies on Sx1a (Chen et al., 2008, Fernandez et al., 1998, Lerman et al., 2000). The discovery of this structured N terminal domain explained previous circular dichroism spectrophotometry findings that although the monomeric non-syntaxin neuronal SNARE proteins have very little α-helical content, monomeric Sx1a contains approximately 43% α-helical content, indicative of a structured domain not present in the other SNARE proteins (Fasshauer et al., 1997a, Fasshauer et al., 1997b; also discussed in section 1.3.1). The N terminal domain of Sx1a is composed of three individual α-helices, domains Ha, Hb and Hc, that align in an up and down bundle, collectively termed the Habc domain (Fernandez et al., 1998). Figure 1.5 *(A)* & *(B)* shows a ribbon representation of the N terminal Habc domain of Sx1a.

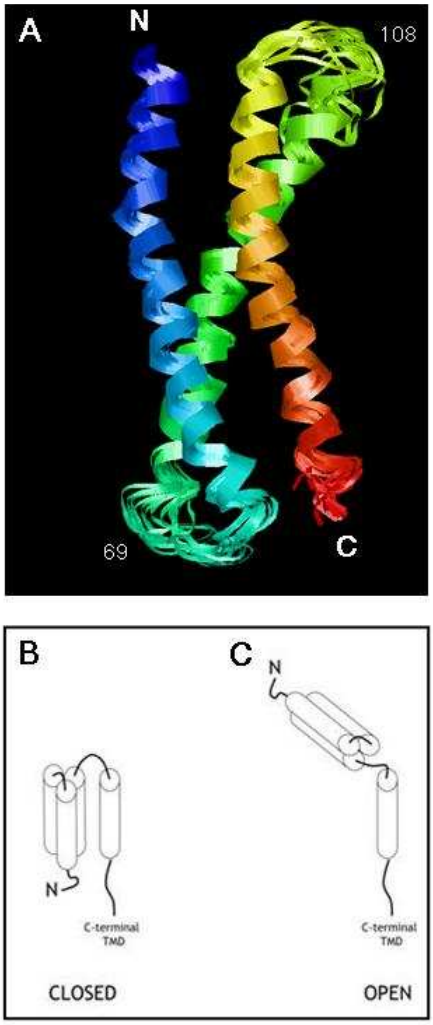

Figure 1.5 Structure of the N terminal Habc domain of Sx1a

(A) The three alpha helices of the Habc domain are shown: Ha domain, residues 28 - 62 (blue); Hb domain, residues 71 - 104 (green); Hc domain, residues 111 - 144 (orange / red). Residues 69 (between Ha and Hb helices) and 108 (between Hb and Hc helices) are also indicated. Crystal structure data (Fernandez et al., 1998) was obtained from the PDB; accession code: 1BRO and modelled using RasMol software. *(C)* Schematic representation of Sx1a in a closed conformation, *(D)* and in an open conformation. In each case the SNARE and Habc domains are indicated by cylinders.

Studies on the linker region of ~40 residues connecting the Habc domain and the SNARE domain revealed it to be largely unstructured (Fernandez et al., 1998). However, the linker region appears to be flexible, in that it cycles between randomly coiled (when Sx1a is interacting with its cognate SNARE partners) and having a defined secondary structure (when Sx1a is in complex with a regulatory Sec1p / Munc18 (SM) protein, Munc18a) (Margittai et al., 2003; discussed in more detail in section 1.5.4.1). This observation was followed by the demonstration that Sx1a adopts two distinct conformations when bound to

either the regulatory SM protein Munc18a, or its cognate SNARE partners (Dulubova et al., 1999). A schematic diagram outlining these two distinct conformations is shown in Figure 1.5 *(C)* & *(D)*. The distinct Sx1a conformation involved with binding to the SM protein was identified in the X-ray crystal structure of Sx1a in complex with Munc18a (Misura et al., 2000). This revealed that the N terminal Habc domain of Sx1a is capable of folding back upon this flexible linker and forming an intramolecular interaction with the SNARE motif, in what is termed a closed conformation (Misura et al., 2000; mode-1 binding, discussed in section 1.5.4.1). As this precludes entry into SNARE complexes it was presumed that the closed conformation of syntaxins acts as a negative regulator on complex assembly and fusion (Dulubova et al., 1999, Misura et al., 2000, Yang et al., 2000). The crystal structures of other syntaxins have been shown to also form a closed conformation that is unfavourable for membrane fusion: the squid Sx1a (Bracher and Weissenhorn, 2004) and the yeast cell-surface Sso1p (Munson et al., 2000). Functional and biochemical studies on other plasma membrane syntaxins (the mammalian Sx4, and the worm UNC-64) have demonstrated that they too regulate complex formation through a conformational switch between these two distinct (open and closed) conformations (Aran et al., 2009, D'Andrea-Merrins et al., 2007, Johnson et al., 2009, Richmond et al., 2001). It was originally presumed that only SNARE proteins localised to the plasma membrane contained Habc domains (Fernandez et al., 1998). More recently it has been shown that, despite poor sequence homology to Sx1a at these N terminal residues, other syntaxins do contain an autonomously folded Habc domain (Antonin et al., 2002a, Dulubova et al., 2001, Dulubova et al., 2002, Misura et al., 2002).

1.4.5 SNAP-25 (Qb & Qc) SNARE family

SNAP-25 is a protein composed of 206 amino acids and differs from the other two SNARE proteins originally identified from the neuronal system, Sx1a and synaptobrevin (Sollner et al., 1993b), as it does not contain a stretch of residues that form a transmembrane domain (Oyler et al., 1989). SNAP-25 contains four closely positioned cysteine residues (Bark and Wilson, 1994), which allow its membrane association through palmitoylation (Hess et al., 1992, Lane and Liu, 1997, Vogel and Roche, 1999). SNAP-25 can bind directly to Sx1a and synaptobrevin (Chapman et al., 1994) in a functional SNARE complex (Weber et al., 1998). SNAP-25 also differs from the other neuronal SNAREs as it contains two conserved SNARE motifs, one at the N terminus and one at the C terminus (Wilson et al.,

1996). SNAP-25 homologues, such as SNAP-23 which is expressed ubiquitously in cells (Ravichandran et al., 1996), and the yeast plasma membrane Sec9p (Brennwald et al., 1994) have been identified. Further sequence alignment analysis on intracellular SNARE proteins revealed that complexes at these locations involved two individual proteins, in addition to the syntaxin and v-SNARE homologues, each protein contributing one motif each (Bock et al., 2001, Weimbs et al., 1997). Based on the homology these proteins have to either the N or C terminal motifs of SNAP-25, they were classified as Qb- and Qc-SNAREs respectively (Bock et al., 2001).

1.4.6 Synaptobrevin (R) SNARE family

The final component of a four helix core SNARE complex bundle containing three Q SNARE motifs is an R-SNARE (Jahn et al., 2003, Pelham, 2001). Before synaptobrevin was isolated as a component of the neuronal SNARE complex (Sollner et al., 1993b), it had been identified as a 120 amino acid protein containing a C terminal transmembrane domain, associated with synaptic vesicles (Trimble et al., 1988). Homologues of synaptobrevin have been identified in various other species (Bock et al., 2001, Hong, 2005). Most R-SNAREs have a C terminal transmembrane domain, one notable exception is the yeast SNARE associated with multiple vacuolar trafficking steps, Ykt6p (Kweon et al., 2003); membrane localization of Ykt6p is mediated by isoprenylation (McNew et al., 1997). The fact Ykt6p has been associated with multiple trafficking routes (Alkaline phosphatase (ALP), cytoplasm-to-vacuole (CVT), and carboxypeptidase Y (CPY) pathways; depicted in Figure 1.11 as grey block arrows), demonstrates that specificity is not reliant on the v- / R-SNARE family alone (Kweon et al., 2003), and that other regulatory factors are involved (discussed in section 1.6).

1.5 SNARE mediated membrane fusion

The SNARE hypothesis proposed that specificity of membrane fusion events could be conferred through various SNARE partners interacting at specific membrane boundaries throughout the cell (Rothman, 1994, Sollner et al., 1993b). A schematic representation of SNARE mediated membrane fusion is shown in Figure 1.6.

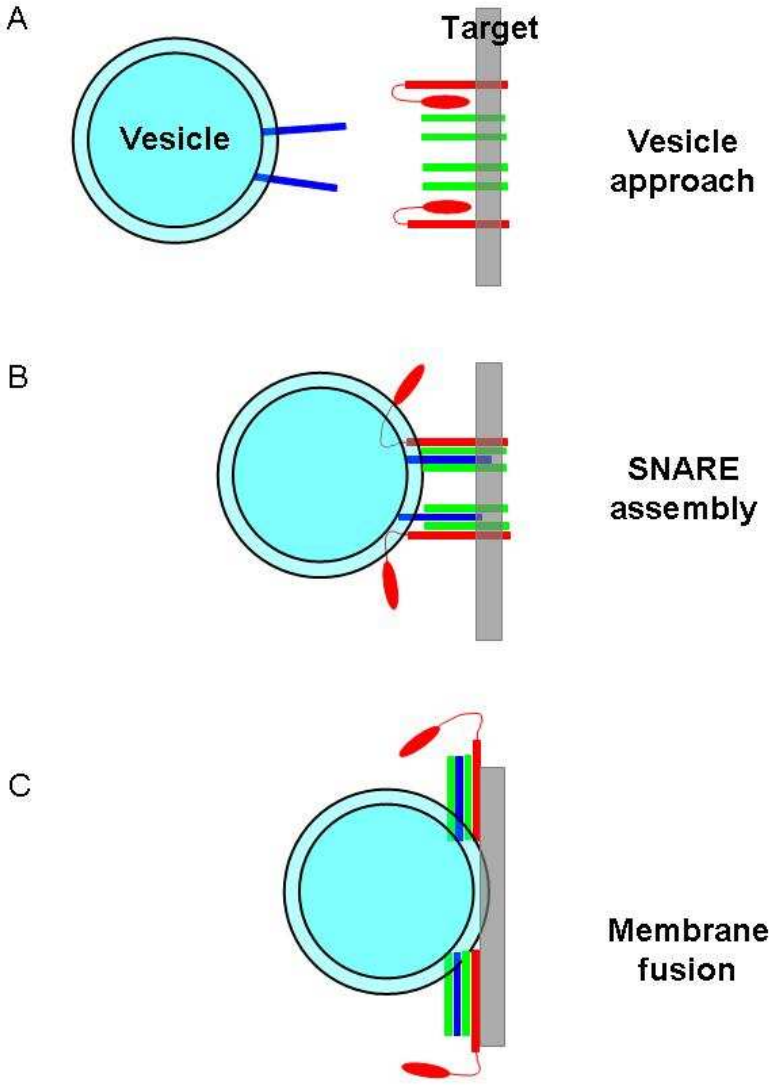

Figure 1.6 Schematic representation of SNARE mediated membrane fusion

(A) A synaptic vesicle (turquoise), containing the v-SNARE synaptobrevin (dark blue) embedded in the vesicle membrane by a C terminal TMD, approaches the target membrane, (in this case, the plasma membrane of a neuronal cell). The target membrane harbours syntaxin molecules (red), anchored to the plasma membrane via a C terminal TMD. The N terminal Habc domain of Sx1a interacts directly with the SNARE motif, in a closed conformation that is incompatible with complex assembly. SNAP-25 (green) is also associated with the target membrane; it is anchored by covalent attachment of palmitate groups to a cysteine rich linker region between the two SNARE motifs of the protein. *(B)* The syntaxin molecules undergo a conformational change which releases the N terminal inhibitory domain and allows the SNARE motif to form a core complex with the two SNAP-25 domains and the synaptobrevin domain. The vesicle is now said to be docked at the membrane via a *trans*-SNARE complex. *(C)* The docked vesicle undergoes membrane fusion, which allows the vesicle cargo to be released. The *cis*-SNARE complex containing Sx1a, SNAP-25 and synaptobrevin on the same membrane then requires ATP driven disassembly to recycle the SNAREs for subsequent fusion events. Taken from (Barrick and Hughson, 2002).

Whilst this was in theory an excellent model to explain the necessary specificity of individual membrane fusion events, further work revealed that specificity is not encoded solely through the SNARE proteins; in fact, many SNARE proteins associated with various transport steps interact promiscuously (Fasshauer et al., 1999, Tsui and Banfield, 2000, Yang et al., 1999). It is especially unsurprising that promiscuous SNARE pairings occur, as the SNARE motifs are so highly conserved (Rizo and Sudhof, 2002). On the other hand, some promiscuous SNARE pairings have been shown to be ineffective at promoting exocytosis in PC12 cells; suggesting that SNAREs do confer some level of specificity to membrane fusion (Scales et al., 2000).

An *in vitro* assay was developed and used to demonstrate that SNARE proteins incorporated into synthetic vesicle membranes were sufficient to drive fusion of the two vesicle populations, one harbouring the v-SNARE and the other the t-SNARE complex (Weber et al., 1998; discussed in detail in Chapter V). This suggests that formation of the energy favourable conformation of the SNARE complex (discussed in section 1.3.2) is sufficient to drive fusion of opposing phospholipid membranes (Weber et al., 1998). This assay was further used to test the ability of various v-SNAREs to promote fusion *in vitro* with known t-SNARE complexes that exist at the Golgi, vacuole or plasma membrane (McNew et al., 2000). This study demonstrated that generally a specific v-SNARE is responsible for promoting fusion with t-SNARE complexes at the various cellular locations (McNew et al., 2000). A more extensive examination of possible t-SNARE complexes with all v-SNAREs in yeast corroborated this report, demonstrating that very few SNARE combinations resulted in fusion; suggesting that cognate SNARE partners localised to specific compartments predominantly facilitate fusion of synthetic membranes (Parlati et al., 2002). A report identifying the yeast SNARE Vti1p used *in vivo* techniques to demonstrate that it could functionally act as a v-SNARE; Vti1p interacts with complexes containing different syntaxin homologues (Sed5p and Pep12p) for two distinct cellular locations: the *cis*-Golgi and the pre-vacuolar compartment, respectively (von Mollard et al., 1997). The discrepancy in specificity observed in various systems may be due to levels of *in vivo* regulation peculiar to any given step; there also may be more attuned regulatory requirements for yeast SNARE proteins, which carry out the various cellular fusion events with fewer homologues of fusion machinery components than are found in higher eukaryotes (Pelham, 2001, Pelham, 1999). The regulatory family of Rab proteins, and their effectors, have been successfully incorporated into liposomes with SNARE proteins (Ohya et al., 2009). This study reported that both machineries work in concert to increase both the specificity and efficiency of membrane fusion (Ohya et al., 2009).

1.6 Regulation of membrane fusion

Although SNARE proteins have been identified as key components of the fusion machinery, it remains clear that there are other essential factors involved in the process of membrane fusion (Ungar and Hughson, 2003). Various proteins have been associated with the regulation of membrane fusion, but their precise roles remain unknown. The following sections will discuss some of the factors that have been implicated in the regulation of SNARE mediated membrane fusion.

1.6.1 Sec1p / Munc18 (SM) proteins

Genetic screening of the nematode worm *Caenorhabditis elegans* revealed a large number of mutations that affected the normal movement behaviour of the animals, termed uncoordinated (Brenner, 1974); one of these genes encodes the canonical SM protein UNC-18. The uncoordinated phenotype observed from deletion of *unc-18* in *C. elegans* was shown to be caused by a block in neuronal vesicular transport (Gengyo-Ando et al., 1993). The first discovered homologue of UNC-18, named Sec1p, was identified in a genetic screen of *S. cerevisiae* isolating secretory mutants that fail to export synthesised protein due to a block in the transport and fusion of secretory vesicles to / with the plasma membrane (Novick et al., 1980). Two functionally related yeast Sec1p homologues involved with intracellular transport, Sly1p and Slp1p, were subsequently identified by sequence alignment techniques (Aalto et al., 1992). Sly1p is involved with ER to Golgi trafficking (Ossig et al., 1991). Genetic and biochemical analysis of Slp1p revealed it to be the same as Vps33p (Robinson et al., 1988); responsible for trafficking from the Golgi to the vacuole (Wada et al., 1990). The final yeast SM protein was identified from a screen of mutants responsible for vacuolar protein sorting defects, named Vps45p (Raymond et al., 1992); which is associated with trafficking at the late Golgi and early endosome system (Cowles et al., 1994, Piper et al., 1994). SM protein family members have been identified in higher eukaryotes also, including ROP in *Drosophila melanogaster* (Harrison et al., 1994) and the mammalian UNC-18 neuronal homologue in rat brain, Munc18 (Hata et al., 1993). Three isoforms of Munc18 have been identified: the original, neuronal specific, Munc18a (Hata et al., 1993); Munc18b, which is predominately expressed in epithelial cells (Riento et al., 1996) and Munc18c, which is ubiquitously expressed in mammalian cells (Katagiri et al., 1995, Tellam et al., 1995).

1.6.2 SM protein structure

All SM proteins are ~600 amino acids in length, and are presumed to form similar structures due to sequence conservation distributed throughout their entire sequences (Halachmi and Lev, 1996, Toonen and Verhage, 2003). This contention is supported by X-ray crystallography studies that set out to characterise the interaction between SM proteins and syntaxins. The first example of this was the crystal structure of Munc18a in complex with Sx1a, which revealed Munc18a forms an arch shape structure with a central cavity (Misura et al., 2000). This structure was confirmed by the crystal structure of Munc18a homologue in the squid *Loligo pealei*, sSec1p (Bracher et al., 2000). Ribbon diagrams generated from the two crystal structures of Munc18a and nSec1p are shown in Figure 1.7. To date, the crystal structures of four SM proteins have been solved: Munc18a (Misura et al., 2000; Figure 1.7 *(A)*); sSec1p (Bracher et al., 2000; Figure 1.7 *(B)*); the yeast protein Sly1p (PBD accession code: 1MQS; Bracher and Weissenhorn, 2002); and Munc18c (PBD accession code: 2PJX; Hu et al., 2007); all of which share this similar arch shaped structure containing a central cavity.

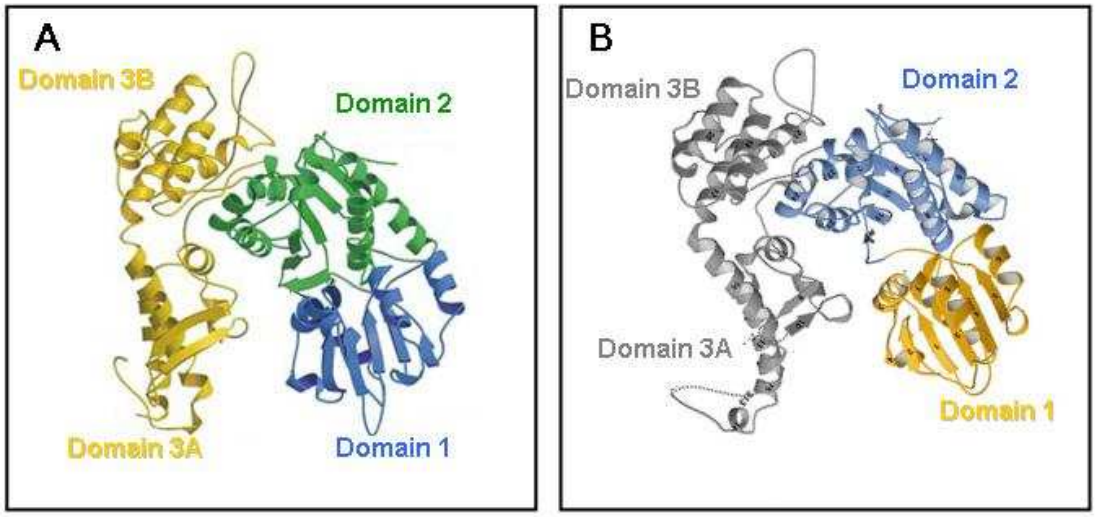

Figure 1.7 X-ray crystal structures of Munc18a and nSec1p

Comparison of the X-ray crystallography structural data generated for two SM protein homologues, α-helices are denoted by spirals, β-sheets by arrows. *(A)* Ribbon representation of Munc18a from rat: domain 1 shown in blue, domain 2 in green and domain 3 in yellow. Approximate dimensions of the protein included with arrows. PDB accession code: 1DN1. Adapted from (Misura et al., 2000). *(B)* Ribbon representation of sSec1 from squid: domain 1 shown in yellow, domain 2 in blue and domain 3 in grey. The approximate distance of the cleft formed between domains 1 and 3 is indicated. PDB accession code: 1FVH. Adapted from (Bracher et al., 2000).

1.6.3 Role of SM proteins

The role of SM proteins is not well understood, but their importance in fusion has been established through various *in vivo* studies. Null mutation of Munc18a and ROP, SM proteins in *Mus musculus* and *D. melanogaster* respectively, both result in a fatal phenotype characterised by severe blockage in neurotransmitter release (Harrison et al., 1994, Verhage et al., 2000). Similarly, severe trafficking phenotypes are observed when SM proteins are mutated or deleted in *S. cerevisiae* (Banta et al., 1990, Cowles et al., 1994, Novick et al., 1980, Ossig et al., 1991, Piper et al., 1994) and *C. elegans* (Gengyo-Ando et al., 1993, Hosono et al., 1992, Weimer et al., 2003). Many of these mutations were responsible for the original identification of individual SM proteins, through the genetic screens mentioned above (section 1.5.1). The SM protein requirement in numerous transport pathways from various species suggests a conserved, fundamental role in membrane fusion.

Despite relatively low sequence identity between this family of proteins, homology is distributed throughout the entire length of the proteins (Halachmi and Lev, 1996, Toonen and Verhage, 2003), suggesting that they share a common function. However, it is unclear whether a universal function can be applied to SM proteins due to seemingly inconsistent data gathered from the various systems studied (Toonen and Verhage, 2003). One recurrent characteristic of SM proteins is their association with members of the syntaxin family, which was first observed when Munc18a was identified as a Sx1a binding partner (Hata et al., 1993), but has since been reported in various other systems (Toonen and Verhage, 2003). It has been suggested that the role of SM proteins is carried out through specific interaction with a syntaxin family member (Jahn, 2000). However, there is not a strict 1:1 relationship between SM proteins and syntaxins, highlighted by the fact the yeast genome has only four SM genes but seven syntaxin genes (Hayashi et al., 1994, Jahn and Sudhof, 1999, Pelham, 2001). Further investigations into SM protein interactions with the syntaxin family has not clarified their role, largely because they have been shown to bind syntaxins via distinct mechanisms and also to interact with non-syntaxin SNARE family members (Toonen and Verhage, 2003; discussed in section 1.6.4.5).

1.6.4 SM protein binding

A wealth of biochemical and structural data have shown SM proteins to interact with SNARE proteins by distinct mechanisms, but the significance of these binding modes remains unclear (Burgoyne and Morgan, 2007). These binding modes have been loosely categorised as mode-1, mode-2 and mode-3 (Burgoyne and Morgan, 2007). However, not all SM-SNARE protein interactions fall neatly into these categories, and there appears to be no obvious reason why different SM proteins should bind their cognate SNAREs by such strikingly different mechanisms, especially considering their apparent conserved structure and function (Jahn, 2000).

1.6.4.1 Mode-1 binding

The first SM binding mode was discovered when the crystal structure of the neuronal SM protein Munc18a in complex with its cognate syntaxin, Sx1a, was solved (Misura et al., 2000; Figure 1.8*(A)*). This study revealed Munc18a forms an arch shaped molecule (discussed in section 1.5.2), and the central cavity interacts with Sx1a in a closed conformation (Misura et al., 2000); this conformation is known to be incompatible with core complex assembly (Dulubova et al., 1999; discussed in section 1.3.4). A cartoon of mode-1 binding is shown in Figure 1.8 *(B)*. The fact that Sx1a interacting with Munc18a via this mode-1 binding precludes its ability to form SNARE complexes (Yang et al., 2000), suggested that SM proteins may act as negative regulators of membrane fusion. However, evidence showing the absolute requirement for Munc18a in neuronal exocytosis (Verhage et al., 2000), alongside the requirement of SM protein family members at other transport steps (Sudhof and Rothman, 2009), supports a model where the interaction between Munc18a and Sx1a destabilises the closed conformation of the syntaxin, thus priming it for entry into SNARE complexes.

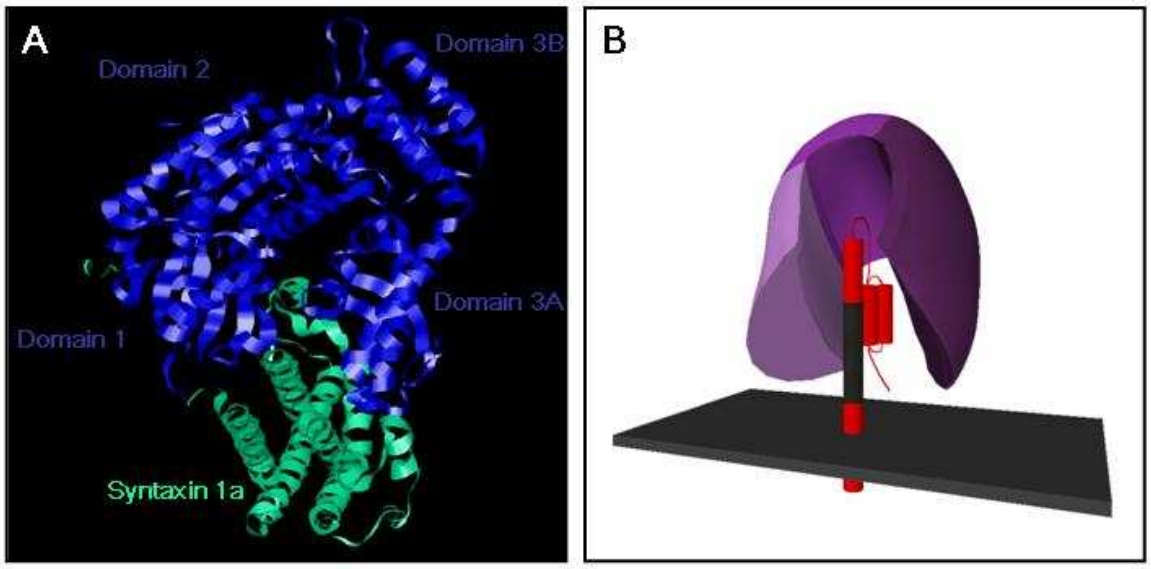

Figure 1.8 Mode-1 binding of SM proteins

(A) Topology diagram indicating the domain structure of Munc18a in complex with Sx1a: Sx1a SNARE domain and Habc domain are shown in green; Munc18a is shown in blue, domains I, II, IIIA and IIIB are indictaed. α-helices are denoted by spirals, β-sheets by arrows. Crystal structure data (Misura et al., 2000) was obtained from the PDB; accession code: 1DN1 and modelled using RasMol software. *(B)* Schematic diagram of mode-1 binding; syntaxin (red), SNARE motif (black), SM protein (purple) and membrane (dark grey) are depicted. The N terminal Habc domain of the syntaxin interacts with the SNARE motif in a closed conformation. The SM protein interacts with the syntaxin by clasping the closed conformation in its central cavity.

1.6.4.2 Mode-2 binding

NMR analysis of the Golgi syntaxin Sed5p revealed that, like Sx1a (discussed in section 1.3.4), Sed5p contains an N terminal Habc domain, with the three α-helices spanning from residues 53 and 168 (Yamaguchi et al., 2002). This study also demonstrated that the distal N terminus of Sed5p preceding the Habc domain (residues 1 - 40) was sufficient to capture its cognate SM protein, Sly1p (Yamaguchi et al., 2002). This was supported by limited proteolysis experiments of the Sed5p-Sly1p complex that showed a 5 kDa N terminal fragment of Sed5p was protected from digestion through its interaction with Sly1p (Bracher and Weissenhorn, 2002). This study resolved the crystal structure of the N terminal fragment (residues 1 - 45) of Sed5p in complex with Sly1p (Bracher and Weissenhorn, 2002; shown in Figure 1.9 *(A)*). This study revealed that SM proteins Sly1p and Munc18a do, in fact, have a very similar arch shaped structure; but the manner by

which Sly1p binds its cognate syntaxin is remarkably different to the binding of Sx1a with Munc18a (Bracher and Weissenhorn, 2002, Misura et al., 2000). The short N terminal peptide of Sed5p forms a point of contact with a hydrophobic pocket (composed of residues Leu137, Leu140, Ala141, Ile153 and Val156) located on the exterior of domain I of Sly1p (Bracher and Weissenhorn, 2002). A cartoon representation of mode-2 binding is shown in Figure 1.9 *(B)*. Mutation of one of the highly conserved hydrophobic residues in the pocket region (L137R, L140K or A141K) results in Sed5p binding being completely abolished; binding is also abolished if a residue in the N terminal peptide of Sed5p is mutated (L10A) (Peng and Gallwitz, 2004).

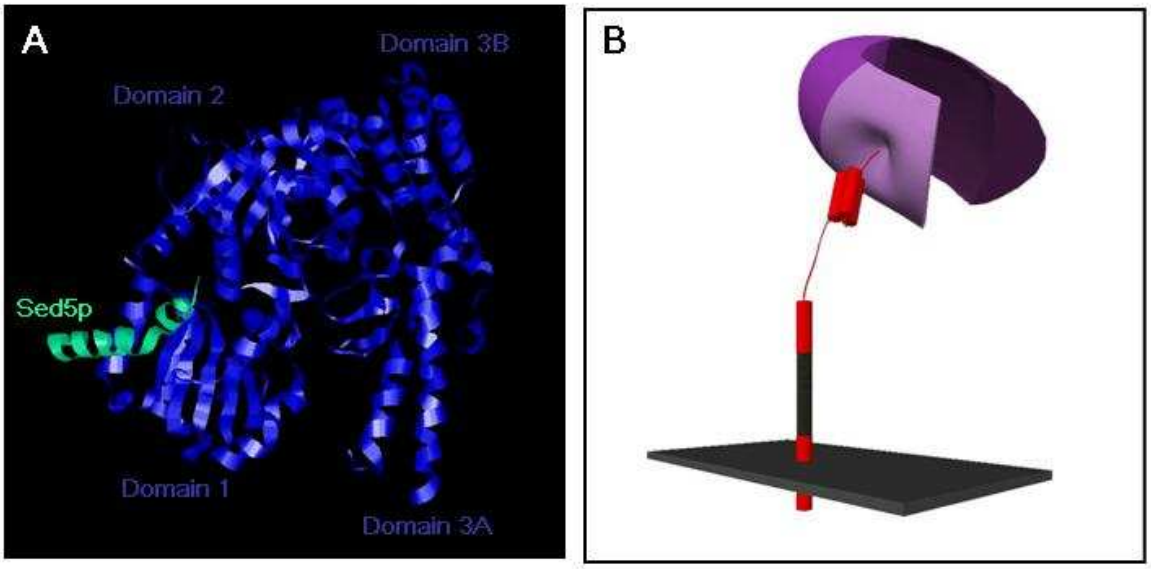

Figure 1.9 Mode-2 binding of SM proteins

(A) Topology diagram indicating the domain structure of Sly1p in complex with the N terminus of Sed5p: Sed5p is shown in green and the three domains of Sly1p are shown in blue. α-helices are denoted by cylinders, β-sheets by arrows. Crystal structure data (Bracher and Weissenhorn, 2002) was obtained from the PDB; accession code: 1DN1 and modelled using RasMol software. *(B)* Schematic diagram of mode-2 binding; syntaxin (red), SNARE motif (black), SM protein (purple) and membrane (dark grey) are depicted. Only the N terminal peptides are included in current crystal structures of a syntaxin molecule interacting with an SM protein via mode-2 binding, therefore the orientation of the proteins in this schematic representation is presumed. The distal N terminal peptide of the syntaxin interacts with a hydrophobic pocket in the exterior of domain I of the SM protein (lightest shade of purple).

Another striking difference between this interaction and mode-1 binding was demonstrated by the ability of Sly1p to interact with Sed5p either as a monomer or when it is in complex with its cognate SNARE partners, with no apparent effect on Sed5p's ability to form SNARE complexes (Peng and Gallwitz, 2002). Sly1p binding to Sed5p was demonstrated to enhance its ability to form *trans*-SNARE complexes (Kosodo et al., 2002). In addition to this, Sly1p bound to Sed5p in the resulting *cis* complexes after fusion has been implicated in the SNARE complex disassembly process, working in conjunction with the ATPase Sec18p (Kosodo et al., 2003). The binding of Sly1p to Sed5p has shown that SM proteins can confer a level of specificity on SNARE complex assembly, as Sed5p in complex with Sly1p precludes formation of complexes with non-cognate v-SNARE partners (Peng and Gallwitz, 2002). Intriguingly, a yeast strain expressing a mutant version of Sly1p abrogated for mode-2 binding (L140K) was found still to localise to Golgi membranes and correctly function in the trafficking of both CPY and invertase (Peng and Gallwitz, 2004). Somewhat surprisingly, *in vitro* binding of the mutant $Sly1p_{L140K}$ to assembled SNARE complexes was greatly reduced, and no Sly1p could be co-immunoprecipitated with Sed5p from yeast cell lysates, suggesting Sly1p function is not directly coupled to assembled SNARE complexes (Peng and Gallwitz, 2004). Mode-2 binding has also been documented for the yeast SM protein Vps45p binding its cognate syntaxin, Tlg2p (Dulubova et al., 2002); and the mammalian SM protein Munc18c binding to Sx4 (Latham et al., 2006), which was further supported by the crystal structure of this complex being solved and found to resemble that of Sed5p-Sly1p (Hu et al., 2007).

1.6.4.3 Mode-3 binding

The crystal structure of the yeast syntaxin responsible for exocytosis, Sso1p, revealed that it adopts a closed conformation, akin to that of Sx1a (Munson et al., 2000). Mutant versions of Sso1p unable to form a closed conformation were used to demonstrate that the Habc domain has a striking inhibitory effect on complex assembly both *in vitro* and *in vivo* (Munson et al., 2000, Munson and Hughson, 2002, Nicholson et al., 1998). It is surprising that the Habc domain of Sso1p has this capacity to inhibit SNARE complex assembly, like that of Sx1a, but does not interact with its cognate SM protein via mode-1 binding (Carr et al., 1999), as characterised for Sx1a binding Munc18a (Dulubova et al., 1999, Misura et al., 2000). It had been previously shown that the Sso1p cognate SM protein, Sec1p, could not bind to monomeric Sso1p (Carr et al., 1999). Both *in vivo* and *in vitro* experiments in

yeast were used to demonstrate that Sec1p binds to preassembled SNARE complexes (Carr et al., 1999, Grote et al., 2000). A cartoon representation of mode-3 binding is shown in Figure 1.10. A small amount of Sec1p-Sso1p binding was documented *in vitro* in another report (Scott et al., 2004), but more extensive *in vivo* searches for an interaction proved fruitless, as did searches for Sec1p binding to any monomeric components of the core complex (Togneri et al., 2006). This has led to the proposal that Sec1p has a direct function related to fusion facilitated by the core complex (Togneri et al., 2006). This is supported by functional studies utilising an *in vitro* liposome fusion assay (discussed in Chapter V), where the binary t-SNARE complex between Sso1p and Sec9p was reconstituted into one population of vesicles, and the cognate v-SNARE Snc2p into another population; the reconstituted SNAREs facilitate fusion of the two liposome populations (Scott et al., 2004). When the cognate SM protein, Sly1p, is reconstituted with the binary t-SNARE complex, the rate of fusion is enhanced almost three fold above the standard fusion reaction, demonstrating that the SM protein is having a direct effect enhancing the rate of fusion (Scott et al., 2004).

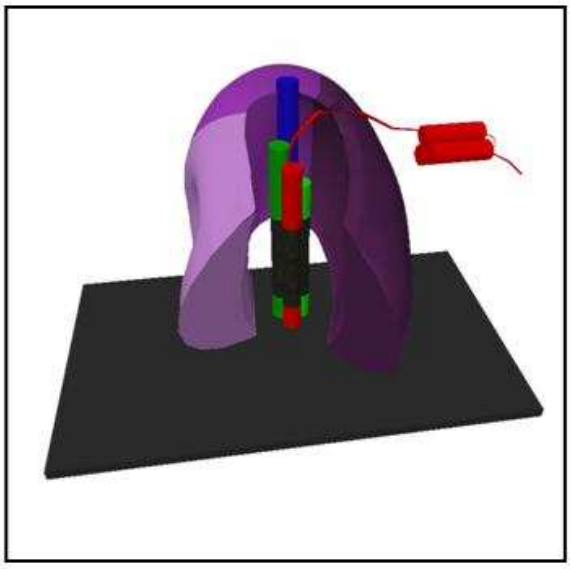

Figure 1.10 Mode-3 binding of SM proteins

There is no crystal structure of a SNARE complex interacting with an SM protein via mode-3 binding; the schematic representation is based on biochemical analysis of the proteins involved, and so the orientation of proteins is again presumed. Syntaxin (red), light chain t-SNARE proteins (green), v-SNARE protein (blue), SNARE domains (black) and SM protein (purple) are depicted. It is not known if Sec1p preferentially binds to complexes on opposing membranes (*trans*-SNARE complexes) or to complexes on the same membrane (*cis*-SNARE complexes), as depicted here.

1.6.4.4 Indirect mode of SM protein binding

Vam3p, the syntaxin that localises to, and regulates traffic into, the yeast vacuole (Sato et al., 1998, Srivastava and Jones, 1998, Wada et al., 1997), differs again in its mode of binding to cognate SM protein Vps33p, in that it does not do so directly (Sato et al., 2000). Sato and colleagues demonstrated that Vps33p is part of a complex (the homotypic fusion and vacuole protein sorting (HOPS) complex; composed of Vps11p, Vps16p, Vps18p, in addition to Vps33p), when it interacts with monomeric Vam3p (Sato et al., 2000). The interaction between this SM protein containing HOPS complex and Vam3p is required for homotypic fusion of vacuolar membranes (Seals et al., 2000). Investigations into Vps33p binding have shown no direct interaction with Vam3p (Dulubova et al., 2001, Price et al., 2000). Functional studies on *D. melanogaster* revealed that a Vps33p homologue also interacts with a complex (Sevrioukov et al., 1999). *In silico* analysis of yeast Vps33p revealed two homologues (Vps33a and Vps33b) in higher eukaryotes: *D. melanogaster*; *Homo sapiens*; *Mus musculus*; *Rattus norvegicus*; *Danio rerio*; *C. elegans* (Gissen et al., 2005). A low affinity interaction has also been demonstrated between Vps33p and the late endosomal syntaxin Pep12p (Subramanian et al., 2004), which is thought to mediate trafficking to the vacuole (Becherer et al., 1996). This is the only documented example of a syntaxin interacting with two SM proteins, as Pep12p has also been shown to interact with Vps45p (Burd et al., 1997, Webb et al., 1997). However, the main binding site of Vps45p has been shown to be Tlg2p, the syntaxin responsible for *trans*-Golgi network (TGN) / early endosome trafficking (Abeliovich et al., 1999, Abeliovich et al., 1998, Bryant and James, 2001, Nichols et al., 1998).

1.6.4.5 SM proteins binding non-syntaxin SNAREs

SM proteins, despite having varied binding modes to their cognate syntaxins were presumed to carry out their function via this interaction; the discovery that SM proteins could also bind to non-syntaxin SNAREs further complicates the proposal of a hypothesis to explain conserved SM protein function(s) (Peng, 2005). The syntaxin Sed5p, which can interact with different cognate SNARE partners to facilitate membrane fusion at the ER-Golgi and intra-Golgi trafficking steps (Parlati et al., 2000, Parlati et al., 2002), is known to bind with a high affinity to SM protein Sly1p (Grabowski and Gallwitz, 1997). As discussed in section 1.5.4.2, Sed5p interacts with Sly1p through mode-2 binding (Bracher

and Weissenhorn, 2002, Yamaguchi et al., 2002). Further investigation of this system, using mutant versions of Sed5p and Sly1p that abolish mode-2 binding, demonstrated that this mode of interaction is not essential for *in vivo* function (Peng and Gallwitz, 2004). The fact that a large fraction of mutant Sly1p unable to interact with Sed5p via mode-2 was still found localised to Golgi membranes, led Peng and Gallwitz to test if Sly1p could interact with non-syntaxin SNAREs (Peng and Gallwitz, 2004). These experiments revealed that Sly1p could directly interact with four non-syntaxin SNARE proteins: two involved in ER-Golgi traffic (Bet1p and Bos1p) and two involved with intra-Golgi traffic (Gos1p and Sft1p) (Peng and Gallwitz, 2004). Furthermore, Sly1p interaction with non-syntaxin SNAREs is not promiscuous, as it does not bind the non-syntaxin SNARE molecules Tlg1p, Vti1p and Nyv1p, which are not associated with these Sed5p related trafficking steps (Peng and Gallwitz, 2004). Another example of an SM protein binding to a non-syntaxin SNARE protein was identified in the yeast TGN / early endosomal system: Vps45p interacts with its cognate v-SNARE Snc2p (Carpp et al., 2006; this interaction is discussed in more detail in Chapter IV), in addition to its better characterised mode-2 interaction with Tlg2p (Abeliovich et al., 1999, Bryant and James, 2001, Dulubova et al., 2002, Nichols et al., 1998).

1.6.4.6 Other SM protein binding

Rab proteins and their effectors have been shown to coordinate various aspects of membrane trafficking, and have also been implicated in conferring a level of specificity to membrane fusion events (Zerial and McBride, 2001; discussed in more detail in section 1.5.5). Rab5 is associated with transport into and through the mammalian early endosome and carries out its function through various effectors recruited to the endosomes (Christoforidis et al., 1999, McBride et al., 1999). The SM protein Vps45 has been shown to indirectly associate with Rab5 through an interaction with one of these effectors, Rabenosyn-5 (Nielsen et al., 2000). A more recent *in vivo* study in *D. melanogaster* demonstrated that the Rabenosyn-Vps45 complex on early endosomes links Rab5 to the syntaxin Avalanche (Avl), and that all four proteins are necessary for vesicle fusion in the early endosome (Morrison et al., 2008).

Another novel interaction, involving the Golgi associated SM protein Sly1 binding directly to a tethering factor, was recently identified (Laufman et al., 2009). Tethering factors are a

family of loosely related proteins that have been implicated in membrane fusion as being the first point of vesicle contact, and also conferring a level of specificity (reviewed in Whyte and Munro, 2002; discussed in section 1.5.6). The conserved oligomeric Golgi (COG) complex is a large multisubunit complex composed of eight individual proteins (Kim et al., 1999, VanRheenen et al., 1999, Whyte and Munro, 2001), which are now labelled Cog1 – Cog8 (or Cog1p - Cog8p in yeast) (Ungar et al., 2002). The COG complex has been shown to interact directly with Golgi syntaxin Sed5p, and its mammalian homologue, Sx5 (Shestakova et al., 2007). More recently, a direct interaction between the Golgi SM protein Sly1 and the N terminal portion of Cog4 has been identified (Laufman et al., 2009). This study further documented that the N terminal portion of Cog4 is also responsible for the Sx5 interaction, although it appears different residues of the Cog4 N terminus are involved in each interaction (Laufman et al., 2009). There are also some documented cases of the neuronal SM protein Munc18a interacting with additional proteins, such as Munc18 interacting proteins (Mints) that are predominantly expressed in the brain (Okamoto and Sudhof, 1997). These proteins / interactions are thought to be specific to neuronal exocytosis (reviewed in Latham and Meunier, 2007).

1.6.4.7 SM proteins binding via multiple modes

The crystal structure of the mode-1 interaction between Munc18a and Sx1a is one of the best characterised examples of an SM protein binding to a syntaxin (Misura et al., 2000). A series of reports have since been published characterising additional modes of Munc18a binding (Verhage and Toonen, 2007), which has helped to reconcile discrepancies between Munc18a apparently only binding an inactive conformation of Sx1a (Dulubova et al., 1999, Yang et al., 2000), whilst being required for neuronal exocytosis (Verhage et al., 2000). Gel filtration and NMR techniques have been used to demonstrate that Munc18a interacts with the assembled core complex (Dulubova et al., 2007). In addition to this, *in vitro* binding studies and *in vivo* co-localisation analysis techniques were used to demonstrate that Munc18a can interact with Sx1a by a mode that is functionally, and spatially, distinct from the closed conformation (Rickman et al., 2007). Similarly, investigations on the effects of arachidonic acid in stimulation of SNARE complex formation showed that Munc18a was in association with the assembled SNARE complex (Connell et al., 2007, Latham et al., 2007). The functional significance of Munc18a association to the SNARE complex was supported in a report that demonstrated that

Munc18a binds to assembled complexes anchored to liposomes *in vitro*, and that this association accelerates the rate of liposome fusion (Shen et al., 2007). It was suggested by Rickman and colleagues that the association of Munc18a to the assembled complex may be facilitated through the N terminus of Sx1a (Rickman et al., 2007). This was confirmed by FRET and NMR analysis, in a study that also demonstrated the functional importance of the N terminal peptide in exocytosis (Khvotchev et al., 2007). This N terminal interaction was suggested to be a link between the Munc18a interactions of the closed conformation and the assembled complex (Khvotchev et al., 2007). Isothermal titration calorimetry (ITC) measurements were used to show that the Sx1a N terminal peptide contributes to its affinity for Munc18a; this led to a refinement to the crystal structure of the Sx1a-Munc18a complex, showing that Munc18a interaction with the closed conformation of Sx1a could occur concurrently with binding to the N terminal peptide (Burkhardt et al., 2008). The authors proposed a model whereby this Munc18a interaction controls accessibility of Sx1a to its cognate partners, a feature that could be common to all SM proteins (Burkhardt et al., 2008).

ITC experiments have also been used to investigate the affinity of mammalian (m)Vps45 for its cognate syntaxin, Sx16; the N terminal peptide of Sx16 binds to mVps45, but longer cytosolic versions have a marked increase in affinity (Burkhardt et al., 2008). This is suggestive of an additional binding mode in the C terminal part of the protein, which additively contributes to the affinity of the N terminal peptide alone. The authors speculate this additional binding mode may be a closed conformation (Burkhardt et al., 2008). Other SM-syntaxin partners have been shown to interact by both mode-1 and mode-2 binding modes, such as the mammalian Sx4 binding to Munc18c (Aran et al., 2009, D'Andrea-Merrins et al., 2007) and UNC-64 binding to UNC-18 in *C. elegans* (Johnson et al., 2009). In addition to this, yeast Vps45p known to interact with Tlg2p via a mode-2 interaction (Dulubova et al., 2002), has been shown to also bind to SNARE complexes by a distinct mechanism (Carpp et al., 2006).

1.6.5 Rab family of proteins

The Rab GTPases are the largest family of small GTPases, homologues of which have been identified in a wide variety of species (Bock et al., 2001, Pereira-Leal and Seabra, 2001). Rab proteins act as molecular switches, alternating between an active GTP bound

form and an inactive GDP bound form, this cycle in activity can impose temporal and spatial regulation on fusion; for this reason Rab proteins have been implicated in a number of roles associated with membrane trafficking (Stenmark, 2009). To achieve their function, activated Rab proteins bind to soluble factors known as effectors (examples listed in Zerial and McBride, 2001). Interestingly, Rabs have been shown to localise to distinct intracellular membranes, the first indication that they may confer specificity to membrane fusion (Chavrier et al., 1990). Mutation of the yeast Rab GTPase Sec4p results in accumulation of vesicles destined for the plasma membrane, indicating that one role of Rab proteins is involved with vesicle docking (Salminen and Novick, 1987). Sec4p has been shown to interact with Sec15p, a component of the exocyst complex (Guo et al., 1999), which acts as a tethering factor that forms long distance contact between secretory vesicles and the plasma membrane (Lipschutz and Mostov, 2002; discussed in section 1.5.6). Rabs have been associated with other aspects of membrane fusion besides being directly involved with vesicle fusion, one such example is at the earlier stage of vesicle budding. Rab5 is an important factor in endocytosis, as a version of Rab5 defective in its ability to bind GTP was shown to drastically reduce the rate of endocytosis, in contrast, over-expression of wild-type Rab5 accelerates uptake of endocytic markers (Bucci et al., 1992). An *in vitro* study later demonstrated that Rab5 is required for formation of clathrin coated vesicles (McLauchlan et al., 1998). Another role Rab proteins have been implicated in is vesicle motility: in *S. cerevisiae*, organelles are delivered to the emerging bud during cell division (Yaffe, 1991). The trafficking of late Golgi compartments along actin cables is mediated by the type V myosin motor Myo2p (Rossanese et al., 2001), the attachment of which is facilitated by the Rab GTPase Ypt11p (Arai et al., 2008). There is an ever increasing volume of data illustrating the essential roles Rab proteins play in fusion related processes. Furthermore, multiple Rab proteins have been shown to coordinate roles at the same location (Stenmark, 2009). The multiple regulatory roles of Rab proteins have led to them being regarded as universal coordinators of membrane fusion.

1.6.6 Tethering factors

The first physical contact between a target membrane and an incoming vesicle is thought to be mediated through a family of poorly understood tethering factors (Pfeffer, 1999). Tethering factors have been grouped into long coiled-coil proteins and large multisubunit complexes (Whyte and Munro, 2002). An example of a long coiled-coil tethering factor is

the yeast Uso1p, which is a parallel homodimer with two globular heads (Yamakawa et al., 1996) and has been shown to mediate binding of ER-derived vesicles (Barlowe, 1997). Electron microscopy has been used to image Uso1p, and revealed that it is a substantial ~160 nm in length (Yamakawa et al., 1996). Furthermore, it has been shown that Uso1p is necessary for formation of functional SNARE complexes to facilitate fusion of ER-Golgi vesicles (Sapperstein et al., 1996). Various other long coiled-coil protein tethering factors have been identified, but they do not all share similar sequence, or even structure (Gillingham and Munro, 2003).

Some multisubunit tethering factors are also diverse from one another; however, several conserved tethering complexes have been identified (Whyte and Munro, 2002). One of the best characterised tethering complexes is the exocyst, which was originally identified in *S. cerevisiae*, where it localizes to sites of exocytosis (Guo et al., 1999, TerBush and Novick, 1995). The exocyst is composed of eight individual subunits (TerBush et al., 1996); homologues of each have been identified and shown to be conserved from yeast to mammals (Guo et al., 2000). The exocyst is included in a subcategory of tethering complexes, termed quatrefoil, which are made up of multiples of four; other members include the COG complex (mentioned in section 1.5.4.6) and the Golgi associated retrograde protein (GARP) complex, associated with intra-Golgi and Golgi-endosomal trafficking respectively (Whyte and Munro, 2002). Comparison of the N termini of all Cog proteins, and indeed components of other quatrefoil tethering factors (exocyst and GARP complexes), revealed a conserved coiled-coil domain (Whyte and Munro, 2001). This is suggestive of a possible common function, which may be facilitated through interactions with other proteins (Whyte and Munro, 2002). Interestingly, protein associations thus far reported include the direct interaction of Cog4 with the fusion machinery (Sed5 and Sly1; section 1.5.4.6; Laufman et al., 2009). Also, the GARP complex has been shown to bind directly to the N terminus of the Qb-SNARE, Tlg1p (Siniossoglou and Pelham, 2002). Other tethering complexes out with the quatrefoil family include: transport protein particle (TRAPP) I complex associated with ER-Golgi traffic, and TRAPP II which has a less well understood association to later Golgi traffic (Sacher et al., 2008); the HOPS complex associated with vacuolar trafficking (Ostrowicz et al., 2008), one component of which is the SM protein Vps33p (mentioned in section 1.5.4.4). Finally, the less well characterised Dsl1p complex (Munson, 2009), that is associated with retrograde traffic from the Golgi to the ER (Andag et al., 2001). Recent structural analysis of Dsl1p components revealed that they resemble subunits of the exocyst complex, suggesting these vastly different tethering complexes may have evolved from a common precursor (Tripathi et al., 2009).

1.7 Membrane trafficking in *S. cerevisiae*

S. cerevisiae has proved an excellent model for studying membrane traffic. Genetic mutational analysis has allowed the identification of key proteins essential in trafficking pathways. One such example is proteins involved in the secretory pathway (Bonifacino and Glick, 2004; Figure 1.11, blue arrows). The use of temperature sensitive *sec* mutants unable to secrete proteins from the cell identified 23 proteins essential for the process, including the SM protein Sec1p (Novick et al., 1980; discussed in section 1.5.1). Electron microscopy (EM) analysis of mutants revealed an accumulation of vesicles unable to dock with the plasma membrane (Novick et al., 1980). The endosomal trafficking pathway (Figure 1.11, red arrows) involves the formation of vesicles at the plasma membrane that are subsequently internalised. There are multiple and distinct endocytic pathways following internalisation (Figure 1.11), with sorting through the early and late endosomes (Wendland et al., 1998). There are various other trafficking pathways in yeast, outlined in Figure 1.11.

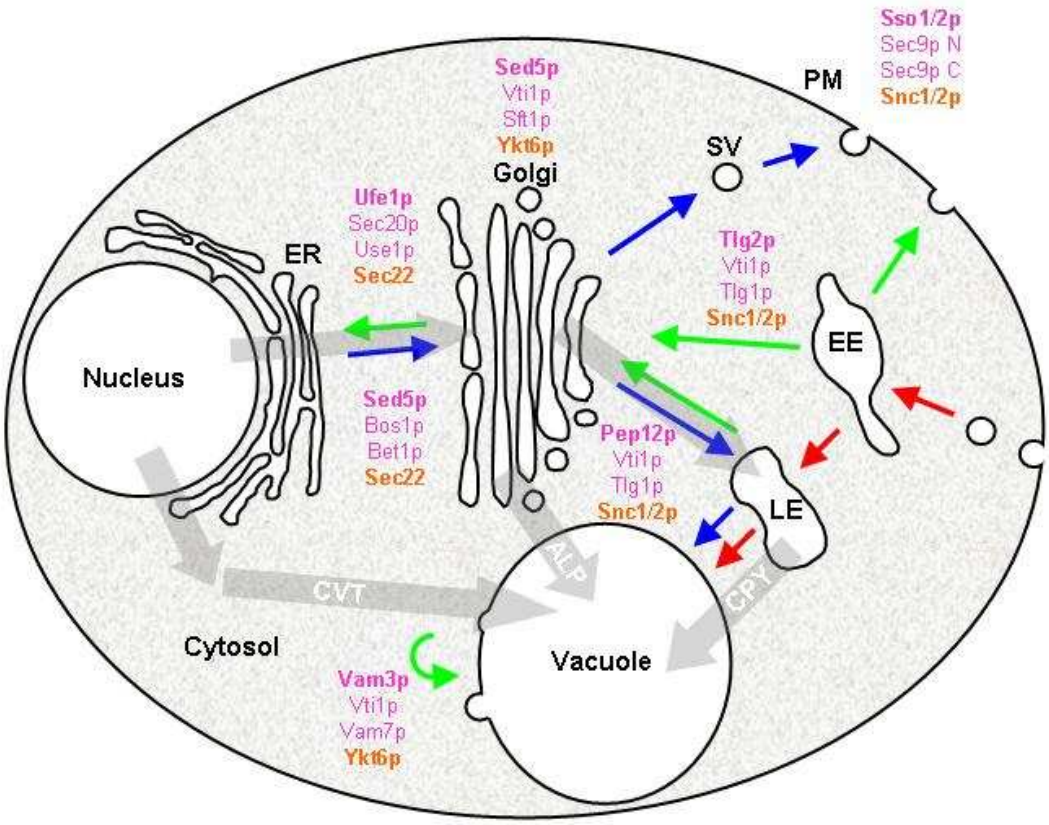

Figure 1.11 Schematic representation of trafficking pathways in yeast.

Compartments of yeast cell are labelled: endoplasmic reticulum (ER); secretory vesicle (SV); plasma membrane (PM); early endosome (EE); late endosome (LE). Trafficking pathways labelled with arrows: secretory pathway (blue); endocytotic pathway (red); other trafficking pathways within the cell (green). The SNARE complexes responsible for each trafficking step are also represented (localisation data taken from Pelham, 2001, Pelham, 1999). t-SNAREs are labelled in pink, the syntaxin molecule in bold; v-SNAREs are labelled in orange. The three trafficking pathways to the vacuole, (ALP, CVT and CYP), are labelled with partially transparent grey arrows.

1.7.1 vps mutants

Protein trafficking from the late Golgi to the vacuole has been intensely investigated and large scale genetic screens have revealed more than 70 proteins involved (Bowers and Stevens, 2005). A precursor of the vacuolar hydroylase CPY is transported through the ER, Golgi and endosome to the vacuole where it is cleaved to its mature form (Figure 1.11; discussed in more detail in Chapter III, section 3.33). Genetic screens based on the perturbation of this pathway, which isolates mutants that secrete a precursor of CPY before

it reaches the vacuole, have been used to identify a large number of vacuolar protein sorting (*vps*) mutants, many of which correspond to gene products (Bankaitis et al., 1986, Bonangelino et al., 2002, Raymond et al., 1992, Robinson et al., 1988, Rothman et al., 1989, Rothman and Stevens, 1986). Some of these proteins were also identified in different genetic screens searching for mutants defective in other aspects of Golgi to vacuole trafficking (Bowers and Stevens, 2005). Such as the *pep* mutants defective for vacuolar protease activity (reduced peptidases) (Jones, 1977); the *vam* mutants, that have abnormal vacuole morphology (Wada et al., 1992); *vac* mutants defective for vacuolar segregation (Weisman et al., 1990); and the *grd* mutants which are Golgi retention defective (Nothwehr et al., 1996). The *vps* mutants have been classified, primarily on vacuolar morphology, into 6 groups (A - F) (Raymond et al., 1992). A 7th class has been proposed, characterised by fragmented vacuoles that appear as clusters of interconnecting tubules (Conibear and Stevens, 2000). These morphological studies have helped identify proteins that function at the same step in the process, and have given better understanding of the multiple processes involved with trafficking to the vacuole (Hedman et al., 2007).

1.7.2 Vps45p

The class D *vps* mutants are characterised by large central vacuoles, defects in vacuole inheritance during cell division, acidification defects and ALP dispersed in membranes of multiple vesicular bodies (Raymond et al., 1992). The gene products of class D *vps* mutants are generally associated with the trafficking step between the late Golgi and the endosomal system (Bryant and Stevens, 1998). One of these genes, *VPS45*, was cloned and the protein Vps45p was characterised by two separate groups (Cowles et al., 1994, Piper et al., 1994). Vps45p was predicted to be a hydrophilic protein of ~67 kDa, and a member of the SM protein family (Cowles et al., 1994, Piper et al., 1994). As mentioned in section 1.6.1, the classification of *vps* mutants groups protein members likely to be involved with the same transport step (Hedman et al., 2007). Other class D *vps* genes encoding proteins proposed to interact at this step are *VPS21* and *VPS6*, which encode a Rab homologue (Rab5; Horazdovsky et al., 1994) and a syntaxin homologue (Pep12p; Becherer et al., 1996, Rothman et al., 1989), respectively; further demonstrating the importance of these three protein families in membrane trafficking events. Both studies that set out to characterise Vps45p reported that some of the hydrophilic protein associates to membranes of the Golgi, the endosome and trafficking vesicles (Cowles et al., 1994,

Piper et al., 1994). Genetic studies suggested that membrane association of Vps45p was mediated through interaction with the syntaxin homologue Pep12p (Burd et al., 1997), but the main binding site was later shown to be through a physical interaction with the syntaxin homologue Tlg2p (Bryant and James, 2001, Dulubova et al., 2002, Nichols et al., 1998). Yeast cells lacking Vps45p were shown to secrete CPY, as expected for *vps* mutants; approximately 70 - 85% CPY was secreted as the precursor to the enzyme (Cowles et al., 1994, Piper et al., 1994). Furthermore, electron microscopy was used to image mutant yeast cells unable to produce Vps45p, which accumulate large numbers of vesicles 40 - 60 nm in diameter (Cowles et al., 1994, Piper et al., 1994). All of this data implicate Vps45p in the targeting and / or fusion pathway between the Golgi and the vacuole (Cowles et al., 1994, Piper et al., 1994).

1.7.3 Tlg2p

Blast searches of the yeast genome based on homology to known syntaxins, the SNARE motif and a C terminal transmembrane domain (Weimbs et al., 1997), identified two possible syntaxin homologues, Tlg1p and Tlg2p (t-SNAREs affecting a late Golgi compartment; Holthuis et al., 1998). Tlg2p has strongest homology to the endosomal and vacuolar syntaxins, Pep12p and Vam3p respectively, but differs from all previously documented syntaxins as it contains a 63 residue luminal domain following its transmembrane domain (Holthuis et al., 1998). This luminal domain was shown not to be essential for its membrane trafficking function, in a study that demonstrated deletion of *TLG2* in yeast results in a CPY trafficking defect, with ~20% being secreted in the precursor form (Abeliovich et al., 1998). In addition to this, studies using internalisation markers showed that Tlg2p is essential for endocytosis (Abeliovich et al., 1998, Seron et al., 1998). Initial localisation of Tlg2p was reported to be at the Golgi (Holthuis et al., 1998), confirmed by fractionation studies showing that it localised with Golgi and endosomal membranes (Abeliovich et al., 1998). Tlg2p and Tlg1p were shown to co-precipitate with Vti1p (Holthuis et al., 1998), and an interaction was found between Tlg2p and the v-SNAREs Snc1p and Snc2p (Abeliovich et al., 1998, Holthuis et al., 1998). Snc1p and Snc2p are functionally redundant v-SNAREs associated with Golgi, endosome and plasma membrane trafficking (Protopopov et al., 1993).

1.7.4 Vps45p interactions

The *PEP12* gene encoding the syntaxin homologue Pep12p (associated with trafficking to the vacuole; Becherer et al., 1996), has been shown to interact genetically with Vps45p (Burd et al., 1997, Webb et al., 1997). However, over-expression of vacuolar syntaxin Vam3p can suppress the CPY trafficking defects of *pep12* delete cells but not those of *VPS45* deletion, suggesting that the sole function of Vps45p is not in regulating Pep12p (Darsow et al., 1997). Soon after this observation was made, binding between Vps45p and Tlg2p was documented (Nichols et al., 1998); it is not surprising that an SM protein can regulate more than one syntaxin, as there are more syntaxins encoded in the yeast genome than there are SM proteins (Pelham, 2001). The Vps45p interaction with Tlg2p was shown to be the main binding site, as Vps45p relies on this interaction, and not that of Pep12p, for its membrane association (Bryant and James, 2001, Nichols et al., 1998). In further support of this, Vps45p co-precipitates with Tlg2p and Tlg1p, and the presence of Vps45p *in vivo* is required to maintain endogenous levels of Tlg2p, but not levels of Pep12p (Bryant and James, 2001, Coe et al., 1999, Nichols et al., 1998). The levels of Tlg2p in *vps45* delete yeast cells can be stabilised in mutant cells lacking proteasomal degradation, indicating that in the absence of Vps45p, Tlg2p is rapidly degraded by the proteasome (Bryant and James, 2001). Mutational analysis of the proteins demonstrated that Vps45p binds to Tlg2p by a mode-2 interaction (Dulubova et al., 2002), which was later shown to be essential for regulation of cellular Tlg2p levels (Carpp et al., 2007). The finding that stabilised Tlg2p levels in the absence of Vps45p can not form SNARE complexes suggested that Vps45p has a role in complex assembly (Bryant and James, 2001). Analysis of a *vps45* delete strain demonstrated that in the absence of Vps45p, Tlg2p is degraded by the proteasome; this degradation can be abolished by using a mutant strain also lacking the activity of two catalytic proteasome subunits (*vps45Δ*, *pre1-1*, *pre2-2*) (Bryant and James, 2001). Co-immunoprecipitation experiments in this strain failed to find Tlg2p bound to its cognate SNARE partners, Vti1p and Tlg1p, unless a version of Tlg2p lacking the Habc domain was used (Bryant and James, 2001). Furthermore, this truncated version of Tlg2p allows trafficking of CPY when the full length version does not, suggesting the complexes formed are functional (Bryant and James, 2001). These data suggest that Vps45p stimulates SNARE complex assembly through an interaction with the N terminus of Tlg2p (Bryant and James, 2001).

Interestingly, a mutant version of Vps45p, analogous to the pocket filled mutant of Sly1p with abrogated mode-2 binding (Peng and Gallwitz, 2004), fails to interact with Tlg2p, but

can still function to correctly traffic CPY (Carpp et al., 2006). This study also reported that Vps45p could bind directly to the v-SNARE Snc2p, and demonstrated that Vps45p could bind to SNARE complexes by a mechanism distinct from mode-2 binding (Carpp et al., 2006). In addition to this, Vps45p has been shown to dissociate from Tlg2p prior to complex assembly, but is later found to bind *cis*-complexes after fusion (Bryant and James, 2003). These distinct binding modes could indicate that Vps45p has more than one role in membrane fusion.

The SNARE domain of Snc2p is responsible for its binding to Vps45p (Carpp et al., 2006). Similarly, the SNARE domains of non-syntaxin proteins Bet1p and Bos1p facilitate their binding to SM protein Sly1p (Peng and Gallwitz, 2004). It has been proposed that the weaker affinity interaction with non-syntaxin SNAREs is a precursor to SM-syntaxin interaction, and that the SM protein may act as a physical bridge between these two phases (Peng and Gallwitz, 2004). Support for this has not been observed with Vps45p *in vitro*, as it cannot bind Tlg2p and Snc2p simultaneously, but it is possible that regulatory factors are required to facilitate the transition of SM protein binding (Carpp et al., 2006). The exact role(s) of Vps45p in complex assembly and membrane fusion has yet to be elucidated.

1.8 Aims of this project

The regulatory factors orchestrating membrane fusion events are extremely complex, and interplay between factors serves to further complicate the issue. My aim was to use the yeast endosomal system to further our understanding of the regulation of SNARE mediated membrane fusion. We consider trafficking at the late Golgi / early endosome of yeast an excellent paradigm to enhance understanding of the SNARE and SM protein families. Vps45p has been heavily implicated in this fusion step; appreciating the significance of its multiple, distinct SNARE interactions could help the formulation of a unifying hypothesis for SM protein family function. The objectives of my investigations presented in this thesis are detailed below.

1.8.1 Aims of Chapter III

The N terminal domain of Tlg2p has been implicated in regulating complex assembly (Bryant and James, 2001), in a manner similar to the exocytotic SNAREs: Sx1a (Dulubova et al., 1999, Misura et al., 2000) and Sso1p (Carr et al., 1999). I wanted to test directly if the Habc domain of Tlg2p has an inhibitory effect on complex assembly. As proof of this, I wanted to test whether Tlg2p can adopt a closed conformation.

Vps45p has been shown to interact with monomeric Tlg2p (Bryant and James, 2001, Nichols et al., 1998), and has been implicated in facilitating a change in Tlg2p which allows it to form SNARE complexes (Bryant and James, 2001). It has been contested that additional *in vivo* factors may be responsible for these observations (Dulubova et al., 2002). Building on the observation that the Habc domain of Tlg2p has a negative role on complex assembly (Bryant and James, 2001; section 1.7.1), we wanted to address this issue, and directly test if Vps45p can alleviate the inhibition on complex assembly imposed by the Tlg2p Habc domain.

1.8.2 Aims of Chapter IV

The significance of the interaction between Vps45p and its cognate v-SNARE Snc2p has yet to be understood. By further characterising this interaction I hoped to reveal any functional relevance it may have.

1.8.3 Aims of Chapter V

Vps45p can bind to assembled complexes by a mechanism distinct from mode-2 (Carpp et al., 2006). We wanted to test if this interaction, or either interaction of Vps45p with Tlg2p or Snc2p, had any functional effect on membrane fusion; as has been demonstrated for SM proteins Sec1p (Scott et al., 2004) and Munc18a (Shen et al., 2007).

Chapter II

Materials & Methods

2.1 Materials

2.1.1 Reagents

General chemicals and reagents were supplied by:

Avanti polar lipids, Alabaster, USA

BioRad Laboratories Ltd, Hemel Hempstead, Hertfordshire, UK

Clontech Laboratories Inc, California, USA

Fisher Scientific Ltd, Loughborough, Leicestershire, UK

GE Healthcare Bio-Sciences Ltd, Buckinghamshire, UK

Invitrogen Ltd, Paisley, UK

Melford Labs Ltd, Ipswich, Suffolk, UK

Qiagen Ltd, Crawley, West Sussex, UK

Roche Diagnostics Ltd, Burgess Hill, UK

Sigma-Aldrich Ltd, Dorset, UK

Spectrum Laboratories Inc, California, USA

Molecular biology enzymes and reagents were supplied by:

Merck Chemicals Ltd, Nottingham, UK

New England Biolabs Ltd, Hertfordshire, UK

Promega Ltd, Southampton, UK

Stratagene Technologies, California, USA

Media used for bacteria and yeast studies were supplied by:

Formedium™, Norfolk, UK

Melford Labs Ltd, Ipswich, Suffolk, UK

Antibodies were supplied by:

Clontech-Takara Bio, Saint-Germain-en-Laye, France

Millipore Ltd, Livingston, UK

Molecular Probes Inc, Oregon, USA.

Roche Diagnostics Ltd, Burgess Hill, UK

Sigma-Aldrich Company Ltd, Dorset, UK

2.1.2 Computer software

Dynamics (DynaPro) V2 - Wyatt Technology Corporation

Image Gauge V4.22 - Fugi Film

Image J: V1.41 - U. S. National Institutes of Health

SIS iTEM Imaging - Olympus

Kaleidagraph V4.0 - Synergy software

Vector NTI V10.3 - Invitrogen Ltd

2.1.3 Primary antibodies

α-cMyc (Clone 9E10) IgG1 monoclonal antibodies raised in mice. Recognises amino acid sequence EQKLISEEDL. Purchased from Sigma-Aldrich Company Ltd (catalogue # C6594). Used at a 1 in 200 dilution from stock solution provided.

α-HA (Clone 3F10) IgG1 monoclonal antibodies raised in rats. Recognises influenza viral protein hemagglutinin (HA) peptide sequence YPYDVPDYA. Purchased from Roche Diagnostics Ltd (catalogue # 11815016001). Used at a 1 in 2,000 dilution from a 100 µg / ml stock.

α-Pgk1p polyclonal antibodies (antisera) raised in rabbits were used as previously described (Piper et al., 1994). Used at a 1 in 20,000 dilution from a ~820 µg / ml stock.

α-Tlg2p polyclonal antibodies generated by Eurogentec were affinity purified from rabbit antiserum to yield antibodies that specifically recognise peptide residues 272 - 287 and 381 - 396 of Tlg2p. Affinity purification performed by Marion Struthers. Used at a 1 in 200 dilution from a ~390 µg / ml stock.

α-Vph1p (Clone 10D7) IgG2 monoclonal antibodies raised in mice. Purchased from Molecular Probes Inc (catalogue # A6426). Used at a 1 in 1,000 dilution from a 250 µg / ml stock.

α-Vps45p polyclonal antibodies generated by Eurogentec were affinity purified from rabbit antiserum to yield antibodies that specifically recognise residues 563-577 of Vps45p. Affinity purification performed by Marion Struthers. Used at a 1 in 1,000 dilution from a ~600 µg / ml stock.

α-Snc2p polyclonal antibodies were raised in rabbits immunised with peptides corresponding to residues 11 - 25 and 72 - 86 of Snc2p (generated by Eurogentec). Antibodies specific to residues 11 - 25 were affinity purified from the rabbit antiserum by Eurogentec. Used at 1 in 1,000 dilution from a ~0.7 mg / ml stock.

2.1.4 Secondary antibodies

All secondary antibodies were purchased from GE Healthcare Bio-Sciences Ltd, Buckinghamshire, UK.

ECL Anti-mouse IgG Horseradish peroxidise-linked species specific whole antibody (from sheep); code NA931. Used at 1: 2,000 dilution from stock solution provided.

ECL Anti-rabbit IgG Horseradish peroxidise-Linked species specific whole antibody (from donkey); code NA934. Used at 1: 5,000 dilution from stock solution provided.

ECL Anti-rat IgG Horseradish peroxidise-Linked species specific whole antibody (from goat); code NA935. Used at 1: 2,000 dilution from stock solution provided.

2.1.5 Bacterial and yeast strains

Strains of *E. coli* and *S. cerevisiae* used are listed in Tables 2.1 and 2.2 respectively. Plasmids were routinely propagated in either *E. coli* host strains XL-1 Blue (Stratagene Technologies) or Top10 (Invitrogen Ltd). Recombinant proteins were generally produced in the *E. coli* host strain BL-21(DE3) (Invitrogen Ltd), and occasionally in strain Rosetta™ 2 (DE3) (Merck Chemicals Ltd).

2.1.6 Bacterial growth media

2YT	1.6% (w / v) tryptone, 1% (w / v) yeast extract, 0.5% (w / v) NaCl
Terrific broth	1.2% (w / v) tryptone, 2.4% (w / v) yeast extract, 0.4% (v / v) glycerol, 0.017 M KH_2PO_4, 0.072 M K_2HPO_4. Purchased from Melford Labs Ltd

SOC	2% (w / v) tryptone, 0.5% yeast extract, 10 mM NaCl, 2.5 mM KCl, 10 mM $MgCl_2$, 10 mM $MgSO_4$, 20 mM glucose

If plated media was required, 2% (w / v) micro agar was added to selective media prior to autoclave sterilisation. Plates were poured in a sterile environment and routinely stored at 4^oC.

Antibiotics were routinely used at a 1 in 1,000 dilution from the stock solutions. Stocks prepared: 100 mg / ml ampicillin sodium salt in water; 36 mg / ml chloramphenicol in 100% ethanol; and 50 mg / ml kanamycin sulphate in water.

2.1.7 Yeast growth media

Yeast was routinely grown on rich media (YPD) or selective minimal synthetic defined (SD) media lacking a particular amino acid.

YPD	1% (w / v) yeast extract, 2% (w / v) peptone, 2% (w / v) glucose
SD -leu	2% (w / v) peptone, 0.7% (w / v) yeast nitrogen base, 0.16% (w / v) leucine dropout supplement
SD -leu,-trp	2% (w / v) peptone, 0.7% (w / v) yeast nitrogen base, 0.16% (w / v) leucine and tryptophan dropout supplement
SD -leu,-trp,-his	2% (w / v) peptone, 0.7% (w / v) yeast nitrogen base, 0.15% (w / v) leucine, tryptophan and histidine dropout supplement

If plated media was required, 2% (w / v) micro agar was added to selective media prior to autoclave sterilisation. Plates were poured in a sterile environment and routinely stored at 4^oC.

2.2 General molecular biology methods

2.2.1 Agarose gel electrophoresis

Agarose powder (0.8 - 2.0% (w / v)) was dissolved in TAE buffer (40 mM Tris Acetate, 1 mM EDTA, pH 8.0) by boiling in a microwave. The solution was allowed to cool to approximately 50^{o}C before Ethidium Bromide (EtBr) was added to a final concentration of 0.5 µg / ml. The solution was left to polymerize in a cassette and then transferred in to a gel tank containing TAE buffer. DNA samples were prepared by addition of 6x DNA loading buffer (40% (w / v), ficoll 0.25% (w / v), bromophenol blue). Samples were loaded onto the gel, alongside a 100 bp or 1kb DNA marker (New England Biolabs Ltd). The gel was then run at 110 volts and DNA samples were visualised with an ultraviolet transilluminator.

2.2.2 Mini DNA preparations

A single colony from fresh bacterial transformation (section 2.3.1) was used to inoculate 5 ml 2YT media containing appropriate antibiotic. Culture was grown overnight at 37^{o}C with shaking. Plasmid DNA was extracted from overnight culture using the Promega Ltd Wizard® Plus SV Mini-prep kit following the manufacturer's instructions. 100 µl of sterile water was generally used to elute DNA from the column. DNA was routinely stored at -20^{o}C.

2.2.3 Gel extraction / purification

Agarose gel electrophoresis (section 2.2.1) was used to separate DNA by size. Specific bands of correct size were identified on a transilluminator, excised from the gel with a scalpel, and then placed in a sterile eppendorf tube. DNA was then extracted and purified from sample using the Qiagen QiaQuick Gel Extraction Kit following the manufacturer's instructions. Depending on subsequent application, between 30 µl and 50 µl sterile water was used to elute DNA from the column.

2.2.4 DNA amplification by Polymerase Chain Reaction (PCR)

Appropriate forward and reverse oligonucleotide primers were designed to amplify the required DNA sequence. Primers were synthesised by York BioScience Ltd, and routinely diluted to 50 pmol with sterile water then stored at -20°C. PCR reactions were set up in thin walled PCR tubes on ice. Genomic or existing plasmid DNA was used as a template. An equal ratio mixture of dATP, dCTP, dGTP and dTTP were used, each at 10 mM concentration. High fidelity proof-reading DNA polymerase, normally *Pfu* (Promega Ltd), was used with the provided buffer. Total volume of reaction mix was made up to 50 µl with nuclease free water. Example of standard reaction:

Template DNA (~1 µg / µl)	1 µl
10 x *Pfu* polymerase buffer	5 µl
Forward primer (5 pmol)	1.5 µl
Reverse primer (5pmol)	1.5 µl
dNTPs (10 mM)	1 µl
Nuclease-free water	39 µl
Pfu DNA polymerase	1 µl

PCR reactions were carried out in a thermocycler. Example of standard conditions:

1. Initial incubation to denature	95°C	2 min
2. Denature	94°C	1 min
3. Annealing of primers	variable (~ 55°C)	1 min
4. Elongation	72°C	2 min / kb
5. Final elongation	72°C	10 min
6. Chill / End	4°C	Hold

Steps 2, 3 and 4 were cycled 30 times before step 5. Size and relative concentration of PCR products were checked by agarose gel electrophoresis (section 2.2.1).

2.2.5 Site directed mutagenesis (SDM)

Desired mutations were incorporated into the designed forward and reverse primers. PCR was then used essentially as described in section 2.2.4, to synthesise mutant DNA, with several alterations: *Pfu* polymerase was used at a reduced temperature of 68^{o}C, for a reduced time of 1 min / kb, and steps 2, 3 and 4 were only cycled 18 times. After the reaction was complete, 1 µl of *Dpn*I was added to each SDM reaction mix and incubated at 37^{o}C for 1 hour to digest the methylated parental DNA. 10 µl of reaction mix was then transformed into Top10 or XL-1 blue *E. coli* cells (section 2.3.1). Successful mutants were selected on antibiotic plates and DNA isolated by mini DNA preparations (section 2.2.2). Mutants were confirmed by sequencing (section 2.2.10).

2.2.6 Restriction endonuclease digestion

Normally DNA / plasmids were digested by 2 restriction endonucleases simultaneously in the same buffer. Reactions were set up in an eppendorf tube, for example:

DNA / plasmid (~1 µg / µl)	5 µl
10 x buffer	1 µl
Restriction enzyme #1	1 µl (20 units)
Restriction enzyme #2	1 µl (20 units)
Sterile water	2 µl

If a double digest could not be completed simultaneously due to incompatibility of buffer requirements, sequential digestions were performed. After the first reaction was completed as above, the DNA was isolated from first buffer using the Qiagen QiaQuick PCR Purification kit. DNA was eluted from the column in 30 µl sterile water, and used in second reaction:

Eluted DNA	30 µl
10 x buffer #2	4 µl
Restriction enzyme #2	1 µl (20 units)
Sterile water	5 µl

Restriction digests were carried out at 37^{o}C for 4 hours. Successful digestion was verified by agarose gel electrophoresis (section 2.2.1).

2.2.7 Ligation reactions

Restriction digests of parent vector and plasmid containing desired fragment were carried out (section 2.2.6). Fragment and vector DNA was then isolated by gel extraction (section 2.2.3). Vector DNA was eluted from the column then incubated with shrimp alkaline phosphatase (SAP) at 37^{o}C for 15 minutes to catalyse the dephosphorylation of 5' phosphates and prevent re-ligation. SAP was deactivated by 15 minute incubation at 65^{o}C before the ligation reaction of the gel purified vector and fragment was set up in PCR tubes on ice. Example of standard reaction:

Vector DNA (~0.5 µg / µl)	2 µl
Fragment DNA (~0.5 µg / µl)	6µl
10 x T4 DNA Ligase buffer	1 µl
T4 DNA Ligase	1 µl

Ligation controls containing only vector DNA, only fragment DNA or no DNA were also prepared. Ligation reactions were carried out at 16^{o}C overnight. 10 µl of each reaction mixture was then transformed into Top10 cells and selected for on antibiotic plates.

2.2.8 Topo® cloning

High fidelity proof-reading PCR was used to amplify DNA (section 2.2.4) which was subsequently gel purified (2.2.6). *Taq* polymerase was used to generate polyadenosine overhangs to the PCR product in the following reaction:

Gel purified DNA (0.5 µg / µl)	20 µl
10 x Mg free buffer	2 µl
$MgCl_2$ (25mM)	1.2 µl
Taq polymerase	0.4 µl (5 units)
dNTPs (10 mM)	0.4 µl

The reaction was set up in PCR tubes and incubated at 72°C for 20 minutes. 2 µl of this *Taq* treated DNA was cloned into the pCR®2.1-TOPO® vector using the Invitrogen pCRII-TOPO® kit. The entire ligation reaction mix was transformed into Top10 cells (section 2.3.1) and selected for on 2YT plates containing appropriate antibiotic and X-gal at a concentration of 0.04 µg / ml. The DNA from white colonies was isolated by mini preparation (section 2.2.2) and sequenced (section 2.2.10) to ensure correct DNA had been cloned.

2.2.9 Estimation of DNA concentration

The concentration of DNA in mini preparations was assessed by ultraviolet absorbance measurements. Absorbance of diluted DNA was measured in a spectrophotometer at 260 nm. Concentration in mg / ml was calculated by multiplying the optical density reading by the dilution factor (normally 100) then by 50, which is the extinction coefficient for double stranded DNA.

2.2.10 Sequencing

Sequencing of DNA was carried out by the University of Dundee Sequencing Service. The correct sequence was confirmed routinely after any molecular cloning techniques involving generation of new DNA.

2.3 General protein methods

2.3.1 Bacterial transformation

Chemically competent bacterial cells (either commercially purchased or prepared in the laboratory, section 2.3.2) were thawed on ice for 15 minutes. 4 µl of plasmid DNA, concentration ~1 µg / µl, was then added to the cells and left on ice for 15 minutes. The cells were then heat shocked at 42^{o}C in a heat block for 45 seconds, before being returned to ice. 250 µl of SOC media was then added to the cells, which were incubated for 1 hour at 37^{o}C with shaking before being spread onto plates containing appropriate antibiotic, allowed to dry for 30 minutes, and then incubated overnight at 37^{o}C.

2.3.2 Preparation of competent bacterial cells

The appropriate bacterial strain was grown in 5 ml 2YT overnight at 37^{o}C in presence of antibiotic if appropriate. 3 ml of culture was then added to 300 ml 2YT and grown at 37^{o}C with shaking to an optical density at 600 nm (OD_{600}) of ~0.6. Cells were then harvested at 1,000 *g* and placed on ice before being gently resuspended in 150 ml of ice cold 50 mM $CaCl_2$ and left on ice for 1 hour. Centrifugation was used to collect cells as before, which were resuspended in 40 ml of 25% (v / v) glycerol, 50 mM $CaCl_2$ and stored in aliquots of 200 µl at -80^{o}C.

2.3.3 Expression of recombinant proteins

A single colony from a fresh transformation was used to inoculate 500 ml 2YT media which was incubated overnight at 37°C with shaking, in the presence of appropriate antibiotic. Cells were then collected by centrifugation at 1,000 *g* for 20 minutes then resuspended in 0.5 - 12 litres of Terrific Broth. Typically cells from 40 ml overnight culture were resuspended in one litre. Cells were incubated at 37°C with shaking in presence of suitable antibiotic to an OD_{600} of 0.6 - 0.8. Expression of recombinant proteins was then induced with 0.2 - 1 mM Isopropyl-β-D-thiogalactopyranoside (IPTG) for 4 hrs at 37°C. In some cases, cells were transferred to lower temperatures (15 - 25°C) at an OD_{600} of 0.4, allowed to grow until the OD_{600} reached 0.6 - 0.8, before being induced with 0.2 - 0.5 mM IPTG overnight at the reduced temperature. Induced cells were harvested at 3,000 *g* for 30 minutes.

2.3.4 General purification of tagged recombinant proteins

Cell pellets (as prepared in 2.3.3) were resuspended in 150 ml cold lysis buffer using a blender before lysis by passage through a Microfluidizer M-110P cell disrupter set to 10,000 psi. DNA was then digested by the addition of DNase I (10 μg / ml) for 30 minutes at 4°C. Cell lysates were then clarified by centrifugation in a Beckman JA-20 rotor for 45 minutes at 20,000 rpm at 4°C. During this spin, appropriate beads were washed and equilibrated, then stored at 4°C. Lysates were then added to beads and incubated on a roller at 4°C to allow tagged proteins to bind. 5 - 10 bead volumes of wash buffer were then added to remove any unspecifically bound proteins. Beads were harvested at 500 *g* for 1 minute, and then the supernatant fluid was discarded. This wash step was repeated as necessary, normally between 5 and 10 repetitions, to obtain as pure a protein sample as possible. If protein of interest was co-expressed with GroEL and GroES chaperone proteins, the final two washes were performed with wash buffer containing 20 mM $MgCl_2$ and 5 mM ATP Na-salt to remove contaminating GroEL and GroES proteins (Rohman and Harrison-Lavoie, 2000, Thain et al., 1996). Protein was then either cleaved from the affinity tag (sections 2.3.4.2 & 2.3.4.3) or eluted from the beads (section 2.3.4.1, 2.3.4.2 & 2.3.4.3) in an appropriate cleavage / elution buffer. The purification of SNARE proteins for use in the *in vitro* fusion assay (Chapter V) was carried out as described in section 2.9.1

2.3.4.1 Purification of His_6 tagged proteins

E. coli cells producing His_6 tagged proteins were resuspended in His_6 lysis buffer (25mM HEPES.KOH pH 7.4, 400 mM KCl, 10% glycerol, 2.5 mM imidazole, 1 mM PMSF, 5 mM β-mercaptoethanol and Complete™ protease inhibitor cocktail (Roche Diagnostics Ltd) before lysis (section 2.3.4). Ni^{2+}-NTA agarose beads were washed 5 times with His_6 wash buffer (lysis buffer containing 20 mM imidazole). Clarified lysates were incubated with washed Ni^{2+}-NTA beads on a roller for ~2 hours at 4°C to allow His_6 tagged proteins to bind. Beads were harvested at 500 *g* for 1 minute and then washed 5 - 10 times with His_6 wash buffer. The His_6 tagged proteins were eluted by incubation for 20 minutes with 1 ml of elution buffer (lysis buffer containing 250 mM imidazole). This process was normally repeated three times and the elutions were pooled. Eluted protein was separated from beads by centrifugation at 500 *g* for 1 minute; supernatant fluid was then removed and stored at -80°C in 200 µl aliquots.

2.3.4.2 Purification of GST tagged proteins

E. coli cells producing GST tagged proteins were resuspended in phosphate buffered saline (PBS; 2.7 mM KCl, 1.8 mM KH_2PO_4, 137 mM NaCl, 10.1 mM Na_2HPO_4) containing 5 mM β-mercaptoethanol and Complete™ protease inhibitor cocktail (Roche Diagnostics Ltd). Cell lysis was then carried out (section 1.3.4) before lysates were clarified by centrifugation at 20,000 rpm in a JA-20 rotor. 3 ml of settled Glutathione Sepharose 4B beads (GE Healthcare Bio-Sciences Ltd) were washed 3x with PBS. Clarified lysates were incubated on a roller overnight at 4°C with washed Glutathione Sepharose beads to allow GST tagged protein to bind. Beads were harvested at 500 *g* for 1 minute then washed 3x with PBS + 1% Triton X-100, 3x with PBS + 0.5 M NaCl and finally 3x with PBS alone. If protein removal from beads was necessary, it was either eluted from the beads using PBS containing 25 mM reduced glutathione or cleaved from the GST affinity tag using thrombin (Chang, 1985; Sigma-Aldrich Ltd) or PreScission protease (Walker et al., 1994; GE Healthcare Bio-Sciences Ltd). Thrombin cleavage was performed by incubating beads with thrombin cleavage buffer (50 mM Tris.HCl pH 8.0, 150 mM NaCl, 2.5 mM $CaCl_2$) containing 0.04 units of thrombin per µl sample at room temperature for 2 hours. PreScission protease cleavage was performed by incubating beads with protease cleavage

buffer (50 mM Tris.HCl pH 7.0, 150 mM NaCl, 1 mM EDTA, 1 mM DTT) containing 0.05 units of PreScission protease per µl sample at 4^{o}C overnight.

2.3.4.3 Purification of Protein A tagged proteins

E. coli cells producing recombinant proteins containing a Protein A tag were resuspended in 150 ml TST buffer (50 mM Tris.HCl pH 7.6, 150 mM NaCl, 0.05% Tween 20) for lysis. Proteins were then purified following the IgG Sepharose™ 6 Fast Flow manufacturer's instructions (GE Healthcare Bio-Sciences Ltd). Protein was either eluted using 0.5 M acetic acid, pH 3.4 or cleaved from the beads using thrombin as described in section 2.3.4.2.

2.3.5 Ion exchange chromatography

Anion exchange separations were carried out on a Mono Q HR (5 / 5) column (GE Healthcare Bio-Sciences Ltd) using Mono Q buffer A (20 mM Tris.HCl pH 8.5, 10% glycerol, 1 mM DTT) and buffer B (20 mM Tris.HCl pH 8.5, 1 M NaCl, 10% glycerol, 1 mM DTT). Cation exchange separations were carried out on a Mono S HR (5 / 5) column (GE Healthcare Bio-Sciences Ltd) using Mono S buffer A (20 mM HEPES.KOH pH 7.0, 1 mM DTT) and Mono S buffer B (20 mM HEPES.KOH pH 7.0, 1 M NaCl, 1 mM DTT). Columns were connected to a fast protein liquid chromatography (FPLC) ACTA system (GE Healthcare Bio-Sciences Ltd) following the manufacturer's instructions.

Protein fractions eluted from affinity purification containing highest concentrations of protein were determined by SDS-PAGE analysis followed by Coomassie staining (sections 2.3.8 & 2.3.9) these fractions were then pooled. Before pooled samples were loaded onto the ion exchange column, the protein in its elution buffer was diluted to 50 mM $NaCl_2$ concentration with buffer A before being filtered through a 0.45 µM syringe filter. The columns were first washed with buffer A, followed by buffer B, and then equilibrated with 5% buffer B (i.e. 50 mM NaCl). Samples were loaded onto the column via a superloop. To elute protein, a gradient from 5% to 50% buffer B (50 mM to 500 mM NaCl) over 20 column volumes was passed through the column. 4 ml fractions were collected and any

displaying absorbance peaks at A_{280} from the chromatograph were analysed by SDS-PAGE and Coomassie staining (sections 2.3.8 & 2.3.9). Fractions containing protein of interest were pooled, concentrated (section 2.3.7) and either stored at -80^{o}C or prepared for further purification (section 2.3.6).

2.3.6 Gel filtration chromatography

Depending on the resolution required, proteins were separated by size on either a Superdex 200 HR (10 / 30) or a Superdex 75 HR (10 / 30) column (GE Healthcare Bio-Sciences Ltd). Columns were connected to an FPLC system as described in the manufacturer's instructions.

The columns were routinely equilibrated overnight with filtered 1x potassium phosphate buffer (170 mM KH_2PO_4, 720 mM K_2HPO_4, 10% (w / v) glycerol, 1 mM DTT). Protein was loaded onto the column 3 ml at a time using a syringe and tubing straight into the FPLC. 1x potassium phosphate buffer was then run through the column at a flow rate of 0.6 ml / min, and 0.5 ml fractions were collected. Fractions with absorbance at A_{280} peaks were analysed by SDS-PAGE and Coomassie staining (sections 2.3.8 & 2.3.9). Fractions containing the protein of interest at highest purity were concentrated (section 2.3.6), and subsequently stored at -80^{o}C after snap freezing in liquid nitrogen.

2.3.7 Concentration of purified protein

Proteins were routinely concentrated using Microcon centrifugation filtration devices (Millipore Ltd, Livingston, UK) following the manufacturer's instructions. Suitable molecular weight cut-off (MWCO) filters were used for each particular protein being concentrated.

2.3.8 SDS PAGE

Discontinuous polyacyrlamide gel electrophoresis was used to resolve proteins as described (Laemmli, 1970). A 30% acrylamide / bisacrylamide mixture (Anachem Ltd, Luton, Bedfordshire, UK) was used to form a stacking mixture of 5% in stacking buffer (25 mM Tris.HCl pH 6.8, 0.2% (w / v) SDS) and a separating mixture of between 7.5 and 15% (v / v) in separating buffer (75 mM Tris.HCl pH 8.8, 0.2% (w / v) SDS). Gels were polymerised by addition of ammonium persulfate (APS) and N, N, N', N' - tetramethylenediamine (TEMED). Gels were then set up in Bio-Rad mini-PROTEAN III apparatus and immersed in running buffer (25 mM Tris base, 190 mM glycine, 0.1% (w / v) SDS). Protein samples were prepared for electrophoresis by incubating at 95^{o}C for 5 minutes in an equal volume of 2x Laemmli sample buffer (LSB; 100 mM Tris.HCl pH 6.8, 4% (w / v) SDS, 20% (v / v) glycerol, 0.2% (w / v) bromophenol blue, 10% (v / v) β-mercaptoethanol). Samples were loaded onto the gel, a BioRad Broadrange Protein Marker was also loaded, and a constant electric potential of 80 volts was applied as proteins migrated through the stack gel. This was increased to 160 volts once the samples had entered the separating gel.

2.3.9 Coomassie staining

Coomassie blue stain was prepared by mixing 0.25% (w / v) Brilliant Blue R-250 (Sigma-Aldrich Ltd) with a solution of 45% methanol, 10% acetic acid (v / v). This solution was thoroughly stirred then filtered through Whatman No 2 filter paper. Resolved SDS-PAGE gels (section 2.3.8) were immersed in staining solution with gentle shaking for a minimum of 1 hour. Gels were de-stained with a solution of 5% methanol, 10% acetic acid (v / v) for as long as necessary.

2.3.10 Western blotting

Proteins to be transferred to a nitrocellulose membrane were first resolved by SDS-PAGE (section 2.3.8). The gels were removed from glass plates and immersed in semi-dry transfer buffer (24 mM Tris base, 20 mM glycine, 0.1% (w / v) SDS) for 30 minutes. Whatman 3 mm filter paper and nitrocellulose membrane (pore size 45 μm) were also

immersed in transfer buffer. Three pieces of filter paper were layered onto the semi dry transfer apparatus, followed by the nitrocellulose membrane. The gel was then carefully placed onto the surface of the membrane, and another 3 pieces of filter paper placed on top. Air bubbles were removed before applying a constant current of 180 mA for 30 minutes at room temperature. Efficiency of transfer was determined by staining the nitrocellulose membrane with Ponceau S solution (0.1% (w / v) Ponceau S, 5% (v / v) acetic acid).

2.3.11 Immunodetection of proteins

Proteins transferred onto a membrane by Western blotting were detected by probing with specific antibodies and visualised using enhanced chemiluminescence (ECL). The nitrocellulose membrane was removed from semi-dry transfer apparatus and washed in PBS-T (2.7 mM KCl, 1.8 mM KH_2PO_4, 137 mM NaCl, 10.1 mM Na_2HPO_4, 0.1% (v / v) tween-20). Non-specific binding to the membrane was reduced by incubating in 5% (w / v) dried milk or BSA in PBS-T for 1 hour. Primary antibodies were diluted to appropriate concentration in 1% (w / v) dried milk in PBS-T and incubated with the membrane for ~2 hours on a roller at room temperature. Unbound antibody was washed off with 6x PBS-T washes over a 30 minute period, before incubation with an appropriate horseradish peroxidise (HRP) linked secondary antibody for 1 hour at room temperature. The excess secondary antibody was washed off as before and labelled proteins were visualised using ECL plus Western Blotting Detection System (GE Healthcare Bio-Sciences Ltd) following the manufacturer's instructions. The membrane was exposed to X-ray film in a light proof cassette before being developed through a Kodak x-omat 2000. Membranes were routinely stripped for re-probing by incubation with 40 ml strip buffer (100 mM glycine.HCl pH 2.2, 150 mM NaCl) for 30 minutes, washing 6x with PBS-T in 30 minutes, then transferring back into blocking solution and following procedure again as described, using a different antibody.

2.3.12 Estimation of protein concentration

2.3.12.1 Absorbance assay at 280 nm

Protein concentrations were estimated by following the manufacturer's instructions of the Bio-Rad protein assay, based on the method of Bradford (Bradford, 1976). All measurements were made on a spectrophotometer at 595 nm. A standard curve was produced by measuring the optical density of a concentration gradient of BSA. Proteins were then measured and relative concentration was calculated from the equation derived from the standard curve.

2.3.12.2 Ninhydrine assay

Protein concentrations were also estimated using ninhydrin colorimetric analysis (Rosen, 1957). 6 point concentration gradients, from 0 - 20 µl, of protein sample and of a 10 mM leucine standard were set up in polypropylene tubes. 150 µl 13 *N* sodium hydroxide was then added to each tube before they were covered with aluminium foil and autoclaved at 116^{o}C for 30 minutes to hydrolyze proteins. Tubes were then cooled to room temperature and each reaction was neutralized by the addition of 250 µl glacial acetic acid. 400 µl CN ninhydrine solution (1.5% (w / v) ninhydrine in 2-methoxyethanol, 50% (v / v) 2-methyoxyethanol, 100 µM sodium cyanide) was then added to each reaction. Tubes were capped and centrifuged at 3,000 *g* for 4 minutes before boiling in water bath for 15 minutes. Immediately after boiling 2 ml 50% isopropanol was added and all tubes were vortexed vigorously then left to cool. Absorbance of all samples was measured at 570 nm in a spectrophotometer. Data was plotted using a linear fit graph. The concentration of amino acids was calculated using a ratio of the 10 mM leucine standard slope and that of the protein samples.

2.3.12.3 Amido black assay

Protein concentration of proteoliposomes was calculated using a modified version of the amido black method (Schaffner and Weissmann, 1973). 20 µl of both proteoliposomes and

BSA standards were prepared for colorimetric analysis. 30 µl 1M Tris.HCl pH 7.5, 2% (w / v) SDS and 50 µl 90% (w / v) trichloroacetic acid (TCA) was added to each sample and vortexed gently prior to incubation at room temperature for 5 minutes. A single 0.45 µm 24 mm filter of mixed cellulose esters (Millipore Ltd) for each sample was pre-wet in 6% (w / v) TCA before samples were applied to filters. Samples were then dried down onto the filters using a vacuum manifold, before the filters were washed with an excess (~500 µl) of 6% (w / v) TCA. Filters of each sample were then incubated for 15 minutes with an excess of 2x amido black staining solution (Sigma-Aldrich Ltd) diluted to 1x with 25% (v / v) isopropanol, 10% acetic acid. Excess stain was then washed off the filters with 3x 30 second washes with 20 ml 25% (v / v) isopropanol, 10% acetic acid, followed by 3x 30 second washes with water. Filters were then dried, chopped up into small pieces and incubated with 1 ml 25 mM NaOH, 0.05 mM EDTA, 50% (v / v) ethanol in a glass test tube. Samples were periodically vortexed during a ten minute incubation at room temperature. The solution in each sample was then removed from the test tube and transferred to a cuvette to measuring absorbance at A_{630} in a spectrophotometer. A standard curve was produced from the BSA samples; the concentration of proteins in each proteoliposome sample was then calculated from the equation derived from the curve.

2.4 General yeast methods

2.4.1 Yeast transformation

100 µl of competent cells per transformation were thawed on ice before addition of ~10 µg of mini prepped plasmid DNA was added. An equivalent volume of 70% (w / v) polyethylene glycol-3350 was added to tubes and mixed gently by inversion. The cells were then incubated on a shaker at 30°C for 45 minutes, followed by a 20 minute heat-shock incubation at 42°C. Cells were pelleted at 3,000 *g* on a bench top centrifuge for 2 minutes and then resuspended in 200 µl sterile water. Cells were then spread under sterile conditions on an agar plate of minimal media lacking appropriate amino acids for selection, allowed to dry, and then placed in a 30°C incubator to allow colonies to form.

2.4.2 Preparation of competent yeast cells

A single colony was used to inoculate a 50 ml culture of YPD media. Cells were incubated at 30°C and grown to an OD_{600} of ~0.8, and then harvested by centrifugation at 1,000 *g* for 2 minutes. Cells were then washed by resuspension in 10 ml LiTE-Sorb (10 mM Tris.HCl pH 7.6, 0.1 M Lithium acetate, 1 mM EDTA, 1.2 M sorbitol) before pelleting again. 1 ml of LiTE-Sorb was then used to resuspend the cells, followed by incubation at 30°C with shaking for 1 hour. Cells were then incubated on ice for at least 20 minutes, and could be used directly for transformation (section 2.4.1). Alternatively, an equivalent volume of ice cold storage buffer (40% (v / v) glycerol, 0.5% (w / v) NaCl) was added to the cells, before aliquoting and snap freezing in liquid nitrogen. Frozen competent cells were stored at -80°C.

2.4.3 Yeast-2-Hybrid assay

2.4.3.1 Expression of proteins in reporter strains

All constructs for the yeast-2-hybrid assays were transformed into an appropriate yeast strain (section 2.4.1). Expression of bait and prey fusion proteins in the host strain was checked by immunoblot analysis of whole cell lysates. Whole cell lysates were prepared by resuspending 10x OD_{600} equivalents of cells in 100 µl TWIRL buffer (5% (w / v) SDS, 8M urea, 10% (v / v) glycerol, 50 mM Tris pH 6.8, 0.2% (w / v) bromophenol blue, 10% (v / v) β-mercaptoethanol), then incubating at 65°C for 10 minutes. A volume equivalent to 1x OD_{600} (10µl) of cell lysates were then resolved on an SDS-PAGE gel (section 2.3.8) followed by immunoblot analysis with appropriate antibodies (sections 2.3.10 & 2.3.11). The vectors containing the Gal4p activation and binding domains also contain N terminal HA and cMyc epitope tags respectively, to allow multiple fusion proteins to be detected simultaneously.

2.4.3.2 Detection of GFP_{S65T} fluorescence expressed in yeast

A C terminal GFP_{S65T} tag was added to constructs containing *VPS45* to allow confirmation of full length translated protein. To detect GFP fluorescence, an overnight culture in selective media was treated with a final volume of 3% (v / v) formaldehyde, and left at room temperature for 10 minutes to fix the cells. Cells from 1 ml of this culture were then collected by centrifugation at 500 *g* for 2 minutes; the pellet was then washed twice with PBS before being resuspended in 1 ml PBS. A glass coverslip was washed in 100% ethanol and left to air dry. To this, 50 µl of washed yeast cells were added and allowed to dry. The coverslip was attached to a glass slide with Immuno-mount (Thermo Shandon Inc, Pittsburgh, PA, USA). Cells were imaged through a 100x oil immersion objective on a Zeiss Axiomat fluorescence microscope (Carl Zeiss, Germany). Images were captured using an Axiocam MRm camera (Carl Zeiss, Germany).

2.5 GST pull down / complex assembly assay

0.36 µg of either GST or the GST fusion proteins bound to Glutathione Sepharose 4B beads were incubated in the presence or absence of a ~10 fold molar excess of His_6-Vti1p, His_6-Snc2p and untagged Sx8 / Tlg1p chimera. The reaction volume was made up to 1400 µl with binding buffer (25 mM HEPES.KOH pH 7.4, 400 mM KCl, 10 (v / v) glycerol, 1% (v / v) Triton X-100, 1 mM DTT, 0.5 mg / ml BSA). Binding reactions were carried out at 4^oC on a 360^o rotator for 20 minutes. Beads were then harvested by centrifugation at 500 *g* at 4^oC for 1 minute. Unbound protein was removed by washing 5 times with 750 µl of binding buffer. The beads were then resuspended in 50 µl of 1x LSB and boiled for 5 minutes. Eluted protein was analysed by running on a 15% SDS-PAGE gel (section 2.3.8) followed by Coomassie staining (section 2.3.9) or immunoblot analysis (sections 2.3.10 & 2.3.11).

2.6 CPY-Invertase secretion assay

Wild-type (BHY10) and *tlg2Δ* (SGSY2) *S. cerevisiae* strains expressing a fusion protein containing the first 50 amino acids of CPY and residues 3 - 512 of mature invertase were

used in this assay. Wild-type and mutant versions of HA-Tlg2p were expressed in yeast; protein expression was checked by SDS-PAGE analysis (section 2.3.8) of yeast cell lysates followed by immunoblot analysis using an α-Tlg2p antibody (sections 2.3.10 & 2.3.11). An equal number of cells from each transformant was then added to a test tube, and made up to 400 µl with 1 M sodium acetate buffer at pH 4.9. Each sample was split into two aliquots, one of which was treated with 5 µl Triton X-100 to lyse the cells, the other was left untreated. 50 µl 0.5 M sucrose solution was then added to each sample and incubated at 30°C for 30 minutes. 300 µl 0.2 M K_2PO_4 pH 10.0 was added to each sample before boiling for 3 minutes in a water bath. Tubes were then chilled on ice before addition of Glucostat reagent (3.5 mM K_2HPO_4, 80 units / ml glucose oxidase, 100 µg / ml Horse radish Peroxidase, 4 mM NEM, 6 mg / ml *o*-dianisidine), and a further incubation at 30°C for 30 minutes. Reactions were then stopped by addition of 2 ml 6 *N* HCl. The absorbance at A_{540} was then measured and lysed samples used to represent total cellular invertase activity, and unlysed samples to show secreted invertase activity.

2.7 Electrophoretic mobility shift assay

2.7.1 Alexa 488 labelling

Prior to binding of the Alexa Fluor® 488 C5 maleimide (Invitrogen Ltd), $Snc2p_{1-94}$ containing a single C terminal cysteine residue was first purified by affinity, ion exchange and gel filtration chromatography, in order to obtain as pure a sample as possible. The sample was then diluted to 50 µM in 1x potassium phosphate buffer containing 1 M Tris (2-carboxyethyl) phosphine (TCEP). The reaction mix was left for 1 hour at room temperature to allow reduction of cysteine residues. To favour the binding reaction to $Snc2p_{1-94}$, a 15 fold excess of dried Alexa 488 was resuspended in phosphate buffer, then added to the sample, bringing the total volume to 200 µl. The reaction was covered in tin-foil to exclude light and left at room temperature for 3 hours. Any precipitate formed was removed by centrifugation at 15,000 *g* at 4°C for 15 minutes, and the supernatant fluid was transferred to a new tube. To this final mix 25 µl of phosphate buffer was added, then the entire sample was loaded onto an FPLC system with 200 µl tubing. The tubing was covered with aluminium foil. The sample was then run through a Superdex 75 HR (10 / 30) gel filtration column (GE Healthcare Bio-Sciences Ltd) to separate the labelled protein.

Mass spectrometry analysis was used to ensure only labelled protein species existed in the sample. Labelled protein was stored at -80^{o}C.

2.7.2 Binding reaction

Binding reactions of Vps45p and Alexa 488 labelled Snc2p$_{1-94}$ were set up in a 96 well plate. 10 µl Alexa 488 labelled Snc2p$_{1-94}$ at a concentration of 10 µM in binding buffer (170 mM KH_2PO_4, 720 mM K_2HPO_4, 10% (w / v) glycerol, 1mM TCEP, 0.1% (v / v) NP-40) was added to 10 wells. A concentration gradient of Vps45p was produced by a $^{3}/_{5}$ serial dilution of 16 µM stock, shown in Table 2.1. 40 µl of undiluted Vps45p was added to first well, then each of the serial dilutions were added to successive wells and no Vps45p added to the last well, to form the decreasing gradient. The reactions were covered in aluminium foil and left to bind in the dark for 3 hours.

Table 2.1 Protein concentrations for Vps45p-Snc2p$_{1-88}$ binding reaction

Reaction / Well	**1**	**2**	**3**	**4**	**5**
[Snc2p$_{1-94}$-Alexa 488] (µM)	10	10	10	10	10
[Vps45p] (µM)	16	9.6	5.76	3.456	2.073
Reaction / Well	**6**	**7**	**8**	**9**	**10**
[Snc2p$_{1-94}$-Alexa 488] (µM)	10	10	10	10	10
[Vps45p] (µM)	1.244	0.746	0.448	0.269	0.161

2.7.3 Gel retardation assay

A 6% native gel (7 mM HEPES.KOH pH 7.4, 8.6 mM imidazole, 6% (v / v) acrylamide / bisacrylamide mixture, 2.5% (v / v) glycerol) was polymerised using TEMED and APS. The gel was then chilled in running buffer at 4^{o}C for 1 hour. 6 µl of 30% (v / v) glycerol containing 0.01% (w / v) bromocresol green dye was added to each binding reaction and mixed thoroughly. 50 µl of each reaction was loaded onto the chilled native gel, which was then run at 125 volts for 4 hours at 4^{o}C. Native gels were carefully transferred to a

glass plate with excess water, and then all air bubbles were removed. Gels were subsequently scanned in an FLA-5000 Phosphorimager (Fuji Film), set with a single laser at 433 nm. Gels were visualised using Image Gauge V4.22 software.

2.8 Competition binding experiments with recombinantly produced proteins

All proteins used for *in vitro* binding experiments were recombinatly produced in *E. coli* then dialysed against 4 L of 1x PBS before storage at 4°C. A His_6 tagged version Vps45p was bound to Ni^{2+}-NTA beads, before incubation on a rotator with a $Snc2p_{1-88}$-PrA fusion protein overnight at 4°C. A sample of the washed beads, alongside the individual inputs was analysed by SDS-PAGE (section 2.3.8) followed by immunoblot analysis (sections 2.3.10 & 2.3.11) using an α-Vps45p antibody to ensure complex had formed. 50 µl settled beads containing ~90µg His_6-Vps45p bound to $Snc2p_{1-88}$-PrA were then added to separate tubes, to which competing proteins or controls were added, before the reaction volume was made up to 1400 µl with PBS. Binding reactions were allowed to proceed for 16 hours at 4ºC on a rotating wheel, after which time non-specifically bound proteins were removed from the beads with 3x 1 ml washes with 1x PBS. An equal volume of 1x LSB was added to the washed beads before boiling at 95°C for 5 minutes, and protein on beads was analysed by SDS-PAGE (section 2.3.8) followed by immunoblot analysis (sections 2.3.10 & 2.3.11).

2.9 Fusion assay

2.9.1 Expression and purification of recombinant SNARE proteins

To purify heterologously expressed SNARE proteins containing their native transmembrane domains, individual overnight cultures were set up in 2YT containing appropriate antibiotic. This was used to inoculate 6 - 12 litres of terrific broth media. Proteins were expressed and harvested as discussed above; after the pellet was resuspended in A_{200} lysis buffer (25 mM HEPES.KOH pH 7.4, 200 mM KCl, 4% (w / v) Triton X-100,

10% (w / v) glycerol, 5 mM β-mercaptoethanol, 1 mM PMSF). Cell lysis was achieved by passage through a Microfluidizer M-110P cell disrupter set at 10,000 psi. Lysates were clarified as discussed previously, and the tagged protein was routinely bound to 3 ml of appropriate beads. The Triton X-100 in the lysis buffer was exchanged for 1% Octyl-β-D-glucopyranoside (OG) in the wash buffer, which was used to wash the beads 10 times. Proteins were eluted from beads in buffer containing 1% (w / v) OG. The eluate was then aliquoted, snap frozen in liquid nitrogen and stored at -80^{o}C.

2.9.2 Lipid stocks

A 15 mM lipid stock of t-SNARE liposomes was made up in chloroform containing 85 mol% POPC and 15 mol% DOPS. For v-SNARE liposomes, a 3 mM lipid stock was made up in chloroform containing 82 mol% POPC, 15 mol% DOPS, 1.5 mol% NBD-DPPE and 1.5 mol% rhodamine-DPPE. Lipid stocks were stored under nitrogen at -80^{o}C.

2.9.3 Formation of proteoliposomes

100 µl of 15mM unlabelled lipid stock, for t-SNARE liposomes, and 500 µl of 3 mM labelled lipid stock, for v-SNARE liposomes were added to separate 12 x 75 mm glass tubes. A gentle stream of compressed nitrogen was then used to evaporate the chloroform from each tube for 15 minutes. Lipid films were then placed in a vacuum desiccator for 30 minutes to completely remove traces of chloroform. 500 µl purified t- or v-SNAREs containing 1% OG were then added to the appropriate tube containing the lipid films. The lipid film was then completely resuspended, by vortexing for 15 minutes. After the lipid film was resuspended, the detergent was diluted below its critical micelle concentration (CMC) level by the addition of 1 ml of buffer A_{200} containing 1 mM DTT; buffer was added drop-wise while the sample was continuously vortexed. The samples were then dialysed against 4 litres A_{200} buffer containing 1 mM DTT overnight at 4^{o}C using 3 ml Float-a-Lyzers (Spectrum Laboratories Inc) with appropriate molecular weight cut offs. 4 g of Bio-Beads (BioRad Laboratories Ltd) were added to dialysis buffer to capture the detergent. Samples were recovered the following day, and each placed in an SW60 tube on ice for subsequent separation using gradient centrifugation.

2.9.4 Proteoliposome recovery

Proteoliposomes were recovered by floatation on a nycodenz ((5-[*N*-(2,3-dihydroxypropyl)acetamido]-2,4,6-triiodo-*N,N'*-bis(2,3-dihydroxypropyl) isophthalamide)) (Sigma-Aldrich Ltd) gradient. 1.5 ml of dialysed liposome sample was added to an equal volume of 80% (w / v) nycodenz (Sigma-Aldrich Ltd) in A_{200} buffer containing 1 mM DTT and mixed extensively. This 40% mixture was carefully overlaid with 1.5 ml 30% (w / v) nycodenz in A_{200} buffer containing 1 mM DTT. Finally, a third layer containing 250 µl of glycerol free A_{200} buffer was carefully overlaid on the top. These gradients were then centrifuged for 4 hours at 46,000 rpm in an SW60 rotor at 4^{o}C. Proteoliposomes float to the interface between the glycerol free A_{200} and the 30% nycodenz layers, due to their lipid content, and free protein remains in the 40% layer. Proteoliposomes were recovered from the top of the gradient by collecting the top 400 µl of sample with a pipette. If necessary, proteoliposomes were snap frozen in liquid nitrogen and stored at -80^{o}C.

2.9.5 Proteoliposome characterisation

2.9.5.1 Lipid recovery

The percentage lipid recovered in proteoliposomes was calculated by scintillation counting tritium added to the stock solutions. 5 µl of recovered proteoliposome sample was added to 4 ml scintillation fluid and counted in a Beckman Coulter LS 6500 scintillation counter set to automatically count using the tritium detection filter for 3 minutes per sample. A 5 µl sample of the stock solution was also measured. The percentage lipid recovery was calculated by comparing the [^{3}H] DPPC counts per minute from recovered material and stock solution.

2.9.5.2 Protein orientation

In order to analyse the percentage of reconstituted SNARE proteins externally orientated in the proteoliposomes, trypsin digests were carried out. To digest externally orientated proteins, 10 µl of recovered liposomes were incubated at 37^{o}C for 3 hours in presence of

2 µl 0.05% trypsin-EDTA (Invitrogen Ltd). To digest the total protein content, including those internally orientated, 10 µl of liposomes were disrupted by addition of 1.5 µl 0.1% (v / v) Triton X-100 and incubated with 2 µl trypsin. As a control, 10 µl of liposomes were incubated at 37°C for 3 hours in the absence of trypsin. The total protein content of each digestion was analysed by SDS-PAGE and Coomassie staining (sections 2.3.8 & 2.3.9). Densitometry analysis of the resultant gel was performed using Image J software, this data was then used to estimate the percentage of externally facing SNAREs.

2.9.5.3 Dynamic light scattering size analysis

Dynamic light scattering (DLS) was used to estimate the average size of donor and acceptor proteoliposomes. 200 µl of recovered samples were diluted $^{1}/_{10}$ in A_{200} buffer then added to a DynaPro 801 Dynamic light scattering instrument (Wyatt Technology Corp.), through a 200 nm filter. All measurements were made at ~37°C, and the laser power was adjusted to keep the intensity between 500,000 counts and 2,000,000 counts. The results were then processed with the programme Dynamics V2 (Wyatt Technology Corporation). The hydrodynamic radii of each population were calculated with the regularisation algorithm provided by this software.

2.9.5.4 Electron microscope size analysis

Samples of recovered proteoliposomes at a $^{1}/_{10}$ dilution were applied to a glow discharged Formvar / Carbon-coated 200 mesh copper grid then dried down with filter paper to a thin layer onto the hydrophilic support film. 20 µl of 1% aqueous methylamine vanadate (Nanovan; Nanoprobes, Stony Brook, NY, USA) stain was applied and the mixture dried down immediately with filter paper to remove excess stain. The samples were then imaged with a LEO 912 energy filtering transmission electron microscope at 120 kV. The size of individual proteoliposomes was measured from images using SIS iTEM soft imaging software (Olympus).

2.9.6 FRET fusion assay

Typically fusion assays were set up on ice by mixing 5 µl of v-SNARE liposome with 45 µl of t-SNARE liposome directly in a well of a chilled 96 well microtitre plate. For assays requiring the addition of soluble v-SNARE, 5 µl of purified protein in buffer A_{200} was added to the t-SNARE liposomes on ice for 10 minutes prior to the addition of v-SNARE liposomes. To correct for the resulting difference in volume 5 µl of A_{200} buffer was added to all other wells in that run. The microtitre plate was warmed to 37^{o}C and then fluorescence was monitored in a FLUOstar Optima plate reader. The fluorescence was measured for 2 hours with the excitation set to 460 nm and the emission recorded at 538 nm at 2 minute intervals. After this period, the plate was removed and 10 µl of 2.5% (w / v) n-dodecylmaltoside was added to each well in order to achieve a maximal fluorescence reading. The plate was then replaced in plate reader, and fluorescence was recorded as before for 40 minutes at 2 minute intervals.

2.9.7 Analysis of raw fluorescence data

Raw fluorescence data was analysed with KaleidaGraph Software. Raw fluorescence was plotted against time. This was then normalised to percentage maximal detergent signal by using the highest fluorescence reading after addition of n-dodecylmaltoside. Percentage maximal detergent signal was then plotted against time.

Table 2.2 E. coli strains used in this study

***E. coli* strains used in this study**		
Strain	**Genotype**	**Source**
BL21(DE3)	F^- *ompT hsd*$S_B(r_B^-m_B^-)$ *gal dcm* (DE3)	Invitrogen Ltd
Rosetta™ 2(DE3)	F^- *ompT hsd*$S_B(r_B^-m_B^-)$ *gal dcm* (DE3) *pRARE2*	Merck Chemicals Ltd
Top10	F^- *mcrA Δ(mrr-hsdRMS-mcrBC) φ80lacZΔM15 ΔlacX74 nupG recA1 araD139 Δ(ara-leu)7697 galE15 galK16 rpsL(*Str^R*) endA1* λ^-	Invitrogen Ltd
XL-1 Blue	*recA1 endA1 gyrA96 thi-1 hsdR17 supE44 relA1 lac* [F´ *proAB* $lacI^qZ\Delta M15$ Tn10 (Tet^r)]	Stratagene Technologies

Table 2.3 Saccharomyces cerevisiae strains used in this study

***S. cerevisiae* strains used in this study**		
Strain (Stock #)	**Genotype**	**Reference**
AH109 **(75)**	*MATa, trp1-901, leu2-3, 112, ura3-52, his3-200, gal4Δ, gal80Δ, LYS2::GAL1UAS-GAL1 TATA-HIS3, GAL2UAS-GAL2TATA-ADE2, URA3::MEL1UAS-MEL1 TATA-lacZ, MEL1*	Clontech Laboratories Inc (James et al., 1996)
BHY10 **(98)**	*MATα, leu2-3,112 ura3-52 his3-A200 trpl-A901 lys2-801 suc2-A9 leu2-3,112::pBHYl 1(CPY-Inv LEU2)*	(Horazdovsky et al., 1994)
MaV103 **(81)**	*MATa, leu2-3, 112 trp-901 his3D200 ade2-1 gal4D gal80D SPAL10::URA3 GAL1::lacZ GAL1::HIS3-LYS2 can1R cyh2R*	(Vidal et al., 1996a)
MaV203 **(82)**	*MATα, leu2-3, 112 trp-901 his3D200 ade2-1 gal4D gal80D SPAL10::URA3 GAL1::lacZ GAL1::HIS3-LYS2 can1R cyh2R*	(Vidal et al., 1996a)
SGSY2 **(100)**	*MATα, leu2-3,112 ura3-52 his3-A200 trpl-A901 lys2-801 suc2-A9 leu2-3,112p::BHYl 1(CPY-Inv LEU2), tlg2::KanMX*	Constructed by Dr. Scott Shanks

Table 2.4 Table of oligonucleotides used in this study

Oligo	Key	Sequence (5' → 3')
3	***Eco*RI**inframe*SNC2*	**GAATTC**GATGTCGTCATCAGTGCCATAGC
4	***Hind*III**stopstop*SNC2*	**AAGCTT**TTATTAATCTTTCCACCACATTTGCT
210	***Bam*HI**start*SXN8*	**GGATCC**TTGGGTTTCGATGAGATCCG
211	*SXN8 TLG1*	GTCCATACCCTCGTCCATATTATCCAACAATTGTCCCTGTTCGTCCAGTTCATTCCCAATCT
212	*TLG1 SXN8*	AAGCAAATGGGCCAGGAGATTGGGAATGAACTGGACGAACAGGGACAATTGTTGGATAATATG
213	***Eco*RI***TLG1*	**GAATCC**TCAAGCAATGAATGCCAAAACTAA
217	*TLG2***F9AL10A***TLG2*	GAGATAGAACTAATTTA**GCTGCA**TCATACCGTAGGACT
218	Reverse complement of 217	AGTCCTACGGTATGA**TGCAGC**TAAATTAGTTCTATCTC
326	***Nco*I**inframe*SNC2*	**CCATGG**GCATGTCGTCATCAGTGCCATACGATC
327	***Bam*HI**stopstop*SNC2*	**GGATCC**TTATTAATCTTTCCACCACATTTGCTTTCTG
328	***Nco*I**inframe*VPS45*	**CCATGG**GCATGAACCTTTTTGATGTGGCTGAC
329	***Bam*HI**stopstop*VPS45*	**GGATCC**ATTATTTTGCAGATCTAATAGAATCC
354	*VPS45**Pac*I**inframe***Bam*HI** pACT2 vector sequence	CTATTAGATCTGCAAAA**TTAATTAA**AA**GGATCC**GAATTCGAGCTC
355	Reverse complement of 354	GAGCTCGAATTC**GGATCC**TT**TTAATTAA**TTTTGCAGATCTAATAG
358	***Pac*I**inframe*GFP*	**TTAATTAA**AATGGGTAAAGGAGAAGAACTTTTC
360	***Pac*I**stopstop*GFP*	**TTAATTAA**TTATTACTAGATCCGGTGGATCCCG
369	*VPS45**Pac*I**inframe***Bam*HI** pGBKT7 vector sequence	TTCTATTAGATCTGCAAAA**TTAATTAA**AA**GGATCC**GTCGACCTGC
370	Reverse complement of 354	GCAGGTCGAC**GGATCC**TT**TTAATTAA**TTTTGCAGATCTAATAGAA
470	*TLG2***I285A***TLG2*	GGACTATTGTGGACAGG**GCT**GATTATAATCTGG
471	Reverse complement of 470	CCAGATTATAATCAGCCCTGTCCACAATAGTCC
474	***Xho*I**stop*VPS45*	**CTCGAG**TTATTTTGCAGATCTAAT
479	***Nco*I***TLG2* SNARE domain	**CCATGG**GCCTCGATATTGAAGACTAT

480	***Bam*HI**stop*TLG2* SNARE domain	**GGATCC**TTATTTTGAGTTCTCTTCTGG
481	***Nco*I***TLG2* Habc domain	**CCATGG**GTACATACCCGATGATG
482	***Bam*HI**stop*TLG2* Habc domain	**GGATCC**TTACAAATCCTTGTTCAAGAA

Table 2.5 Table of parental vectors used for cloning in this study

Parent Vectors	**Description**	**Source**
pACT2	ColE1 *ori*, Ap^R. Yeast expression plasmid (2μ, *LEU2*).	Clontech Laboratories Inc (Li et al., 1994)
pACYCDuet-1	P15A *ori*, *lacI*, Cm^R; *E. coli* expression vector.	Merck Chemicals Ltd
pCOG022	*E. coli* expression vector encoding two repeats of the IgG binding domains of *S. aureus* protein A.	*Xho*I and *Pac*I were used to remove C terminal S tag ORF from pETDuet-1, Sequence encoding two synthetic repeats of the IgG binding domains of *S. aureus* protein preceded by a thrombin cleavage site then inserted with the same sites. Created by Dr. Lindsay Carpp.
pCR®2.1-TOPO®	pUC *ori*, f1 *ori*, Ap^R, Kn^R, *E. coli* cloning vector.	Invitrogen Ltd
pET28(a-c)	F1 *ori*, *lacI*, Kn^R; *E. coli* expression vector.	Merck Chemicals Ltd
pETDuet-1	ColE1 *ori*, *lacI*, Ap^R; *E. coli* expression vector.	Merck Chemicals Ltd
pETDuet-1 GST	*E. coli* expression vector encoding glutathione *S* transferase (GST).	*Xho*I and *Pac*I were used to remove C terminal S tag ORF from pETDuet-1, GST ORF sequence preceded by a thrombin cleavage site then inserted with the same sites. Created by Dr. Fiona Brandie.
pGEX-3T-1	pBR322 *ori*, *lacI*, Ap^R; *E. coli* expression vector.	GE Healthcare Bio-Sciences Ltd
pGEX-4T-1	pBR322 *ori*, *lacI*, Ap^R; *E. coli* expression vector.	GE Healthcare Bio-Sciences Ltd
pGEX-6P-1	pBR322 *ori*, *lacI*, Ap^R; *E. coli* expression vector.	GE Healthcare Bio-Sciences Ltd
pQE-TriSystem	pUC *ori*, *lacO*, Ap^R. *E. coli* expression vector.	Qiagen Ltd

Table 2.6 Plasmids constructed / used in this study

Stock #	Plasmid name	Description	Source
455	pCMD001	Fragment encoding chimera containing Sx8 residues 135 - 179 followed by Tlg1p residues 166 - 244. Flanked by *Bam*HI and *Eco*RI sites in pCR®2.1-TOPO®.	PCR SOEing reaction using *TLG1* and *SXN8* cDNA was performed using external oligos 210 and 213 containing *Bam*HI and *Eco*RI sites. These oligos were used in conjunction with internal oligos 211 and 212. Resulting PCR product was *Taq*-treated and sub-cloned into pCR®2.1-TOPO®.
456	pCMD002	*E. coli* expression vector encoding an N-terminally His_6-tagged version of the Sx8 / Tlg1p chimera.	*Bam*HI / *Eco*RI fragment sub-cloned from pCMD001 into pET28a cut with the same enzymes.
457	pCMD003	*E. coli* expression vector encoding an N-terminally GST-tagged version of the Sx8 / Tlg1p chimera.	*Bam*HI / *Eco*RI fragment sub-cloned from pCMD001 into pGEX-4T-1 cut with the same enzymes.
458	pCMD004	*E. coli* expression vector encoding an N-terminally GST-tagged version of the Sx8 / Tlg1p chimera.	(Struthers et al., 2009)
467	pCMD007	*E. coli* expression vector encoding a C-terminally GST-tagged version of cytosolic Tlg2p, residues 221 - 309.	(Struthers et al., 2009)
480	pCMD008	*E. coli* expression vector encoding a C-terminally GST-tagged version of cytosolic Tlg2p, residues 1 - 309.	(Struthers et al., 2009)
481	pCMD009	Fragment encoding GFP_{S65T} flanked by *Pac*I sites, in pCR2.1-TOPO®.	Sequence encoding GFP_{S65T} was PCR amplified from template pGO036 (Odorizzi et al., 2003) using oligos 358 and 360 to incorporate *Pac*I sites. Resulting PCR product was *Taq*-treated and sub-cloned into pCR®2.1-TOPO®.
490	pCMD011	Yeast expression plasmid (2μ, *URA3*) driving production of HA-$Tlg2p_{F9A/L10A/I285A}$.	SDM was performed on pCMD013 using oligos 217 and 218.

466	pCMD013	Yeast expression plasmid (2µ, *URA3*) driving production of HA-Tlg2p$_{I285A}$.	SDM was performed on pHA-TLG2 using oligos 470 and 471.
493	pCMD014	Fragment encoding Vps45p flanked by *Nco*I and *Xho*I sites, in pCR2.1-TOPO®.	Sequence encoding Vps45p was PCR amplified from template pNB710 using oligos 328 and 474 to incorporate *Nco*I and *Xho*I sites. Resulting PCR product was *Taq*-treated and sub-cloned into pCR®2.1-TOPO®.
494	pCMD015	*E. coli* expression vector encoding a C-terminally His$_6$-tagged version of Vps45p.	*Nco*I / *Xho*I fragment encoding full length Vps45p from pCMD014 was sub-cloned into pET28b cut with the same enzymes.
495	pCMD016	Yeast expression plasmid (2µ, *TRP1*) driving expression of Gal4p BD-cMyc-Vps45p-GFP$_{S65T}$.	*Pac*I fragment encoding GFP$_{S65T}$ from pCMD009 was sub-cloned into pCOG085 cut with the same enzymes.
496	pCMD017	Yeast expression plasmid (2µ, *LEU2*) driving expression of Gal4p AD-HA-Vps45p-GFP$_{S65T}$.	*Pac*I fragment encoding GFP$_{S65T}$ from pCMD009 was sub-cloned into pCOG084 cut with the same enzymes.
499	pCMD018	Fragment encoding Tlg2p residues 37 - 192 flanked by *Nco*I and *Bam*HI sites, in pCR®2.1-TOPO®.	Sequence encoding Tlg2p$_{37-192}$ was PCR amplified from template pHA-TLG2 using oligos 481 and 482 to incorporate *Nco*I and *Bam*HI sites. Resulting PCR product was *Taq*-treated and sub-cloned into pCR®2.1-TOPO®.
500	pCMD019	Yeast expression plasmid (2µ, *LEU2*) driving expression of Gal4p AD-HA-Tlg2p$_{37-192}$.	*Nco*I / *Bam*HI fragment encoding Tlg2p$_{37-192}$ sub-cloned from pCMD018 into pACT2 cut with the same enzymes.
501	pCMD020	Yeast expression plasmid (2µ, *TRP1*) driving expression of Gal4p BD-cMyc-Tlg2p$_{37-192}$.	*Nco*I / *Bam*HI fragment encoding Tlg2p$_{37-192}$ sub-cloned from pCMD018 into pGBKT7-p53 cut with the same enzymes, to drop out p53 gene.
503	pCMD021	Fragment encoding Tlg2p residues 221 - 318 flanked by *Nco*I and *Bam*HI sites, in pCR®2.1-TOPO®.	Sequence encoding Tlg2p$_{221-318}$ was PCR amplified from template pHA-TLG2 (Seron et al., 1998) using oligos 479 and 480 to incorporate *Nco*I and *Bam*HI sites. Resulting PCR product was *Taq*-treated and sub-cloned into pCR®2.1-TOPO®.

504	pCMD022	Yeast expression plasmid (2μ, *LEU2*) driving expression of Gal4p AD-HA-Tlg2p$_{221-318}$.	*Nco*I / *Bam*HI fragment encoding Tlg2p$_{221-318}$ sub-cloned from pCMD021 into pACT2 cut with the same enzymes.
505	pCMD023	Yeast expression plasmid (2μ, *TRP1*) driving expression of Gal4p BD-cMyc-Tlg2p$_{221-318}$.	*Nco*I / *Bam*HI fragment encoding Tlg2p$_{221-318}$ sub-cloned from pCMD021 into pGBKT7-p53 cut with the same enzymes, to drop out p53 gene.
35	pCOG002*	Fragment encoding cytosolic Snc2p$_{1-88}$ flanked by *Eco*RI and *Hind*III sites, in pCR®2.1-TOPO®.	Sequence encoding the cytosolic domain of Snc2p was PCR amplified from genomic DNA prepared from a 9Dα strain using oligos 3 and 4 to incorporate *Eco*RI and *Hind*III sites. Resulting PCR product was *Taq*-treated and sub-cloned into pCR®2.1-TOPO®.
39	pCOG006*	*E. coli* expression vector encoding an N-terminal His$_6$ tagged version of cytosolic Snc2p, residues 1 - 88.	*Eco*RI / *Hind*III fragment sub-cloned from pCOG002 into pCAYCDuet-1 cut with the same enzymes.
87	pCOG025*	*E. coli* expression vector encoding a C-terminally PrA -tagged version of the cytosolic domain of Tlg2p, residues 1 - 309.	(Carpp et al., 2006)
201	pCOG045*	*E. coli* expression vector encoding a C-terminally PrA -tagged version of the cytosolic domain of Snc2p, residues 1 - 88.	*Kpn*I / *Xho*I fragment encoding cytosolic domain from pCOG043 was sub-cloned into pCOG022 cut with the same enzymes.
297	pCOG066*	Yeast expression plasmid (2μ, *URA3*) driving production of HA-Tlg2p$_{F9A/L10A}$.	SDM was performed on pHA-TLG2 using oligos 217 and 218.
317	pCOG067*	*E. coli* expression vector encoding His$_6$-Vps45p$_{L117R}$.	(Carpp et al., 2006)
357	pCOG076*	*E. coli* expression vector encoding a C-terminally PrA -tagged version of cytosolic, (residues 1 - 309) Tlg2p$_{F9A/L10A}$.	SDM was performed on pCOG025 using oligos 217 and 218.
371	pCOG077*	Fragment encoding Snc2p flanked by *Bam*HI and *Nco*I sites, in pCR2.1-TOPO®.	Sequence encoding Snc2p was PCR amplified from template pCOG006 using oligos 326 and 327 to incorporate *Bam*HI and *Nco*I sites. Resulting PCR product was *Taq*-treated and sub-cloned into pCR®2.1-TOPO®.

372	pCOG078*	Fragment encoding Vps45p flanked by *Bam*HI and *Nco*I sites, in pCR2.1-TOPO®.	Sequence encoding Vps45p was PCR amplified from template pNB710 using oligos 328 and 329 to incorporate *Bam*HI and *Nco*I sites. Resulting PCR product was *Taq*-treated and sub-cloned into pCR®2.1-TOPO®.
385	pCOG079*	Yeast expression plasmid (2µ, *LEU2*) driving expression of Gal4p AD-HA-Snc2p.	*Bam*HI / *Nco*I fragment encoding full length Snc2p from pCOG077 was sub-cloned into pACT2 cut with the same enzymes.
386	pCOG080*	Yeast expression plasmid (2µ, *TRP1*) driving expression of Gal4p BD-cMyc-Snc2p.	*Bam*HI / *Nco*I fragment encoding full length Snc2p from pCOG077 was sub-cloned into pGBKT7-p53 cut with the same enzymes, to drop out p53 gene.
387	pCOG081*	Yeast expression plasmid (2µ, *LEU2*) driving expression of Gal4p AD-HA-Vps45p.	*Bam*HI / *Nco*I fragment encoding full length Vps45p from pCOG078 was sub-cloned into pACT2 cut with the same enzymes.
388	pCOG082*	Yeast expression plasmid (2µ, *TRP1*) driving expression of Gal4p BD-cMyc-Vps45p.	*Bam*HI / *Nco*I fragment encoding full length Vps45p from pCOG078 was sub-cloned into pGBKT7-p53 cut with the same enzymes, to drop out p53 gene.
393	pCOG084*	pCOG081 with a *Pac*I site inserted immediately after the *VPS45* gene.	SDM was performed on pCOG081 using oligos 354 and 355.
412	pCOG085*	pCOG082 with a *Pac*I site inserted immediately after the *VPS45* gene.	SDM was performed on pCOG082 using oligos 369 and 370.
N / A	pFB09 / 2	*E. coli* expression vector encoding a C-terminally GST-tagged version of the cytosolic domain of Sx4.	Sequence encoding Sx4 cloned into pGEX4T-1. Constructed by Dr. Fiona Brandie.
366	pGBKT7-LamC	Yeast expression plasmid (2µ, *TRP1*) driving production of Gal4p-BD-Lamin C (residues 66 - 230).	Clontech Laboratories Inc
365	pGBKT7-p53	Yeast expression plasmid (2µ, *TRP1*) driving production of Gal4p-BD-p53 (residues 72 - 390).	Clontech Laboratories Inc
50	pHA-TLG2	Yeast expression plasmid (2µ, *URA3*) driving production of HA-Tlg2p.	(Seron et al., 1998)

239	pJM081	*E. coli* expression vector encoding a C-terminally His_6-tagged version Snc2p.	(McNew et al., 2000)
244	pJM132	*E. coli* expression vector encoding an N-terminally His_6-tagged version of Vti1p.	(Fukuda et al., 2000)
240	pJM106	*E. coli* expression vector encoding an N-terminally His_6-tagged version of Tlg2p, residues 37 - 397.	Sequence encoding $Tlg2p_{37-397}$ cloned into pET28a. Gift from Dr. James McNew.
242	pJM124	*E. coli* expression vector encoding an N-terminally His_6-tagged version of Tlg1p.	(McNew et al., 2000)
246	pJM325	*E. coli* expression vector encoding an N-terminally His_6-tagged version of Tlg2p, residues 1 - 335.	Sequence encoding $Tlg2p_{1-335}$ cloned into pET28a. Gift from Dr. James McNew.
N / A	pKIM001	*E. coli* expression vector encoding an N-terminally His_6-tagged version of Tlg2p.	Sequence encoding Munc18c flanked by *Bam*HI and *Xho*I sites was PCR amplified and cloned directly into pQE-TriSystem cut with the same enzymes. Performed by Kim Boney
479	pMM472	*E. coli* expression vector encoding an N-terminal GST tagged version of cytosolic Snc2p, residues 1 - 94.	Sequence encoding $Snc2p_{1-94}$ cloned into pGEX3T-1. Gift from Dr. Mary Munson.
56	pNB710	*E. coli* expression vector encoding a N-terminally His_6-tagged version Vps45p.	(Carpp et al., 2006)
368	pTD1-1	Yeast expression plasmid (2μ, *LEU2*) driving production of Gal4p-AD-SV40 Large T antigen (residues 87 - 708).	Clontech Laboratories Inc (Li and Fields, 1993)
N / A	pT-GroE	*E. coli* expression vector encoding GroEL and GroES chaperone proteins.	(Yasukawa et al., 1995)

** All pCOG plasmids were constructed by Dr. Lindsay Carpp.*

Chapter III

Regulatory mechanisms of Vps45p and Tlg2p

3.1 Introduction

Regulation of SNARE complex assembly is integral to controlling membrane fusion events within the eukaryotic cell (Jahn and Scheller, 2006). The syntaxin and SM protein families are essential for this process, but the mechanisms by which they confer regulation are not fully understood (Jahn, 2000, Sudhof and Rothman, 2009). Structural studies on the syntaxin family member responsible for neuronal exocytosis, Sx1a, have revealed that it contains an autonomously folded Habc domain (Fernandez et al., 1998), that can fold back and form intramolecular interactions with the SNARE motif, thereby prohibiting its entry into a SNARE complex (Dulubova et al., 1999). This has been described as a closed conformation (Dulubova et al., 1999), and syntaxin family members from other systems have been shown to regulate complex assembly, and fusion, by adopting this conformation: the yeast exocytotic Sso1p (Fiebig et al., 1999, Nicholson et al., 1998); mammalian Sx4 in adipocytes (Aran et al., 2009, D'Andrea-Merrins et al., 2007); and UNC-64 in *C. elegans* (Johnson et al., 2009, Richmond et al., 2001).

SM proteins have been identified as essential regulators of vesicle trafficking, but the exact role of these highly conserved proteins remains unclear (Sudhof and Rothman, 2009, Toonen and Verhage, 2003). Failure to construct a unifying hypothesis for the role of SM proteins has largely been due to apparently conflicting data from studies on various transport steps in different experimental systems (Toonen and Verhage, 2003). The crystal structure of the neuronal Sx1a in complex with its cognate SM protein Munc18a revealed that the SM protein has an arch shape, with a central cavity that cradles Sx1a in a closed conformation (Misura et al., 2000). The closed conformation of Sx1a is known to be incompatible with complex assembly (Dulubova et al., 1999). This structural data was supported by a study that demonstrated binding of Sx1a to its SNARE partners precluded binding to Munc18a, and *vice versa* (Yang et al., 2000). Binding of Sx1a in a closed conformation to Munc18a is perturbed if a double mutation, that disrupts the closed conformation (L165A, E166A), is introduced into the linker region between Habc and SNARE domains of Sx1a (Dulubova et al., 1999). These findings have been interpreted as indicating that the SM protein has an inhibitory role on complex assembly by actively prohibiting the syntaxin from entering into complex (Misura et al., 2000, Yang et al., 2000). However, deletion of Munc18a in mice results in a complete lack of synaptic neurotransmitter release (Verhage et al., 2000), which is not what would be expected upon removal of a negative regulator, and suggests a positive role for the SM protein in membrane fusion. These data taken together suggest that the interaction of Munc18a with

the closed conformation of Sx1a is a necessary regulatory step that results in complex formation and membrane fusion.

Understanding the exact mechanisms that control membrane fusion events in the yeast endosomal system has also been made difficult by seemingly conflicting data. In agreement with the *in vivo* Munc18a deletion experiments in mice (Verhage et al., 2000), deletion of Vps45p in yeast (*vps45Δ*) has a profound affect on their ability to correctly traffic the vacuolar hydrolase CPY (Cowles et al., 1994, Piper et al., 1994). A model whereby Vps45p facilitates a switch of Tlg2p from a closed (inactive) to an open conformation that is able to form SNARE complexes, and thus drive fusion, is supported by the observation that the requirement of Vps45p in CPY trafficking can be bypassed by expressing a mutant version of Tlg2p; the mutant version of Tlg2p lacks the N terminal Habc domain, and is therefore unable to adopt a closed conformation (Bryant and James, 2001). However, the above model has been contested by NMR studies that suggest Tlg2p cannot form a closed conformation, and exclusively binds Vps45p via a distinct mechanism (mode-2 binding) involving a small N terminal peptide of Tlg2p (Dulubova et al., 2002). This mode of binding is analogous to the yeast Golgi syntaxin Sed5p interacting with cognate SM protein Sly1p (Bracher and Weissenhorn, 2002, Yamaguchi et al., 2002). The authors of this study suggested that an unidentified inhibitory factor acting on the N terminal portion of Tlg2p may account for the suppression of *vps45Δ* trafficking defects by the version of Tlg2p lacking the Habc domain, since this would not be able to bind to any such inhibitory factor (Dulubova et al., 2002). However, it could be argued that the recombinant proteins used for NMR analysis are not physiologically relevant due to necessary truncations used to obtain sufficient concentrations of soluble protein for analysis; it is possible that these missing residues are important for stabilising a closed conformation. More experimental data is required to distinguish between these two models. Recently, support for a model of Vps45p interacting with Tlg2p by a mode distinct from mode-2 has been inferred from studies on a mammalian homologue of Tlg2p, Sx16. Although the short N terminal peptide of Sx16 is sufficient for binding mVps45, full length Sx16 has a greatly enhanced affinity for the SM protein (Burkhardt et al., 2008). This study also documented a refined crystal structure of the Sx1a-Munc18a complex, which demonstrated that Sx1a could in fact bind Munc18a through its N terminal peptide (mode-2) in addition to its well characterised mode-1 binding (Burkhardt et al., 2008). This refined crystal structure is in agreement with a previous report that used both *in vivo* and *in vitro* techniques to demonstrate that Munc18a could bind to Sx1a via mode-2 binding (Rickman et al., 2007). The originally confounding discovery of the highly

conserved family of SM proteins binding SNARE proteins by multiple, structurally disparate, binding modes is becoming more lucid by such demonstrations of individual SM proteins binding via multiple modes. Convergence in experimental data, such as these examples, may ease the formulation of unifying hypotheses to describe SM protein function.

3.2 Aims of this Chapter

We propose a model whereby Tlg2p forms a closed conformation incompatible with complex assembly; this conformation then undergoes a switch, facilitated by Vps45p, to allow complex formation. To directly test the hypothesis that the presence of the Tlg2p Habc domain inhibits formation of SNARE complexes, I set out to use a simplified *in vitro* assay void of any additional regulatory factors that may influence the process. Once this technique was established to assay complex formation, I aimed to add recombinant Vps45p, to see if any direct effect could be detected by addition of the SM protein to the system. Further to this, I aimed to use a yeast-2-hybrid technique to test whether an intramolecular interaction between the Habc domain and the SNARE domain of Tlg2p could be detected, in support of the syntaxin forming a closed conformation. Finally, using mutant versions of Tlg2p in an *in vivo* trafficking assay we set out to elucidate the functional significance of Vps45p binding modes. Specifically we tested whether abrogating the hypothetical mode-1 binding of Vps45p to a closed conformation of Tlg2p has functional consequences *in vivo*.

3.3 Results

3.3.1 Complex assembly assay

Tlg2p is unable to bind cognate SNARE partners Tlg1p and Vti1p in the absence of Vps45p *in vivo*, but a mutant version of Tlg2p lacking the N terminal Habc domain overcomes this inability to form complexes (Bryant and James, 2001). This led to our hypothesis that Tlg2p forms a closed conformation where the Habc domain interacts with the SNARE motif, thus rendering the protein incompatible with complex formation.

Furthermore, CPY trafficking is blocked in absence of Vps45p, but this effect can be relieved by using a version of Tlg2p lacking the Habc domain (Bryant and James, 2001). This led us to propose that Vps45p facilitates a switch in the conformation of Tlg2p, thus allowing it to enter into functional complexes. These observations can not exclude the possibility that, in the absence of Vps45p, an unidentified inhibitory factor binds to the N terminus of Tlg2p, restricting its ability to enter into SNARE complex *in vivo* (Dulubova et al., 2002). To distinguish between these two models, we designed a GST pull down assay to examine the ability of Tlg2p to form complexes with cognate SNAREs Vti1p, Tlg1p and Snc2p *in vitro*.

All the proteins for the GST pull down assay were produced recombinantly in *E. coli*. To determine the effect the Tlg2p Habc domain has on complex assembly, two Tlg2p-GST fusion proteins were recombinantly produced. The first expressing the entire cytosolic domain, residues 1 - 309, from plasmid pCMD008; the second expressing a version lacking the Habc domain ($_{\Delta Habc}$Tlg2p), containing residues 221 - 309, from pCMD007. Figure 3.1 shows samples analysed by SDS-PAGE followed by Coomassie staining from each step in the purification process of both Tlg2p (upper panel) and $_{\Delta Habc}$Tlg2p (lower panel). The truncated version of Tlg2p lacking the Habc domain expresses at a much higher concentration than the full length version, which is more susceptible to degradation *in vitro* (Carpp et al., 2006). For this reason we used a larger culture (12 fold) of *E. coli* cells expressing full length protein; more IPTG was also used for a longer induction period to raise concentration of full length Tlg2p. These adjustments resulted in similar concentrations of the two Tlg2p-GST fusion proteins produced.

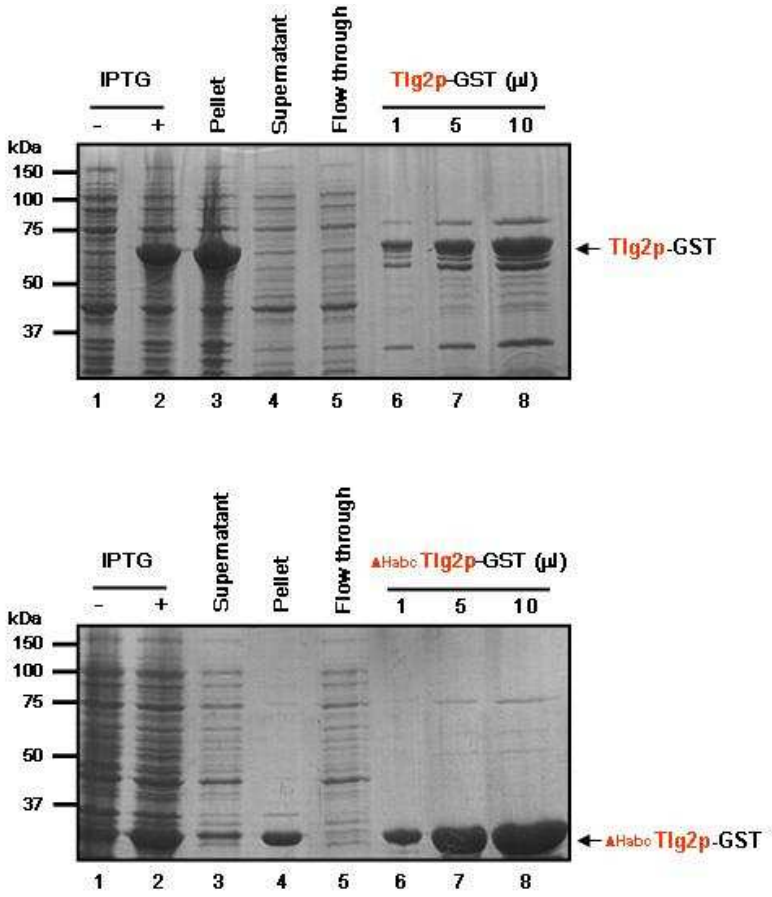

Figure 3.1 GST fusion proteins of Tlg2p for complex assembly assay

Recombinant cytosolic truncations of Tlg2p were produced as GST fusions: plasmids pCMD007 and pCMD008 were used to express Tlg2p residues 1 - 309 (full length; upper panel) and residues 221 - 309 ($_{\Delta Habc}$Tlg2p; lower panel), respectively; each with a C terminal GST tag. Full length Tlg2p-GST protein was expressed from a 3 L culture; cells were induced with 1 M IPTG overnight at 22^{o}C upon reaching OD_{600} of ~0.8 cells. $_{\Delta Habc}$Tlg2p-GST protein was expressed from a 250 ml culture; upon reaching OD_{600} of ~0.8, cells were induced with 0.2 M IPTG at 37^{o}C for 1 hour. Each expressed GST fusion protein was purified by binding to 1 ml settled Glutathione Sepharose 4B beads (GE Healthcare), as described in section 2.3.4.2. Purity of proteins were analysed at various stages by SDS-PAGE on a 12% gel followed by Coomassie staining: samples of culture before and after IPTG induction (Lanes 1 & 2; 5 µl each); soluble protein produced (Lane 4, upper panel; 5 µl & Lane 3, lower panel; 5 µl) compared to protein lost as insoluble (Lane 3, upper panel; 5 µl & Lane 4, lower panel; 5 µl); protein not bound to beads (Lane 5; 5 µl). Finally an equal volume 1x LSB was added to a sample of the washed beads before boiling to analyse protein bound to beads by SDS-PAGE, 3 volumes were run: 1 µl, 5 µl, and 10 µl (Lanes 6 - 8; 5 µl each). Molecular weight markers are indicated.

Next, we created versions of the Tlg2p cognate binding partners: Vti1p, Tlg1p and Snc2p. A chimera, containing the N terminal portion of the Sx8 SNARE motif and the C terminus of Tlg1p (subsequently labelled as Sx8 / Tlg1p), was chosen in place of full length Tlg1p, which has been shown to require additional activation to fuse liposomes *in vitro* (Paumet et al., 2005; discussed in more detail in Chapter V, sections 5.4.1.2 & 5.4.5). We wanted to eliminate this additional level of regulation in order to directly test the effects of the Habc domain and Vps45p on complex assembly. Figure 3.2 shows SDS-PAGE analysis of purified His_6-Vti1p (Lanes 1 - 3), untagged Sx8 / Tlg1p (Lanes 4 - 6) and His_6-Snc2p (Lanes 7 - 9) samples.

Reactions were set up with 0.36 μg of either Tlg2p-GST or $_{\Delta Habc}$Tlg2p-GST bound to Glutathione Sepharose 4B beads (shown in Figure 3.1). Beads were incubated for 20 minutes or 120 minutes in the presence or absence of a ~10 fold molar excess of the cognate SNARE partners shown in Figure 3.2. The beads were then extensively washed in reaction buffer, and the proteins bound to the beads were analysed by SDS-PAGE and immunoblot analysis using an α-Snc2p antibody, shown in Figure 3.3 *(A)* lower panel. Snc2p does not bind directly to Tlg2p, but can enter into an assembled SNARE complex in the presence of the partner t-SNAREs Vti1p and Tlg1p (Carpp et al., 2006). Snc2p, detected on the beads containing the Tlg2p fusion proteins after washing, can therefore be used as an indicator of assembled complexes. Figure 3.3 *(A)* upper panel shows that approximately equal amounts of full length (Tlg2p) and truncated ($_{\Delta Habc}$Tlg2p) versions of Tlg2p have been used in the assay. The lower panel shows that the version lacking the Habc domain ($_{\Delta Habc}$Tlg2p) forms complexes more efficiently than the full length version at the 20 minute time point (compare Lanes 4 & 5). The binding reactions carried out for 120 minutes show little difference in assembled complexes (Lanes 6 & 7). This shows that the full length version of Tlg2p is equally capable of forming SNARE complexes; it is just doing so more slowly than the version lacking the Habc domain. These experiments were carried out four times, the average ability of full length Tlg2p to form complexes compared with the more efficient $_{\Delta Habc}$Tlg2p version (taken as 100%), is presented as a histogram in Figure 3.3 *(B)*. Since these experiments were performed with purified proteins produced in *E. coli*, the inhibitory effect of the Habc domain is not due to the binding of another unidentified factor, as suggested by Dulubova and colleagues (Dulubova et al., 2002). These results support our model whereby the Habc domain of Tlg2p acts to inhibit complex assembly.

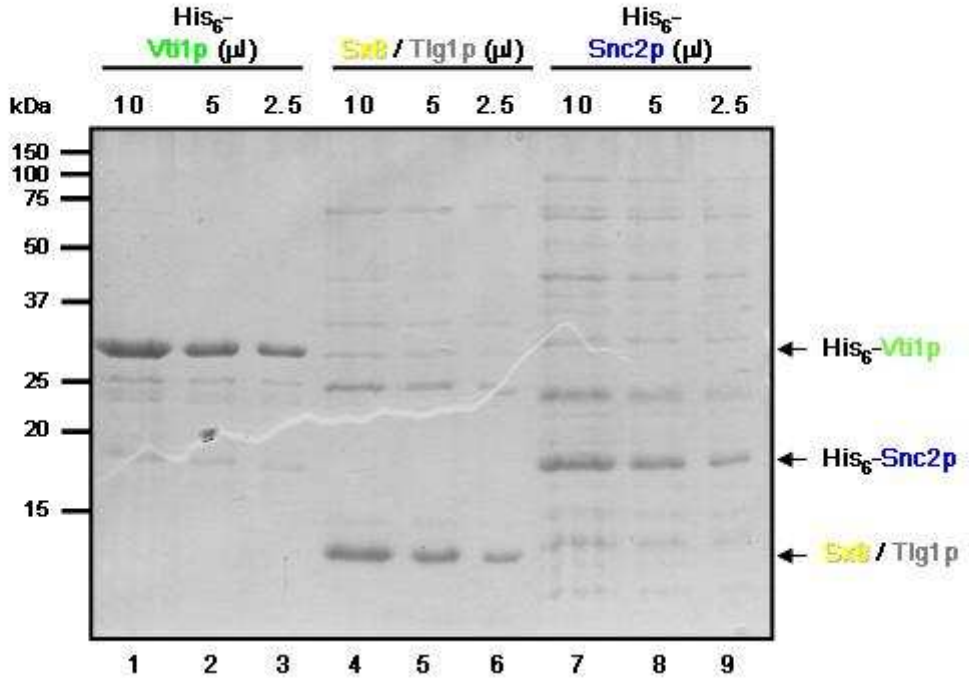

Figure 3.2 Recombinant input SNARE proteins for complex assembly assay

Plasmids pJM132 and pJM081 were respectively used to produce versions of full length Vti1p and Snc2p, each with an N terminal His_6 tag. Proteins were purified as described in section 2.3.4.1. Plasmid pCMD004 was used to produce the Sx8 / Tlg1p chimera with an N terminal GST tag, purified as described in section 2.3.4.2. 0.04 units / µl PreScission protease was used to cleave the purified Sx8 / Tlg1p protein from beads. All proteins were initially analysed by SDS-PAGE followed by Coomassie staining. Proteins were diluted to equal molar concentrations with reaction buffer (400mM KCl, 25 mM imidazole, 4% (w / v) Triton X-100, 5 mM β-mercaptoethanol). A serial dilution of each protein was then analysed on a second 15% gel: His_6-Vti1p (Lanes 1 - 3), Sx8 / Tlg1p (Lanes 4 - 6) and His_6-Snc2p (Lanes 7 - 9), to ensure equal concentrations. Molecular weight markers are indicated.

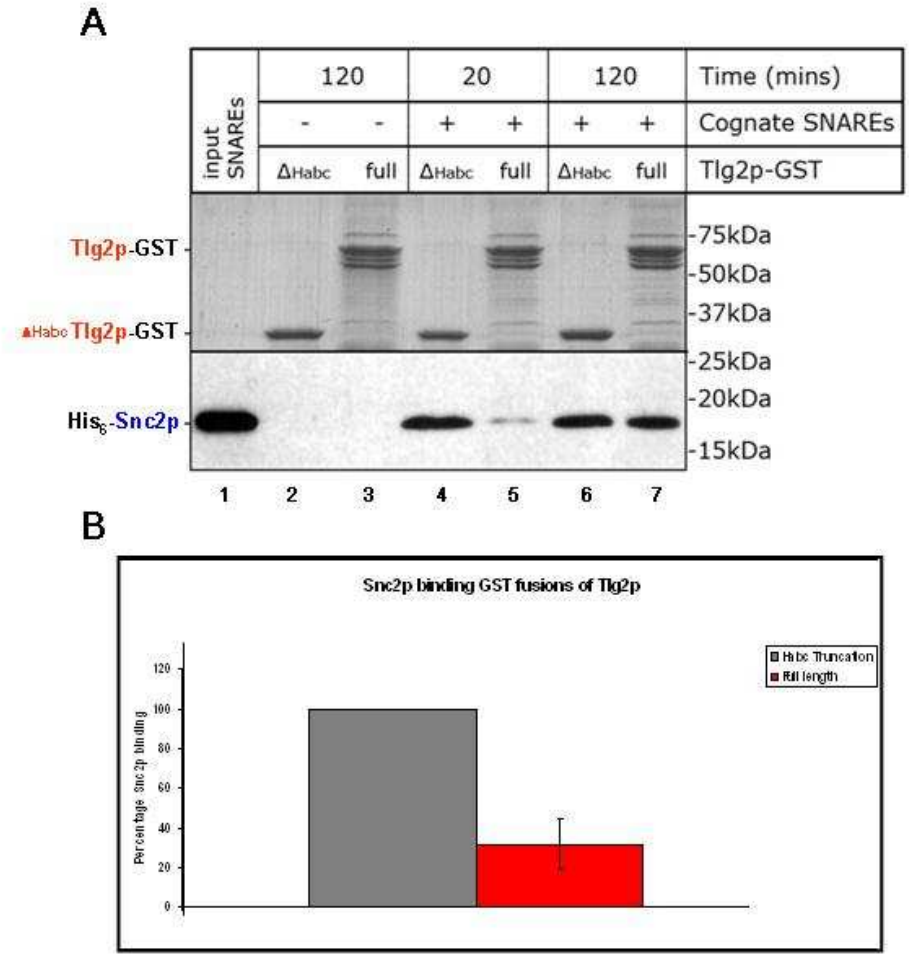

Figure 3.3 In vitro SNARE complex assembly of Tlg2p and $_{\Delta Habc}$Tlg2p

(A) 5 µl of beads containing Tlg2p-GST fusions (shown in Figure 3.1) were incubated in the presence of a ten fold molar excess of the cognate SNARE proteins, His_6-Vti1p, His_6-Snc2p and untagged Sx8 / Tlg1p (shown in Figure 3.2). Reactions were incubated at 4°C on a rotator for 20 and 120 minutes before unbound protein was washed from beads 3x with reaction buffer. Beads were then boiled in 50 µl 1x LSB buffer; 10 µl of each sample was run out on two 15% SDS-PAGE gels. The first was Coomassie stained to show equal loading of Tlg2p fusions (upper panel), the second gel was transferred to a nitrocellulose membrane and then subjected to immunoblot analysis with an α-Snc2p antibody (lower panel). Positions of molecular weight markers are indicated. *(B)* The levels of Snc2p bound to full length Tlg2p-GST compared to $_{\Delta Habc}$Tlg2p-GST from four experiments were analysed by densitometry using Image J software. The average Snc2p bound to $_{\Delta Habc}$Tlg2p-GST was taken as 100% (grey) and compared with average Snc2p bound to full length Tlg2p-GST (red). The standard deviation is indicated by an error bar.

To test whether the addition of the SM protein Vps45p has any effect on the ability of Tlg2p to form complexes in our system, His_6-Vps45p expressed from pNB710 (Carpp et al., 2006) was purified as described in section 2.3.4.1. Figure 3.4 *(A)* shows purified Vps45p used in the complex assembly assay. The assays were set up as described previously, this time also in the presence or absence of Vps45p. Figure 3.4 *(B)* shows protein samples from beads analysed by SDS-PAGE: one gel being Coomassie stained to confirm that equal amounts of full length and ΔHabc Tlg2p-GST fusion proteins were used (upper panel); the other being transferred to a nitrocellulose membrane for immunoblot analysis with an α-Snc2p antibody, to determine the extent of complex formation in each reaction (lower panel). Binding reactions were run for 20 minutes and proteins bound to beads were analysed by SDS-PAGE and immunoblot analysis. Addition of Vps45p has no effect on the rate at which complexes containing truncated $_{\Delta Habc}$Tlg2p are assembled (compare Lanes 1 & 3). However, Vps45p relieves the kinetic delay of complex assembly observed with full length Tlg2p (Lanes 2 & 4), resulting in levels of assembly comparable with the version of Tlg2p lacking the Habc domain (compare Lanes 3 & 4). These data suggest that the Habc domain of Tlg2p confers a negative level of regulation upon SNARE complex assembly *in vitro*, which is alleviated by Vps45p. The simplest explanation for a conformation that precludes complex assembly is a "closed" conformation, previously observed in Tlg2p homologues Sx1a and Sso1p (Dulubova et al., 1999, Nicholson et al., 1998). More recently Sx16, a mammalian homologue of Tlg2p, has been proposed to also form a closed conformation (Burkhardt et al., 2008). The data presented here indicate that like these syntaxin homologues, Tlg2p also forms a closed conformation, which regulates its entry into SNARE complexes. Further to this, and in agreement with *in vivo* CPY trafficking studies (Bryant and James, 2001), a positive regulatory role for the SM protein Vps45p in SNARE complex assembly has been demonstrated. These experiments were published, (Struthers et al., 2009; Appendix III).

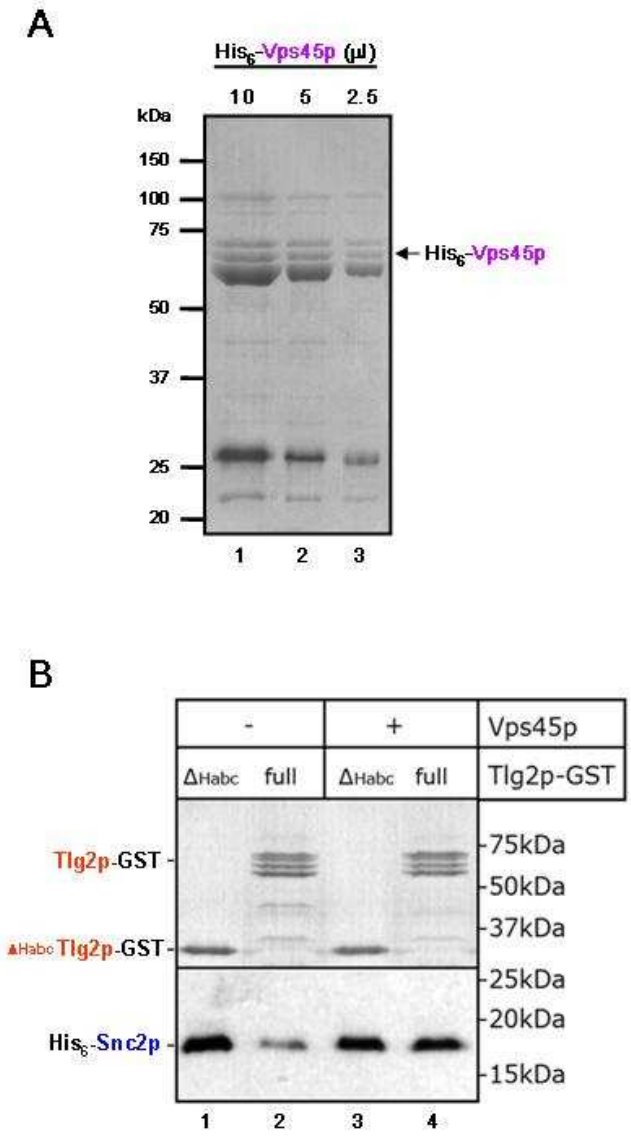

Figure 3.4 In vitro assay to assess complex assembly in presence of Vps45p

(A) Plasmid pNB710 was co-expressed with pT-GroE plasmid in *E coli* strain BL21 (DE3) to produce recombinant His_6-Vps45p in presence of GroEL and GroES chaperone proteins, as described in section 2.4.3.1. Three separate dilutions of protein were analysed on a 12% SDS-PAGE gel (Lanes 1 - 3) in order to estimate protein concentration. *(B)* The *in vitro* complex assembly assay was set up as described previously. 5 µl beads containing either full length or ΔHabc versions of Tlg2p were incubated in the presence of a 10 fold excess of the cognate SNARE partners His_6-Vti1p, His_6-Snc2p and untagged Sx8 / Tlg1p. These reaction mixtures were incubated for 20 minutes at 4^{o}C in the presence of absence of an 8 fold (to the cognate SNARE inputs) excess recombinant His_6-Vps45p. Protein was analysed, as before, by SDS-PAGE (upper panel) and immunoblot analysis using an α-Snc2p antibody (lower panel).

3.3.2 Yeast-2-hybrid assay

I set up a yeast-2-hybrid assay, a well characterised system to evaluate protein interactions (McAlister-Henn et al., 1999), in attempt to demonstrate an intramolecular interaction between the Habc domain and the SNARE domain of Tlg2p. The yeast-2-hybrid technique was developed in *S. cerevisiae* and is used to study protein-protein interactions (Fields and Song, 1989). The assay takes advantage of the native yeast protein Gal4p, which is a transcriptional activator encoded by a member of the family of *GAL* genes, all of which encode enzymes required for galactose utilization (Johnston, 1987). Gal4p is a large protein of 881 residues which activates transcription at specific upstream promoter DNA sequences of each *GAL* gene (Laughon and Gesteland, 1984). A relatively short N terminal domain of the protein is required to actually bind the upstream activating DNA sequence (Keegan et al., 1986), and another domain at the distal C terminus is responsible for the transcriptional activation of the *GAL* genes (Ma and Ptashne, 1987). In order to use the assay to test if two proteins interact, they are produced as fusions with the individual Gal4p domains responsible for DNA binding and transcriptional activation, and then subsequently expressed in a host yeast strain (Chien et al., 1991). The host strain contains a selective auxotrophic marker exclusively under the control of a *GAL* promoter; if the proteins interact, the reconstituted Gal4p domains induce transcription of the selective reporter gene. Yeast transformants capable of growth on selective media are then used to identify protein partners that interact. The principles of a yeast-2-hybrid assay are outlined in Figure 3.5.

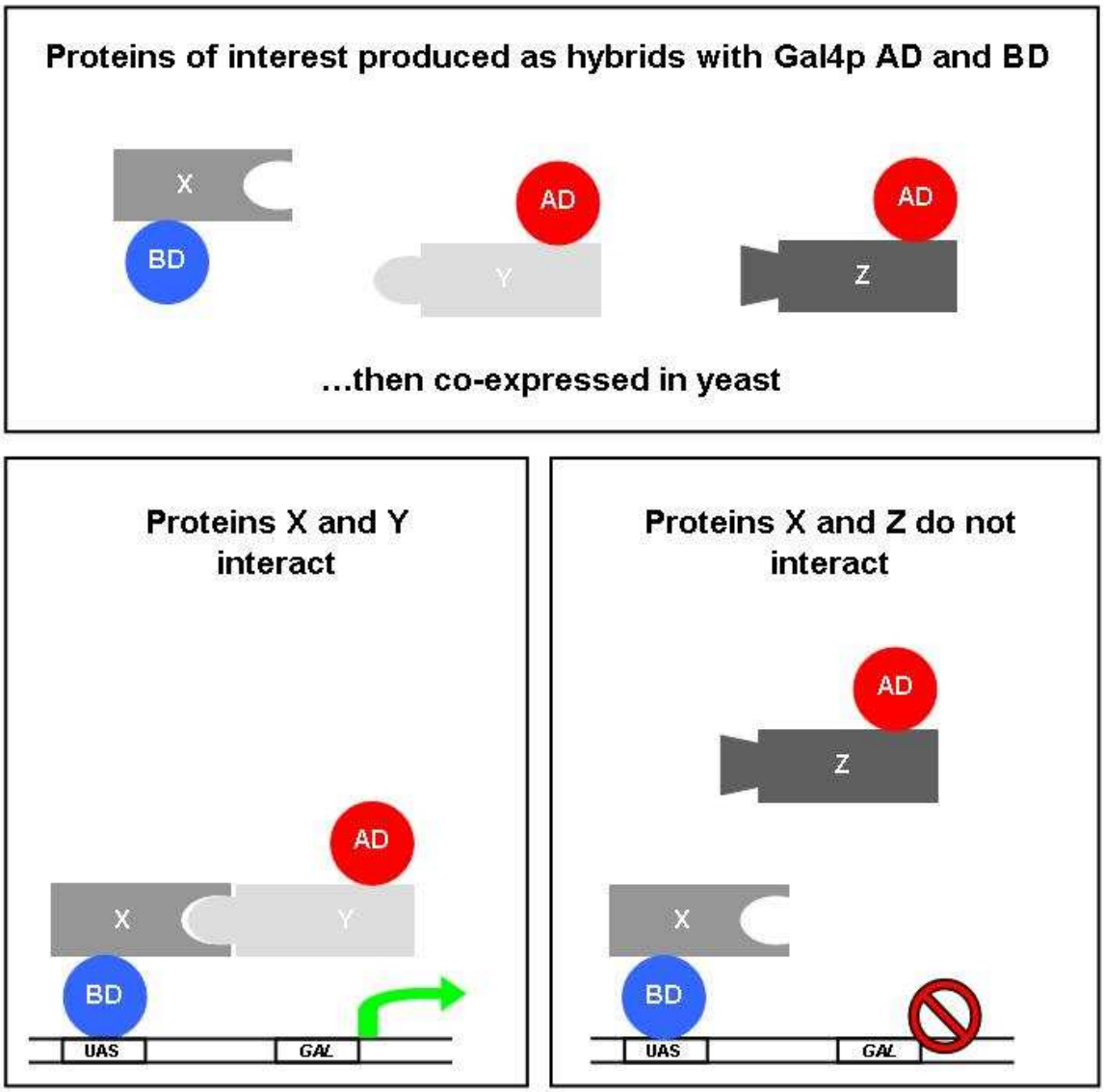

Figure 3.5 Principles of the yeast-2-hybrid assay

A yeast-2-hybrid assay that can detect possible interactions of protein X with either protein Y or protein Z. Protein X is expressed as a fusion with the DNA binding domain of Gal4p (blue), and proteins Y and Z are expressed as fusions with the Gal4p activation domain (red) in host yeast strain (upper panel). Protein X-BD fusion is co-expressed with either Y-AD (left panel) or Z-AD (right panel) fusion proteins; in each case protein X is localised to the upstream activating sequence (UAS) of a *GAL* promoter by the DNA binding domain. If proteins interact, such as X and Y (left panel), the Gal4p AD is in proximity of the promoter sequence, which induces transcription of a downstream reporter gene (green arrow). This reporter gene remains silent if proteins do not interact, as shown with X and Z (right panel). Yeast expressing the fusion proteins are then grown in a selective environment to ascertain whether the reporter gene has been activated.

The yeast-2-hybrid parent vectors pACT2 and pGBKT7, designed by Clontech Laboratories Inc, were used to produce a range of constructs for the assay. The former vector encodes residues 768 - 881 of the activating domain (AD) of the Gal4p protein, and the latter encodes residues 1 - 147 of the Gal4p DNA binding domain (BD). The coding sequences of either the Habc domain or the SNARE domain of Tlg2p were incorporated into the multiple cloning sites following the Gal4p domains in each vector. This allowed hybrid fusion proteins to be produced; fusions of each Tlg2p domain with both Gal4p domains were created. The assay is based on the yeast *S. cerevisiae* expressing two fusions proteins at the same time, the first is a Gal4p AD fusion, the second a Gal4p BD fusion. The plasmids encoding these fusion proteins were co-expressed in yeast strain AH109. Table 3.1 outlines the 8 co-transformation reactions carried out. Expression of the fusion proteins was confirmed by immunoblot analysis of all transformant cell lysates. Plasmids encoding an AD fusion protein also contain an influenza viral protein HA epitope sequence (YPYDVPDYA); Figure 3.6 shows all transformants expressing an AD fusion protein through expression of the HA epitope. BD fusion plasmids contain a cMyc epitope sequence (EEQKLISEEDL), for easy identification of fusion protein expression. Figure 3.7 shows all transformants expressing a BD fusion protein.

Transformant #	1st Transformation		2nd Transformation	
	Plasmid	Expressing	Plasmid	Expressing
1	pTD1-1	AD-HA-Large TAg	pGBK7-Lam	BD-myc-Lam C
2	pTD1-1	AD-HA-Large TAg	pGBKT7-53	BD-myc-p53
3	pTD1-1	AD-HA-Large TAg	pCMD020	BD-myc-Habc
4	pTD1-1	AD-HA-Large TAg	pCMD023	BD-myc-SNARE
5	pCMD019	AD-HA-Habc	pGBKT7-53	BD-myc-p53
6	pCMD019	AD-HA-Habc	pCMD023	BD-myc-SNARE
7	pCMD022	AD-HA-SNARE	pGBKT7-53	BD-myc-p53
8	pCMD022	AD-HA-SNARE	pCMD020	BD-myc-Habc

Table 3.1 Table of transformants for yeast-2-hybrid assay

The *S. cerevisiae* host strain AH109 was co-transformed with various combinations of Gal4p activating domain (AD) and DNA binding domain (BD) containing plasmids for the yeast-2-hybrid assay. The genetic sequence for both the Habc (residues 37 - 192) and the SNARE (residues 221 - 318) domains of Tlg2p were incorporated into both pACT2 and pGBKT7 to give fusions of each domain with either an activating or binding domain. The SNARE domain AD and BD fusions were co-transformed with Habc AD and BD fusions (transformants 16 & 18). Transformant 2 is an internal positive control containing plasmids encoding two proteins known to interact as fusions with the functional Gal4p domains. The other combinations are controls to ensure random components of the assay do not give positive reporter gene activation.

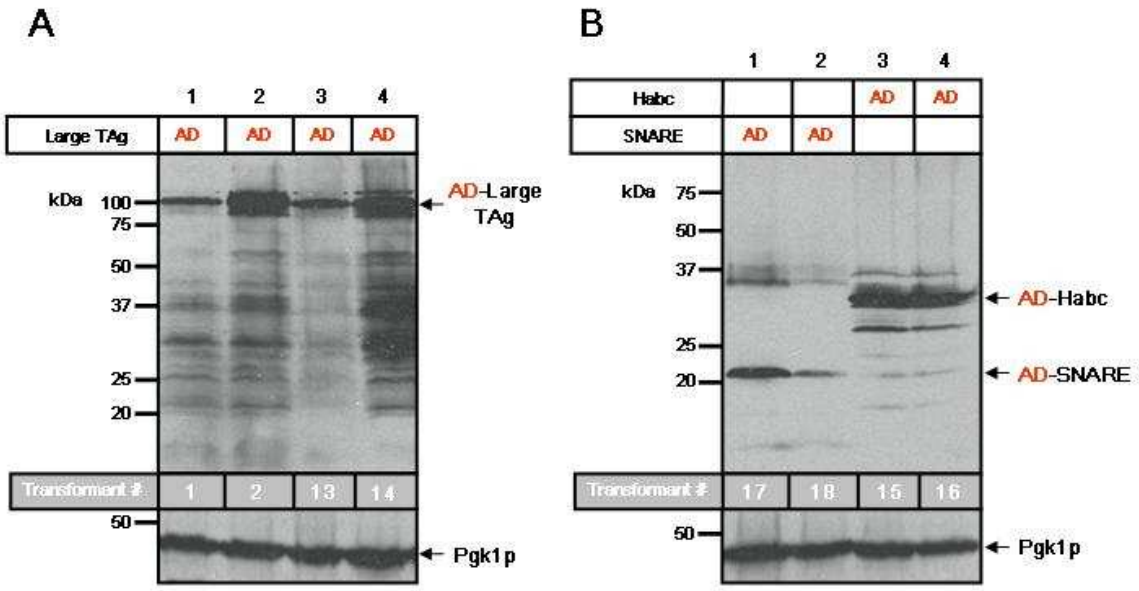

Figure 3.6 Expression of yeast-2-hybrid Gal4p AD fusion proteins

S. cerevisiae strain AH109 was co-transformed with plasmids encoding the Gal4p activating domain (AD; red) with our proteins of interest or control proteins (see Table 3.1), preceded by an HA tag. Equal number of cells from each transformant, equivalent to 10x OD_{600}, were resuspended in 100 µl 2x Laemmli sample buffer containing 8 M urea, then heated at 65°C for 10 minutes. 10 µl of each sample was separated by SDS-PAGE on a 12% gel, transferred to a nitrocellulose membrane and then subjected to immunoblot analysis to detect the fusion proteins using an α-HA antibody. *(A)* Upper panel shows transformants containing pTD1-1 (Clontech Laboratories Inc), used to express AD-SV40 large T antigen (residues 87 - 708) AD fusion protein of predicted molecular weight 83.3 kDa (Lanes 1 - 4). *(B)* Upper panel shows transformants containing plasmids pCMD022 and pCMD019, respectively expressing AD-SNARE, of predicted molecular weight 24.7 kDa; and AD-Habc, of predicted molecular weight of 31.2 kDa. Membranes were stripped and re-probed with an α-Pgk1p antibody to detect levels of the 44.7 kDa cytosolic enzyme, 3-phosphoglycerate kinase (Watson et al., 1982), as a loading control, shown in lower panels. The relative transformants from Table 3.1 are shown in the gray coloured boxes above each loading control. Molecular weight markers are indicated.

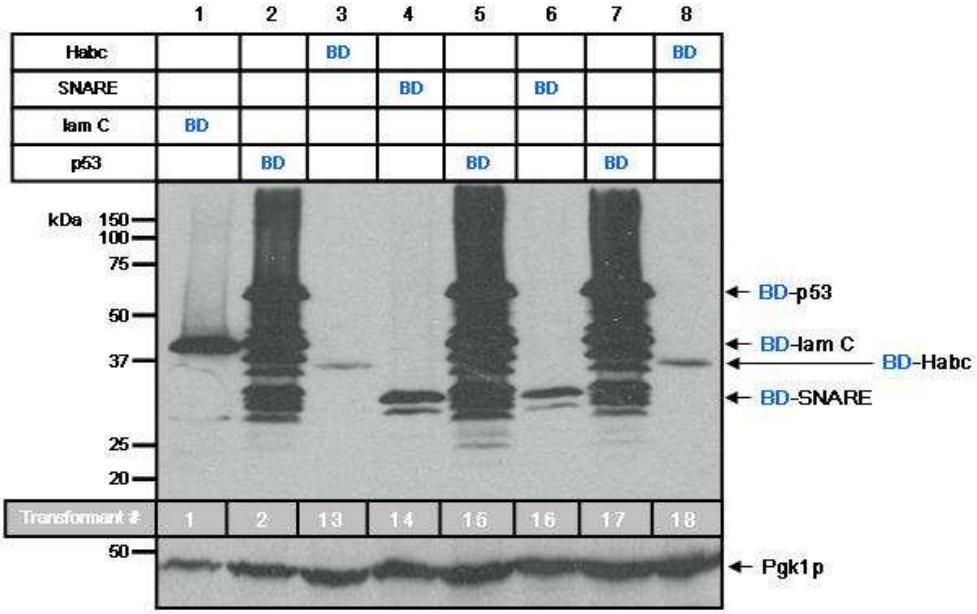

Figure 3.7 Expression of yeast-2-hybrid Gal4p BD fusion proteins

S. cerevisiae strain AH109 was co-transformed with plasmids encoding the Gal4p binding domain (BD; blue) fusions with our proteins of interest or control proteins (see Table 3.1), preceded by a cMyc tag. Equal number of cells from each transformant, equivalent to 10x OD_{600}, were resuspended in 100 µl 2x Laemmli sample buffer containing 8 M urea, and then heated at 65°C for 10 minutes. 10 µl of each sample was separated by SDS-PAGE on a 12% gel, transferred to a nitrocellulose membrane and then subjected to immunoblot analysis to detect the fusion proteins using an α-cMyc antibody. Upper panel shows transformants containing plasmids pGBKT7-Lam C, pGBKT7-53, pCMD023 and pCMD020, respectively used to express BD fusions of: human lamin C (residues 66 - 230), predicted molecular weight 35.7 kDa (Lane 1); p53 (residues 72 - 390), predicted molecular weight 52.8 kDa (Lanes 2, 5 & 7); Tlg2p SNARE domain (residues 221 - 318), predicted molecular weight 28.2 kDa (Lanes 4 & 6); and Tlg2p Habc domain (residues 37 - 192), predicted molecular weight 34.7 kDa (Lanes 3 & 8). Membranes were stripped and re-probed with an α-Pgk1p antibody to detect levels of the 44.7 kDa cytosolic enzyme, 3-phosphoglycerate kinase (Watson et al., 1982), as a loading control, shown in lower panel. The relative transformants from Table 3.1 are shown in the gray coloured box above the loading control. Molecular weight markers are indicated.

One important genotypic feature of strain AH109, which is a derivative of PJ69-2A (James et al., 1996), is that yeast cells cannot synthesise the amino acids leucine (leu) and tryptophan (trp); due to mutations in the *LEU2* (*leu2-3, 112*) and *TRP1* (*trp1-901*) genes, respectively. Successful transformants were identified by complementation of these auxotrophic markers. Transformants containing plasmids derived from pACT2 and pGBKT7 have the ability to grow on leucine and tryptophan synthetic drop out plates (as they carry the *LEU2* and *TRP1* auxotrophic markers, respectively). Transformants harbouring plasmids for both AD and BD fusion proteins can grow on media lacking both these amino acids (SD -leu, -trp). Figure 3.8 *(A)* shows each transformant streaked out on -leu, -trp plates. Figure 3.8 *(B)* shows the same transformants streaked out on plates also lacking histidine (SD -leu, -trp, -his). Interaction of the fusion proteins brings the two Gal4p domains into close proximity and triggers activation of the *GAL1* regulated histidine reporter gene (*HIS3*). Yeast capable of growing on histidine deficient plates *(B)* display intact Gal4p transcriptional activity, due to the BD fusion protein localising to the *GAL1* upstream activating sequence and interacting with the AD fusion protein, which subsequently triggers transcription of the gene. The positive control interaction between p53 and the SV40 large T antigen results in successful yeast growth on plates lacking histidine (transformant 2). The combination of BD-SNARE and AD-Habc did give activation of the histidine reporter gene (transformant 16), but unfortunately the BD-SNARE fusion also resulted in a positive reporter signal when co-expressed with the SV40 large T antigen (transformant 14). Taken together with the fact that absolutely no growth is detected with the opposite combination of AD-SNARE and BD-Habc on histidine lacking plates (transformant 18), we assume that the assay is not sensitive enough to detect an interaction between the domains, or that additional residues are necessary to stabilise an intramolecular Tlg2p interaction. It is worth noting that the effective concentrations of the two domains *in vivo*, where they exist on the same polypeptide, are considerably higher than we could create in the yeast-2-hybrid system.

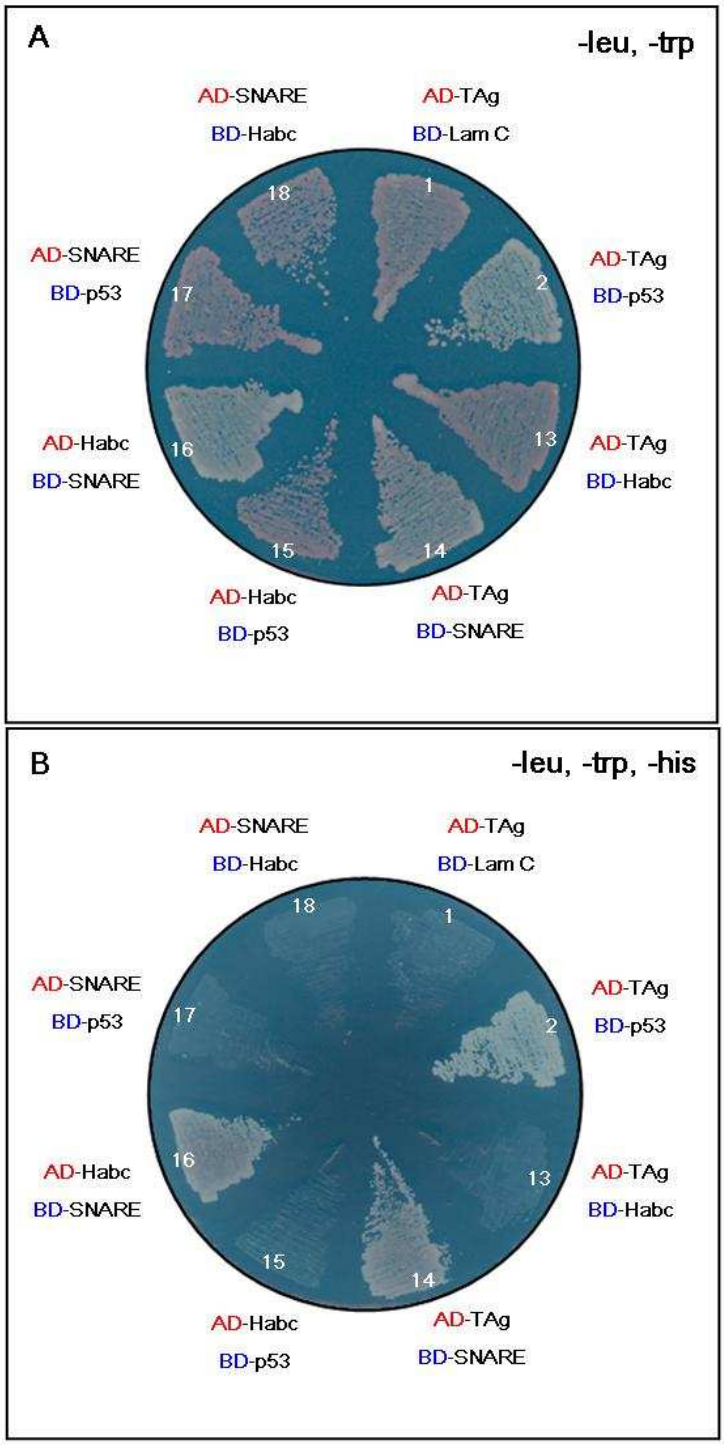

Figure 3.8 Yeast-2-hybrid assay

A single colony of each transformant (Table 3.1) was incubated in 10 ml liquid media lacking amino acids leucine and tryptophan (SD -leu, -trp) overnight at 30°C. Cells were then diluted to 0.2 OD_{600} in fresh SD -leu, -trp media and grown to mid log phase at 30°C. An equivalent volume of 1 ml cells at 0.8 OD_{600} were harvested by centrifugation at 1,000 *g* in a table top centrifuge. Cells were then resuspended in 1 ml dH_2O; 10 µl of each culture was then streaked out on selective plates lacking leucine and tryptophan (upper panel) and onto plates lacking leucine, tryptophan and histidine (lower panel). All plates were then incubated at 30°C and yeast growth was recorded after 5 days. Transformants relative to Table 3.1 are labelled on plates in white. Plates are representative of three individual co-transformation reactions.

3.3.3 Carboxypeptidase Y trafficking assay

The trafficking of newly synthesised CPY through the ER and Golgi to the vacuole is a well characterised biosynthetic pathway (Stevens et al., 1982). CPY is synthesised with a signal peptide that directs its translocation to the ER before cleavage, leaving a core glycosylated 67 kDa precursor protein (p1CPY) remaining (Hasilik and Tanner, 1978). p1CPY is modified by oligosaccharide trimming and addition as it traverses the Golgi, resulting in a 69 kDa p2CPY precursor of the active enzyme (Stevens et al., 1982, Trimble et al., 1983). p2CPY is then transported to the vacuole where it is cleaved by resident proteases to give the mature active 61 kDa enzyme, mCPY (Hasilik and Tanner, 1978). Perturbation of trafficking through the endosomal system results in the missorting of CPY and the subsequent secretion of p2CPY into the extracellular media (Rothman and Stevens, 1986). The CPY pathway, and the missorting of CPY in *vps* mutants, is outlined in Figure 3.9 *(A)*.

Deletion of either Vps45p or Tlg2p in yeast cells results in an obvious CPY secretion phenotype (Abeliovich et al., 1998, Cowles et al., 1994, Piper et al., 1994). However, it has been previously shown that abrogation of mode 2 binding between the hydrophobic pocket of Vps45p and the N terminal peptide of Tlg2p does not perturb the trafficking of CPY (Carpp et al., 2006), so we hypothesised that another binding mode between Tlg2p and Vps45p may be required for CPY sorting. As described earlier in this Chapter, a closed conformation would explain why full length Tlg2p can form SNARE complexes less readily than a version lacking the Habc domain *in vitro*, until Vps45p is added to relieve the kinetic delay. The yeast-2-hybrid analysis of the Habc and SNARE domains alone did not reveal a closed conformation, so we sought an *in vivo* approach to test this hypothesis.

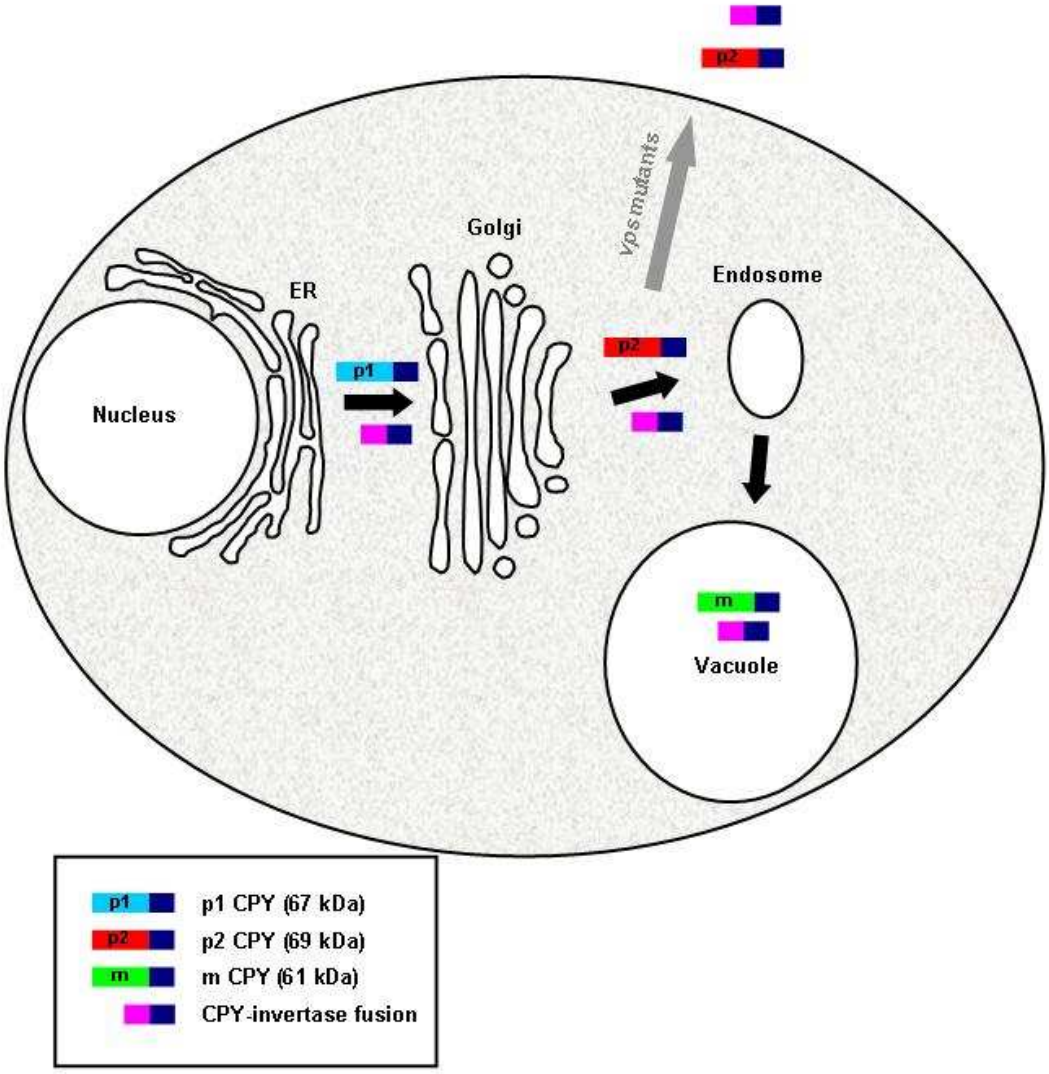

Figure 3.9 The CPY pathway & principles of the CPY-invertase secretion assay

(A) The CPY pathway is shown by the black arrows. The inactive enzyme precursor of CPY is synthesised in the nucleus. The N terminal portion of CPY, that is sufficient for the correct trafficking of the vacuolar hydrolyase through the pathway, is shown in dark blue. CPY is translocated into the endoplasmic reticulum (ER), where is modified to a 67 kDa p1CPY version (shown in light blue). p1CPY is then trafficked through the Golgi, where further post translational modifications generate the 69 kDa p2CPY (shown in red). p2CPY is then transported through the endosomal system to the vacuole, where it is cleaved to its final 61 kDa mature form, mCPY (shown in green). If trafficking in the endosomal system is perturbed by mutation of a key component in the pathway (*vps* mutants), cells secrete the p2CPY version (shown by the grey arrow). *(B)* The CPY-invertase secretion assay utilises a fusion containing the N terminal portion of CPY responsible for correct sorting of CPY (shown in dark blue) and the active element of the enzyme invertase (shown in pink); which is expressed in an *S. cerevisiae* that cannot synthesise native invertase. The substrate sucrose is used to identify the enzymatic activity of invertase. Total invertase activity is compared with activity exclusively in the extracellular fluid. Enzymatic activity of invertase in extracellular fluid is representative of a trafficking defect that has caused the CPY-invertase fusion protein to be missorted.

Sx1a is the best characterised example of a SNARE protein in a closed conformation (Dulubova et al., 1999). The isoleucine 233 residue of the SNARE domain of Sx1a is known to contact with the central cavity of Munc18a (Misura et al., 2000). Mutation of the analogous isoleucine residue to alanine (I236A) of Sx1a in *D. melanogaster* was shown to abolish affinity to its cognate SM protein, ROP (Wu et al., 1999). This mutation is thought to disrupt the closed conformation, thereby disallowing interaction with SM protein via mode-1 binding (Misura et al., 2000). ITC affinity calculations of mammalian Sx1a containing the isoleucine 233 to alanine (I233A) mutant dramatically reduce affinity to Munc18a (Burkhardt et al., 2008). The analogous mutation in Tlg2p, I285A, was created in order to investigate further the hypothesis that Tlg2p can form a closed conformation akin to that of Sx1a (Dulubova et al., 1999) *in vivo*. For this purpose $Tlg2p_{I285A}$, along with a mutant version unable to bind Vps45p via mode-2 binding ($Tlg2p_{F9A/L10A}$) and a version carrying all three mutations ($Tlg2p_{F9A/L10A/I285A}$) were created in a yeast expression vector, each with an N terminal HA tag. To test if these mutant versions of Tlg2p expressed in place of the wild-type protein *in vivo* resulted in any observable phenotype, a CPY-invertase assay was used (Darsow et al., 2000).

This assay uses a fusion of CPY and invertase, taking advantage of the cell's ability to correctly traffic the vacuolar hydrolase CPY and using invertase enzymatic activity to quantify any trafficking defects (Darsow et al., 2000). If the CPY pathway is perturbed by genetic mutation of a gene required for trafficking, (*vps* mutants; discussed in section 1.7.1), CPY is secreted from the cell as the precursor p2CPY (Bowers and Stevens, 2005). In cells lacking Tlg2p, (*tlg2Δ*), about 20% of the total CPY synthesised is secreted as the p2CPY precursor (Abeliovich et al., 1998). The basis of the assay, described by Darsow and colleagues (Darsow et al., 2000), is to replace endogenous invertase with a fusion protein containing the active element of invertase and the N terminal portion of CPY containing the information that targets the protein to the vacuole (Johnson et al., 1987). The enzymatic activity of invertase is measured as a total fraction and compared to that of the invertase secreted through its association with the CPY signal peptide. The basis of the assay is outlined in Figure 3.9 *(B)*. The enzymatic hydrolysis of sucrose by invertase results in the production of glucose, which is then oxidised by glucose oxidase. A by-product of this reaction is H_2O_2, which can be used by peroxidase to oxidise *o*-dianisidine resulting in a precipitate; absorbance of solution containing precipitate at A_{540} can be indirectly used to quantitatively assess extent of invertase activity (Darsow et al., 2000).

Figure 3.10 *(A)* shows SDS-PAGE analysis of yeast cell lysates from *tlg2Δ* strain SGSY2 expressing the relevant plasmids for wild-type Tlg2p and the mutants described above. An equal number of cells from each transformant were then used in the CPY-invertase assay as described in methods section 2.6; this experiment was performed in collaboration with Dr. Scott Shanks. The average invertase activity of each transformant from four separate experiments is presented in Figure 3.10 *(B)* as a histogram. From this we observe a basal level of ~5% CPY-invertase secretion from wild-type cells (Lane 1), which is increased to ~25% when secretion is measured in a strain lacking Tlg2p (Lane 2). This is in accordance with previously reported levels of CPY secretion in *tlg2Δ* cells being ~ 20% (Abeliovich et al., 1998). Reintroduction of Tlg2p expressed from plasmid pHA-Tlg2p (Seron et al., 1998) in *tlg2Δ* cells rescues the CPY-invertase secretion phenotype, with secretion of the CPY-invertase fusion reduced to ~10% (Lane 3). The rescued phenotype of ~10% CPY-invertase secretion by expression of wild-type Tlg2p in the *tlg2Δ* strain is also observed by introduction of mutant versions of Tlg2p. Introduction of mutant versions of Tlg2p harbouring either the I285A mutation (abrogated mode-1 binding) or the F9A/L10A mutation (abrogated mode-2 binding) into the assay results in the same levels of secretion as observed with wild-type (compare Lanes 3 with 4 & 5), this suggests that either binding mode is sufficient for Tlg2p function. It is unsurprising that the F9A/L10A mutant of Tlg2p, that abrogates binding via mode-2, does not block CPY-invertase trafficking, as previous experiments have demonstrated CPY could still be correctly trafficked in cells expressing a version of Vps45p incapable of interacting with Tlg2p via mode-2 binding (Carpp et al., 2006). Interestingly, when the triple mutant version of Tlg2p (F9A/L10A/I285A), which cannot bind to Vps45p via mode-1 or mode-2, is expressed in *tlg2Δ* cells, CPY is secreted at levels comparable with the *tlg2Δ* strain alone (Lane 5). This suggests that Tlg2p can facilitate trafficking to the vacuole by binding to Vps45p by either mode-1 or mode-2, but cannot function if both binding modes are perturbed. These experiments were published, (Furgason et al., 2009; appendix III).

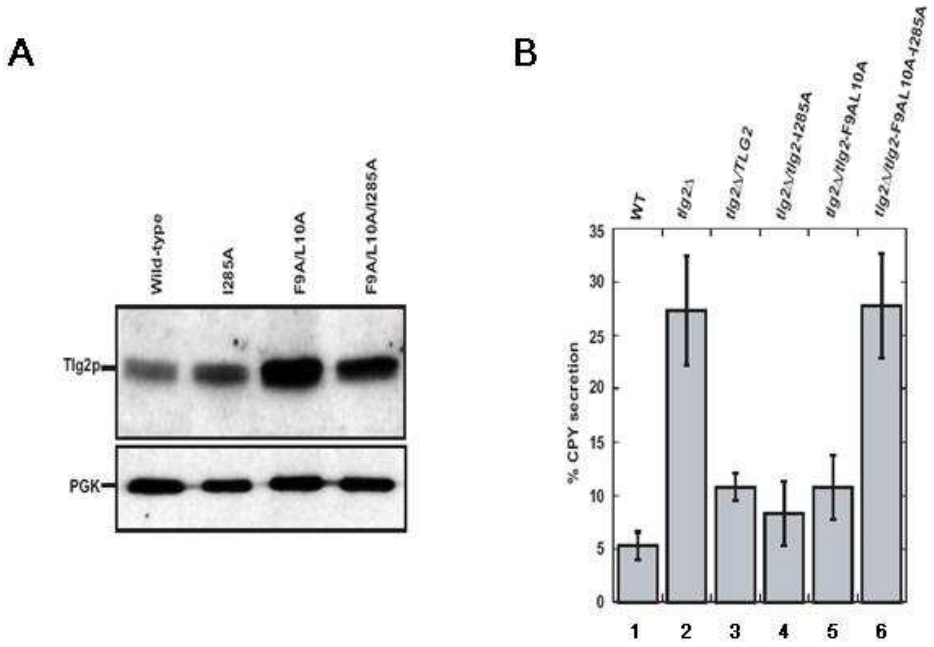

Figure 3.10 Carboxypeptidase Y- invertase trafficking assay

Wild-type (BHY10) and *tlg2Δ* (SGSY2) *S. cerevisiae* strains were used to express a fusion protein containing the first 50 amino acids of CPY and residues 3 - 512 of mature invertase. Both these strains lack endogenous invertase. *(A)* The *tlg2Δ* strain was transformed with the following plasmids: pHA-TLG2 to express wild-type HA-tagged Tlg2p; pCMD013, pCOG066 and pCMD011 to respectively express mutant HA-tagged versions $Tlg2p_{I285A}$, $Tlg2p_{F9A/L10A}$ and $Tlg2p_{I285A/F9A/L10A}$. Protein expression was checked by SDS-PAGE analysis of yeast cell lysates followed by immunoblot analysis using an α-Tlg2p antibody (upper panel). As a loading control, membranes were stripped and re-probed with an α-Pgk1p antibody (lower panel). *(B)* Equal numbers of cells were collected from each transformant / strain, topped up to 400 µl with sodium acetate buffer. Each sample was split into two aliquots, one of which was treated with 5 µl Triton X-100 to lyse the cells. 50 µl 0.5 M sucrose solution was then added to each sample and incubated at 30°C for 30 minutes. 300 µl 0.2 M K_2PO_4 pH 10.0 was added to each sample before boiling for 3 minutes in a water bath. Tubes were then chilled on ice before addition of glucostat reagent (3.5 mM K_2HPO_4, 80 units / ml glucose oxidase, 100 µg / ml Horse radish Peroxidase, 4 mM NEM, 6 mg / ml *o*-dianisidine), and a further incubation at 30°C for 30 minutes. Reactions were then stopped by addition of 2 ml 6 *N* HCl. The absorbance at A_{540} was then measured and lysed samples used to represent total cellular invertase activity, and unlysed samples to show secreted invertase activity. This experiment was performed by Dr. Scott Shanks.

3.4 Chapter summary

Using recombinantly produced SNARE proteins from the yeast endosomal system we have shown that a version of Tlg2p lacking the Habc domain forms SNARE complexes more readily than full length Tlg2p. Furthermore, we have demonstrated that the kinetic delay on complex assembly experienced by full length Tlg2p *in vitro* can be relieved by addition of recombinant Vps45p. This is in agreement with previous *in vivo* data suggesting Vps45p facilitates a conformational change in Tlg2p to accommodate SNARE complex assembly (Bryant and James, 2001). Also, as these experiments were performed *in vitro* with purified proteins, we have excluded the possibility that the inhibitory effect of full length Tlg2p is not via an unidentified factor in yeast (Dulubova et al., 2002). To test whether Tlg2p could form a closed conformation that prohibits complex formation, akin to that of Sx1a (Dulubova et al., 1999), we used two different approaches. The first was a yeast-2-hybrid assay, used in attempt to detect a Tlg2p intramolecular interaction. This was done by expressing the Habc and SNARE domains separately as Gal4p fusion proteins, and using their ability to reconstitute the transcriptional machinery of a reporter gene to signify an interaction. This assay was inconclusive as although a positive interaction was detected between the Habc and SNARE domains of Tlg2p, there was also reporter gene activation in a control transformant. It is possible that the yeast-2-hybrid technique is not sensitive enough to detect such an intramolecular interaction, or that the constructs we used did not have essential residues beyond the two domains that are necessary to stabilise an interaction. The second approach we used to investigate a closed conformation of Tlg2p was an *in vivo* assay to determine the ability of wild-type and mutant versions of Tlg2p to traffic a CPY-invertase fusion protein. To this assay we introduced mutant versions of Tlg2p abrogated in mode-1, mode-2 and both binding modes. The basis of this assay is that sorting defects cause the reporter fusion protein to be secreted. Extracellular invertase activity was compared to total activity, revealing the extent of CPY-invertase secretion in the various transformants. In a *tlg2Δ* strain, secretion of the reporter protein was elevated to ~25%. This phenotype could be rescued by addition of an HA-tagged version of wild-type Tlg2p, which reduced secretion to ~10%; these levels are similar to a wild-type strain used as a control. Introduction of $Tlg2p_{F9A/L10A}$, a mutant known to abrogate mode-2 binding, resulted in no effect on this reduced CPY-invertase secretion of ~10%. The same levels were again observed when $Tlg2p_{I285A}$, a mutant analogous to a Sx1a mutant incapable of binding Munc18a via mode-1 binding, was expressed in the *tlg2Δ* background. This suggests that abrogation of either mode-1 or

mode-2 binding of Vps45p does not result in a trafficking defect. Interestingly, when the triple mutant Tlg2p$_{F9A/L10A/I285A}$ was introduced into the *tlg2Δ* strain, the CPY-invertase secretion was elevated to ~25%, resembling levels of secretion observed in the *tlg2Δ* strain alone. This suggests that Vps45p can bind Tlg2p in a closed conformation, in a manner analogous to Sx1a, and that either this mode of binding or mode-2 binding is sufficient to facilitate proper trafficking through the cell. However, abrogation by mutation of both binding modes results in complete loss of Tlg2p function.

Chapter IV

Further Characterisation of the Vps45p-Snc2p Interaction

4.1 Introduction

Initial studies of SM proteins indicated that their regulatory role was carried out through interaction with the cognate syntaxin (Peng, 2005). The yeast syntaxin Sed5p, which regulates ER-Golgi (Hardwick and Pelham, 1992) and intra-Golgi (Holthuis et al., 1998) trafficking, binds its cognate SM protein Sly1p through the first identified example of mode-2 binding, through a short N terminal peptide of Sed5p (Yamaguchi et al., 2002). X-ray crystallography studies on Sly1p in complex with the N terminal peptide of Sed5p revealed that Sly1p has an arch shaped structure similar to that of Munc18a, but the central cavity plays no role in binding the Sed5p peptide (Bracher and Weissenhorn, 2002). This is in stark contrast to mode-1 binding where the SM protein Munc18a cradles the closed conformation of Sx1a in this cavity (Misura et al., 2000). Instead, for mode-2 binding, as defined by the Sly1p / Sed5p crystal structure, a small hydrophobic pocket on the exterior of domain I of Sly1p forms the sole point of interaction with the Sed5p N terminal peptide (Bracher and Weissenhorn, 2002).

Further studies on Sly1p revealed its capacity to bind non-syntaxin SNARE proteins: GST pulldown experiments were used to demonstrate that Sly1p could interact with the R-SNAREs Bet1p and Sft1p, as well as the non-syntaxin Q-SNAREs Bos1p and Gos1p (Peng and Gallwitz, 2004). The finding that SM proteins have the capacity to bind non-syntaxin SNARE proteins adds a new dimension to the unresolved issue of explaining SM protein function in membrane fusion. Like Sly1p, the syntaxin responsible for trafficking through the yeast TGN / endosomal system, Tlg2p, also binds its cognate SM protein Vps45p via a mode-2 interaction (Carpp et al., 2006, Dulubova et al., 2002). Tlg2p forms a functional SNARE complex with Vti1p, Tlg1p and the v-SNARE Snc2p (Bryant and James, 2001, Paumet et al., 2001). Investigations into the interaction of Vps45p with these non-syntaxin SNARE proteins revealed that recombinantly produced His_6 tagged Vps45p binds specifically to the cytosolic domain of Snc2p, but no interaction was detected between Vps45p and either Vti1p or Tlg1p (Carpp et al., 2006). Furthermore, the short N terminal domain of Snc2p preceding the SNARE domain is not required for its binding to Vps45p since a version lacking the N terminal peptide ($Snc2p_{\Delta 1\text{-}19}$) can be pulled down by Vps45p in a manner comparable to full length Snc2p; thus Vps45p binds directly to the SNARE motif of Snc2p (Carpp et al., 2006). These studies also demonstrated that Snc2p bound to Vps45p can be displaced by Tlg2p, but Snc2p cannot displace Tlg2p bound to Vps45p, even at high concentrations (Carpp et al., 2006). Very little is known about the

mechanism by which SM proteins interact with non-syntaxin SNAREs, and the functional relevance of these interactions remains to be elucidated.

4.2 Aims of this Chapter

The initial aim of this Chapter was to further study the interaction originally described between the SM protein Vps45p and the v-SNARE Snc2p (Carpp et al., 2006). I first set out to use a yeast-2-hybrid assay to confirm an interaction between Vps45p and Snc2p. The second approach used to confirm that Vps45p can form a complex with Snc2p was the more quantitative electrophoretic mobility shift assay (EMSA), which separates unbound protein from species in complex through a gel. Finally, we wanted to further investigate the capabilities of Tlg2p to displace Snc2p in complex with Vps45p.

4.3 Results

4.3.1 Yeast-2-hybrid assay

The principles behind the yeast-2-hybrid technique are discussed in detail in section 3.3.2 and outlined in Figure 3.5. The yeast-2-hybrid parent vectors pACT2 and pGBKT7 (Clontech Laboratories Inc), were utilised to produce the necessary constructs and controls to test for an interaction between Vps45p and Snc2p. In addition to confirming a protein-protein interaction between Snc2p and Vps45p, we wanted to design a reverse-2-hybrid screen (Vidal et al., 1996a) which could then be used to identify mutant versions of Vps45p that are unable to bind Snc2p, thereby allowing us to map residues involved with the interaction. To eliminate Vps45p mutants in the reverse screen that do not bind Snc2p due to the introduction of a premature stop codon, we created a construct containing a green fluorescent protein (GFP) sequence directly after the *VPS45* gene. The GFP sequence encodes a 26.9 kDa protein originally identified in the jellyfish *Aequorea Victoria* (Prasher et al., 1992), which can be used to detect gene expression and protein location in living organisms (Chalfie et al., 1994). A version of GFP containing a single residue mutation, serine 65 to threonine (GFP_{S65T}), was used; this mutation results in increased fluorescence and photostability (Heim et al., 1995). Detection of the GFP_{S65T} tag

would confirm that any mutant versions of Vps45p identified in the reverse screen were full length. For this reason AD and BD fusions of Vps45p containing a C terminal GFP_{S65T} tag were created during the course of this study (see Table 4.1).

Transformant #	1st Transformation		2nd Transformation	
	Plasmid	Expressing	Plasmid	Expressing
1	pTD1-1	AD-HA-Large TAg	pGBK7-Lam	BD-myc-Lam C
2	pTD1-1	AD-HA-Large TAg	pGBKT7-53	BD-myc-p53
3	pTD1-1	AD-HA-Large TAg	pCOG080	BD-myc-Snc2p
4	pTD1-1	AD-HA-Large TAg	pCOG082	BD-myc-Vps45p
5	pTD1-1	AD-HA-Large TAg	pCMD016	BD-myc-Vps45p-GFP
6	pCOG079	AD-HA-Snc2p	pGBKT7-53	BD-myc-p53
7	pCOG079	AD-HA-Snc2p	pCOG082	BD-myc-Vps45p
8	pCOG079	AD-HA-Snc2p	pCMD016	BD-myc-Vps45p-GFP
9	pCOG81	AD-HA-Vps45p	pGBKT7-53	BD-myc-p53
10	pCOG081	AD-HA-Vps45p	pCOG080	BD-myc-Snc2p
11	pCMD017	AD-HA-Vps45p-GFP	pGBKT7-53	BD-myc-p53
12	pCMD017	AD-HA-Vps45p-GFP	pCOG080	BD-myc-Snc2p

Table 4.1 Transformations of Saccharomyces cerevisiae strain AH109

The *S. cerevisiae* host strain AH109 was co-transformed with various combinations of Gal4p activating domain (AD) and DNA binding domain (BD) containing plasmids for the yeast-2-hybrid assay. There are 4 possible combinations for Snc2p expression with either Vps45p or a version containing a C terminal GFP_{S65T} tag (transformants 7, 8, 10 & 12). Transformant 2 is an internal positive control containing plasmids encoding two proteins known to interact as fusions with the functional Gal4p domains. The other 7 combinations are controls to ensure non-specific binding events are not responsible for any positive assay results.

4.3.1.1 Expression of Gal4p AD fusion proteins

The genetic sequences encoding the cytosolic domain of Snc2p and full length Vps45p were incorporated into the pACT2 vector (Clontech Laboratories Inc) before transformation into *S. cerevisiae* yeast strain AH109. A third construct was designed to place sequence encoding the GFP_{S65T} protein in frame at the C terminus of Vps45p, as discussed above. Expression of all fusion proteins in yeast was regulated by the *ADH1* promoter. The pACT2 vector also contains an influenza viral protein HA epitope sequence (YPYDVPDYA) which was used to check the expression of each fusion using an α-HA antibody. Figure 4.1 shows yeast cell lysates of transformants expressing: *(A)* AD-HA-Snc2p; *(B)* AD-HA-Vps45p and the fluorescently tagged version, AD-HA-Vps45p-GFP_{S65T}; *(C)* an AD-HA fusion with the Simian virus 40 (SV40) large T antigen (TAg), was included as an internal positive control for the assay.

4.3.1.2 Expression of Gal4p BD fusion proteins

The complimentary vector pGBKT7 (Clontech Laboratories Inc) containing the sequence for the Gal4p binding domain (BD) was used to create constructs containing cytosolic *SNC2* and full length *VPS45* genetic sequences. As with the pACT2 cloning procedure, we created a construct that incorporates the GFP_{S65T} sequence at the 3' end of the *VPS45* gene. Expression of all BD-containing fusion proteins was again regulated by the *ADH1* promoter. To allow easy detection of the expressed fusions, the pGBKT7 parent vector contains a *c-myc* proto-oncogene sequence, which encodes an epitope from the cMyc transcription factor (EEQKLISEEDL), at the N terminus of the protein encoded by the inserted gene. Figure 4.2 shows yeast cell lysates of all transformants containing BD-fusions that have been resolved by SDS-PAGE and subjected to immunoblot analysis to detect the cMyc peptide. Figure 4.2 *(A)* shows Snc2p and control BD fusion proteins. The BD-p53 fusion protein is a positive control as it interacts with the AD-SV40 large T antigen (Tag). The BD-lam C fusion protein is used as a negative control, as it does not bind to the SV40 large TAg. Figure 4.2 *(B)* shows BD-Vps45p and BD-Vps45p-GFP_{S65T} fusion proteins being expressed.

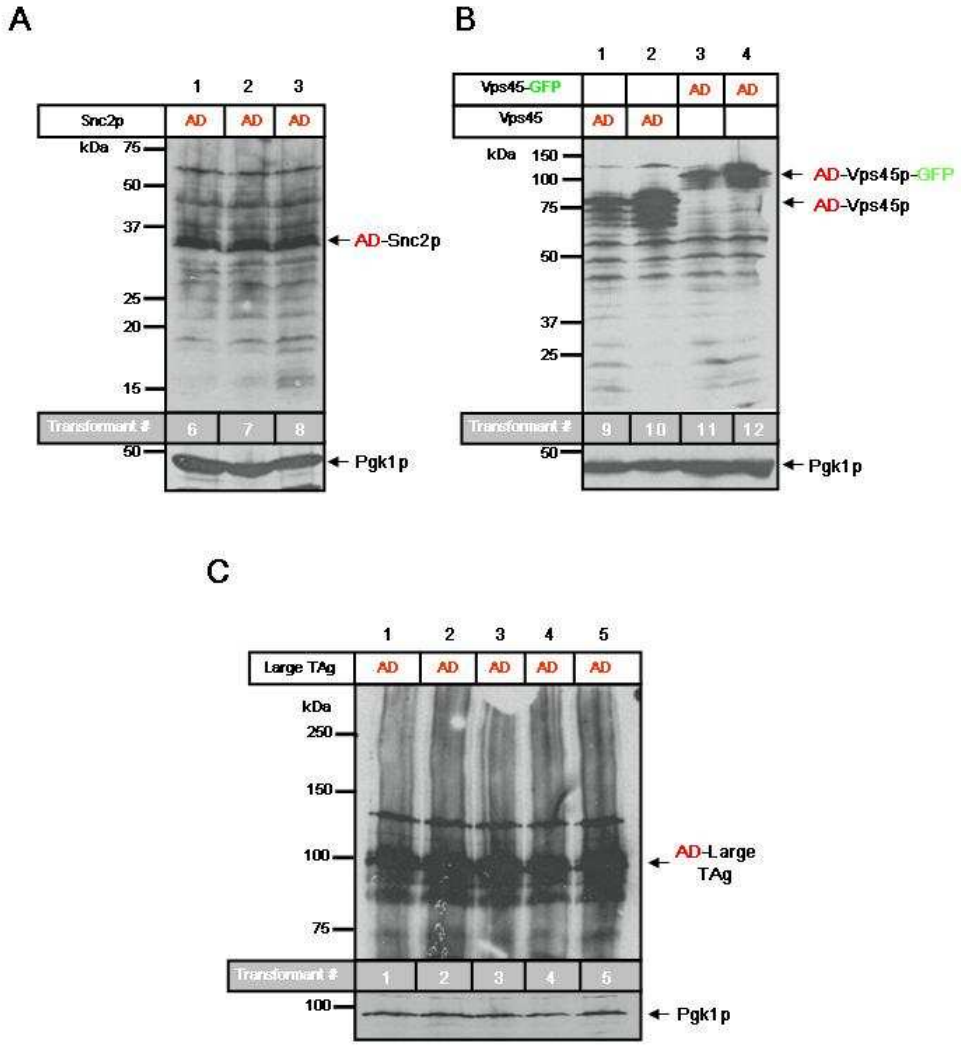

Figure 4.1 Expression of AD fusion proteins in yeast strain AH109

S. cerevisiae strain AH109 was transformed with plasmids encoding the Gal4p activating domain (AD) fusion harbouring our proteins of interest or controls (see Table 4.1), preceded by an HA tag. Equal number of cells equivalent to 10x OD_{600} were resuspended in 100 µl 2x Laemmli sample buffer containing 8 M urea, then heated at 65°C for 10 minutes. 10 µl of each sample was separated by SDS-PAGE (*(A)* 7.5%, *(B)* & *(C)* 10% gels), transferred to a nitrocellulose membrane then subjected to immunoblot analysis to detect the fusion proteins using an α-HA antibody. *(A)* Transformants containing pCOG079 were used to express AD-Snc2p at molecular weight 26.8 kDa (upper panel, Lanes 1-3). *(B)* Upper panel shows transformants containing plasmids pCOG081 and pCMD017, respectively expressing AD-Vps45p of predicted molecular weight 78.1 kDa (Lanes 1 & 2) and a GFP_{S65T} tagged version AD-Vps45p-GFP_{S65T} of predicted molecular weight 104.6 kDa (Lanes 3 & 4). Membranes were stripped and re-probed with an α-Pgk1p antibody (*(A)* & *(B)* lower panels) to detect levels of the 44.7 kDa cytosolic enzyme, 3-phosphoglycerate kinase (Watson et al., 1982), as a loading control. *(C)* Transformants containing positive control plasmid pTD1-1 (Clontech Laboratories Inc) was used to express AD-SV40 large T antigen (residues 87 - 708) fusion protein of predicted molecular weight 83.3 kDa (upper panel, Lanes 1 - 5). The membrane was then stripped and re-probed using an α-Vph1p antibody as a loading control showing expression of the 95.5 kDa vacuolar integral membrane protein Vph1p (Manolson et al., 1992) (lower panel). The relative transformants from Table 4.1 are shown in the gray coloured boxes above each loading control. Molecular weight markers are indicated.

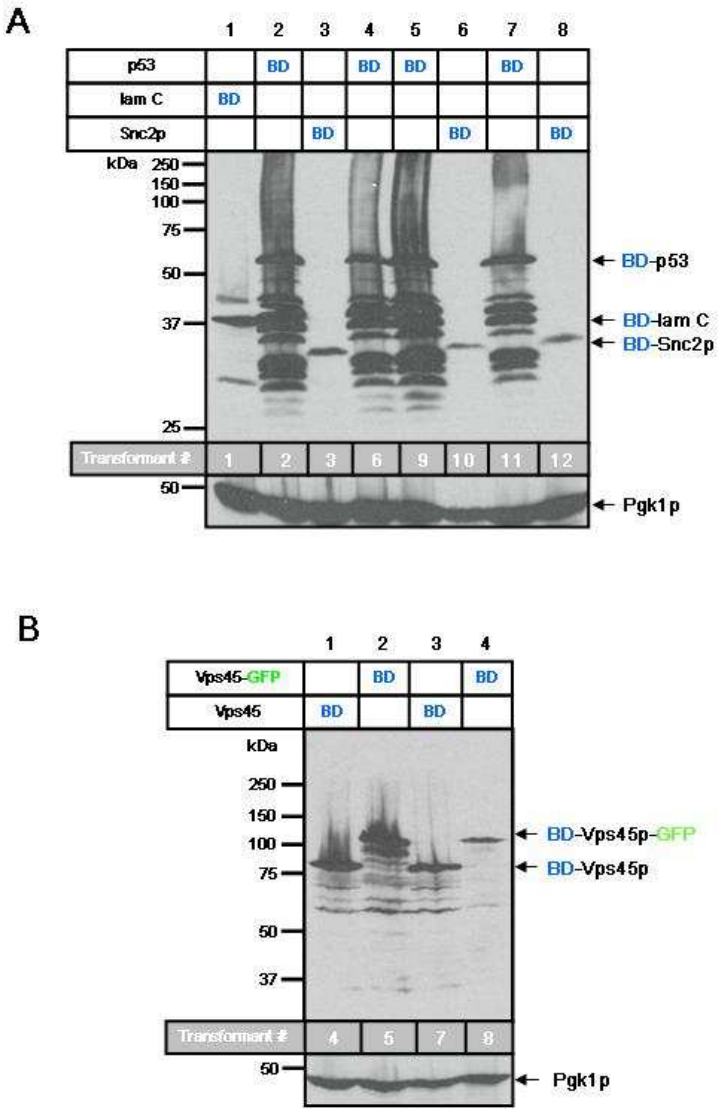

Figure 4.2 Expression of BD fusion proteins in yeast strain AH109

Strain AH109 harbouring an AD fusion plasmids were subsequently transformed with plasmids encoding the Gal4p BD fusion protein preceded by a cMyc epitope tag. An equal number of cells equivalent to 10x OD_{600} were resuspended in 100 µl 2x LSB containing 8 M urea, then heated at 65°C for 10 minutes. 10 µl of each sample was resolved on *(A)* 12%, *(B)* 10% gels by SDS-PAGE, before gels were transferred to a nitrocellulose membrane and immunoblot analysis with an α-cMyc antibody. *(A)* Control plasmids pGBKT7-Lam C and pGBKT7-53 were respectively used to express BD fusions of human lamin C (residues 66 - 230), predicted molecular weight 35.7 kDa (Lane 1) and p53 (residues 72 - 390), predicted molecular weight 52.8 kDa (Lanes 2,4,5 & 7). Yeast expressing pCOG080 produced BD-Snc2p fusion protein of predicted molecular weight 30.3 kDa (Lanes 3,6 & 8). *(B)* Transformants containing plasmids pCOG082 and pCMD016 produced proteins of 81.6 and 108.1 kDa, respectively representing BD-Vps45p and BD-Vps45p-GFP_{S65T} fusions. Membranes from *(A)* & *(B)* were stripped and re-probed with an α-Pgk1p antibody, showing expression of Pgk1p at 45.7 kDa as a loading control. The relative transformants from Table 4.1 are shown in the gray coloured boxes above each loading control. Molecular weight markers are indicated.

4.3.1.3 Yeast-2-hybrid assay in strain AH109

The various transformations (outlined in Table 4.1) were carried out in the *S. cerevisiae* strain AH109. As described in Chapter III, the yeast strain AH109 has mutations that prevent it from growing in media lacking the amino acids leucine, tryptophan and histidine. This characteristic was used to isolate successful transformations that contain AD and BD fusion plasmids, conferring ability to grow on media lacking leucine and tryptophan respectively. Figure 4.3, upper panel shows that the 12 double transformations required have been successful, as demonstrated by their ability to grow on the leucine and tryptophan deficient selective media (SD -leu-trp), even at $^{1}/_{10}$ and $^{1}/_{100}$ dilution.

Strain AH109 is incapable of producing histidine, due to the *his3-200* mutation in the *HIS3* gene, and therefore will not grow in media lacking this amino acid (-his). The strain does however have a functional histidine (*HIS3*) reporter gene under the control of the *GAL1* promoter, which is the basis for the assay. Transformants grown on SD -leu -trp media above were also spotted out in serial dilution on SD -leu -trp -his selective plates. Growth on these plates demonstrates that the expressed fusion proteins interact, thus reconstituting the functional Gal4p transcriptional machinery at the upstream activating sequence of the *GAL1* promoter, resulting in activation of the histidine reporter gene. Figure 4.3, lower panel shows the transformants ability to grow on SD -leu -trp -his selective media. Transformant 2 (Lane 2), containing positive control fusions of AD-SV40 and BD-p53 shows growth at all dilutions, reflecting the strong interaction of the fusions triggering activation of the reporter gene. None of the negative control transformants show any growth on histidine selective plates (Lanes 1, 3, 4, 5, 6, 9 & 11), showing that non-specific binding between our proteins of interest and the other components of the assay are not responsible for activation of the histidine reporter gene. Vps45p and Snc2p can be seen to interact with each other regardless of which Gal4p domain they are produced as fusions with (Lanes 7 & 10). The addition of a C terminal GFP_{S65T} tag to Vps45p appears to reduce the efficiency of the interaction somewhat (compare Lane 7 with 8 & 10 with 12), but a level of reporter gene activation is detectable, suggesting this would be a viable system to use in a reverse screen for mutant versions of Vps45p that do not interact with Snc2p.

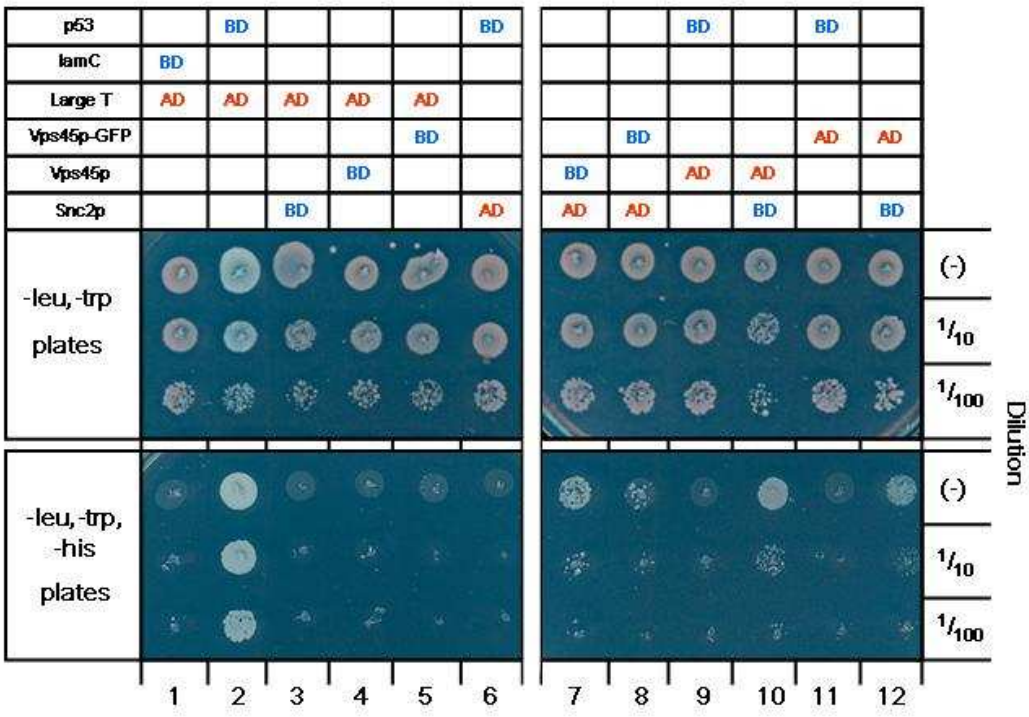

Figure 4.3 Yeast-2-hybrid assay

A single colony of each transformant (Table 4.1) was incubated in 10 ml liquid SD minimal media lacking amino acids leucine and tryptophan (SD -leu, -trp) overnight at 30°C. Cells were then diluted to 0.2 OD_{600} in fresh SD -leu, -trp media and grown up to mid log phase at 30°C. An equivalent volume of 1 ml cells at 0.8 OD_{600} were harvested by centrifugation at 1,000 *g* in a table top centrifuge. Cells were then resuspended in 1 ml dH_2O and a ten-fold serial dilution was created. 5 µl of each dilution was then spotted out onto selective plates lacking leucine and tryptophan (upper panels) and onto plates lacking leucine, tryptophan and histidine (lower panels). All plates were then incubated at 30°C and yeast growth was recorded after 5 days. Plates are representative of three individual co-transformation reactions, each spotted multiple times on selective plates.

4.3.1.4 Expression of C terminal GFP_{S65T} tag

The results presented in Figure 4.3 demonstrate that a version of Vps45p containing a GFP_{S65T} tag at the C terminus is capable of interacting with Snc2p, as detected by the yeast-2-hybrid technique. To check that this version of Vps45p expresses the fluorescent tag, all transformants containing the C terminal GFP_{S65T} sequence were grown to mid-log phase before being fixed and imaged under a microscope. Figure 4.4 shows fluorescence microscopy at 100x magnification of yeast transformants expressing GFP_{S65T}, both brightfield (left panels) and fluorescent (right panels) images are shown. Figure 4.4 *(A)*

shows the transformants expressing AD-Vps45p-GFP_{S65T} show fluorescence with diffuse GFP_{S65T} detected throughout the cell, with most of the GFP accumulated in a small compartment in each cell. Figure 4.4 *(B)* shows images of cells expressing BD-Vps45p-GFP_{S65T}, here both transformants display a similar distribution of GFP_{S65T} labelled Vps45p as with the AD fusions. As a control, cells from other transformants containing unlabelled Vps45p (transformants 5, 7, 9 & 10) were imaged under the same conditions, but no fluorescence could be detected. These data demonstrate that both constructs can be used to successfully produce versions of Vps45p expressing a detectable C terminal GFP_{S65T} tag.

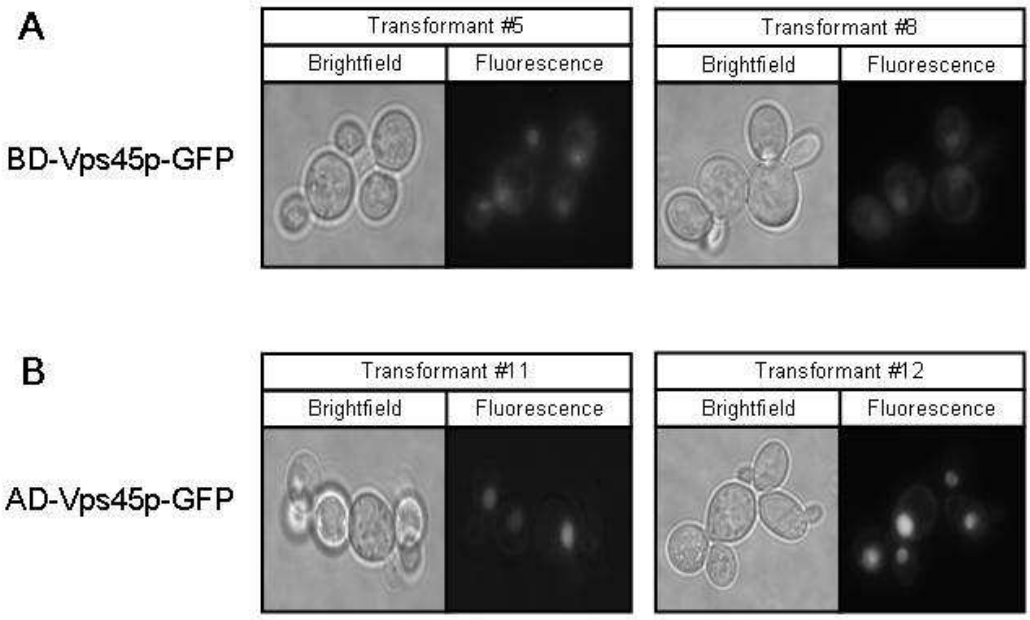

Figure 4.4 GFP_{S65T} expression in strain AH109

Transformants expressing Vps45p with a C terminal GFP tag (5, 8, 11 & 12) were grown to mid-log phase before being fixed with 3% formaldehyde and imaged through an 100x oil immersion objective on a Zeiss Axiomat fluorescence microscope (Carl Zeiss, Germany). Brightfield images were recorded at 15 ms exposure (left panels) and fluorescent images at 1.2 s (right panels). The fluorescence images were recorded *(A)* Transformants 5 and 8 expressing GFP fluorescence from BD-Vps45p-GFP_{S65T}. *(B)* Transformants 11 and 12 expressing GFP fluorescence from AD-Vps45p-GFP_{S65T}.

4.3.2 Electrophoretic mobility shift assay

The electrophoretic mobility shift assay (EMSA) relies on the altered mobility of a molecule through a gel upon binding with a partner molecule. It was originally developed to identify DNA binding proteins (Fried and Crothers, 1981, Garner and Revzin, 1981), but has more recently been adapted to investigate protein-protein interactions (Park and Raines, 1997). The protein of interest is labelled to allow its detection in a native gel. Progress of unbound labelled protein is monitored through the gel and compared to the progress of protein samples pre-incubated with the proposed binding partner. If the proteins form a complex there is a detectable change in the mobility of the labelled species.

We wanted to use this technique to investigate the interaction between Vps45p and Snc2p. The experimental design for these experiments is outlined in Figure 4.5. Firstly, Vps45p and the cytosolic domain of Snc2p were expressed in *E. coli* and then extensively purified in order to obtain pure and concentrated samples. This was achieved using 3 independent chromatographic steps, separating our expressed proteins from impurities according to: affinity for the specific resin, charge (ion exchange) and size (gel filtration). Finally, samples were concentrated using centrifugal filtration devices. To account for the loss of protein during each of these steps, initial culture volumes were increased appropriately. A ninhydrin assay (Rosen, 1957) was used to give an accurate estimate of final protein concentrations before the labelling and binding reactions were calculated. We chose the Alexa 488 fluorophore to label the cytosolic domain of Snc2p, to allow us to detect its progress through a gel.

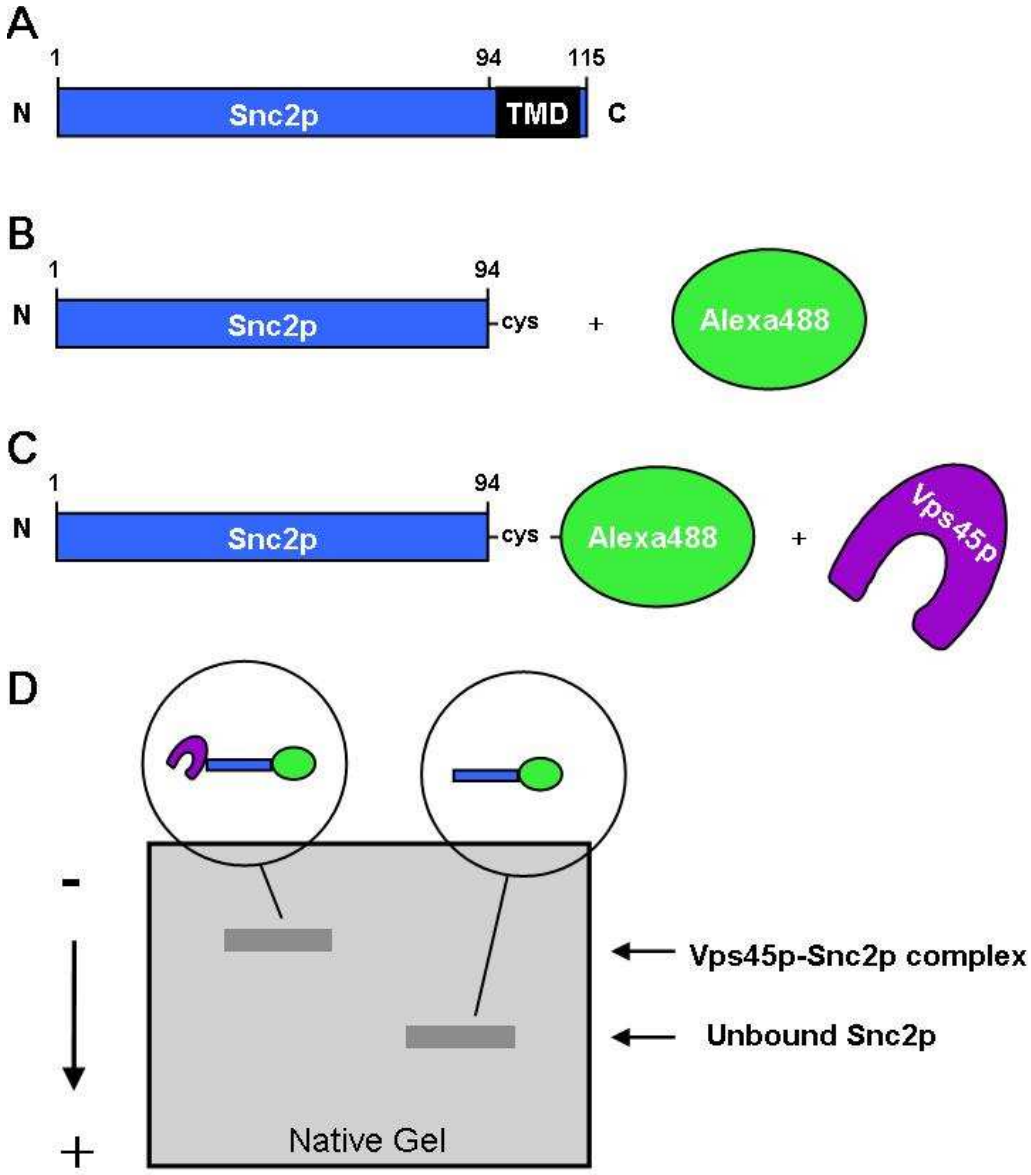

Figure 4.5 Schematic diagram of experimental design for the EMSA assay

(A) Full length Snc2p protein (blue), containing cytosolic N terminal residues 1 - 95, including the SNARE motif. The additional C terminal residues, (96 - 115) make up the hydrophobic transmembrane domain. *(B)* Production of a truncated Snc2p protein, containing cytosolic residues 1 - 94. Note that the 94th residue of Snc2p is the protein's only native cysteine residue. $Snc2p_{1\text{-}94}$ incubated with the thiol-reactive Alexa 488 fluorophore (green) which covalently binds to the cysteine residues of $Snc2p_{1\text{-}94}$. Labelled species is then isolated from excess Alexa 488 fluorophore by size exclusion chromatography. *(C)* Labelled $Snc2p_{1\text{-}94}$ is then incubated with Vps45p to allow them to bind; varying concentrations of proteins can be used for each reaction. A control reaction containing no Vps45p is also prepared. (*D)* Binding reactions are then analysed by native gel electrophoresis followed by scanning in a phosphorimager to detect Alexa 488 fluorescence; only labelled protein will be detected. On the right hand side of the gel the mobility of the control reaction containing only $Snc2_{1\text{-}94}$ bound to Alexa 488 is shown. If the binding reaction containing Vps45p and labelled $Snc2p_{1\text{-}94}$ results in formation of a complex, it will have an altered mobility in the gel compared to the control reaction containing only labelled $Snc2p_{1\text{-}94}$. Consequently, complexes can be identified by their slower mobility through the gel, where they run higher, as shown on the left hand side of the gel.

4.3.2.1 Expression and purification of Vps45p

Vps45p containing an N terminal His_6 tag was expressed in BL21 (DE3) *E. coli* cells from the plasmid pNB710 (Carpp et al., 2006). Co-production of the chaperone proteins GroEL and GroES was induced at the same time from the pT-GroE plasmid (Yasukawa et al., 1995; described in more detail in Chapter V, section 5.4.1.4). Proteins were induced with IPTG overnight at a reduced temperature of 15^{o}C. A sample taken from each step in the purification process was analysed by SDS-PAGE and visualised by Coomassie staining, as shown in Figure 4.6. The single band product of the Vps45p purification runs at its predicted molecular weight of 67.0 kDa.

4.3.2.2 Expression and purification of $Snc2p_{1-94}$

A truncated version of Snc2p lacking the transmembrane domain was expressed as a GST fusion protein from plasmid pMM472. Residues 1 - 94 were expressed, to allow the native cysteine at position 94 to be utilised in the subsequent application of labelling. The protein was expressed in BL21 (DE3) *E. coli* cells and purified as outlined in section 2.3.4.2. Figure 4.7 shows a Coomassie stained gel of samples from each step in the purification process after analysis by SDS-PAGE. The Snc2p truncation was cleaved from the N terminal GST tag after the affinity purification step using an optimal concentration of Factor X, determined by a trial cleavage with a range of protease concentrations, shown in Figure 4.8 *(A)*. A 1:500 dilution (Lane 8) was deemed the optimal concentration; although a large proportion of $Snc2p_{1-94}$-GST is not cleaved at this dilution, the protein that results from cleavage has a single band product. Figure 4.8 *(B)* shows a Coomassie stained gel of the final concentrated sample after the cleaved product had been further purified by ion exchange and gel filtration chromatography.

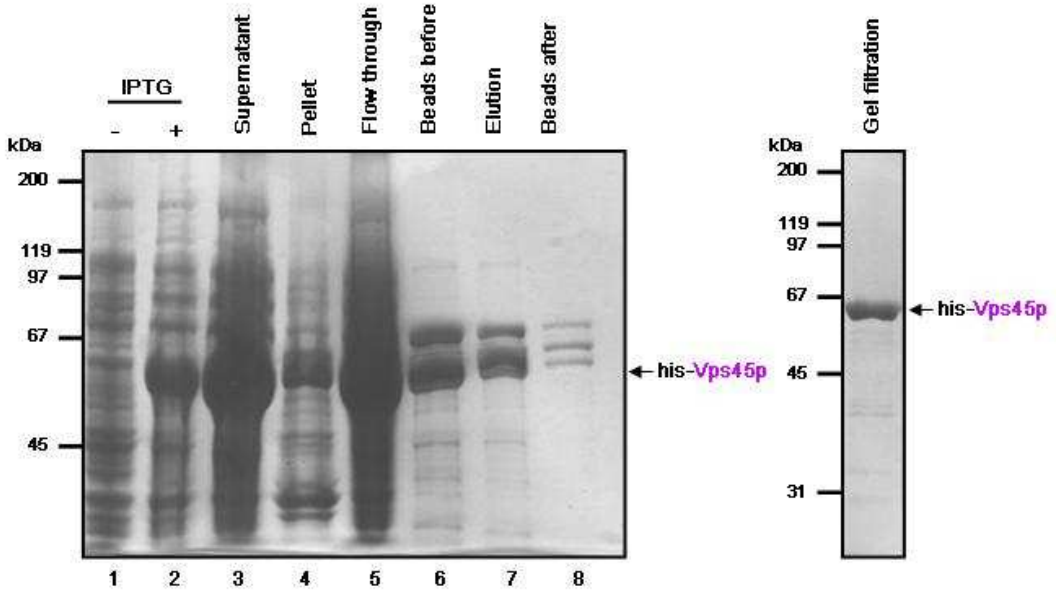

Figure 4.6 Expression and purification of Vps45p

Plasmid pNB710 was used to produce a recombinant His_6 tagged version of Vps45p; the plasmid was transformed into BL21 (DE3) cells already containing plasmid pT-GroE, which expresses the *E. coli* chaperone proteins GroEL and GroES. Purity of protein was analysed at various stages by SDS-PAGE on a 10% gel followed by Coomassie staining (left panel). Protein expression was induced overnight at 15^{o}C by addition of 0.5 M IPTG (Lanes 1 & 2; 7.5 µl each). Protein was expressed and purified from 10 L of culture as outlined in methods section (2.3.4.1). Soluble protein (Lane 3; 7.5 µl) was bound to 5 ml of washed Ni^{2+}-NTA beads for 1 hour. The amount of protein lost as insoluble protein (Lane 4; 7.5 µl) and not bound to column (Lane 5; 7.5 µl) is shown. Protein bound to beads (Lane 6; 7.5 µl) was eluted from column with buffer containing 250 mM imidazole. Eluted protein was then bound to a Mono Q (10 / 10) ion exchange column and eluted with an increasing NaCl concentration gradient. There were 3 absorbance peaks at A_{280}, fractions containing Vps45p were identified by SDS-PAGE then pooled and concentrated to approximately 6 mls. Concentrated protein was then loaded onto a Superdex 200 (16 / 60) gel filtration column. Again, fractions of interest were analysed by SDS-PAGE on a 12% gel and fractions containing purest samples of Vps45p (right panel; 10 µl) were pooled and concentrated, before snap freezing in liquid nitrogen. Positions of molecular weight markers are indicated.

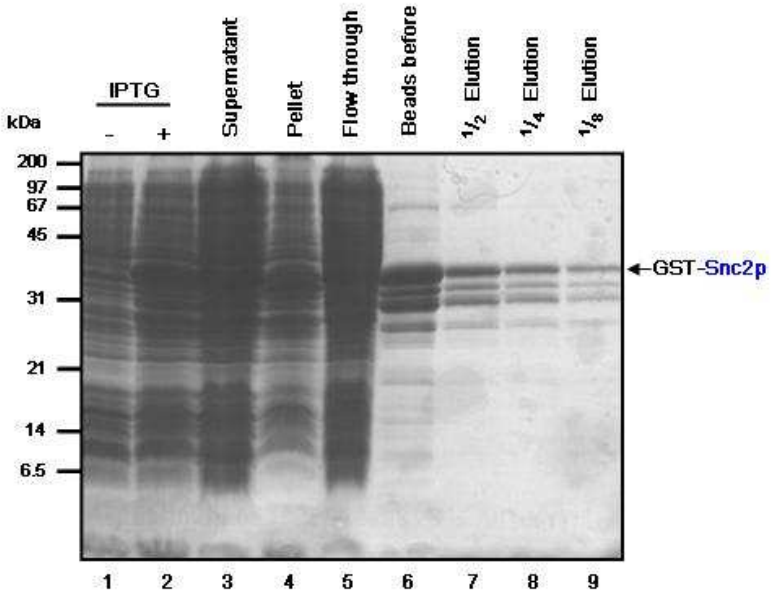

Figure 4.7 Expression and purification of Snc2p$_{1-94}$

Plasmid pMM472 was used to recombinantly produce a truncated version of Snc2p containing the first 94 N terminal residues. The protein was expressed as a GST fusion protein, and then purified from 10 L of culture as outlined in methods section (2.3.4.2). Purity of protein was analysed at various stages by SDS-PAGE on a 15% gel followed by Coomassie staining. Protein expression was induced by addition of 1 M IPTG for 2 hours at 37^{o}C (Lanes 1 & 2; 7.5 µl of each). Soluble protein (Lane 3; 7.5 µl) was bound to 5 ml Glutathione Sepharose 4B beads for 1 hour. The amounts lost as insoluble protein (Lane 4; 7.5 µl) and not bound to column (Lane 5; 7.5 µl,) are shown. Protein was eluted from beads with buffer containing 25 mM reduced glutathione, the elution was then diluted by $^{1}/_{2}$, $^{1}/_{4}$ and $^{1}/_{8}$ (Lanes 7 - 9; 5 µl each), before SDS-PAGE analysis. Positions of molecular weight markers are indicated.

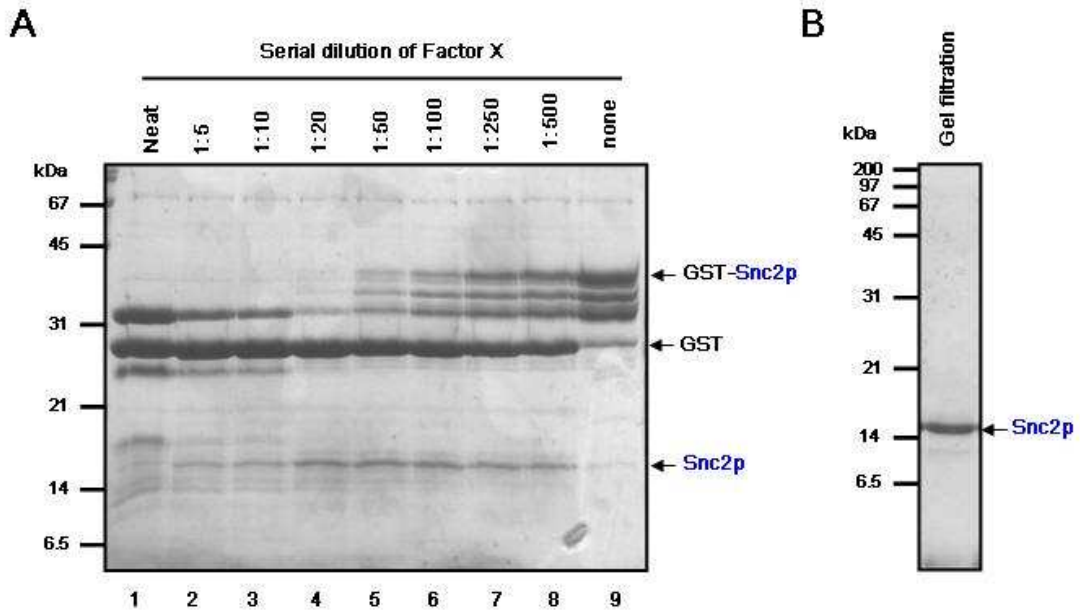

Figure 4.8 Further purification of Snc2p$_{1-94}$

(A) A trial cleavage of GST from Snc2p was set up with 2.5 µl of eluted protein and 2 µl of Factor X (or a serial dilution thereof) and allowed to cleave at 4^{o}C for 18 hours. 5 µl of each dilution was then analysed by SDS-PAGE on a 15% gel (Lanes 1 - 8; 5 µl each), including a sample incubated in same conditions with no factor X (Lane 9; 5 µl). A 1:500 dilution of Factor X was estimated to be the optimal concentration for cleavage and used to cleave Snc2p from GST in remainder of sample. Protein was then bound to a Mono S (5 / 5) ion exchange column and eluted with an increasing NaCl concentration gradient. Fractions containing Snc2p$_{1-94}$ were identified by SDS-PAGE then pooled and concentrated to approximately 3 mls. Protein was then loaded onto a Superdex 75 (16 / 60) gel filtration column. *(B)* Fractions displaying high absorbance peaks at A$_{280}$ were analysed by SDS-PAGE on 15% gel and elutions containing purest samples of Snc2p$_{1-94}$ (right panel; 15 µl) were pooled and concentrated before snap freezing in liquid nitrogen. Positions of molecular weight markers are indicated.

4.3.2.3 Labelling Snc2p1-94 with Alexa 488 fluorophore

I took advantage of the unique native cysteine in the cytosolic Snc2p, found at residue 94, to covalently bind the thiol-reactive Alexa Fluor® 488 C5 maleimide (Invitrogen) label. Cysteine contains the nucleophillic thiol side chain group, which is easily oxidized and ideal for this application. A binding reaction was set up with purified $Snc2p_{1-94}$ and a 15 fold molar excess of the Alexa 488 fluorophore. All buffers used in the labelling procedure contained TCEP as a reducing agent, in place of DTT, as it does not interfere with the attachment of thiol-reactive probes (Getz et al., 1999). The reaction mixture was left for 3 hours at room temperature to allow the Alexa 488 fluorophore to bind the reduced cysteine residues of the cytosolic version of Snc2p, before being passed over a gel filtration column. This process allows the labelled $Snc2p_{1-94}$ to be separated from the excess fluorophore and TCEP, shown in Figure 4.9 *(A)*. The fractions collected from the gel filtration column were analysed on a 15% gel by SDS-PAGE and then viewed in a phosphorimager under a blue laser at 433 nm. This demonstrates that Alexa 488 labelled $Snc2p_{1-94}$ can be visualised from the gel, shown in Figure 4.9 *(B)* lower panel. After imaging, the SDS-PAGE gel was stained with Coomassie blue, shown in Figure 4.9 *(B)* upper panel. $Snc2p_{1-94}$ fractions that have been successfully labelled with Alexa 488 are seen to run at a higher molecular weight than the unlabelled sample of purified $Snc2p_{1-94}$ (compare Lane 1 with Lanes 4, 5, 6 & 7).

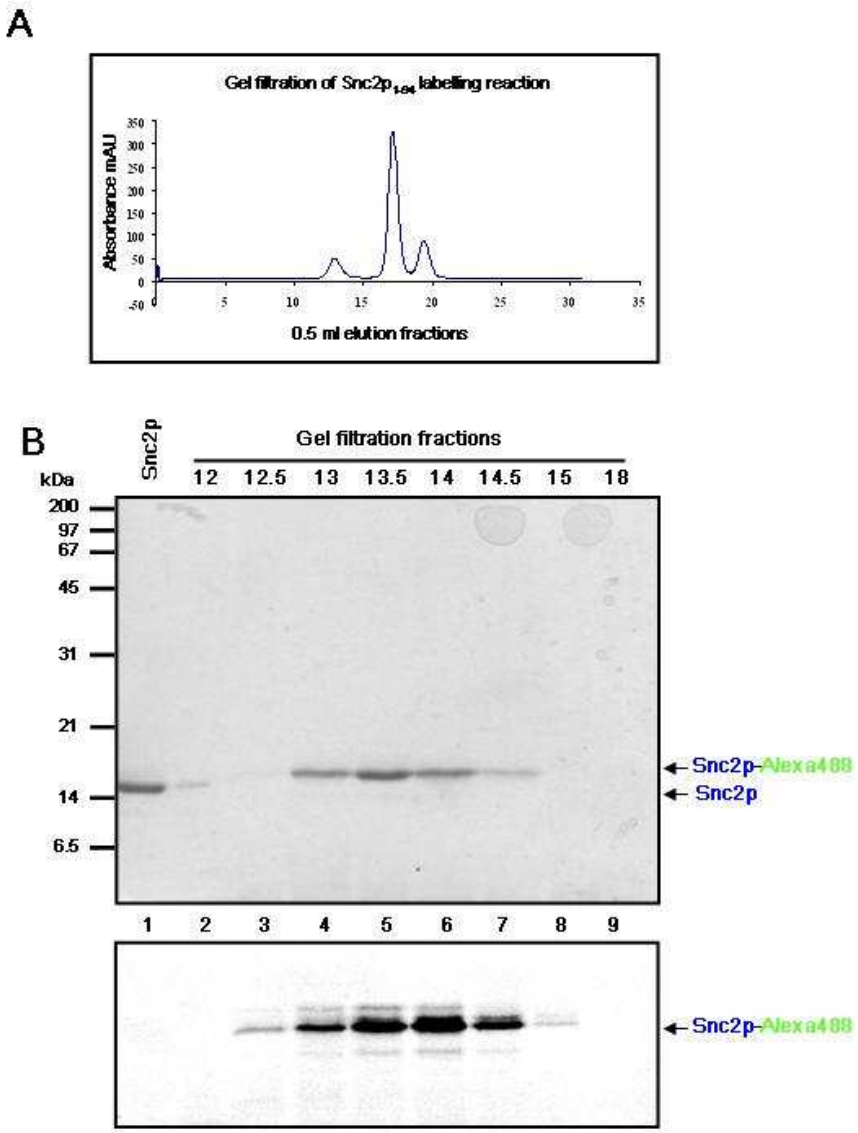

Figure 4.9 Labelling of Snc2p$_{1-94}$ with Alexa 488 fluorophore

A sample of purified Snc2p$_{1-94}$ was diluted in phosphate buffer containing 1 mM TCEP and left for 1 hour at room temperature to reduce cysteine residues. A 15 fold molar excess of Alexa 488 was then added drop-wise to the meniscus of Snc2p$_{1-94}$ sample. The labelling reaction was then sealed from external light and allowed to run for 3 hours. Samples were then loaded onto a Superdex75 (10 / 30) gel filtration column and 0.5 ml fractions were collected. *(A)* Chromatograph showing absorbance at A_{280} from all fractions from the gel filtration column. *(B)* Fractions of interest were analysed by SDS-PAGE on a 15% gel. The gel was scanned using a phosphorimager with a single laser at 433 nm to detect fluorescence of Alexa 488 (lower panel) before Coomassie staining (upper panel). A sample of unlabelled Snc2p was run (Lane 1; 10 µl), followed by fractions of interest (Lanes 2 - 9; 12.5 µl each). Fractions of Snc2p containing detectable concentrations of bound Alexa 488 were collated. Positions of molecular weight markers are indicated.

4.3.2.4 Mobility of Alexa 488 labelled Snc2p1-94 in native gel conditions

Before attempting to quantify binding of labelled $Snc2p_{1-94}$ to Vps45p, we wanted to optimise the conditions of the protein moving through a native gel. The choice of the gel matrix can amplify or attenuate the mobility experienced by a particular protein (Ryder et al., 2008). Preliminary gels were run in order to identify the overall charge of the protein at several pH values; this was uncertain as the predicted isoelectric point of full length Snc2p is 9.28 and the Alexa 488 fluorophore carries an overall negative charge. Once I had established that the protein would move towards the anode when an electric potential was applied across the field, we set out to optimise the native gel conditions. We predicted that the electrophoretic separation of labelled $Snc2p_{1-94}$ from a Vps45p bound version would be best at an alkaline pH, so native slab gels were prepared with TBE at pH 8.4 and pH 9.0. Vps45p was incubated with labelled Snc2p for 3 hours to allow complex formation, before loading on the gels. A sample of unbound labelled $Snc2p_{1-94}$ was also loaded before the gels were run. As shown in the two right hand columns of Figure 4.10, distinct bands could not be detected at 1 or 2 hour time points and the protein had significantly diffused into the gel by the 4 hour time point. In an attempt to better resolve the unbound $Snc2p_{1-94}$ from protein in complex with Vps45p, a native gel of HEPES / imidazole at physiological pH 7.4 was prepared and run as previously described. The proteins moved slower through the gel, but distinct bands were better observed, as shown in the left column of Figure 4.8. We deemed this method most suitable for the gel shift assay.

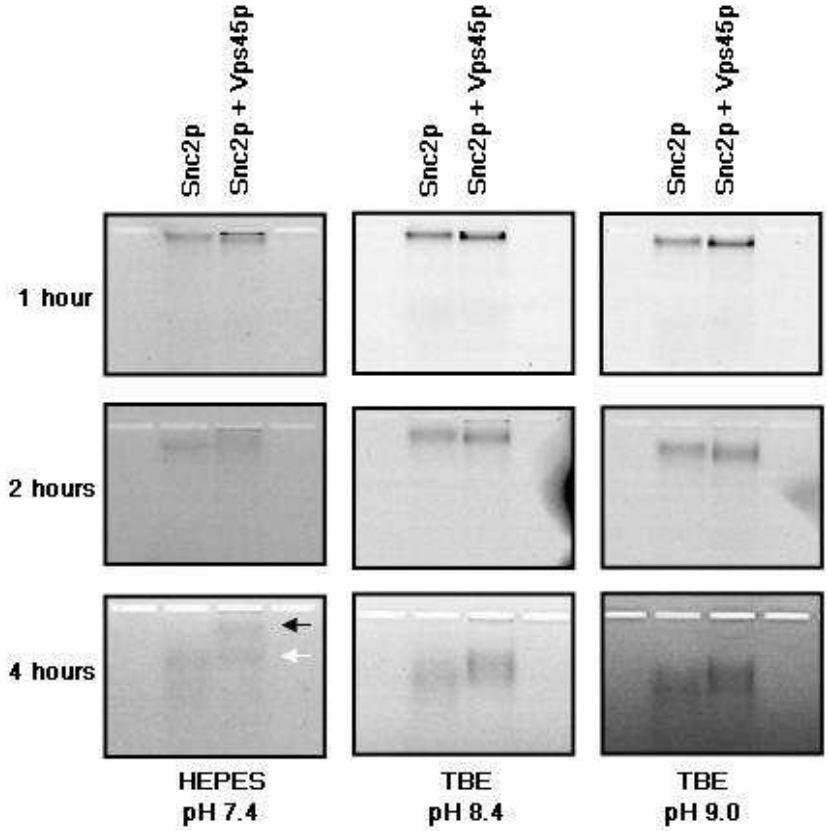

Figure 4.10 Optimisation of conditions for gel shift assay

Binding reactions were prepared containing 2 µM Alexa 488 labelled Snc2p with or without 10 µM Vps45p, made up to 60 µl in potassium phosphate buffer containing 1 mM TCEP and 0.1% NP-40. The reactions were allowed to bind for 3 hours at room temperature in the dark. A 6% native HEPES / imidazole gel and two 6% TBE gels of pH 8.4 and pH 9.0 were prepared and immersed in appropriate cold running buffer for 1 hour prior to loading. 6 µl of 30% glycerol containing 0.01% (w / v) bromocresol dye was added to each binding reaction before 50 µl of sample was loaded onto each of the gels. Gels were each run at 125 volts at 4°C and imaged at the 1 hour (top row), 2 hour (middle row), and 4 hour (bottom row) time points. For images, gels were scanned in a phosphorimager with a 433 nm laser at each of the time points to detect fluorescence of Alexa 488. Bands detected shown by black and white arrows.

4.3.2.5 Complex determination by gel shift assay

Binding reactions of $Snc2p_{1-94}$ at a concentration of 10 µM were set up with a decreasing concentration gradient of Vps45p, beginning at 16 µM. The exact concentrations of Vps45p in each binding reaction are shown in Chapter II, Table 2.1. The reactions were left to bind for 3 hours before being prepared for electrophoresis as described in section 2.1.3.4. All 10 reactions were loaded onto a large scale HEPES / imidazole native gel at

pH 7.4, and then run at constant voltage. The progress of labelled Snc2p$_{1-94}$ was monitored by scanning in a phosphorimager. After the gel had been run for 2 hours, different bands representing unbound and complexed Snc2p$_{1-94}$ could not be detected, as shown in the upper panel of Figure 4.11. It does appear that the samples pre-incubated with highest concentrations of Vps45p migrate out of wells more slowly than samples containing more dilute, or completely lacking, Vps45p. After 2 hours (upper panel) the samples containing most bound Snc2p$_{1-94}$ (Lanes 1 - 4) had not migrated far from the wells. After the gel had been run for 4 hours a band shift could be detected at high Vps45p concentrations, shown in Figure 4.11 lower panel. The first 5 Lanes show two distinct bands, the concentration of Snc2p$_{1-94}$ in the higher band appears to be proportional to the concentration of Vps45p. It is important to note that even the binding reaction containing the highest concentration of Vps45p (Lane 1) did not achieve 100% complex formation, as two bands can still be detected. Samples pre-incubated with lowest concentrations of Vps45p (Lanes 6 - 9) migrate through the gel similarly to the unbound Snc2p control sample (Lane 10), suggesting that the concentration was too low to allow detectable complex formation. As the highest concentration of Vps45p was insufficient to achieve 100% binding to Snc2p$_{1-94}$, the K_d of the interaction could not be accurately calculated. However, ~50% binding could be observed between Vps45p concentrations of 16 µM (Lane 1) and 5.76 µM (Lane 3). We therefore estimate the K_d of the Vps45p-Snc2p interaction to be approximately 10 µM.

The EMSA technique has also been used to investigate the binding affinity between Tlg2p and Vps45p. Reactions were set up as described above for investigating the Vps45p-Snc2p interaction, but an Alexa 488 labelled version of cytosolic Tlg2p lacking the first 36 N terminal residues (Tlg2p$_{37-318}$) was incubated with Vps45p. A full range of binding was achieved; the calculated affinity of the interaction from this assay is 280 nM (Furgason et al., 2009). Unlabelled full length cytosolic Tlg2p (Tlg2p$_{1-318}$) was also added to a reaction as described above; this allowed the competition between the unlabelled Tlg2p$_{1-318}$ and the labelled Tlg2p$_{36-318}$ to be assessed. The binding competency, and therefore the apparent affinity, of the unlabelled molecule can then be calculated (Furgason et al., 2009). From these experiments the full length molecule was shown to have a K_d of 190 nM (Furgason et al., 2009). Both these experiments demonstrate that the affinity of Vps45p for Tlg2p is significantly greater than its affinity for Snc2p. These experiments were published, (Furgason et al., 2009; Appendix III).

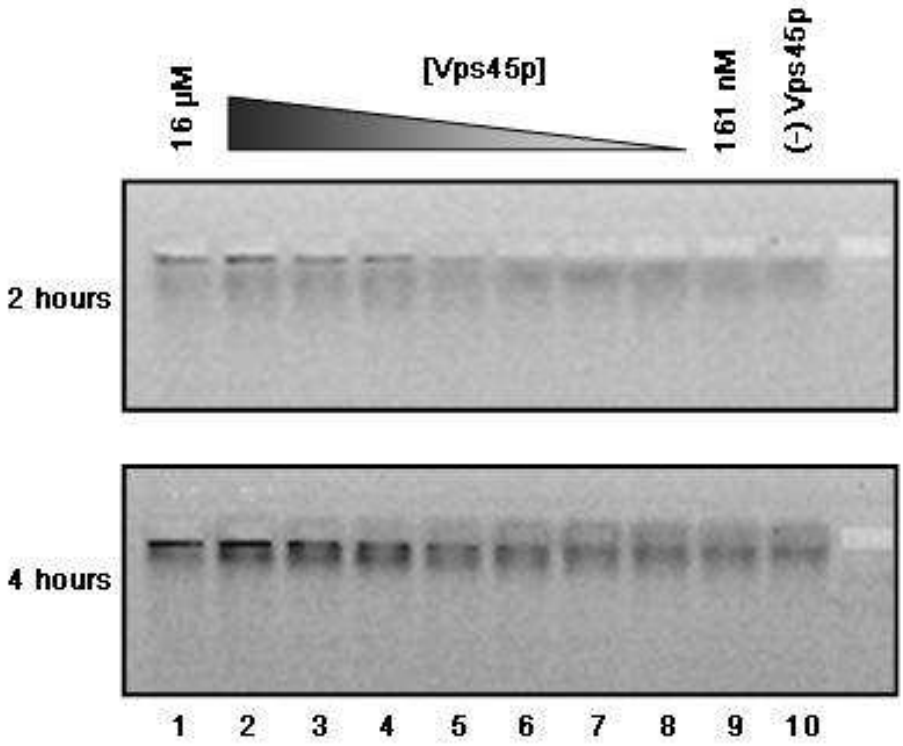

Figure 4.11 Gel shift assay with concentration gradient of Vps45p

A concentration gradient of Vps45p was added to equal samples of $Snc2p_{1-94}$ to produce 10 individual binding reactions. 10 µl Alexa 488 labelled Snc2p at a concentration of 10 µM in binding buffer containing 1mM TCEP and 0.1% NP-40 was added to 10 wells of a 96 well plate. Vps45p at a concentration of 16 µM was used to create a 9 point $^3/_5$ serial dilution from 16 µM to 161 nM (exact concentrations shown in Table 2.1). 40 µl of each of these dilutions were added to the wells containing labelled Snc2p, no Vps45p was added to the final well (Lane 10). The reactions were left to bind in the dark for 3 hours and then 6 µl of 30% glycerol containing 0.01% (w / v) bromocresol dye was added to each binding reaction. A 6% HEPES / imidazole native gel was prepared and chilled in running buffer at 4°C for 1 hour before 50 µl of each sample was loaded onto the gel, which was then run at 125 volts for 4 hours. Gels were scanned in a phosphorimager with a 433 nm laser at 2 (upper panel) and 4 (lower panel) hour time points to detect fluorescence of Alexa 488.

4.3.3 Competition binding experiments

It has been previously shown using an *in vitro* pull down assay that Tlg2p can displace the cytosolic domain of Snc2p ($Snc2p_{1-88}$) from Vps45p (Carpp et al., 2006). The reverse of this is not true, and even high concentrations of $Snc2p_{1-88}$ will not displace Tlg2p in complex with Vps45p (Carpp et al., 2006). This is unsurprising given that we have previously shown in this Chapter that the interaction between Vps45p and $Snc2p_{1-94}$ to be in the micromolar range (~10 µM), which is relatively weak compared to its affinity with

the cytosolic domain of Tlg2p (190 nM; Furgason et al., 2009; discussed in section 4.4.1.5). These experiments were repeated with a better defined concentration gradient of Tlg2p. We also used mutant versions of Vps45p and Tlg2p unable to bind via mode-2, to test if the ability of Tlg2p to displace $Snc2p_{1-88}$ in complex with Vps45p was mediated through this binding mode.

The experiment was set up as previously described (Carpp et al., 2006). Briefly, a His_6 tagged version of wild-type Vps45p was bound to Ni^{2+}-NTA agarose beads. An identical binding reaction was set up with His_6 tagged mutant Vps45p that cannot interact via mode-2 ($Vps45p_{L117R}$). Unbound protein was then washed from the beads before each set of reactions were incubated with a Protein A tagged version of $Snc2p_{1-88}$. The complexes bound to beads were then washed again to remove any uncomplexed Snc2p. The proteins used to form complexes of wild-type Vps45p and the mutant $Vps45p_{L117R}$ are shown in Figure 4.12 *(A)* and *(B)* respectively. 50 µl of settled beads containing complexes were added to a series of tubes, to which the competing proteins were added. Figure 4.12 *(C)* shows SDS-PAGE analyses of the competing proteins produced in *E. coli*: wild-type Tlg2p (Lanes 1 & 2); a version of Tlg2p containing a double alanine mutation ($Tlg2p_{F9A/L10A}$) which disrupts mode-2 binding (Lanes 3 & 4); and Sx4, a mammalian syntaxin that does not bind Vps45p (Struthers et al., 2009), used here as a negative control (Lanes 5 & 6). These proteins were normalised so that they were all of equal molar concentrations (22.8 µM). 300 µl of competing protein, or dilutions thereof, was added to each tube containing beads bound to wild-type or mutant Vps45p in complex with $Snc2p_{1-88}$. 300 µl of Tlg2p and $Tlg2p_{F9A/L10A}$ samples were added undiluted or at a 1:2 or a 1:4 dilution. Reactions were made up to 1 ml with reaction buffer. As controls, tubes were set up and incubated with either 1 ml reaction buffer alone or 300 µl 25 µM mammalian Sx4; 700 µl reaction buffer was also added to this control reaction so all volume were equal. The competing proteins were incubated for 3 hours on a rotator at 4^oC, before being washed 3x with PBS containing 20 mM imidazole. The proteins bound to beads were resolved by SDS-PAGE followed by immunoblot analysis using an α-Vps45p antibody, which also detects the IgG domain of the protein A tag.

The competition analysis of $Snc2p_{1-88}$-PrA bound to either wild-type or mutant Vps45p is shown in Figure 4.13 *(A)* and *(B)* respectively. In each case, addition of reaction buffer alone or Sx4 does not result in any displacement of $Snc2p_{1-88}$ bound to versions of Vps45p (Lanes 1 & 2 in both *(A)* & *(B)*). In contrast, addition of Tlg2p to either Vps45p-$Snc2p_{1-88}$ or $Vps45p_{L117R}$-$Snc2p_{1-88}$ complexes displaces Snc2p in a concentration dependent manner

(Lanes 3 - 5 in both *(A)* & *(B)* respectively). This suggests that mode-2 binding is not involved with the ability of Tlg2p to displace $Snc2p_{1-88}$ in complex with Vps45p. This is corroborated by the fact that addition of $Tlg2p_{F9A/L10A}$, which cannot interact via mode-2 binding, displaces $Snc2p_{1-88}$ from Vps45p similarly to wild-type Tlg2p (compare Lanes 3 - 5 & 6 - 8 in Figure 4.13 *(A)*). There is also no detectable difference between displacement from $Vps45p_{L117R}$ bound to $Snc2p_{1-88}$ with wild-type Tlg2p and $Tlg2p_{F9A/L10A}$, again demonstrating that mode-2 is not important for Tlg2p to bind Vps45p and displace $Snc2p_{1-88}$ (Carpp et al., 2006).

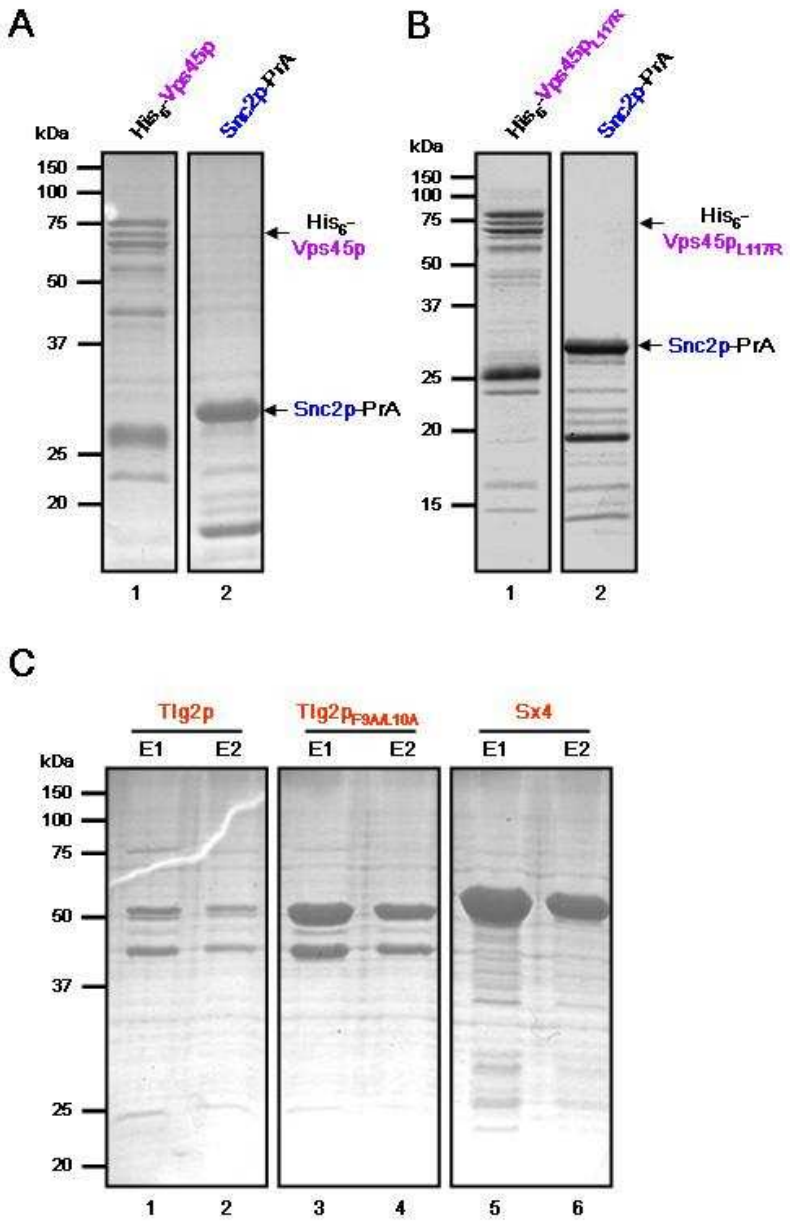

Figure 4.12 Proteins for competition binding assay

For the binding reactions, plasmids pNB710 and pCOG067 were respectively used to produce wild-type Vps45p and a version containing the single residue mutation, Vps45p$_{L117R}$. Both versions of Vps45p were co-expressed with chaperone proteins GroEL and GroES (as described in section 3.4.4) then purified as described in section 2.3.4.1. Left panels of *(A)* & *(B)* show samples from each 1 ml elution of both versions of Vps45p running at 68 kDa (Lanes 1, 5 µl each). Plasmid pCOG045 was used to express the cytosolic domain of Snc2p with two IgG-binding domains of PrA at the C terminus, as described in section 2.3.4.3. Two separate preparations are shown in *(A)* and *(B)* right panels (Lanes 2; 5 µl each). The input proteins for the experiment were also produced with a double IgG-binding domains PrA tag for Tlg2p, the mutant Tlg2p$_{F9A/L10A}$, and the mammalian Sx4 with a C terminal GST tag, were all produced in BL21 (DE3) *E. coli* from plasmids pCOG025, pCOG076 and pFB09 / 2 respectively. *(C)* shows samples from the 1 ml first and second elutions from input protein purifications (Lanes 1 - 6; 5 µl each). All proteins were dialysed against 4 L 1x PBS before stored at 4^{o}C.

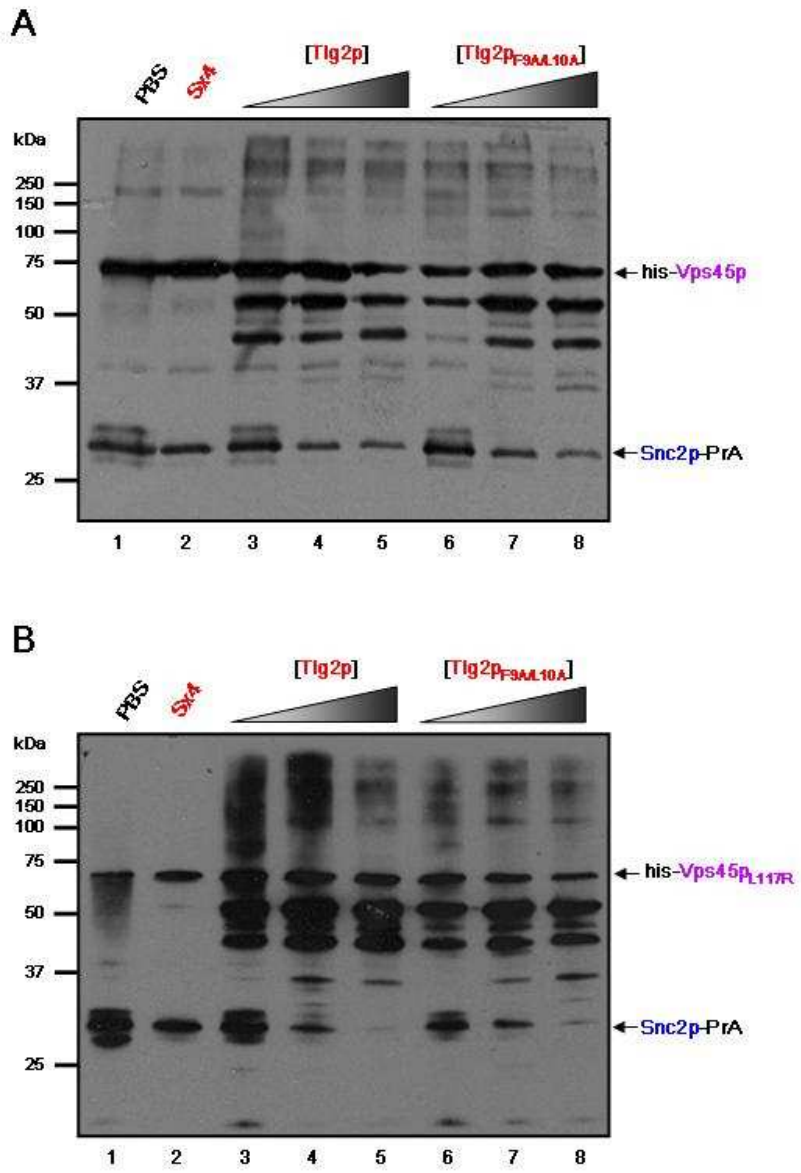

Figure 4.13 Competition binding studies

Recombinant proteins, shown in Figure 4.12, were used to prepare the binding experiments. 200 µl of either wild-type His_6-Vps45 or His_6-$Vps45p_{L117R}$ was added to 500 µl settled Ni^{2+}-NTA agarose beads (Qiagen) and left to rotate at 4°C for 1 hour. Beads were then washed 3x with 1 ml PBS containing 20 mM imidazole. 900 µl of cytosolic Snc2p-PrA was then added to each tube of beads containing version of Vps45p and left to incubate on a rotator overnight at 4°C. Beads were again washed 3x with PBS containing 20 mM imidazole, before 50 µl of settled beads containing Vps45p-Snc2p complexes was then added to separate tubes. Before input proteins were added to beads they were normalised so that they were of equal concentrations; 25 µl, 100 µl and 300 µl of both Tlg2p and $Tlg2p_{F9A/L10A}$ were added to separate tubes containing beads. As controls, 300 µl of PBS or Sx4 was also added to different tubes. Tubes were left to incubate at 4°C for ~16 hours, before another 3x washes with PBS. 50 µl 1x LSB was then added to each sample of beads and boiled at 95°C for 5 minutes. Samples were resolved on a 12% gel by SDS-PAGE followed by transfer to a nitrocellulose membrane and immunoblot analysis using an α-Vps45p antibody to detect the Vps45p protein or the IgG binding domain of the double PrA tag. Immunoblot analysis from competition experiments of Vps45p-Snc2p and $Vps45p_{L117R}$-Snc2p are presented in *(A)* & *(B)* respectively.

4.4 Chapter summary

The data presented in this Chapter confirm the observations that the yeast SM protein Vps45p interacts directly with the v-SNARE Snc2p (Carpp et al., 2006). The protein-protein interaction can be detected through a yeast-2-hybrid assay. Further to this, we have created two plasmids that express Vps45p with a C terminal GFP_{S65T} tag and shown it to also interact via the yeast-2-hybrid technique. The full length fusion protein is identifiable through expression of the GFP_{S65T} tag; we plan to utilise this characteristic in future experiments to screen a library of randomly mutated Vps45p proteins, and then assay their ability to form a complex with Snc2p. The second section of this Chapter has used a complimentary technique, an electrophoretic mobility shift assay, to demonstrate the Vps45p-Snc2p interaction. The advantage of this approach, that involves determining the ability of Snc2p to bind a concentration gradient of Vps45p, is that estimations of affinity can be calculated from the results. Unfortunately accurate calculations could not be performed in this instance, because the concentrations required to achieve a complete range of binding were unattainable. We did however observe more than 50% binding, and a rough estimation of the dissociation constant (K_d) reveals the interaction to be very weak, approximately 10 µM. Another more sensitive approach may be required to make accurate affinity estimations of the Vps45p-Snc2p interaction. Biacore surface plasmon resonance (SPR) and isothermal titration calorimetry (ITC) are two such techniques discussed in Chapter VI. Finally, Snc2p that is bound to Vps45p can be displaced by Tlg2p in a concentration dependent manner. Further to this, we have eliminated this displacement occurring via mode-2 binding using mutant versions of both Vps45p and Tlg2p. The ability of Tlg2p to displace Snc2p from Vps45p may be indicative of a sequential binding model, (a bridging role of the SM protein, discussed in Chapter I). The respective affinities of Tlg2p and Snc2p for Vps45p also support a model whereby Vps45p is carried to the site of action with a weak interaction with the v-SNARE, and then binds to the syntaxin through a higher affinity interaction to fulfil its role.

Chapter V

In vitro fusion of yeast endosomal SNARE proteins

5.1 Introduction

In vitro protein based assays, such as those described in Chapters III and IV, are conducive to understanding simplistic factors of SNARE mediated membrane fusion events; however, they may not accurately represent intracellular conditions. On the other hand, it can be difficult to identify factors responsible for any individual event in the complex series of membrane fusion steps from studies of whole cells and / or organisms. A variety of simplified assays have been developed, using either partially intact cellular components or completely synthetic membranes, in order to bridge this gap (Avery et al., 1999). One such system, designed in the early 1980's by Struck and colleagues, monitors the rate of fusion using fluorescence resonance energy transfer (FRET) (Struck et al., 1981). The FRET pair used in the assay are two fluorophores: NBD (N-(7-nitro-2,1,3-benzoxadizol-4-yl) and rhodamine (N-(lissamine rhodamine B sulfonyl) (Struck et al., 1981). The emission band of NBD, which acts as the energy donor, overlaps with the excitation band of the acceptor rhodamine; when the two probes are in close proximity the NBD fluorescence is quenched by rhodamine (Fung and Stryer, 1978). These probes are used to label the polar headgroups of phosphatidylethanolamine, before the lipid is used to generate liposomes, which can contain other lipid(s) as desired (Struck et al., 1981). The basis of the assay is to mix a vesicle population containing these labelled lipids with an unlabelled vesicle population. If the vesicles fuse, the labelled probes will be distanced spatially as the unlabelled membrane dilutes the labelled membrane, resulting in a decrease in rhodamine quenching, and an increase in NBD fluorescence (Struck et al., 1981). The principles of the *in vitro* fusion assay are outlined in Figure 5.1

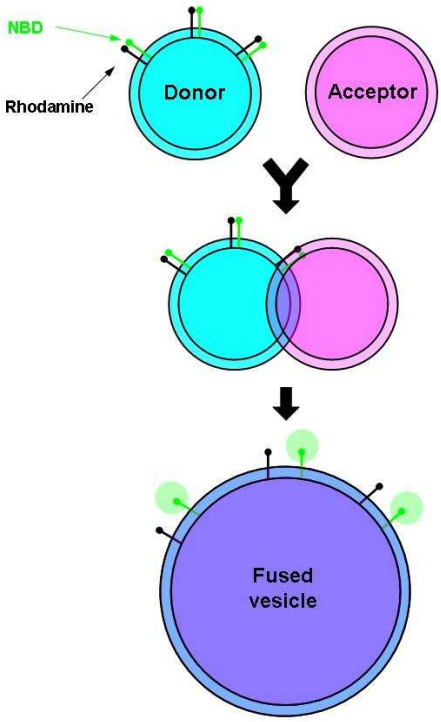

Figure 5.1 Principles of the in vitro fusion assay

Schematic diagram of the *in vitro* fusion assay. Fluorescently labelled lipids are reconstituted into the phospholipid bilayer of donor vesicles. The fluorescence resonance energy transfer (FRET) pair NBD (light spheres) and rhodamine (dark spheres) are reconstituted at a concentration in which NBD fluorescence is quenched by rhodamine through FRET. When donor vesicles fuse with acceptor vesicles the fluorescently labelled lipids are diluted in the membrane and fluorescence quenching by FRET is decreased. The resultant increase in NBD fluorescence over time can be used as an indicator of the rate of fusion. Taken from (Scott et al., 2003).

This simplified *in vitro* fusion assay was further developed to allow incorporation of SNARE proteins into generated vesicle populations (Weber et al., 1998). SNARE proteins that contain hydrophobic transmembrane domains can be purified in the presence of detergent then added to a lipid mixture. Liposomes are created by diluting the detergent below its critical micelle concentration (CMC), the threshold at which the detergent can no longer maintain the lipids in solution. Dilution results in spontaneous formation of liposomes composed from the lipid mixtures, with SNARE proteins integrated into the membrane through their transmembrane domains (Weber et al., 1998). Resultant proteoliposomes are then used to investigate the fusogenic properties of the reconstituted SNARE proteins in this simplified system that, in many ways, mimics biological membranes. This study was used to support the hypothesis that SNARE proteins alone are sufficient to drive fusion of opposing lipid membranes (Weber et al., 1998). The fusion observed was confirmed as SNARE dependent by the inclusion of a negative control in which the t-SNARE containing liposomes are pre-incubated with the cytosolic domain of

the v-SNARE (Weber et al., 1998). These t-SNARE complexes are then unable to form functional SNARE complexes when the v-SNARE containing liposomes are added, and fusion is thus inhibited (Weber et al., 1998).

This *in vitro* fusion assay has been widely used to study SNARE mediated membrane fusion, and can be used to investigate the regulation of this process. The regulatory role of SM proteins on SNARE mediated membrane fusion has been examined using this assay. The first example of this involved the addition of the yeast SM protein Sec1p to the exocytotic t-SNARE complex of Sso1p / Sec9p before reconstitution into liposomes (Scott et al., 2004). Sec1p addition enhances the rate of fusion recorded with liposomes harbouring v-SNARE Snc2p approximately three fold over fusion lacking Sec1p (Scott et al., 2004). A similar effect is observed with liposomes reconstituted with the neuronal exocytotic t- and v-SNARE proteins, Sx1a / SNAP-25 and VAMP respectively (Shen et al., 2007). In this study, proteoliposomes were pre-docked at low temperature (4^{o}C), which prohibits fusion but allows complex formation (Parlati et al., 1999); subsequent addition of cognate SM protein Munc18a to docked liposomes enhances the rate of liposome fusion upon incubation at 37^{o}C (Shen et al., 2007). A third study reported that SM protein Munc18c has an inhibitory effect on the rate of liposome fusion of its cognate SNARE proteins responsible for exocytosis at the mammalian plasma membrane, Sx4 / SNAP-23 and VAMP2; this system likely has additional regulatory requirements to promote fusion *in vitro* (Brandie et al., 2008).

The yeast endosomal syntaxin Tlg2p interacts with Vti1p and Tlg1p to form a ternary t-SNARE complex capable of forming a functional SNARE complex with v-SNARE Snc2p (Bryant and James, 2001, Coe et al., 1999). These proteins have been shown to facilitate fusion of synthetic liposomes in the *in vitro* fusion assay described (Paumet et al., 2001). Vps45p is required for formation of functional Tlg2p containing complexes *in vivo*, which suggests that the SM protein has a positive regulatory role on complex assembly and fusion (Bryant and James, 2001).

5.2 Aims of this Chapter

The aim of this Chapter was to establish the liposome fusion assay using the SNAREs responsible for endosomal trafficking in the yeast *S. cerevisiae*: Tlg2p, Vti1p, Tlg1p and Snc2p. Further to this, I planned to examine the role of Vps45p on membrane fusion mediated by this SNARE complex

5.3 Results

5.3.1 Producing protein components of in vitro liposome assay

Recombinant SNARE proteins were produced in *E. coli*, and then purified by affinity chromatography. To allow reconstitution into synthetic lipid membranes it was necessary that the proteins produced contained their C terminal transmembrane domain. To stop these hydrophobic residues causing aggregation and precipitation of protein, all SNARE protein purifications were carried out in the presence of the detergent Octyl-β-D-glucopyranoside (OG), which solubilises the transmembrane domain. This particular detergent was chosen on account of its small size, which allows easy removal by dialysis after proteoliposome production (Weber et al., 1998).

Where possible full length SNARE proteins were created for the assay, however, this was not possible for Tlg2p and Tlg1p, so alternative versions of these proteins were used, discussed in the following sections. Plasmids encoding Tlg2p and truncations thereof, Vti1p, Tlg1p and Snc2p were kind gifts from Dr. James McNew, Rice University, Texas, USA.

5.3.1.1 Expression and purification of Tlg2p

Tlg2p contains a C terminal luminal domain that is not essential for its membrane trafficking function (Abeliovich et al., 1998); plasmid pJM135 was used to produce a His_6 tagged version of Tlg2p lacking this region, $Tlg2p_{1\text{-}335}$, which expresses better than the full length protein (Paumet et al., 2001). In agreement with Paumet and colleagues, our

attempts to optimise the purification of this protein did not result in sufficient concentrations to allow reconstitution (Paumet et al., 2001); this was unsurprising, as degradation of Tlg2p *in vitro* has been previously documented (Carpp et al., 2006). For this reason a version of Tlg2p lacking the first 36 N terminal residues ($Tlg2p_{37-397}$), a truncation known to significantly enhance protein expression, was produced in *E. coli* from plasmid pJM325 (Paumet et al., 2001). Figure 5.2 shows SDS-PAGE analysis of $Tlg2p_{37-397}$ samples from each step in the purification process.

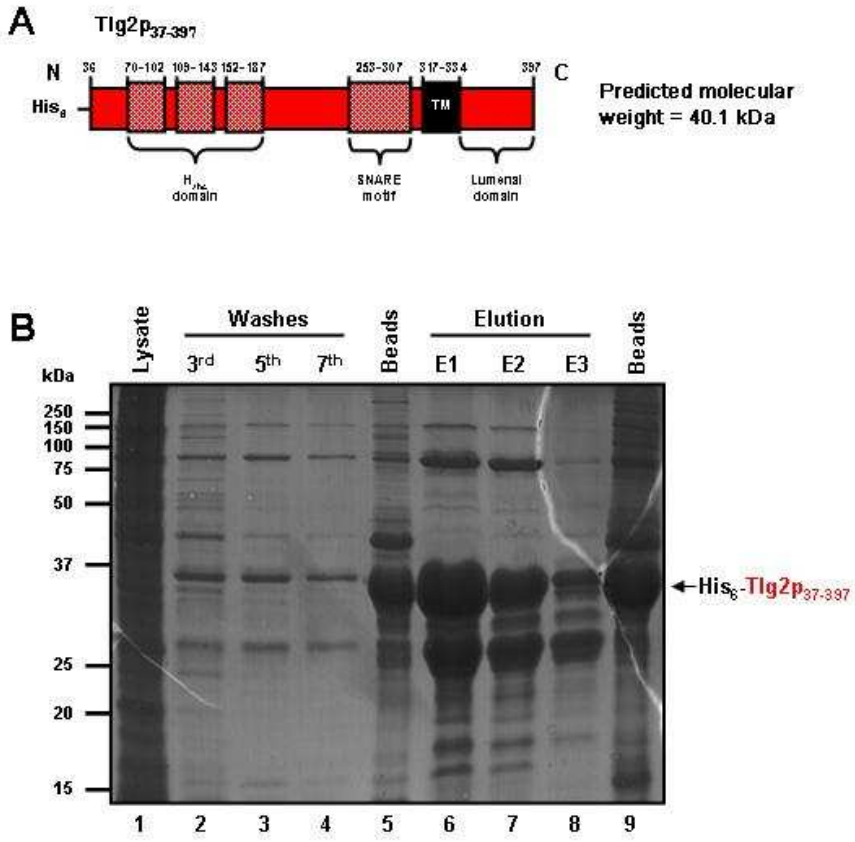

Figure 5.2 Expression and purification of $Tlg2p_{37-397}$

(A) Schematic diagram of $Tlg2p_{37-397}$. *(B)* Plasmid pJM106 was used to recombinantly produce a truncated version of Tlg2p lacking the first 36 N terminal residues in BL21 (DE3) *E. coli* cells. The His_6 tagged protein was expressed and purified from 12 L of culture, as outlined in methods section (2.3.4.1). Purity of protein was analysed at various stages by SDS-PAGE on a 12% gel followed by Coomassie staining. Lysate after 4 hour induction with 1 mM IPTG (Lane 1; 0.001%); examples of the 5 ml washes with 20 mM imidazole (Lanes 2 - 4; 0.1% of each); protein on beads before elution (Lane 5; 5 µl); 1 ml elutions with 250 mM imidazole (Lanes 6 - 8; 5 µl of each); protein on beads after elutions (Lane 9; 20 µl). Positions of molecular weight markers are indicated.

5.3.1.2 Expression and purification of Vti1p and Tlg1p

His_6 tagged versions of Vti1p and Tlg1p were expressed from plasmids pJM132 (Fukuda et al., 2000) and pJM124 (McNew et al., 2000) respectively; both proteins expressed well and resulted in large quantities of purified protein, as shown in Figures 5.3 and 5.4. The reason full length Tlg1p was not used for the *in vitro* fusion assay is that it has previously been shown to require additional activation to fuse synthetic vesicles *in vitro* (Paumet et al., 2001). The additional activation required is the presence of a short C terminal peptide of the v-SNARE motif of Snc2p which reversibly binds the t-SNARE complex, structurally priming it for entry into SNARE complexes (Melia et al., 2002). The SNARE domain of Tlg1p alone reconstituted into this system with cognate t-SNAREs also requires this activation (Paumet et al., 2004). This feature appears not to be conserved through evolution, as the SNARE domain of Sx8, the mammalian homologue of Tlg1p, functions to fuse liposomes in place of Tlg1p without requiring any activation (Paumet et al., 2005). Paumet and colleagues identified the N terminal portion of the Tlg1p SNARE domain to be responsible for this additional regulatory requirement of complexes containing the entire Tlg1p SNARE domain; by demonstrating that chimeric versions of the Tlg1p and Sx8 SNARE domains would only facilitate fusion if the N terminus of Tlg1p was replaced by that of Sx8 (Paumet et al., 2005). Given that our primary aim was to investigate any regulatory role Vps45p may have on SNARE fusion, it was therefore preferable to eliminate this second level of regulation from our experiments. For this reason, a chimeric protein containing the N terminus of Sx8 SNARE motif and the C terminus of Tlg1p was created, (depicted in Figure 5.5). The expression and purification of the Sx8 / Tlg1p chimera required considerable optimisation to yield a final sample of sufficient concentration to reconstitute into liposomes.

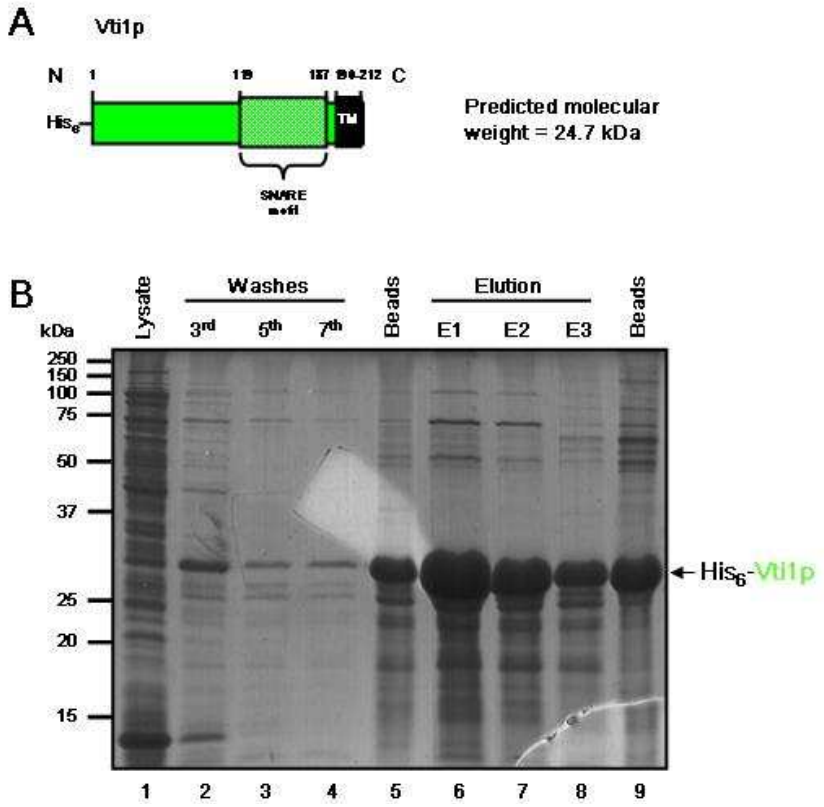

Figure 5.3 Expression and purification of full length Vti1p

(A) Schematic diagram of Vti1p. *(B)* Plasmid pJM132 was used to produce full length recombinant Vti1p. The protein was expressed with an N terminal His_6 tag in BL21 (DE3) *E. coli* cells, and then purified from 12 L of culture as outlined in methods section (2.3.4.1). Purity of protein was analysed at various stages by SDS-PAGE on a 12% gel followed by Coomassie staining. Lysate after 4 hour induction with 1 mM IPTG (Lane 1; 0.001%); examples of the 5 ml washes with 20 mM imidazole (Lanes 2 - 4; 0.1% of each); protein on beads before elution (Lane 5; 5µl); 1 ml elutions with 250 mM imidazole (Lanes 6 - 8; 5 µl of each); protein on beads after elutions (Lane 9; 20 µl). Molecular weight markers are indicated.

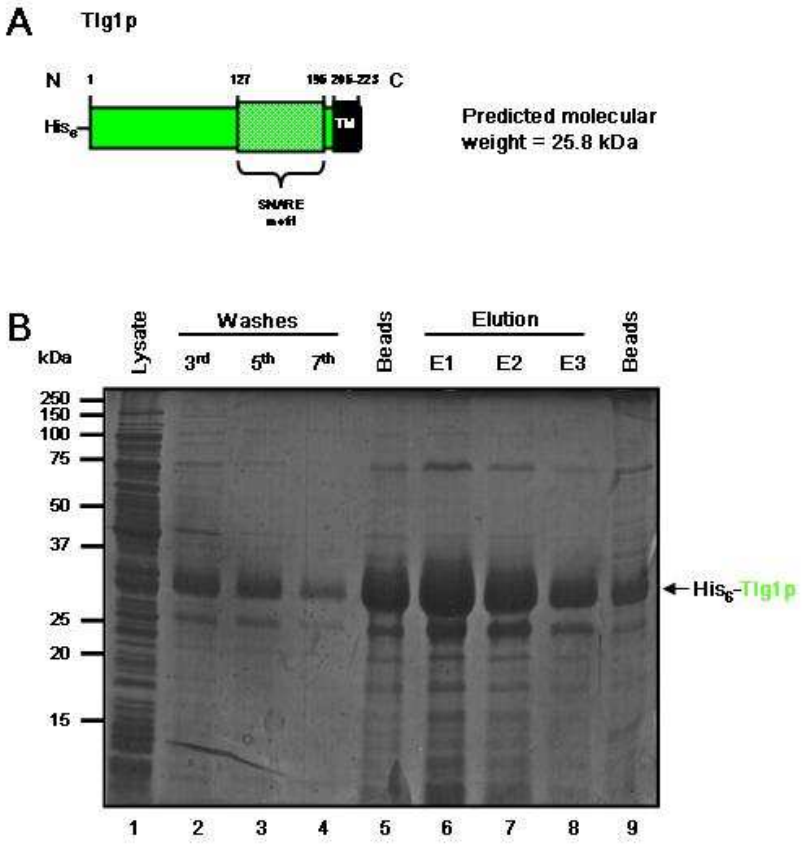

Figure 5.4 Expression and purification of full length Tlg1p

(A) Schematic diagram of Tlg1p. *(B)* Plasmid pJM124 was used to recombinantly produce full length Tlg1p in BL21 (DE3) *E. coli* cells. The His_6 tagged protein was expressed and purified from 12 L of culture as outlined in methods section (2.3.4.1). Purity of protein was analysed at various stages by SDS-PAGE on a 12% gel followed by Coomassie staining. Lysate after 4 hour induction with 1 mM IPTG (Lane 1; 0.001%); examples of the 5 ml washes with 20 mM imidazole (Lanes 2 - 4; 0.1% of each); protein on beads before elution (Lane 5; 5 µl); 1 ml elutions with 250 mM imidazole (Lanes 6 - 8; 5 µl of each); protein on beads after elutions (Lane 9; 20 µl). Positions of molecular weight markers are indicated.

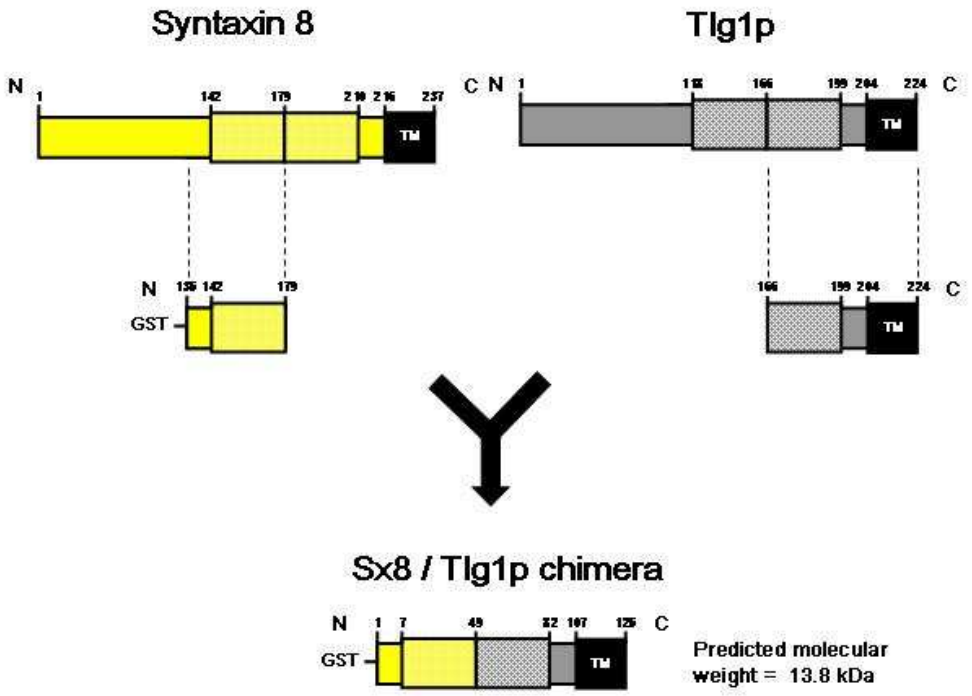

Figure 5.5 Syntaxin 8 / Tlg1p chimera

Schematic representaions of mammalian Syntaxin 8 (yellow) and Tlg1p (grey) are depicted. The hatched boxes represent each SNARE domain. The chimera consists of the N terminal residues of the Sx8 SNARE domain (residues 135 - 179), directly followed by Tlg1p residues from the zero layer to the end of the transmembrane domain (residues 165 - 224). Adapted from (Paumet et al., 2005).

Initial attempts to purify a His_6 tagged version were unsuccessful, with very little protein being expressed. For this reason I constructed pCMD003, which was used to express a version of the Sx8 / Tlg1p chimera harbouring an N terminal GST tag; an approach which sometimes increases yield of expression and solubility of recombinant proteins (Smith and Johnson, 1988). The parent vector, pGEX4T-1 (GE Healthcare) is designed to encode a thrombin cleavage site (Leu-Val-Pro-Arg-Gly-Ser) to allow the GST tag to be removed from recombinant proteins after purification, as shown in Figure 5.6 *(A)*. The low final concentration of cleaved protein was partially due to the instability of the protein at room temperature (the optimal temperature for thrombin cleavage is 25^{o}C; Chang, 1985). Utilisation of filtration devices to concentrate the Sx8 / Tlg1p chimera was reasonably effective at increasing the concentration, shown in Figure 5.6 *(B)*. This was a time consuming exercise involving protein being purified from 4 separate 12 L cultures being concentrated to give less than 1 ml of protein at 48 μM; giving enough material for 4 liposome reconstitutions. For this reason I sought an alternative method, and created pCMD004 based on parent vector pGEX6P-1 (GE Healthcare), to produce another GST fusion of the Sx8 / Tlg1p chimera, which contains a PreScission protease cleavage site

(Leu-Glu-Val-Leu-Phe-Gln / Gly-Pro) to assist with removal of the GST tag (Walker et al., 1994). This protease optimally cleaves at 4°C (Walker et al., 1994), which overcame the degradation problem encountered with thrombin cleavage and allowed sufficient protein concentration for 4 reconstitution procedures to be obtained from a single 6 L culture. Figure 5.6 *(C)* compares the yield obtained from these two vectors. The only fundamental difference between these two systems was the ability of the different proteases to cleave protein from the GST tag at different temperatures; the stability of protein at 4°C results in substantially higher concentrations of protein obtained.

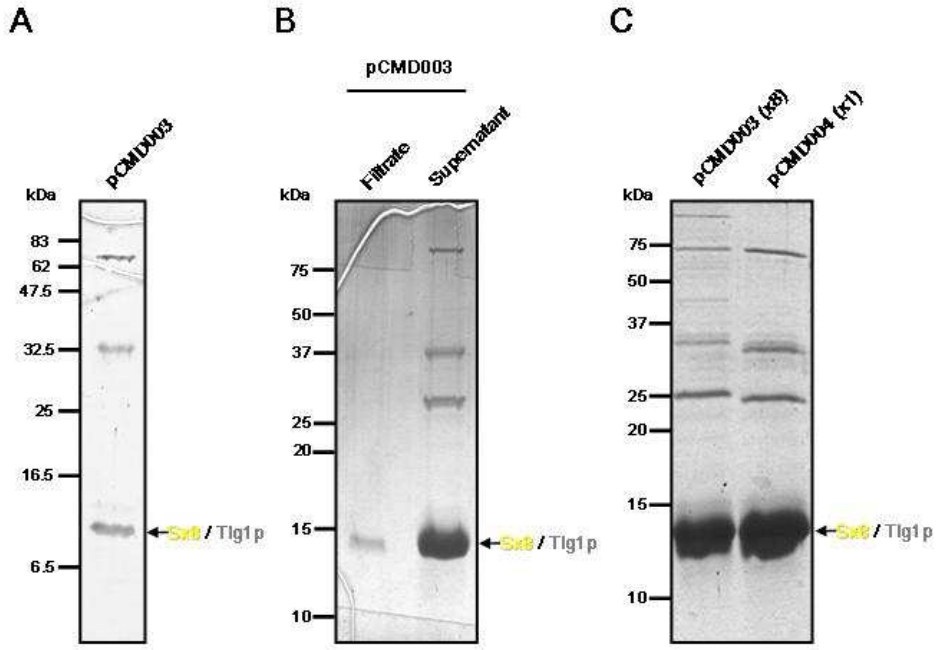

Figure 5.6 Optimisation of expression and purification of Sx8 / Tlg1p chimera

The Sx8 / Tlg1p chimera was produced as a GST fusion protein from two vectors: pCMD003, which contains a thrombin cleavage site; and pCMD004, which contains a PreScission protease cleavage site. Proteins were expressed in Rosetta™ 2 (DE3) *E. coli* cells and purified onto Glutathione Sepharose 4B beads (GE Healthcare), as described in section 2.3.4.2. The respective proteases were used to cleave protein from beads, following the manufacturer's instructions (GE Healthcare), before samples were separated on 15% SDS-PAGE gels then stained with Coomassie Blue. *(A)* Sx8 / Tlg1p chimera produced from pCMD003 was cleaved from beads using 0.05 units / µl thrombin, 5µl was resolved on gel. *(B)* Protein produced from pCMD003 was concentrated using a centrifugal filtration device (Millipore) with a molecular weight cut off of 3 kDa. Samples were centrifuged at 3,000 *g* for 15 minutes at 4°C; this centrifugation step was repeated until ~8 ml of the Sx8 / Tlg1p sample had been reduced to ~1 ml. Panel shows filtrate (left Lane, 5 µl) and final product (right Lane, 5 µl) from concentration process. *(C)* A sample of Sx8 / Tlg1p produced from pCMD004 and cleaved from beads using 0.04 units / µl PreScission protease (right Lane, 5 µl) was compared with the ~8 fold concentrated sample from pCMD003 (left Lane, 5 µl). Positions of molecular weight markers are shown.

5.3.1.3 Expression and purification of Snc2p

For reconstitution of labelled donor liposomes an N terminally His_6 tagged version of full length Snc2p was expressed from plasmid pJM081 (McNew et al., 2000). Purified Snc2p runs significantly higher than its predicted molecular weight of 12.9 kDa, as shown in Figure 5.8; this is consistent with a previous report (Protopopov et al., 1993). In order to create a negative control that could block the entry of this full length v-SNARE into SNARE complexes, a cytosolic version of Snc2p, containing only residues 1 - 88 and harbouring an N terminal His_6 tag, was produced from plasmid pCOG006, shown in Figure 5.7 *(B)*. Protein was snap frozen in liquid nitrogen and stored at -80°C in aliquots of 100 µl.

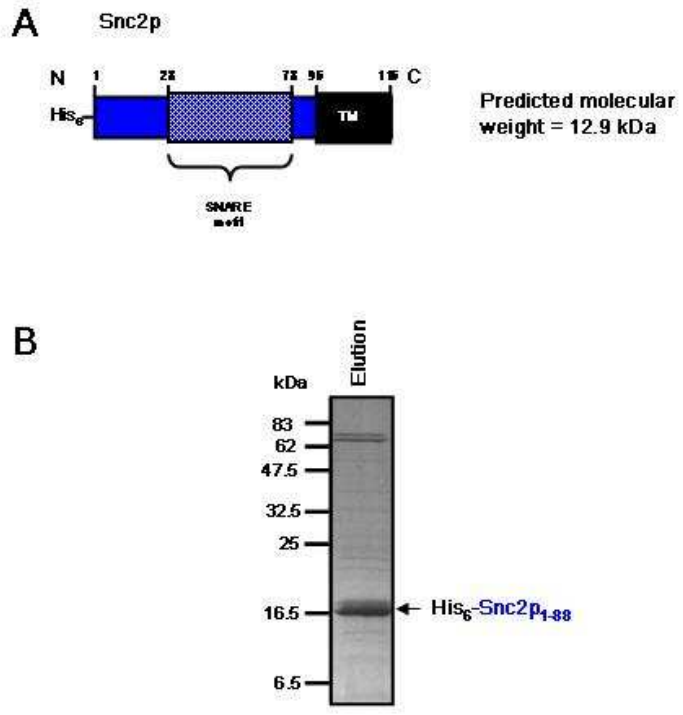

Figure 5.7 Expression and purification cytosolic Snc2p$_{1-88}$

(A) Schematic diagram of Snc2p. *(B)* Plasmid pCOG006 was used to recombinantly produce a version of Snc2p lacking the transmembrane domain, expressing only residues 1 - 88. The His_6 tagged protein was expressed and purified from 6 L of culture as outlined in methods section (2.3.1.4). Expression was induced with 1 mM IPTG for 4 hours at 37°C. Protein was then bound to 2 ml settled Ni^{2+}- NTA beads and eluted with buffer containing 250 mM imidazole after several washes. 5 µl of elution was run on a 15% SDS-PAGE gel, and visualized by Coomassie staining. Molecular weight markers are indicated.

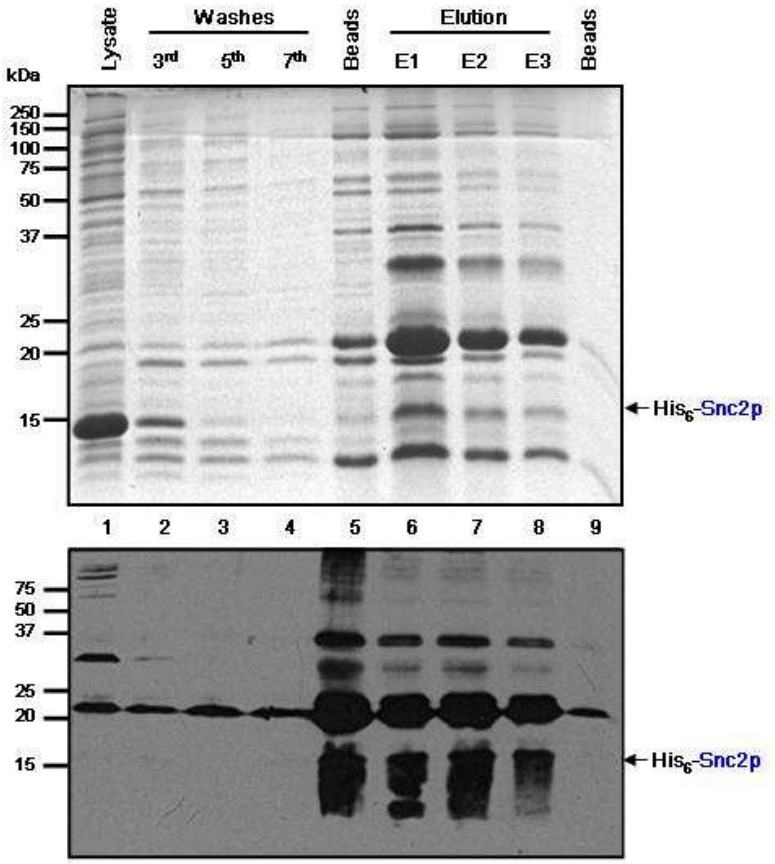

Figure 5.8 Expression and purification of full length Snc2p

Plasmid pJM081 was used to recombinantly produce full length Snc2p with an N terminal His_6 tag. The protein was expressed in BL21 (DE3) *E. coli* cells and purified from 12 L of culture as outlined in methods section (2.3.4.1). Purity of protein was analysed at various stages by SDS-PAGE on a 12% gel followed by Coomassie staining (upper panel). Lysate after 4 hour induction with 1 mM IPTG (Lane 1; 0.001%); examples of the 5 ml washes with 20 mM imidazole (Lanes 2 - 4; 0.1% of each); protein on beads before elution (Lane 5; 20µl); 1 ml elutions with 250 mM imidazole (Lanes 6 - 8; 5 µl of each); protein on beads after elutions (Lane 9; 5 µl). The same samples were run on a second SDS-PAGE gel, and subsequently transferred to a nitrocellulose membrane for immunoblot analysis with α-Snc2p antibody (lower panel). Molecular weight markers are indicated.

5.3.1.4 Expression and purification of Vps45p

Production of recombinant protein in *E. coli* often results in large amounts of insoluble aggregates due to improper protein folding. A large family of chaperone proteins function *in vivo* by stabilising partially folded protein intermediates allowing correct conformation to be achieved (Gething and Sambrook, 1992). One member of the chaperone family found in bacteria is the oligomer GroEL, which forms a functional complex with its

regulator oligomer GroES (Chandrasekhar et al., 1986). Partially folded proteins are bound and released by the GroESL complex in a sequential cycle (Martin et al., 1993, Weissman et al., 1994), which allows progressive ATP dependent folding of the protein (Azem et al., 1994). The GroEL and GroES chaperone proteins were used to increase the concentration of soluble Vps45p achieved from affinity purification.

Recombinant production of the SM protein Sec1p has previously been shown to be enhanced by co-expression with the bacterial chaperone protein GroEL and its regulator GroES (Scott et al., 2004). Protein yield from purifications of Vps45p with and without GroEL and GroES co-expression were compared, keeping all other parameters in the process identical. The pT-GroE plasmid (Yasukawa et al., 1995) was used to produce both GroEL and GroES. This plasmid was co-expressed in *E. coli* with pNB710 (Carpp et al., 2006), which encodes a version of Vps45p with an N terminal His_6 tag. Proteins were purified as described in methods section (2.3.4.1). I found that inducing production of proteins with 0.2 mM IPTG overnight at 15^{o}C was the best method to obtain highest levels of soluble Vps45p. Figure 5.9 *(A)* shows samples of protein eluted from each purification. Vps45p concentrations obtained are much greater when co-expressed with GroEL and GroES (compare - and + Lanes for each elution, E1 - E4). Vps45p of predicted molecular weight 68.0 kDa can be more easily identified after Western blot analysis, shown in Figure 5.9 *(B)*.

To ensure that any observed effects of Vps45p addition to the system were not due to the N terminal affinity tag, I created plasmid pCMD015, which was used to express a version of Vps45p with a C terminal His_6 tag. Both the N and C terminally His_6 tagged versions of Vps45p were purified under exactly the same conditions, to ensure they were added to the assay in equal concentrations. Both proteins were then concentrated using centrifugal filtration devices until there was visible signs of precipitation. Figure 5.10 shows samples of N and C tagged Vps45p both before and after centrifugal filtration. The protein concentration of Vps45p alone, and not that of chaperone proteins and impurities, was estimated by analysing samples on an 8.5% SDS-PAGE gel, alongside BSA standards, followed by Coomassie staining. The relative concentration of each band was determined by densitometry using Image J software. The concentration of samples was estimated from the equation derived from a calibration curve plotted of the BSA standards. The concentrations of Vps45p are very similar regardless of which side the tag is on; example preparations shown in Figure 5.10 were calculated as N terminally tagged Vps45p being 31.9 μM and C terminally tagged 30.1 μM.

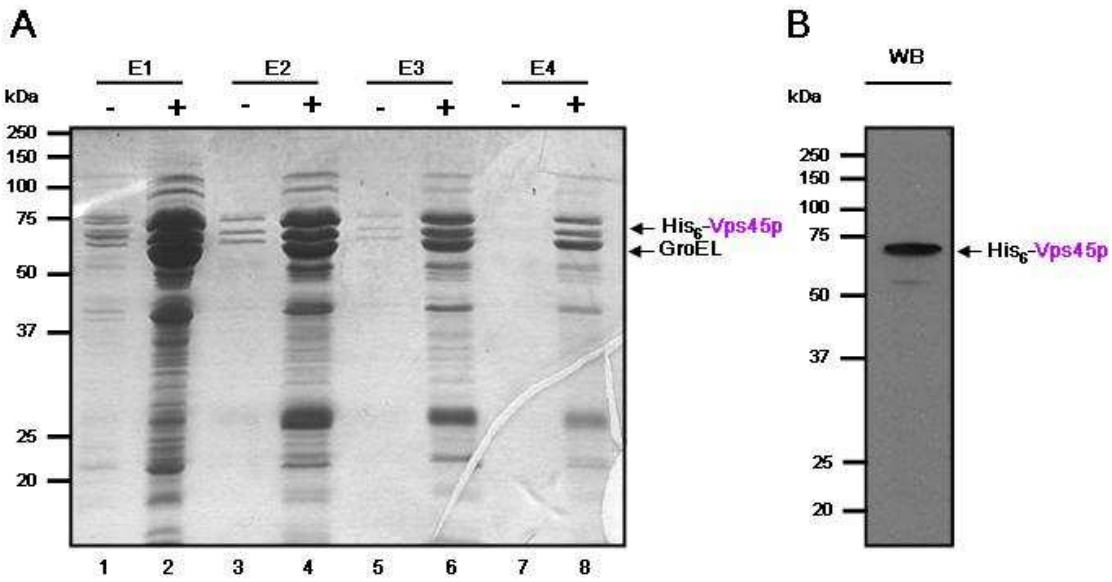

Figure 5.9 Co-expression of Vps45p with GroEL and GroES

Plasmid pNB710 was used to recombinantly produce an N terminally tagged version of Vps45p into BL21 (DE3) *E. coli* cells. The same construct was also used to express protein in BL21 (DE3) cells harbouring plasmid pT-GroE, which expresses the *E. coli* chaperone proteins GroEL and GroES. 6 L cultures of each transformation were grown to OD_{600} ~0.6 before expression of proteins was induced by 0.2 M IPTG overnight at 15^{o}C. Proteins from each culture were purified in exactly the same manner, as outlined in methods section (2.3.4.1). Both purified lysates were bound to 2 ml settled Ni^{2+}-NTA beads for 1 hour before 4x 1 ml elutions in buffer containing 250 mM were carried out. *(A)* 5 µl of each elution (E1 - E4), with (+) and without (-) co-expression of chaperone proteins, was boiled in 2x LSB and then analysed by SDS-PAGE on a 12% gel before Coomassie staining. Vps45p and GroEL, predicted molecular weights 68 and 58 kDa respectively, are indicated. *(B)* 5 µl of sample co-expressed with GroEL and GroES (Lane 1) was also run on a 12% gel then transferred to a nitrocellulose membrane and subjected to immunoblot analysis using an α-Vps45p antibody. Positions of molecular weight markers are indicated.

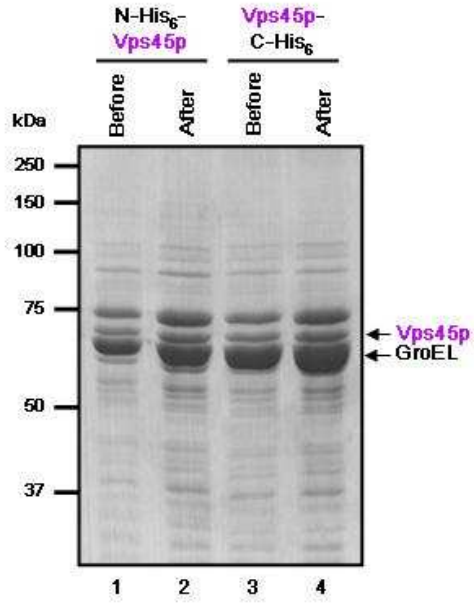

Figure 5.10 Comparison of N and C terminally His_6 tagged Vps45p

Plasmids pNB710 and pCMD015 were respectively used to express versions of Vps45p containing either an N or C terminal His_6 tag in *E. coli* cells as described above. Purifications of both proteins were carried out as before (described above); all parameters and conditions were identical. Samples were then concentrated using centrifugal filtration devices with a molecular weight cut off of 30 kDa. All samples were analysed on an 8.5% SDS-PAGE gel followed by Coomassie staining. Both N and C terminally tagged versions before (Lane 1 & 3; 5 µl each) and after (Lane 2 & 4; 5µl each) centrifugal concentration are analysed. Positions of molecular weight markers are indicated.

5.3.2 Reconstitution of recombinant SNARE proteins into liposomes

To produce unlabelled acceptor liposomes, the t-SNARE proteins were added to a lipid mixture consisting of 85 mol% 1-palmitoyl-2-oleoyl phosphatidylcholine (POPC) and 15 mol% 1,2-dioleoylphosphatidylserine (DOPS). To produce donor liposomes a lipid mixture of 82 mol% POPC and 15 mol% DOPS was used, with fluorescent probes NBD and rhodamine added as head group labels of 1,2-dipalmitoyl phosphatidylethanolamine (DPPE), at 1.5 mol% each. POPC was chosen by Rothman and colleagues to be the main constituent of the synthetic lipid membrane for SNARE protein incorporation as it is relatively inert, the addition of DOPS was due to the negative charge of

phosphatidylserine, which appears to assist with protein reconstitution (Liu et al., 2007, Scott et al., 2003, Weber et al., 1998).

In order to reconstitute the t-SNARE proteins in an assembled ternary complex, $Tlg2p_{37-397}$, Vti1p and Sx8 / Tlg1p proteins were pre-incubated overnight at 4°C; these proteins were added at an equal molar ratio (reactions typically contained ~250 µl $Tlg2p_{37-397}$ at ~21 µM; ~150 µl Vti1p at ~37 µM; and ~100 µl Sx8 / Tlg1p chimera at ~48 µM). The overnight t-SNARE sample was then added to the dried down lipid mixture of 85% POPC and 15% DOPS to create an acceptor liposome population. The stock solution of Snc2p was thawed from storage at -80°C, subjected to centrifugation at 18,000 *g* at 4°C to remove any precipitate, and then transferred to the donor lipid mix containing 15% DOPS and a slightly reduced concentration of 82% POPC, to accommodate addition of the fluorescently labelled lipids (1.5% DPPE-NBD and 1.5% DPPE-rhodamine). Proteoliposome populations of both t- and v-SNAREs were created by diluting the OG concentration below its CMC (19 - 25 mM; le Maire et al., 2000) to form liposome populations. The detergent was removed by dialysis against A_{200} buffer after production of proteoliposomes to ensure it did not interfere with any subsequent applications. Proteoliposomes were then separated from soluble protein by floatation on a gradient of Nycodenz (Sigma-Aldrich Ltd).

To determine success of reconstitution, samples were analysed by SDS-PAGE both before and after the procedure. Figure 5.11 shows the samples of premixed $Tlg2p_{37-397}$, Vti1p, Sx8 / Tlg1p and Snc2p before (Lanes 1 & 3) and after (Lanes 2 & 4) the reconstitution process. This demonstrates that all proteins have been successfully incorporated into their respective vesicles. The additional protein bands from the affinity purification seen on the gel before reconstitution are not reconstituted, presumably because they do not contain a transmembrane domain to facilitate incorporation into the lipid membrane.

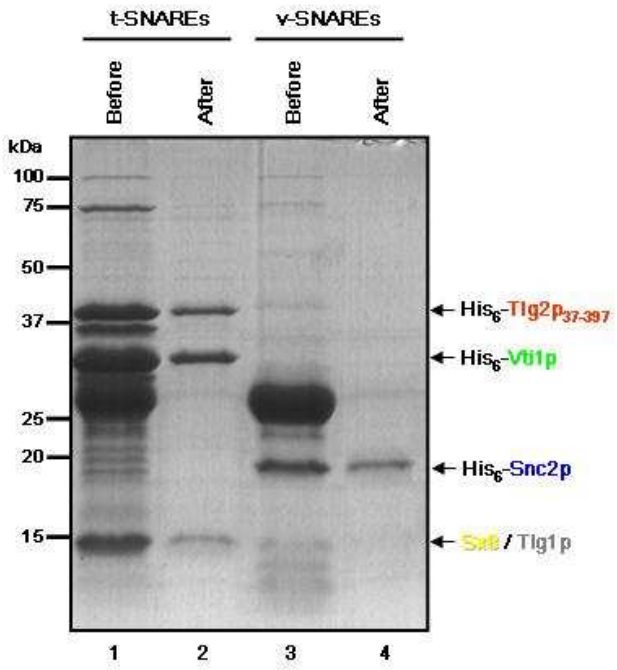

Figure 5.11 Reconstitution of yeast endosomal SNAREs into liposomes

Purified t-SNAREs $Tlg2p_{37-397}$, Vti1p and Sx8 / Tlg1p chimera were mixed together to a total volume of 500 µl at a molar ratio of 1:1:1 on a rotator overnight at 4°C, to allow ternary complex formation in preparation for acceptor liposome reconstitution. 100 µl of purified Snc2p stock was thawed for reconstitution into donor liposomes, and added to 400 µl A_{200} buffer containing 1% OG. 100 µl of 15 mM acceptor lipid mixtures and 500 µl of 3 mM donor lipid mixtures, stored in chloroform, were dried down under a stream of nitrogen gas before vacuum desiccation. Purified t- and v-SNAREs were added to lipids respectively, and then thoroughly mixed by vortexing. The 500 µl solution of each lipid-protein mixture was then diluted, by the addition of 1 ml A_{200} buffer (200 mM KCl, 25 mM HEPES), below the CMC of OG, to allow spontaneous formation of liposomes. The lipid mixture of each reaction was then dialysed against 4 L of A_{200} buffer containing 4 g BioBeads (BioRad Laboratories Ltd) to assist with removal of detergent. Dialysed t- and v-SNARE populations were then mixed with 1.5 ml 80% (w / v) Nycodenz (Sigma-Aldrich Ltd) in A_{200} buffer in a SW60 tube (Beckman Coulter Ltd, London, UK). A 1 ml layer of 30 % (w / v) Nycodenz in A_{200} buffer was then carefully overlaid onto each mixture, before a 250 µl layer of A_{200} buffer was finally overlaid on top. Formed proteoliposomes were separated through the Nycodenz gradient by centrifugation in a Beckman Coulter SW60 rotor at 46,000 rpm for 4 hours at 4°C. t and v-SNARE populations were harvested from the top layer and the interface between the 30% layer. 10 µl of each population was then analysed by SDS-PAGE (Lanes 2 & 4) and compared with 10 µl samples from before the reconstitution (Lanes 1 & 3). Molecular weight markers are indicated.

5.3.3 Characterisation of proteoliposomes

In addition to checking SNARE proteins had been successfully reconstituted into liposomes by SDS-PAGE analysis, it was important to characterise the liposomes. This is necessary to gauge how accurately fusion observed represents the biological system we have based our investigations on. Firstly, I wanted to know the protein and lipid content of each liposome population. Size determination is another important factor, as if the liposome sizes vary dramatically then the results obtained from the dequenching assay may not represent the actual rate of fusion. I also wished to investigate the orientation of the proteins in the reconstituted liposomes, as a large amount of internally orientated proteins may result in misinterpretation of any fusion assay results correlated to the total protein concentrations.

5.3.3.1 Estimation of protein and lipid content

The total protein concentration in reconstituted liposomes was determined by amido black protein assay (Schaffner and Weissmann, 1973), which has previously been used to accurately determine protein content in presence of high lipid concentrations (Kaplan and Pedersen, 1989), described in methods section 2.3.12.3. The molar concentrations of Snc2p in donor liposomes were generally 6 - 10 fold greater than t-SNARE proteins in acceptor liposomes. The calculated molar concentrations for Snc2p and the t-SNARE complex samples shown in Figure 5.11 were 32.9 μM and 5.6 μM respectively. The lipid recovery was calculated by addition of trace amounts of tritiated 1,2-dipalmitoyl phosphatidylcholine ([^{3}H]DPPC) to the lipid stocks. Samples from both the lipid stocks and the harvested liposomes were compared by measuring radioactivity from equivalent volumes in a scintillation counter.

5.3.3.2 Estimating size of proteoliposomes

A dynamic light scattering (DLS) technique was used to estimate the size of reconstituted proteoliposomes containing either t- or v-SNAREs. This technique relies on the scattering experienced by light when it collides with particles of smaller wavelength (Rayleigh

scattering). The Brownian motion experienced by particles in solution causes fluctuations in the scattered light; a digital correlator can be used to determine the intensity auto-correlation function, which can be used to calculate the hydrodynamic radii of the liposomes (Kinuta and Takei, 2002). The DynaLS algorithm (DynaPro; Wyatt Technology Corp.) was used to invert the correlation function to find the best fitting size distribution. Measurements of both populations of proteoliposomes were made; Figure 5.12 *(A)* shows the range of hydrodynamic radii for the donor population containing Snc2p. The measurements for this v-SNARE proteoliposome population were used to estimate an average size of 43.3 ± 6.42 nm. Figure 5.12 *(B)* shows the size distribution of the acceptor liposomes containing $Tlg2p_{37\text{-}397}$, Vti1p and the Sx8 / Tlg1p chimera. The scattering measurements for this population were more varied and disallowed an accurate estimate to be achieved. From the graph we can see that the range of liposome sizes was between 10-90 nm, which is the same range as our donor liposomes, which we would expect, although we cannot accurately estimate their size from these measurements. The raw data from the dynamic light scattering measurements are displayed in appendix I.

To complement the dynamic light scattering size estimations, and with the hope of getting a better approximation of the t-SNARE liposome size, transmission electron microscopy was used to image the liposomes and measure their size directly. The samples were diluted $^{1}/_{10}$ before being imaged at 16,000x magnification. Figure 5.13 *(A)* and *(B)* shows examples of images taken from liposomes containing the yeast endosomal t-SNAREs and v-SNAREs respectively. Proteoliposome diameters from several preparations of each population were estimated from the images using SIS iTEM software (Olympus). The range of diameters from each population is presented as a percentage of the total, shown in Figure 5.13 *(C)* and *(D)*. This data shows that the liposomes ranged in size between 10 and 100 nm, with the majority measuring between 40 and 70 nm in size, which is in agreement with the dynamic light scattering results previously described in this section.

Both our dynamic light scattering and electron microscopy results correlate well with other examples of reconstituted yeast SNARE proteins in liposomes composed of 85% POPC and 15% DOPS (Scott et al., 2003).

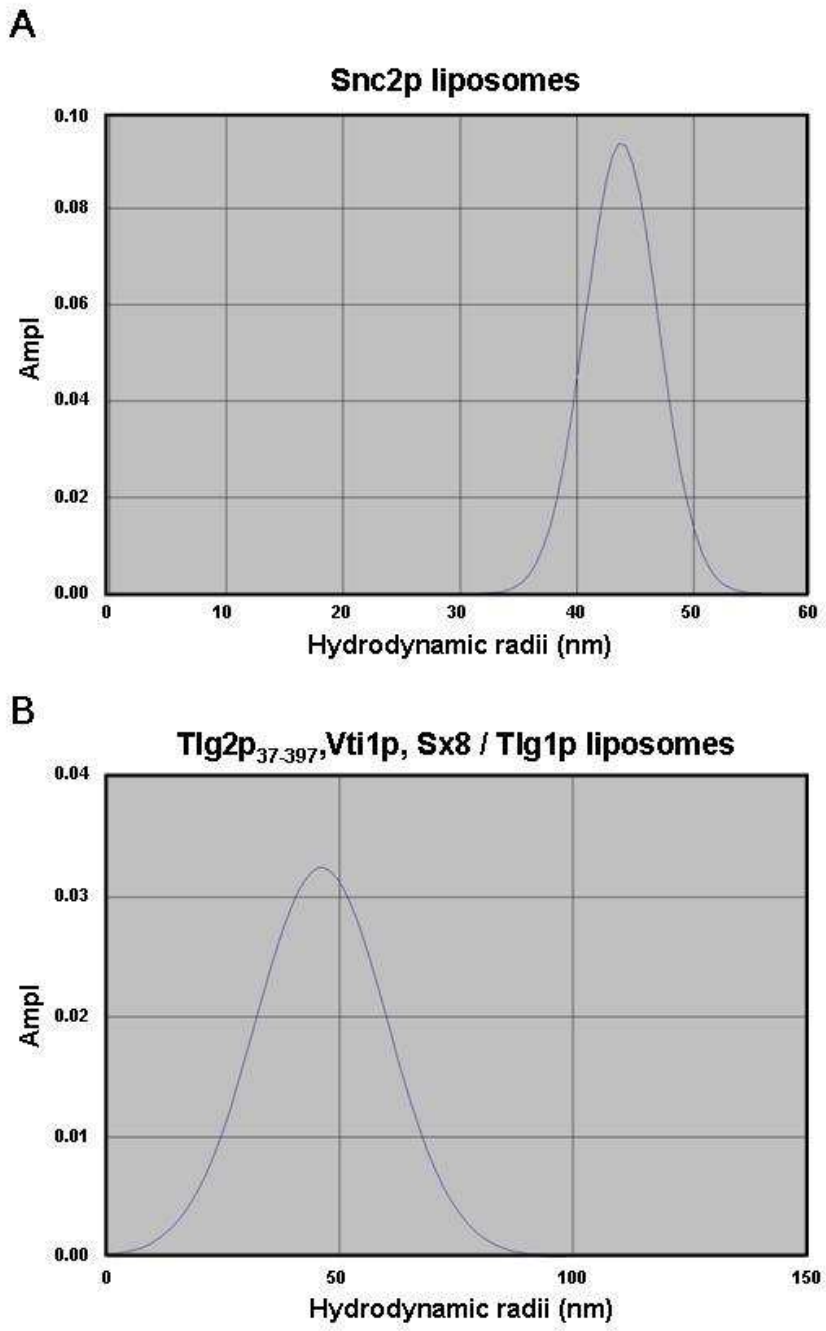

Figure 5.12 Determination of proteoliposome size by dynamic light scattering

Each population of donor and acceptor liposomes was diluted $^{1}/_{20}$ with A_{200} buffer and then centrifuged at 18,000 *g* for 10 minutes. Samples were applied through a 200 nm filter into a DynaPro 801 Dynamic light scattering instrument (Wyatt Technology Corp.). Measurements were taken at ~37^{o}C. The laser power was adjusted to keep the intensity between 500,000 counts and 2,000,000 counts. The results were then processed with the program Dynamics V2 software (Wyatt Technology Corporation). The hydrodynamic radii of each population were calculated with the regularisation algorithm provided by this software.

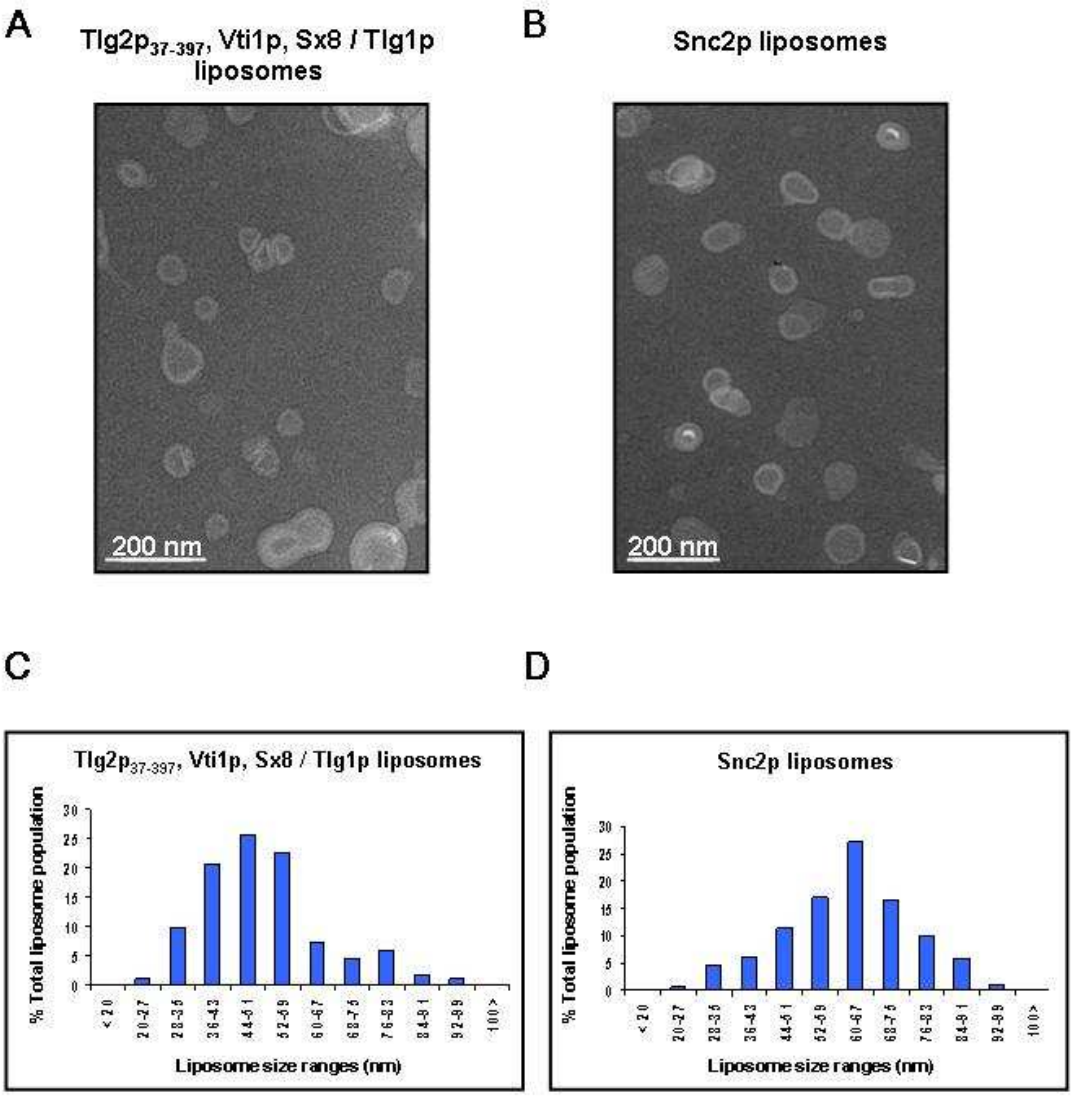

Figure 5.13 Determination of proteoliposome size by electron microscopy

Recovered acceptor and donor proteoliposomes were diluted $^{1}/_{10}$ before 10 µl of each sample was applied to a glow discharged copper grid. 1% aqueous methylamine vanadate was then applied as a negative stain before samples were imaged with a LEO 912 energy filtering transmission electron microscope at 120 kV. Representative images of both acceptor liposomes containing Tlg2p$_{37-397}$, Vti1p and Sx8 / Tlg1p chimera *(A)* and donor lipsomes containing Snc2p *(B)* are shown. Scale bars indicated. Liposome diameters were measured directly from images produced from several different grids from each sample using SIS iTEM soft imaging software (Olympus). Data presented as a percentage of total liposome population in histograms for acceptor *(C)* and donor *(D)* liposomes.

5.3.3.3 Estimating orientation of reconstituted SNARE proteins

The external orientation of SNARE proteins is crucial for their ability to interact with cognate partners and facilitate fusion. For this reason I designed a technique to allow the percentage of technically redundant, internally orientated, SNARE proteins to be estimated. Trypsin was used to digest the external portion of the SNARE proteins; this was compared to a trypsin digest where the internal SNAREs were also made accessible to the protease by addition of detergent to disrupt the liposomes. Figure 5.14 *(A)* shows an example of a trypsin digest to estimate the orientation of proteins. Proteoliposomes were incubated at 37^{o}C as a control (Lanes 1 & 4), external SNAREs were digested with trypsin and compared with total SNARE digestion, when Triton X-100 was also added (compare Lanes 2 with 3 & 5 with 6). Figure 5.14 *(B)* shows average external orientation of SNAREs from at least 5 separate reconstitutions. The Sx8 / Tlg1p chimera is not represented; it resolved poorly on the gel due to its small size; the resultant images were not suitable for densitometry analysis.

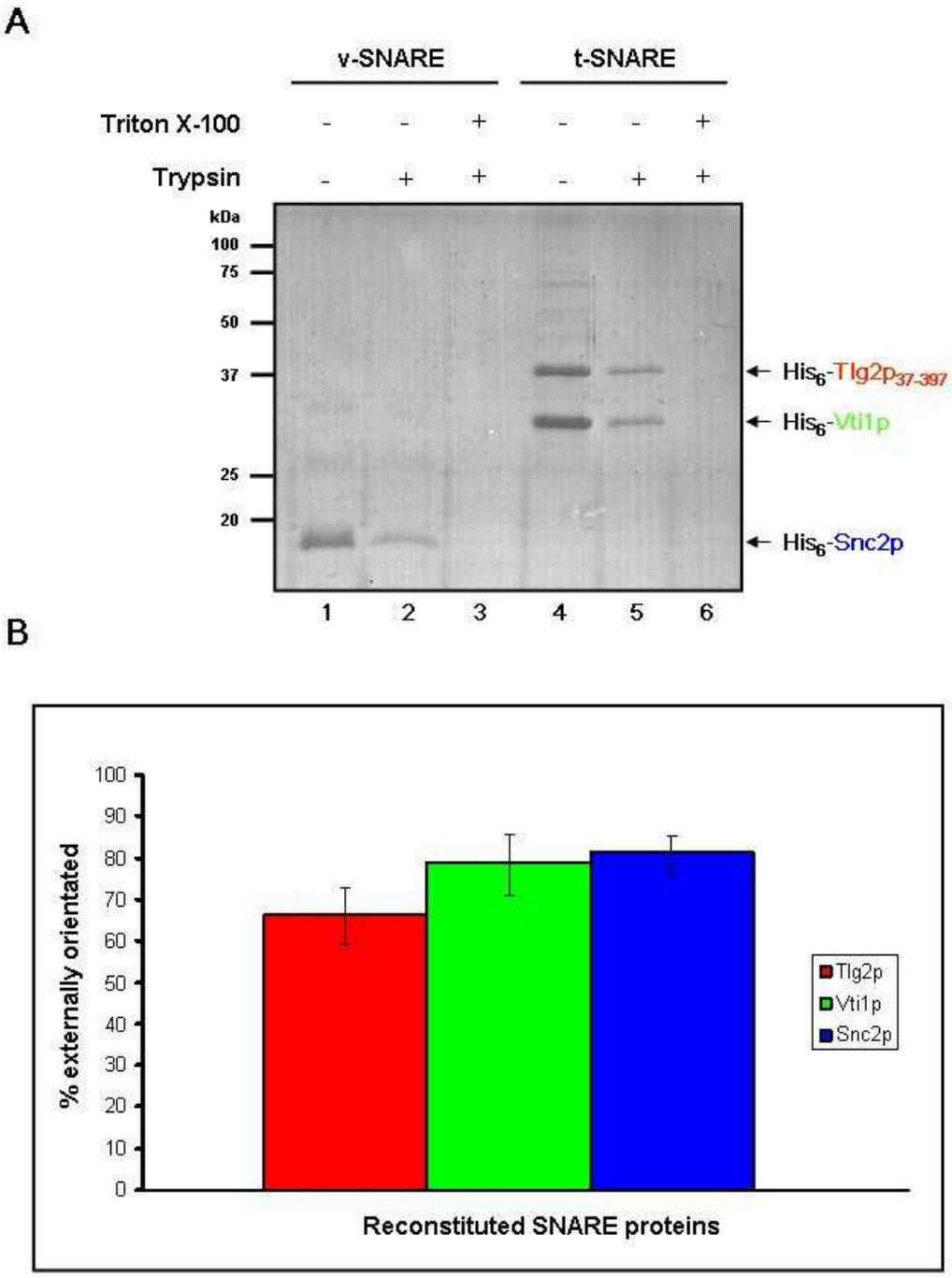

Figure 5.14 Orientation determination of reconstituted proteins in liposomes

(A) Example of an SDS-PAGE gel used to determine the orientation of SNARE proteins reconstituted into acceptor and donor liposomes. 10 µl of liposomes were incubated at 37°C for 3 hours in the presence of trypsin either with or without Triton X-100. v-SNARE liposomes contain Snc2p, and t-SNARE liposomes contain Tlg2p, Vti1p and Sx8 / Tlg1p chimera. Each reaction was then analysed by SDS-PAGE followed by Coomassie staining. As a control a 10 µl sample from each population was also incubated with no trypsin (Lanes 1 & 4). Molecular weight markers indicated. *(B)* Histogram displaying average externally orientated SNARE proteins from at least 5 separate reconstitutions. The standard deviation of each externally orientated SNARE protein is indicated by error bars.

5.3.4 In vitro fusion of liposomes containing the yeast endosomal SNAREs

Reconstituted acceptor and donor liposomes were used to set up an *in vitro* fusion assay. Two reactions were prepared, each with 45 µl of the acceptor liposome population containing $Tlg2p_{37-397}$, Vti1p and Sx8 / Tlg1p chimera at 4°C. To the first reaction 5 µl of A_{200} buffer was added, to the second reaction 5 µl of cytosolic $Snc2p_{1-88}$ was added as a negative control, to ensure that any increase in fluorescence was due to SNARE mediated membrane fusion. Reactions were then incubated at 4°C for 1 hour to allow the binding of $Snc2p_{1-88}$ to the ternary t-SNARE complex. 5 µl of donor liposomes containing reconstituted Snc2p were then added to each reaction. The reason an excess of t-SNARE liposomes are added to the reaction is to account for the higher concentration of v-SNAREs per liposome, at these volumes the ratio of t-SNARE complexes to v-SNARE is approximately 1:1 (Parlati et al., 1999). Since there is a ~10 fold excess of Snc2p proteins per liposome in the donor population, each vesicle can undergo fusion with multiple acceptor liposomes mediated via different t-SNARE complexes. Once the v-SNAREs had been added to the reaction and thoroughly mixed, the microtitre plates containing the reactions were transferred to the spectrophotometer pre-heated to 37°C. Following a 5 minute incubation, NBD fluorescence was measured at 2 minute intervals for 2 hours. Maximal fluorescence was then determined by the addition of n-dodecylmaltoside to each reaction and fluorescence measurements recorded for a further 40 minutes. Figure 5.15 shows the data normalised to the maximal fluorescence measurements for each reaction. The gradual increase in NBD fluorescence measured due to the decrease in rhodamine quenching as the acceptor liposomes dilute the donor liposomes, thus represents fusion (solid blue line). The fusion of liposome populations is due to the formation of SNARE complexes, demonstrated by the inability of the same populations to fuse in the control reaction pre-incubated with cytosolic Snc2p (red dotted line). The cytosolic $Snc2p_{1-88}$ competitively interacts with t-SNARE complexes rendering them inaccessible to Snc2p carried by the donor vesicles. The raw fluorescence data recorded is shown in appendix II.

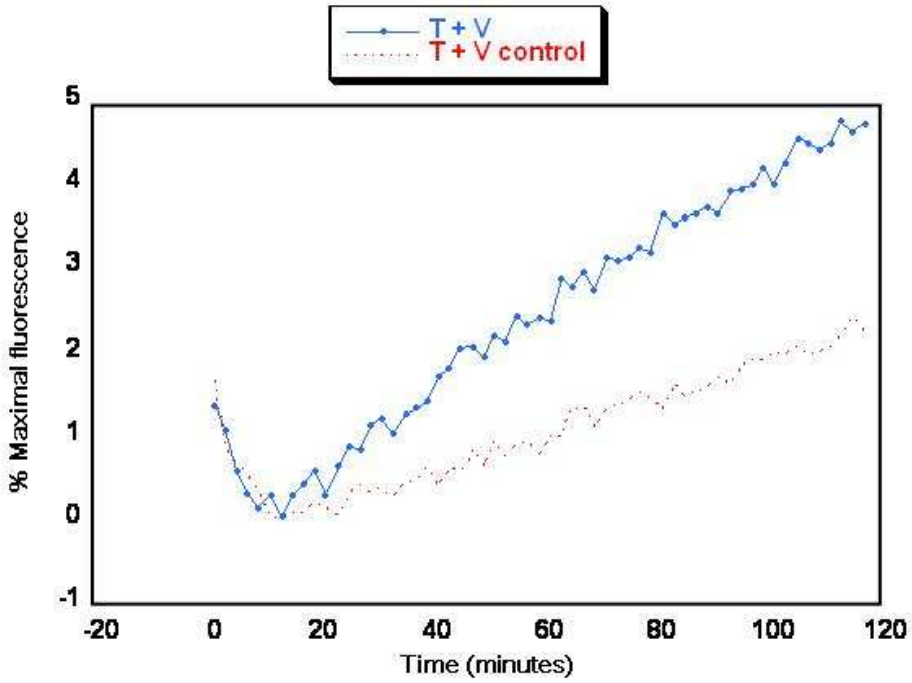

Figure 5.15 Reconstituted endosomal yeast SNAREs form a functional complex

Fusion assays were set up with 45 µl acceptor t-SNARE and 5 µl v-SNARE liposomes. Populations were mixed in a 96 well plate before transfer to a FLUOstar Optima spectrophotometer at 37°C. Samples were incubated for 10 minutes before NBD fluorescence was measured at 2 minute intervals for 2 hours, with the excitation set to 460 nm and the emission set to 535 nm. 10 µl 2.5% (w / v) n-dodecylmaltoside detergent was then added to each reaction, and fluorescence was measured for a subsequent 40 minutes. The maximal fluorescence was determined by this addition of detergent, raw fluorescence measurements were then normalised to this maximum. Graph shows normalised data for t-SNAREs containing Tlg2p$_{37-397}$, Vti1p, Sx8 / Tlg1p and v-SNARE Snc2p (blue line, filled circles). As a control, a replica reaction was set up with the t-SNAREs previously incubated for 1 hour with 5 µl soluble Snc2p$_{1-88}$ before mixing with donor liposomes (red dotted line). The raw fluorescence measurements for this experiment are presented in Appendix II.

5.3.5 Tlg1p SNARE complexes cannot facilitate fusion of vesicles *in vitro*

It has previously been shown that the N terminal residues of the Tlg1p SNARE motif contain a regulatory element that inhibits its ability to facilitate fusion of vesicles *in vitro* (Paumet et al., 2005). To confirm that Tlg1p could not fuse vesicles in our system we compared acceptor liposomes reconstituted with t-SNARE complexes containing $Tlg2p_{37-397}$ and Vti1p with either Tlg1p or the Sx8 / Tlg1p chimera. Fusion assays containing 45 µl of the two populations of acceptor liposomes containing either Tlg1p or Sx8 / Tlg1p were set up with 5 µl of the same population of donor liposomes containing Snc2p. Control reactions were again prepared in which the cytosolic domain of $Snc2p_{1-88}$ was pre-incubated with t-SNARE complexes for an hour at $4^{o}C$ to block fusion. Figure 5.16 shows the NBD fluorescence results normalised against maximal fluorescence determined by liposome disruption with detergent. Successful fusion of Snc2p donor liposomes with acceptor liposomes containing t-SNARE complexes with the Sx8 / Tlg1p chimera is observed, as previously described (solid blue line). Acceptor lipsomes containing Tlg1p do not fuse with the donor vesicles, indicated by no increase in NBD fluorescence above controls (solid red line compared with blue and red dotted lines). This confirms the previously reported observation that Tlg1p is not capable of facilitating fusion of vesicles *in vitro* whereas a chimeric version, replacing the N terminal residues of the SNARE motif with those of mammalian Sx8, results in fusion of synthetic liposomes (Paumet et al., 2005).

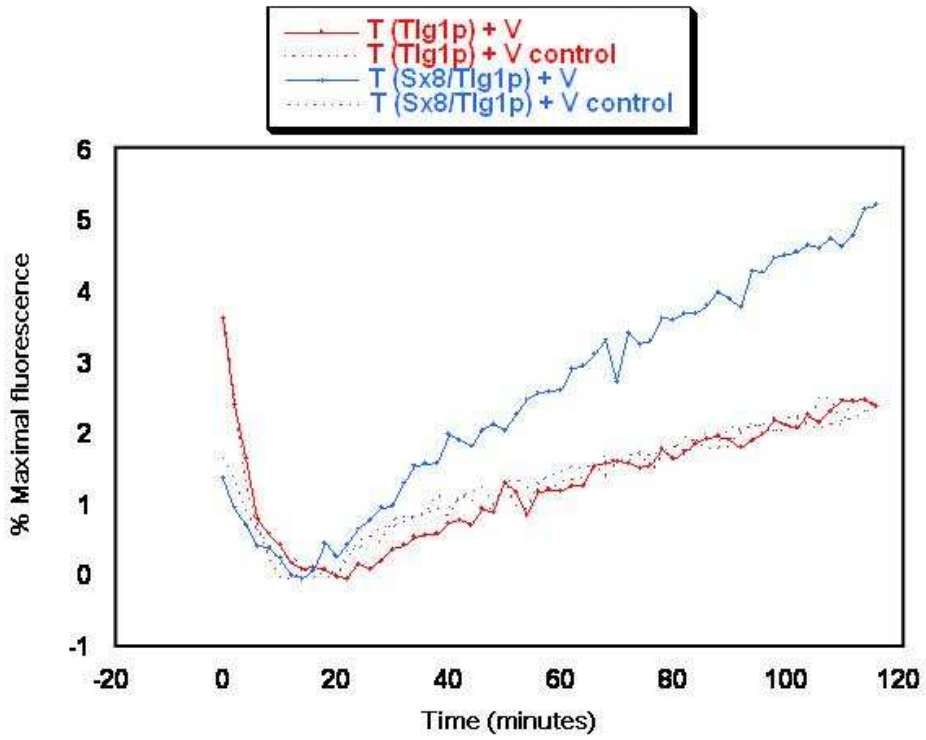

Figure 5.16 N terminal domain of Tlg1p SNARE motif inhibits fusion

Fusion assays were set up as described previously. 45 µl t-SNARE populations containing $Tlg2p_{37-397}$, Vti1p, and either Tlg1p (red) or Sx8 / Tlg1p (blue) were mixed with Snc2p containing donor liposomes. NBD fluorescence at 535 nm was measured at 2 minute intervals, data was normalised to a percentage of maximal fluorescence, determined by addition of n-dodecylmaltoside after 2 hours. Control reactions were set up with the addition of cytosolic Snc2p for 1 hour with Tlg1p and Sx8 / Tlg1p containing acceptor liposomes (red and blue dotted lines respectively). The raw fluorescence measurements for this experiment are presented in Appendix II.

5.3.6 Inhibition of SNARE mediated membrane fusion

The addition of cytosolic v-SNARE to competitively interact with t-SNARE complexes, thus inhibiting fusion of liposomes containing these t-SNAREs, is a necessary control to demonstrate that the fusion observed is SNARE dependent (Weber et al., 1998). A small gradual increase in fluorescence in these control reactions is still detected (dotted lines in Figure 5.15 and 5.16). I wanted to ensure that maximum inhibition was being achieved in these reactions. In order to do this, I wanted to test if varying concentrations of $Snc2p_{1-88}$ resulted in a concentration dependent inhibition. As we had previously been using 5 µl $Snc2p_{1-88}$ at 38.4 µM to inhibit fusion, we chose to add 1 µl and 10 µlof $Snc2p_{1-88}$ at 38.4 µM to the t-SNARE liposomes prior to mixing with v-SNARE liposomes. If the 5 µl $Snc2p_{1-88}$ we were using previously was only partially inhibiting fusion, we should see more inhibition with 10 µl and less with 1µl. As with previous experiments, $Snc2p_{1-88}$ samples were added to 45 µl t-SNARE containing liposomes and incubated for 1 hour at 4^oC. A_{200} buffer was added to ensure reactions contained the same volume. 5 µl v-SNARE liposomes were then added to each reaction, and the rate of fusion was measured as before and normalised to the maximal fluorescence achieved by addition of detergent. Figure 5.17 shows that 1 µl of $Snc2p_{1-88}$ is sufficient to block fusion to the levels that I have previously documented from the in the *in vitro* fusion assay, approximately 2% after 2 hours (solid red line). Increasing the volume of $Snc2p_{1-88}$ incubated with 45 µl of the same t-SNARE populations to 10 µl results in no additional inhibition of fusion (solid blue line).

An intrinsic property of the fluorescently labelled lipids in the donor population at 37^oC (e.g. induction of liposome disruption by an unknown factor) may account for this basal increase in fluorescence detected in the control experiments. To test this explanation, a control reaction containing only 5 µl of the Snc2p containing donor liposomes was prepared, and again A_{200} buffer was added to make all volumes equal. Donor liposomes alone do not result in any fluorescence (Figure 5.17, black dotted line), so we can exclude liposome lysis or any artefact associated with the donor liposomes alone causing this basal level of fusion observed.

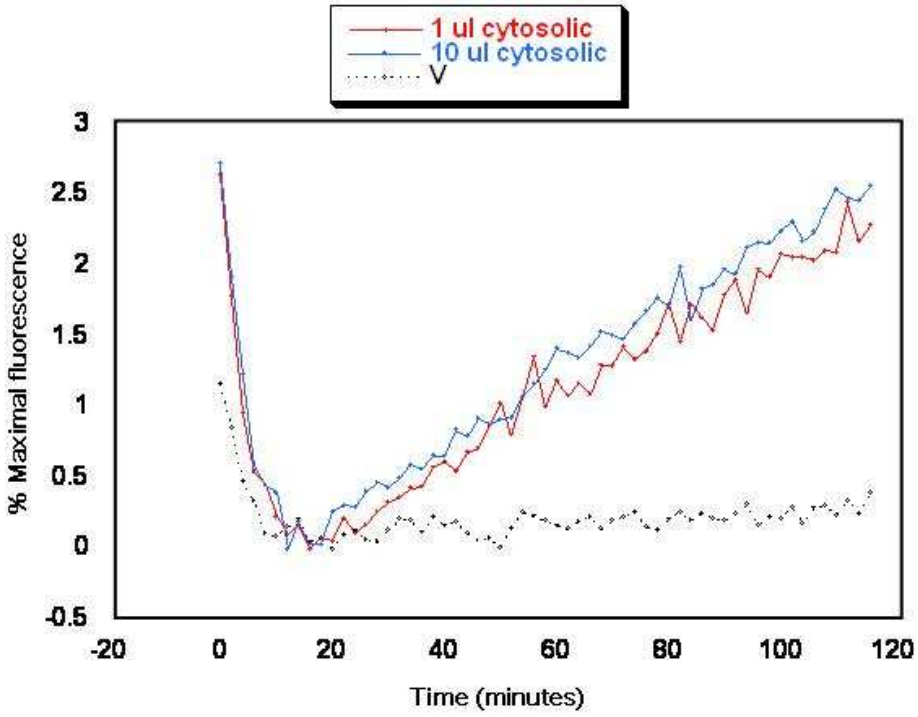

Figure 5.17 Optimising cytosolic Snc2p$_{1-88}$ control reactions

Fusion assays were set up as described previously. 45 µl of liposomes containing reconstituted Tlg2p$_{37-397}$, Vti1p, Sx8 / Tlg1p were incubated with 1 µl or 10 µl cytosolic Snc2p$_{1-88}$ for 1 hour at 4°C to inhibit complex assembly. 5 µl of Snc2p containing donor liposomes was then added to each reaction. A third reaction containing only 5 µl Snc2p liposomes and 55 µl A$_{200}$ buffer was also prepared in a separate well. NBD fluorescence at 535 nm was measured. Graph shows fluorescence data normalised to a maximum determined by addition of detergent to achieve maximum fluorescence. Blue and red lines represent fusion of yeast SNARE liposomes previously inhibited with 1 µl or 10 µl Snc2p$_{1-88}$ respectively. Black dotted line depicts fluorescence of donor liposomes alone over 2 hours at 37°C. The raw fluorescence measurements for this experiment are presented in Appendix II.

In order to ascertain if this basal level of fusion observed in control reactions occurred through some non-SNARE mediated fusion event, fusion reactions mixing proteoliposomes and empty liposomes were prepared. 45 µl of either t-SNARE (T) or empty (T*) acceptor liposomes were incubated with 5 µl of both v-SNARE (V) and empty (V*) donor liposomes. Assays were run as previously described. Figure 5.18 shows no fusion occurs between Tlg2p$_{37-397}$, Vti1p, Sx8 / Tlg1p and empty donor liposomes (blue line) or Snc2p and empty acceptor liposomes (red line). Both empty liposome controls show a basal rate of fusion which correlates with the control reaction previously incubated with Snc2p$_{1-88}$ to inhibit fusion (black dotted line). We then assume the basal rate is

representative of maximum inhibition achieved in our control reaction and is an unavoidable artefact from the assay conditions. We consequently assume SNARE inhibition is maximised by addition of cytosolic $Snc2p_{1-88}$ in our previous experiments, and fusion above this level represents the fusogenic effects of the SNARE proteins.

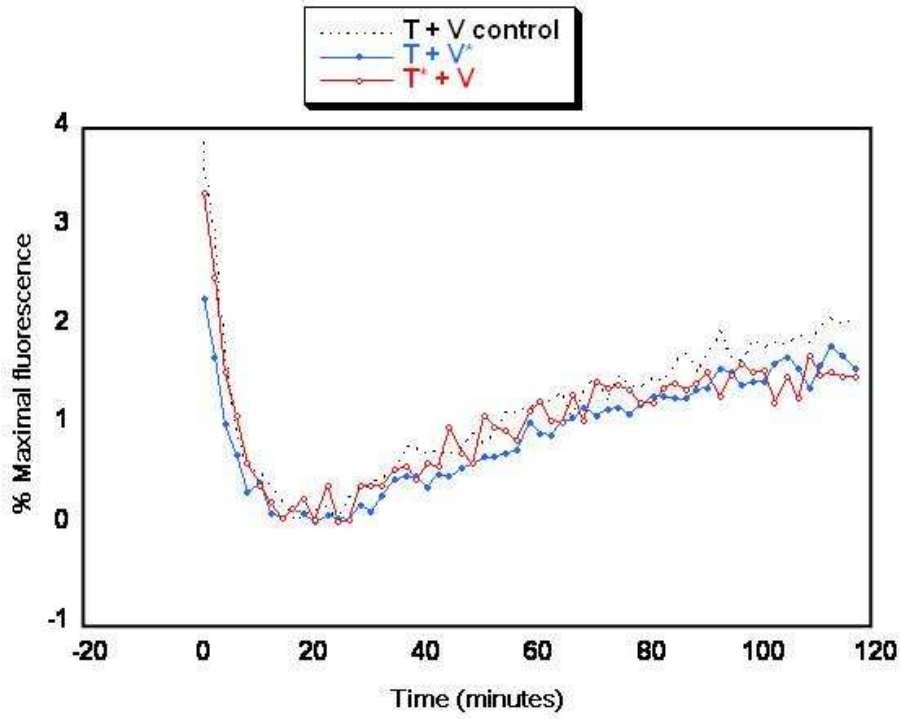

Figure 5.18 Control fusion assay with liposomes lacking SNARE proteins

Fusion assays were set up as described previously. 45 µl of liposomes containing reconstituted $Tlg2p_{37-397}$, Vti1p, Sx8 / Tlg1p were incubated with 5 µl cytosolic $Snc2p_{1-88}$ for 1 hour at 4°C as a negative control. Fusion reactions containing 45 µl t-SNARE with 5 µl empty donor liposomes (V*) or 45 µl empty acceptor (T*) and 5 µl Snc2p donor liposomes were incubated at 37°C; NBD fluorescence at 535 nm was measured. Graph shows fluorescence data normalised to a maximum determined by addition of detergent to achieve maximum fluorescence. The black dotted line depicts fluorescence of control reaction previously incubated with $Snc2p_{1-88}$. Blue and red lines represent fusion of yeast SNARE liposomes with empty donor and acceptor liposomes respectively. The raw fluorescence measurements for this experiment are presented in Appendix II.

5.3.7 Addition of Vps45p to in vitro fusion assay

Firstly, to introduce the SM protein Vps45p into the fusion assay directly, we set up reactions (including controls) as previously described: 45 µl of t-SNARE liposomes pre-incubated with 5 µl v-SNARE liposomes overnight at 4°C, to allow complex formation. Reactions were then incubated in the presence or absence of 80 µl C terminally His_6 tagged Vps45p at a concentration of 30.1 µM. The rate of fusion was measured as described previously, and compared to the maximal signal determined by liposome disruption with detergent. Figure 5.19 shows the NBD fluorescence measurements. Unfortunately the fusion reaction lacking SM protein showed no fusion above that of the cytosolic control (compare solid and dotted red lines). This has been observed previously, but we have not ascertained the exact cause. Certainly liposomes stored at 4°C for more than several days appear to lose their fusogenic capabilities, possibly due to degradation of proteins reconstituted in the liposomes; there are possibly other contributory factors that result in no fusion that we have yet to identify. All reaction volumes for fusion assays are identical; this suggests that dilution of the liposomes does not affect their ability to fuse. The reaction containing Vps45p does show elevated levels of fusion (solid blue line), that may suggest fusion has been stimulated above the basal rate in these reaction conditions, but without a control reaction resulting in fusion we cannot make these assumptions.

A second approach was also used to incorporate Vps45p into the fusion assay. 45 µl t-SNARE liposomes were incubated with 80 µl C terminally His_6 tagged Vps45p or Munc18c for 24 hours at 4°C. We thought it necessary to include a control reaction containing a non-cognate SM protein, so a C terminally His_6 tagged version of Munc18c was expressed from pKIM001 and purified as described in section 2.3.4.1. This was primarily because it is known that Vps45p can interact directly with cytosolic Snc2p *in vitro* (Carpp et al., 2006). Since this was likely during an overnight incubation, we feared this would invalidate the control reaction. As before, a control was set up incubating 45 µl t-SNAREs with cytosolic $Snc2p_{1-88}$ before the 24 hour incubation step. A_{200} buffer was added to reactions not containing SM proteins, so that all reactions contained an equal volume. Each reaction was then heated to 37°C before addition of 5 µl v-SNARE liposomes. NBD fluorescence was measured as before and compared to the maximum signal, determined by addition of detergent. Figure 5.20 shows these results. There appears to be no difference in the fusion reactions containing only buffer (red solid line) or Vps45p (blue solid line). The control reaction is greater than we have observed for

previous cytosolic control reactions (red dotted line), possibly fusion has not been inhibited to its maximum in this reaction. Addition of the control SM protein also appears to have no effect (green solid line); it is slightly less than the reactions containing Vps45p and buffer. These experiments would have to be repeated to ascertain if this reduction in rate of fusion is significant or not.

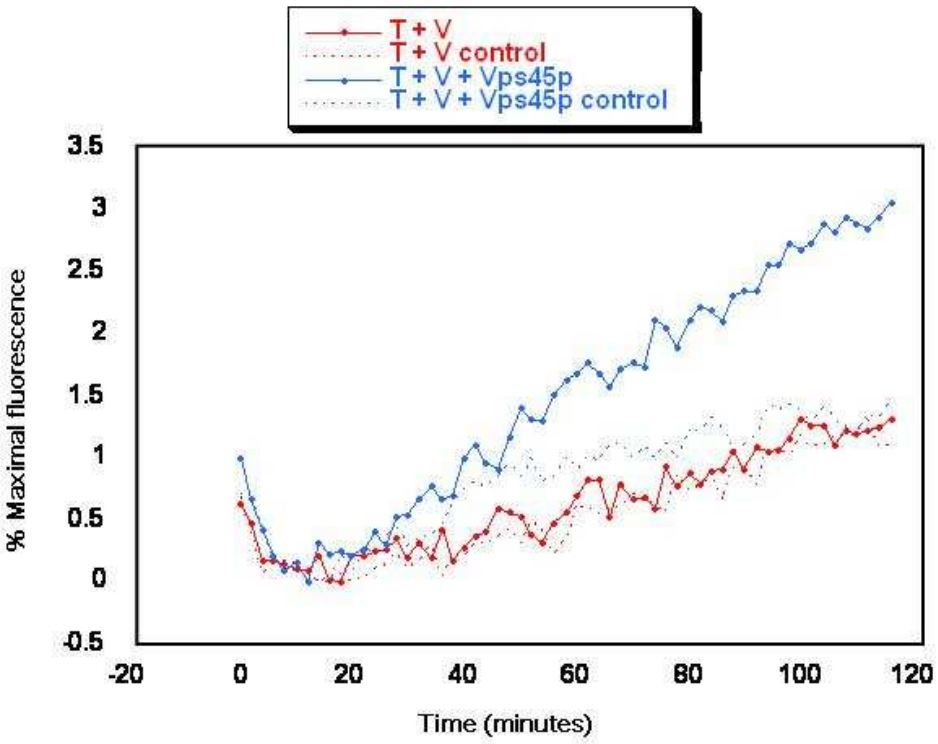

Figure 5.19 Addition of Vps45p to in vitro fusion assay

Fusion assay reactions were prepared consisting of 45 µl t-SNARE liposomes containing $Tlg2p_{37-397}$, Vti1p, Sx8 / Tlg1p and 5 µl v-SNARE liposomes containing Snc2p. Liposome populations were incubated overnight at 4°C to allow complex formation. The reaction mixtures were then incubated with either 80 µl Vps45p (at concentration 26.4 µM) or 80 µl A_{200} buffer; reactions were then incubated at 4°C for a further 3 hours. As for previous experiments, identical control reactions were prepared, in which 5 µl cytosolic $Snc2p_{1-88}$ was incubated with the t-SNARE liposomes for 1 hour at 4°C, before addition of v-SNARE liposomes. Liposomes were then incubated at 37°C for 10 minutes, before NBD fluorescence at 535 nm was measured every 2 minutes. Graph shows fluorescence data normalised to a maximum determined by addition of detergent. Reactions containing only buffer are shown in red, those pre-incubated in the presence of Vps45p are shown in blue. The control reactions of each assay are presented as dotted lines. The raw fluorescence measurements for this experiment are presented in Appendix II.

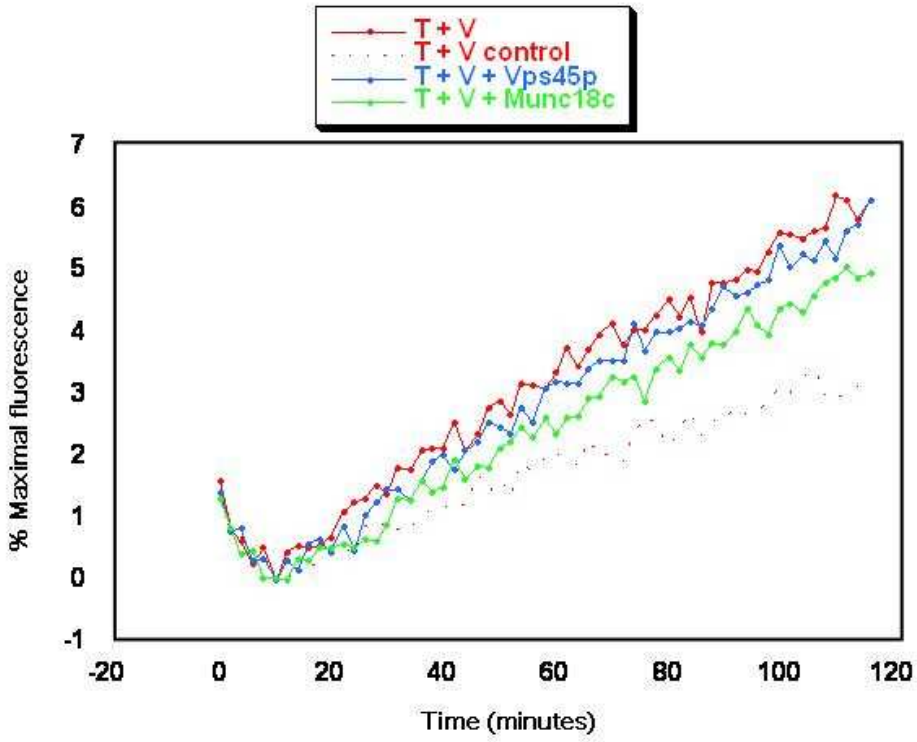

Figure 5.20 Addition of Vps45p and Munc18c to fusion assay

Fusion assay reactions were prepared consisting of 45 µl t-SNARE liposomes containing $Tlg2p_{37-397}$, Vti1p, Sx8 / Tlg1p, a control reaction containing 5 µl cytosolic $Snc2p_{1-88}$ was incubated with 45 µl t-SNARE liposomes for 1 hour at 4°C. 80 µl of either A_{200} buffer, Vps45p (25 µM) or Munc18c (25 µM) was added to each reaction (75 µl A_{200} buffer was added to the cytosolic control reaction, so all volumes were equal), and incubated for 24 hours at 4°C. Fusion reactions were heated to 37°C before 5 µl of v-SNARE liposomes was added to each reaction. Fusion reactions were then incubated at 37°C and NBD fluorescence at 535 nm was measured every 2 minutes. Graph shows fluorescence data normalised to a maximum determined by addition of detergent. The reaction lacking SM protein (solid line), and its control pre-incubated with cytosolic $Snc2p_{1-88}$ (dotted line) are shown in red. The reactions pre-incubated with Vps45p and Munc18c are shown in blue and green respectively. The raw fluorescence measurements for this experiment are presented in Appendix II.

5.4 Chapter summary

This Chapter has discussed the development of an *in vitro* fusion assay, which has been successfully used to demonstrate that versions of the SNARE proteins localised to the TGN / endosomal system of *S. cerevisiae* (Tlg2p$_{37-397}$, Vti1p, Sx8 / Tlg1p chimera) are capable of fusing synthetic liposomes. In addition to this, we have confirmed the finding that t-SNARE complexes containing full length Tlg1p are incapable of facilitating fusion of synthetic membranes (Paumet et al., 2005). Our preliminary attempts to incorporate Vps45p into the fusion assay have not revealed any functional role the SM protein may have. Addition of Vps45p to the t-SNARE liposomes overnight was seen to have no effect on fusion. A stimulatory effect was observed when Vps45p was added to liposomes that had already been pre-incubated to allow complex formation, but this result was inconclusive as the standard reaction did not result in fusion. It is possibly that we need to optimise the conditions of Vps45p addition to the liposome fusion assay. Also, it is important to note that the version of Tlg2p we were using did not contain the first 36 N terminal residues, so it is unable to bind to Vps45p via mode-2 binding. An obvious next step would be to reconstitute Vps45p pre-bound to Tlg2p, or indeed to Snc2p, into liposomes.

Chapter VI

Discussion

The work presented in this thesis was aimed at understanding the regulation of SNARE dependent membrane fusion, using the yeast endosomal system as a model. To this end, I have demonstrated several key features of the syntaxin homologue Tlg2p, and the SM protein Vps45p, which are important for fusion.

6.1 Discussion of results

In Chapter III, I presented data in support of our hypothesis that Tlg2p forms a closed conformation which is inhibitory to complex formation. This is contentious, as it disagrees with NMR data demonstrating that no intramolcular interactions were observed in Tlg2p, suggesting that it can not adopt a closed conformation (Dulubova et al., 2002). One restriction of the recombinantly produced fragments used in the NMR analysis is that due to the insolubility of the full length protein, truncated versions of Tlg2p were used (Dulubova et al., 2002). NMR analysis of Tlg2p fragments containing residues 60 - 283 (representing the entire cytosolic domain) and residues 65 - 192 (representing the Habc domain) were compared to see if any difference in structure could imply an intramolecular interaction (Dulubova et al., 2002). Unfortunately, these fragments lack more than half the SNARE motif and the carboxy-terminal residues preceding the transmembrane domain, which may be important for the stabilisation of a closed conformation. Existing evidence for the N terminal domain of Tlg2p playing an inhibitory role include the finding that removal of the Habc domain alleviates the requirement for SM protein Vps45p to allow complex formation (Bryant and James, 2001). My data are in agreement with this, as versions of Tlg2p lacking the Habc domain form complexes more readily than the full length version *in vitro* (Figure 3.3), suggesting these *in vivo* observations (Bryant and James, 2001) are directly due to the lack of the Habc domain.

The most obvious explanation for a conformation of Tlg2p that has an inhibitory effect on complex formation, is that Tlg2p forms a closed conformation, akin to that of its homologues Sx1a (Dulubova et al., 1999, Misura et al., 2000) and Sso1p (Carr et al., 1999, Munson et al., 2000), as outlined in our hypothesis. Our attempts to identify a direct interaction between the Habc domain and the SNARE domain of Tlg2p using a yeast-2-hybrid assay proved unsuccessful; this could be explained by the fragments used not being sufficient to stabilise a closed conformation. Also, the concentrations of each domain produced in the yeast-2-hybrid assay may be too low to detect an interaction, as the

effective concentration of the two domains situated on the same polypeptide (as it occurs *in vivo*), is much greater than can be achieved when they are produced individually.

The closed conformation of Sx1a is intrinsically linked to the SM protein, Munc18a, which interacts directly with Sx1a in this conformation that is incompatible with SNARE complex assembly (Dulubova et al., 1999, Misura et al., 2000). Studies investigating the inhibitory domain of Tlg2p must therefore also examine its interaction with the SM protein, Vps45p. A study looking at the interaction of Sx16, a mammalian homologue of Tlg2p, with mammalian Vps45 concluded that Sx16 can adopt a closed conformation which interacts with Vps45 (Burkhardt et al., 2008). This study used ITC to demonstrate that the apparent affinity of the entire cytosolic domain of Sx16 is greater than that of the N terminal peptide alone (the portion that facilitates mode-2 binding) (Burkhardt et al., 2008). A similar effect was observed in quantitative analysis of yeast-2-hybrid results testing the affinity of Vps45p for various truncations of Tlg2p, where a stronger reporter signal is detected for the full length cytosolic domain than that of the N terminal peptide alone; this observation was not commented on by the authors (Dulubova et al., 2002).

More direct evidence for a Tlg2p closed conformation was produced using size exclusion chromatography, demonstrating that Vps45p can interact with a Tlg2p fragment lacking the N terminal peptide, through an interaction distinct from mode-2 binding (Furgason et al., 2009). This study went on to further characterise the affinity of this other binding mode with Vps45p, using a quantitative competition EMSA technique. These experiments estimated the affinity of the N terminal domain of Tlg2p (residues 1 - 33) for Vps45p to be 35 ± 3 nM and that of the C terminal binding site to be 280 ± 4 nM (Furgason et al., 2009). Mutant versions of Tlg2p, predicted to either disrupt mode-1 binding (I285A) or to produce a version of Tlg2p that cannot adopt a closed conformation (K134A/K137A/K163A), were created based on homology to other known mutants, (Burkhardt et al., 2008, Wu et al., 1999) and (Munson et al., 2000, Munson and Hughson, 2002), respectively (Furgason et al., 2009). When these mutants were combined with the N terminal truncation ($Tlg2p_{\Delta 1\text{-}33}$), no apparent affinity was observed, suggesting that the second C terminal binding site of Tlg2p corresponds to a closed conformation (Furgason et al., 2009). Interestingly, the N terminal binding mode of Tlg2p competes with the closed conformation for Vps45p binding (Furgason et al., 2009), the exact functional relevance of this remains to be understood.

Understanding the significance of Vps45p binding to Tlg2p by these two distinct mechanisms may be advantageous to understand SM protein function in general. Abrogation of Vps45p binding through either a mode-1 interaction with the closed conformation, or a mode-2 interaction with the N terminal peptide had no effect on the cell's ability to correctly sort the vacuolar hydrolase CPY (Figure 3.10). However, an essential role of Vps45p was shown when both binding modes were abolished, which resulted in defects in the trafficking pathway of CPY (Figure 3.10). The finding that Vps45p relieves the kinetic delay on complex assembly experienced by full length Tlg2p *in vitro* (Figure 3.4), suggests that Vps45p has a direct role in SNARE complex assembly preceding fusion: priming SNAREs for assembly by activating Tlg2p. This supports our hypothesis that Vps45p facilitates a conformational switch in Tlg2p, whereupon the Habc domain disengages with the SNARE domain, rendering it accessible to the cognate SNARE partners.

Chapter IV details my analysis of Vps45p's interaction with the v-SNARE Snc2p (Carpp et al., 2006). I used a yeast-2-hybrid system to confirm the interaction, shown in Figure 4.3, and further developed this assay to serve as a tool for mapping the binding sites of Vps45p to the Snc2p SNARE motif (discussed in section 6.2). It is noteworthy that addition of the C terminal GFP tag to Vps45p reduced the levels of reporter gene activation in the assay, suggesting a weaker interaction than untagged Vps45p (Figure 4.3). This may be due to the proximity of the GFP tag to the Snc2p binding site of Vps45p. Introducing mutation in this area first may be the fastest course of action to determine the essential residues for the interaction.

The interaction between Vps45p and Snc2p was also confirmed using an EMSA assay (Figures 4.10 & 4.11). The EMSA assay was prepared with the aim of accurately determining the affinity of the interaction between Snc2p and Vps45p, as demonstrated for Tlg2p binding to Vps45p (Furgason et al., 2009). This was not possible, as we were unable to obtain the high concentrations of recombinant protein required to accurately measure this low affinity interaction. We can however estimate the K_d of the interaction to be approximately 10 µM. This is a weaker interaction than either of the two binding modes between Tlg2p and Vps45p (Furgason et al., 2009). This is consistent with our model: Vps45p travels to the site of membrane fusion on the transport vesicle through its interaction with Snc2p and is then transferred to Tlg2p in a closed conformation (discussed in section 6.3). This model predicts that Vps45p would have a greater affinity for Tlg2p than Snc2p.

In conjunction with the EMSA assay, I attempted a fluorescence polarisation (FP) assay (Park and Raines, 2004), using similar binding conditions as described in the preparation of the EMSA (Chapter IV). The FP assay is more sensitive than the EMSA, and has the advantage of being able to record measurements in solution. This would eliminate any factor the gel matrix has on protein-protein interactions or protein mobility. The principle of the assay is to distinguish unbound labelled protein from that which is in complex with another protein (Heyduk et al., 1996). This can be achieved by measuring the fluorescence anisotropy of the samples in solution; the Vps45p-Snc2p complex will have a detectably slower rotational motion value than uncoupled Snc2p. The size difference between the two proteins is favourable for these measurements. Unfortunately, these results were inconclusive, but the method could potentially be used in the future to accurately measure the K_d of the Vps45p-Snc2p interaction. Other possibly avenues of investigation to achieve this goal are discussed in section 6.2.

As competition experiments could not be used in the EMSA assay, we used *in vitro* competition binding studies to investigate the relative affinities of Vps45p for Tlg2p and Snc2p. In agreement with a previous report, Tlg2p can displace binding of Snc2p to Vps45p (Carpp et al., 2006). Further to this, I demonstrated that the displacement of Snc2p occurs in a concentration dependent manner, and that the mode-2 interaction is dispensable for this displacement (Figure 4.13). This is also in agreement with a model whereby Vps45p is transferred from Snc2p to the higher affinity binding of the closed conformation of Tlg2p (mode-1).

My final results Chapter deals with developing an *in vitro* fusion assay. I have successfully incorporated the SNARE proteins of the yeast endosomal system into synthetic liposomes, and demonstrated that they are capable of fusing the liposomes (Figure 5.15). Further to this, in agreement with a previous report (Paumet et al., 2005), I have shown that the N terminal portion of the Tlg1p SNARE domain imposes a level of negative regulation on fusion (Figure 5.16). Using a chimeric protein, that replaces the N terminus of the Tlg1p SNARE domain with that of the mammalian homologue, Sx8, relieves this inhibition (Figure 5.16).

I spent considerable time and effort trying to optimise the *in vitro* assay, so that it can be used to investigate the role of Vps45p in membrane fusion. I have extensively characterised the proteoliposomes produced in the process, so that we can assess their lipid and protein content, and what orientation the proteins are in (discussed in section 5.3.3).

In addition to this we have estimated the size of the liposomes; ensuring populations are of similar size distribution to each other. This will also aide any "rounds of fusion" calculations, a physical parameter used to demonstrate the extent of fusion in donor vesicles (Parlati et al., 1999), which can now be calculated more accurately. I also had some trouble maximising the inhibition of the cytosolic control, but my observation that liposomes lacking SNARE proteins results in a small increase in fluorescence that can not be reduced any further in the control fusion reaction, suggests this is unavoidable (Figure 5.18).

My attempts to incorporate Vps45p into the assay have as yet been unsuccessful in yielding any functional data on its SNARE interactions. Addition of Vps45p to liposomes incorporated with SNARE proteins that had previously been allowed to form complexes at 4^{o}C was unsuccessful, but this may be have been due to the fluorescence equilibration I detect as the temperature is increased. There is a high fluorescence at the start of the assays, as the temperature is changed from 4^{o}C to 37^{o}C (Vicogne and Pessin, 2008). The neuronal Sx1a binds Munc18a via mode-2 during this stage, and enhances the rate of fusion (Shen et al., 2007). If Vps45p is having an effect on fusion at this stage, it will only do so for the first round of liposome fusion from the pre-docked samples. The first round of pre-docked liposomes containing the neuronal SNARE proteins occurs most significantly in the first 20 minutes (Shen et al., 2007). If this is the also the case in our system, the effect will be drowned out by the high fluorescence background experienced at the start of the assay. This is unavoidable, as the liposomes cannot be left to dock through SNARE interaction at 37^{o}C, as fusion will also occur.

Alternatively, as we are using a version of Tlg2p that cannot interact with Vps45p via a mode-2 interaction, maybe it cannot exert influence on the process. Or, possibly, our system differs from the exocytotic systems thus far characterised using the *in vitro* fusion assay (Scott et al., 2004, Shen et al., 2007). It has been shown previously that Vps45p dissociates from *trans*-SNARE complexes and then re-associates with the *cis*-SNARE complex after fusion (Bryant and James, 2003), so possibly the interaction between Vps45p and the SNARE complex by a mode distinct from mode-2 observed *in vitro* (Carpp et al., 2006) represents the *cis* complex, and Vps45p has no direct role on fusion *per se*. Functional analysis of the full length Tlg2p protein is required to differentiate between these possibilities.

Interestingly, the reaction that was prepared in presence of Vps45p resulted in fusion (Figure 5.19). We cannot say that this is an enhanced effect, as the standard reaction did not work; it may be standard fusion observed in the reaction containing Vps45p, and the basal fusion reaction did not work for some unknown reason.

I also attempted to incorporate Vps45p into the assay before complex formation. This did not result in any observable difference in the rate of fusion (Figure 5.20), but it is worth noting that addition of yeast Sec1p had a very marginal effect on increasing the rate of fusion, and it was only when the SM protein was reconstituted with the t-SNARE complex (Sso1p and Sec9p), that a 3 fold increase in the rate of liposome fusion was observed (Scott et al., 2004). My initial attempts to reconstitute Vps45p with the t-SNARE complex, or that of the v-SNARE Snc2p, resulted in vast amounts of precipitation and no detectable protein reconstitution. Also, it is again possible that the full length Tlg2p protein will have to be used in this manner to test the effect of Vps45p. These difficulties may require considerable work to overcome.

The physiological relevance of this *in vitro* fusion assay has been questioned, primarily due to its inability to replicate fusion at rates anywhere near those which must occur in the neuronal synapse (Chernomordik and Melikov, 2006, Rizo and Sudhof, 2002). Also, it has been suggested that the number of reconstituted SNARE proteins per liposome may not represent physiological conditions (Chernomordik and Melikov, 2006), however estimates of this number for the neuronal system are not agreed upon (Brunger, 2005, Dennison et al., 2006). Characterisation of proteoliposomes, such as those described in section 5.3.3, allows this information to be known prior to any fusion assays, so the results can be directly correlated, for example, to the amount of externally facing v-SNAREs in a donor liposome. Also, the protein to lipid content can be adjusted at the preparation stage, to increase or decrease the number of SNAREs per liposome. It has also been assumed that additional regulatory factors are required to allow fusion to occur at a faster rate (Weber et al., 1998), as there are many *in vivo* factors, such as the Rab and tethering protein families (discussed in sections 1.5.5 & 1.5.6) that are not represented in this system. This has been supported by one study that successfully incorporated the Rab-SNARE machinery necessary for mammalian endosomal traffic into liposomes, and demonstrated that fusion is more efficient with the entire complement of Rab-SNARE machinery than SNAREs alone (Ohya et al., 2009). Although the *in vitro* fusion assay is a simplified system, it does mimic both proteins and lipids involved with membrane fusion. This reductionist approach remains a useful tool to reveal data related to function of the factors involved.

6.2 Future work

In the light of a confirmed Tlg2p closed conformation (Furgason et al., 2009), it might be useful to repeat the competition binding experiments (Figure 4.13) with the mutants abrogated for mode-1 binding used in this study ($Tlg2p_{I285A}$ and $Tlg2p_{K134A/K137A/K163A}$), both alone and in combination with the mutants used to abrogate mode-2 binding ($Vps45p_{L117R}$ and $Tlg2p_{F9A/L10A}$). This would allow us to test if the mode-1 interaction of Tlg2p is necessary to displace Snc2p, as we know mode-2 is not important (Figure 4.13). These studies could reveal more about the importance of each binding mode, and would confirm our hypothesis that the Vps45p binding to Snc2p precedes its interaction with the closed conformation of Tlg2p.

We would also like to further characterise the Snc2p binding mode. As the EMSA proved an inappropriate technique to estimate the affinity of the interaction, the more sensitive Biacore SPR may be a better technique. One requirement of this method is to bind protein of interest to a chip, which is subsequently flushed with the interacting protein partner (Fivash et al., 1998). The native cysteine in Snc2p, at residue 94, would be ideal to immobilise the protein on a chip (O'Shannessy et al., 1992) via a thiol reaction similar to the Alexa 488 labelling reaction we carried out for the EMSA technique (Section 4.3.2.3). Competition binding experiments could also be done through the Biacore technique. We hope to carry out these experiments in collaboration with Dr. Sharon Kelly, University of Glasgow, UK. My initial attempts to purify Vps45p either without GroEL, or to separate the GroEL by more extensive purification, proved unsuccessful. Optimisation of the ion exchange chromatography could result in relatively rapid production of the necessary proteins for these Biacore experiments. ITC is another more sensitive technique that has been recently used to estimate the affinity of SM protein binding (Burkhardt et al., 2008), which could be used to investigate the relative affinity of the Vps45p-Snc2p interaction.

The yeast-2-hybrid assay discussed in Chapter IV is now ready to be moved into a different host strain that will allow a reverse selection to identify binding partners that do not interact. Several reverse-2-hybrid techniques have been developed, the most common of which uses *URA3* as a positive selection forward assay, then uses the toxic 5-fluororotic acid (5-FOA) drug to positively select for mutants that no longer interact (Vidal et al., 1996b). We attempted to do this with the yeast strains MaV103 and Mav203 (Vidal et al., 1996a), and use the reconstitution of the transcriptional machinery to activate the *URA3* gene in these strains. 5-FOA is toxic to cells in the presence of uracil, as it converts uracil

to 5-fluro-deoxyuracil, which is toxic to yeast cells (Boeke et al., 1987). Therefore, 5-FOA can be used to counter select yeast harbouring versions of Vps45p unable to interact with Snc2p. Truncation mutants can be avoided by prior screening for the C terminal GFP tag that ensures the entire *VPS45* gene has been translated. Unfortunately the *URA3* selection in the forward assay did not work consistently, so we are in search of a new reverse screen. Other systems involve using different agents that allow counter selection, such as 3-aminotriazole (3-AT): a drug which competitively interacts with a critical enzyme in the biosynthetic pathway of histidine (Walhout and Vidal, 2001). The best course of action for us is to use a yeast strain that allows selective incorporation of our constructs based on parent vectors pACT2 and pGBKT7. This would be prudent as the forward assay has been shown to work well and consistently (Figure 4.3), also, the full length mutants will be easily identifiable by the C terminal GFP_{S65T} tag, that has been successfully incorporated into both AD and BD versions of Vps45p and shown to express well (Figure 4.4). Alterations of selective markers or genetic modifications to a yeast strain genome are both difficult and time consuming tasks which could be avoided by choice of strain. We have recently identified a model which could work with our system, the strain CY770 that contains a mutant *cyh2* gene (which is resistant to cyclohexamide), could be used in conjunction with a plasmid that confers sensitivity to the drug through a *GAL* activated promoter (GALUAS-*CYH2*) (Young et al., 1998). Resistance to this drug would allow us to isolate hybrid combinations that no longer interact. Sequence analysis of a library of mutants that can no longer interact should indicate areas of the Vps45p molecule that are important for this interaction. Further, site specific, mutations would then allow us to produce recombinant protein that was abrogated for this mode of binding. We could then use this mutant, in conjunction with other mutant proteins abrogated for other binding modes, in various assays (including the *in vitro* fusion assay; discussed in Chapter V) to help us appreciate the significance of Vps45p binding SNAREs by multiple, distinct binding modes.

We would like to do several things with the *in vitro* fusion assay, primarily to incorporate Vps45p in some way that will reveal its functional significance. Our attempts thus far to do so have been unsuccessful, but sufficient time has not been spent to optimise conditions to a satisfactorily degree; further investigation could still prove fruitful. Addition of Vps45p that has been more extensively purified (as is necessary for Biacore SPR analysis) could also be beneficial to these studies. Also, optimisation of the purification and reconstitution of full length version of Tlg2p (containing the first 36 residues), allowing its

incorporation into liposomes, would allow us to directly test if Vps45p binding via mode-2 has any effect on membrane fusion.

Taking the arguments against the physiological relevance of the *in vitro* fusion assay into account (section 6.1), we still consider it a valuable tool to reveal the functional relevance of certain aspects of our model system. The use of our existing mutant proteins versions could still reveal the importance of the various Vps45p binding modes. Testing the ability of versions of Tlg2p both with the Habc domain truncated and a constitutively open protein could show us if the N terminal Habc domain / closed conformation has a reduced rate of fusion. Also, versions of Vps45p abrogated for mode-1, mode-2 and the ill-defined Snc2p binding modes would allow us to test the role of each mode in the actual fusion event. If experiments are correctly controlled internally, we see no reason why this type of data would not contribute to our overall understanding of membrane fusion.

6.3 Proposed model

A model for the proposed series of events resulting in fusion of trafficked vesicles at the yeast TGN / early endosome is outlined in Figure 6.1. The novel interaction between Vps45p and Snc2p (Carpp et al., 2006; Chapter IV) allows the transportation of the SM protein to the target membrane harbouring the t-SNARE proteins. To ensure non-functional SNARE complexes are not formed, the Tlg2p molecule is in its closed conformation, with the Habc domain folded back and interacting with the SNARE motif (Chapter III; Furgason et al., 2009). As Vps45p has a greater affinity for the closed conformation of Tlg2p (K_d = ~ 280 nM; Furgason et al., 2009) than Snc2p (K_d = ~1,000 nM; Chapter IV), the SM protein is transferred to the Tlg2p molecule. Mode-2 binding of Tlg2p is not required for it to displace Snc2p (Chapter IV), so presumably Vps45p interacts with Tlg2p through a mode-1 interaction. As Vps45p cannot bind to Tlg2p and Snc2p at the same time (Carpp et al., 2006), as would be predicted for the simplest bridging hypothesis (Peng and Gallwitz, 2004), we speculate additional *in vivo* factors may work in concert with the proteins to allow the transfer. It seems likely other proteins would be involved at this step, the GARP complex for example (Oka and Krieger, 2005), due to the temporal and spatial regulatory requirements of these distinct binding modes. Upon binding, Vps45p then facilitates a conformational change in Tlg2p, relieving the inhibitory effect of the Habc domain on that of the SNARE domain and allowing it to form

a ternary complex with Vti1p and Tlg1p (Bryant and James, 2001). We are unsure of the fate of Vps45p at this juncture, but based on the Sx1a-Munc18a model, we propose that Vps45p interacts with the SNARE partners at this point (through a mode-2 interaction; K_d = ~35 nM), possibly enhancing the rate of fusion. As the N terminal binding site and the binding site of the closed conformation compete for interaction (Furgason et al., 2009), we must assume there are additional factors that allow the binding to the closed conformation to be favourable in the first instance. Tlg2p differs from Sx1a in that its SM protein competes for these two binding modes (Furgason et al., 2009); we plan to use the *in vitro* fusion assay to test if Vps45p has an effect on the fusion rate, which would be suggestive of an interaction at this stage. Mutant versions could then be used to test if, like Sx1a (Shen et al., 2007), Tlg2p binds via mode-2 at this point. As the vesicle containing Snc2p, that delivered Vps45p to the inactive Tlg2p molecule, is in close proximity, a *trans*-SNARE complex is then favourable; this allows the vesicle to dock at the target membrane site. At this point Vps45p dissociates from the complex (Bryant and James, 2003). After this, the *trans*-complex facilitates fusion of the opposing membranes. Vps45p re-associates with the membrane through an interaction (possible mode-3 binding) with the *cis*-complex (Bryant and James, 2003); which may have been the *in vivo* scenario replicated by the *in vitro* binding experiments demonstrating that Vps45p associates to SNARE complexes via a mode distinct from mode-2 (Carpp et al., 2006). This interaction may be associated with a distinct role from the earlier events in the fusion process, possibly associated with the disassembly process, which the other yeast SM protein, Sly1p, has been implicated in (Kosodo et al., 2003).

The production of Vps45p mutants abrogated in Snc2p binding (as discussed for the yeast-2-hybrid reverse screen) would allow us to check if this binding *in vivo* functions to correctly traffic vesicles to the endosomal membranes. Also, I have not discussed the role Vps45p plays in stabilising endogenous levels of Tlg2p, by protecting it from proteasomal degradation (Bryant and James, 2001, Carpp et al., 2007). I have hinted at additional regulatory factors having roles in this model, one such example could be phosphorylation. It has been shown *in vitro* that Tlg2p can be phosphorylated, which prohibits its entry into SNARE complexes (Gurunathan et al., 2002). It might be that this is a sublevel of regulation, which works in concert with Vps45p to regulate both Tlg2p levels and its proclivity to form SNARE complexes.

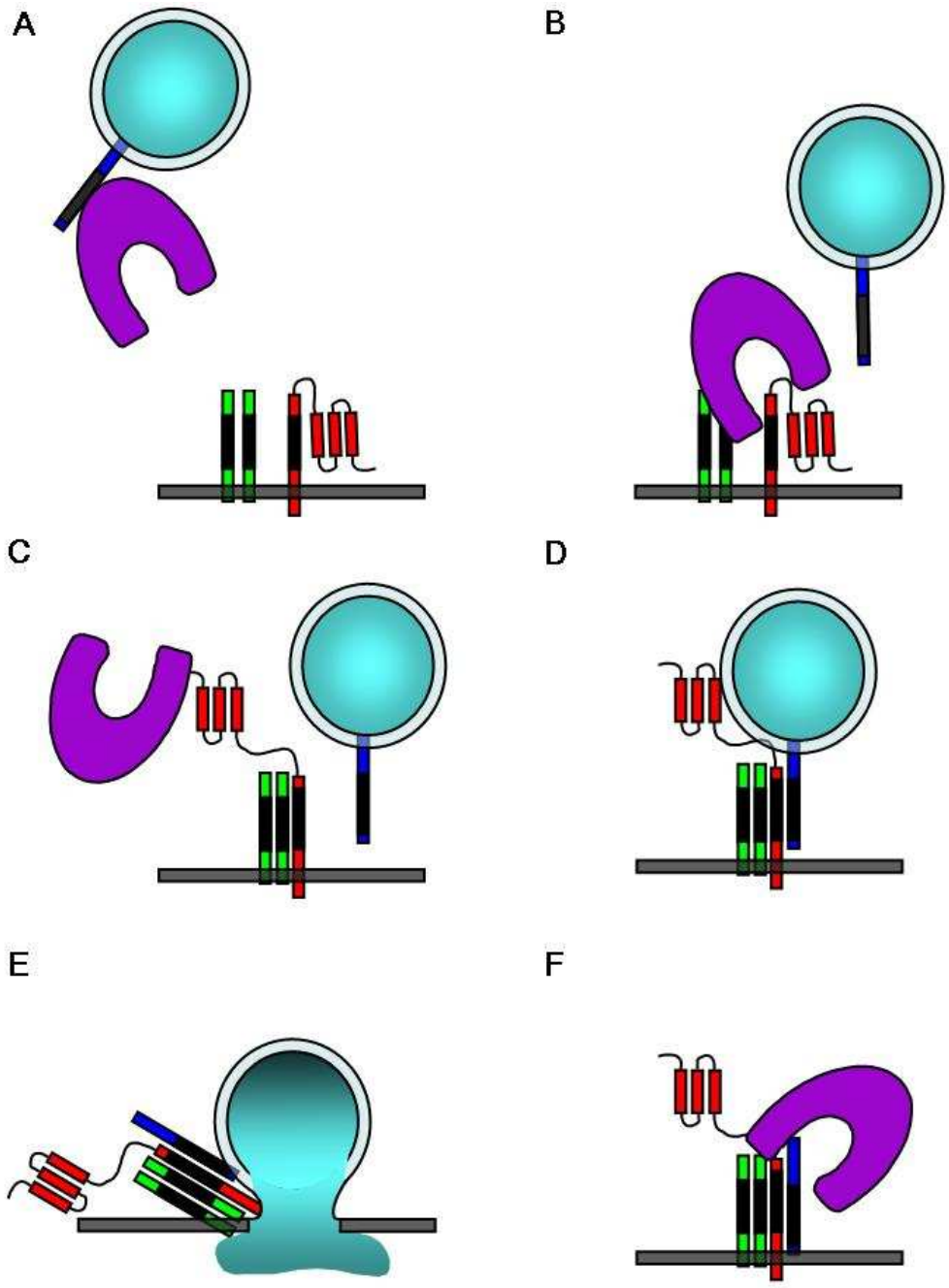

Figure 6.1 Proposed model

(A) The weak affinity interaction between Vps45p (purple) and Snc2p (blue) anchored to a transport vesicle, localises the SM protein to target membrane. Tlg2p (red) is in a closed conformation at the target membrane, with the Habc domain interacting with the SNARE motif (black); and not interacting with cognate t-SNAREs Vti1p and Tlg1p (both in green). *(B)* Upon its arrival at the target destination, Vps45p detaches from Snc2p and interacts with Tlg2p via a mode-1 interaction. This binding results in a conformational switch in Tlg2p, releasing the Habc domain from the SNARE domain. *(C)* The Tlg2p SNARE domain is free to form a ternary complex with Vti1p and Tlg1p; Vps45p binds Tlg2p via mode-2 interaction. *(D) trans*-SNARE complex formation, docking the vesicle at then target membrane; Vps45p dissociates at this point. *(E)* SNARE complex facilitates fusion of opposing membranes, releasing cargo (turquoise). *(F)* Vps45p interacts with the *cis*-SNARE complex through a mode distinct from mode-2 (possibly mode-3). Complex is disassembled; SNAREs are recycled and ready for another round of fusion *(A)*.

Chapter VII

Appendices

7.1 Appendix I: Dynamic light scattering raw data

Data readout from the DynaPro 801 Dynamic light scattering instrument was analysed using dynamics V2 software (Wyatt Technology Corp.). Readout from hydrodynamic radii estimations made on t-SNARE acceptor liposomes and v-SNARE donor liposomes.

Dynamic light scattering measurements for Tlg2p$_{37-397}$,Vti1p, Sx8/Tlg1p liposomes

Msr#	Time(s)	Temp(C)	Count Rate	Ampl	Diff Coeff	Radius(nm)	Polyd(nm)	PolydIndx	MW(KDa)	%Mass	Baseline	Sos Error
1*	0.0	34.3	1262193	1.149	65.8	46.1	14.1	0.09	3.13e+004	100.0	2.006	6.10
2*	53.0	34.3	1247888	1.123	67.8	44.7	11.8	0.07	2.91e+004	100.0	2.002	6.42
3*	107.0	34.1	1217924	1.156	67.3	44.8	8.71	0.04	2.93e+004	100.0	2.005	2.99
4*	162.0	34.3	1209813	1.169	66.6	45.5	12.9	0.08	3.05e+004	100.0	1.994	5.73
5*	216.0	34.3	1203717	1.167	66.2	45.8	11.0	0.06	3.09e+004	100.0	2.005	4.17
6*	271.0	34.3	1161284	1.155	68.6	44.2	15.2	0.12	2.83e+004	100.0	1.995	5.16
7*	323.0	34.3	1185647	1.152	66.0	45.9	16.5	0.13	3.11e+004	100.0	2.001	4.18
Aves:												
Mono		0.0	0	0.000	0.000	0.000	0.000	0.00	0.000	100.0	0.000	0.000
Bi-1		0.0	0	0.000	0.000	0.000	---	---	0.000	0.0	0.000	0.000
Bi-2				0.000	0.000	0.000			0.000	0.0		

Figure 7.1 DLS raw data for t-SNARE liposome size estimations

Data print out from the dynamic light scattering measurements made to calculate the hydrodynamic radii of t-SNARE acceptor liposomes.

Dynamic light scattering measurements for Snc2p liposomes

Msr#	Time(s)	Temp(C)	Count Rate	Ampl	Diff Coeff	Radius(nm)	Polyd(nm)	PolydIndx	MW(KDa)	%Mass	Baseline	Sos Error
1	0.0	34.2	977852	0.738	69.0	43.8	3.14	0.01	2.78e+004	100.0	1.003	0.846
2	33.0	34.2	936782	0.745	70.0	43.2	7.98	0.03	2.68e+004	100.0	1.000	1.10
3	41.0	34.3	891687	0.732	73.6	41.2	6.67	0.03	2.39e+004	100.0	0.996	0.753
4	48.0	34.3	866049	0.752	74.7	40.6	0.0284	0.00	2.30e+004	100.0	1.006	1.81
5	56.0	34.2	850150	0.748	72.4	41.8	9.47	0.05	2.47e+004	100.0	0.997	3.97
6	64.0	34.2	835295	0.753	68.5	44.1	6.23	0.02	2.83e+004	100.0	0.994	0.544
7	72.0	34.4	793947	0.760	71.6	42.5	0.0297	0.00	2.57e+004	100.0	1.011	1.28
8	79.0	34.3	796243	0.758	72.8	41.6	2.86	0.00	2.45e+004	100.0	1.012	0.781
9	87.0	34.3	825629	0.781	66.8	45.4	4.31	0.01	3.02e+004	100.0	0.992	1.17
10	95.0	34.3	753980	0.768	72.7	41.7	3.26	0.01	2.46e+004	100.0	1.002	1.04
11	102.0	34.3	788870	0.750	67.8	44.7	6.41	0.02	2.92e+004	100.0	0.993	4.10
12	110.0	34.2	788471	0.755	69.7	43.4	11.2	0.07	2.71e+004	100.0	0.992	1.17
13	118.0	34.2	726719	0.765	71.8	42.1	0.0295	0.00	2.52e+004	100.0	1.006	2.10
14	125.0	34.3	755018	0.774	67.2	45.1	11.0	0.06	2.98e+004	100.0	0.987	1.65
15	133.0	34.2	718714	0.792	68.1	44.4	11.5	0.07	2.87e+004	100.0	1.001	1.21
16	141.0	34.3	708001	0.789	70.3	43.1	4.79	0.01	2.67e+004	100.0	1.003	0.216
17	150.0	34.3	699365	0.784	68.5	44.2	2.27	0.00	2.84e+004	100.0	0.999	0.513
18	159.0	34.3	660278	0.767	69.3	43.7	12.2	0.08	2.76e+004	100.0	1.002	1.63
19	167.0	34.4	652318	0.777	71.7	42.4	0.0297	0.00	2.56e+004	100.0	1.001	1.54
20	176.0	34.2	651479	0.781	69.8	43.3	10.2	0.06	2.70e+004	100.0	0.996	1.46
21	185.0	34.3	630782	0.750	68.6	44.2	9.16	0.04	2.83e+004	100.0	1.004	4.08
22	194.0	34.2	611792	0.780	70.7	42.8	15.4	0.13	2.62e+004	100.0	1.002	2.24
23	203.0	34.3	616842	0.793	67.2	45.1	7.06	0.02	2.97e+004	100.0	0.996	2.37
24	211.0	34.5	591019	0.790	67.3	45.3	8.85	0.04	3.00e+004	100.0	1.007	0.851
Aves:												
Mono		34.3	755303	0.766	70.0	43.3	6.42	0.03	2.71e+004	100.0	1.000	1.60
Bi-1		0.0	0	0.000	0.000	0.000	---	---	0.000	0.0	0.000	0.000
Bi-2				0.000	0.000	0.000			0.000	0.0		

Figure 7.2 DLS raw data for v-SNARE liposome size estimations

Data print out from the dynamic light scattering measurements made to calculate the hydrodynamic radii of v- SNARE donor liposomes.

7.2 Appendix II: Fusion assay raw fluorescence data

NBD fluorescence measured from fusion assays indicated, both tables of data and a graph depicting the fluorescence from the dequenching assay before and after the addition of detergent to achieve a maximal signal, which is subsequently used to normalize data.

Time	Raw Fluorescence	
(minutes)	T + V	T + V control
0	11706	10709
2	11607	10404
4	11442	10345
6	11348	10294
8	11283	10204
10	11342	10097
12	11250	10107
14	11335	10115
16	11385	10116
18	11435	10170
20	11340	10147
22	11458	10102
24	11537	10207
26	11524	10246
28	11629	10216
30	11652	10221
32	11592	10182
34	11675	10250
36	11694	10265
38	11724	10326
40	11827	10231
42	11862	10309
44	11945	10306
46	11952	10406
48	11908	10322
50	11997	10445
52	11972	10372
54	12071	10427
56	12040	10446
58	12064	10384
60	12055	10465
62	12230	10467
64	12188	10592
66	12251	10606
68	12180	10502
70	12314	10584
72	12303	10611
74	12317	10618
76	12356	10660
78	12334	10641
80	12500	10585

Time	Raw Fluorescence	
(minutes)	T + V	T + V control
82	12455	10700
84	12476	10646
86	12496	10668
88	12529	10685
90	12497	10726
92	12587	10700
94	12592	10790
96	12610	10814
98	12682	10806
100	12616	10847
102	12704	10829
104	12805	10869
106	12786	10830
108	12762	10850
110	12788	10865
112	12877	10919
114	12831	11004
116	12863	10929
118	45034	47410
120	45509	47937
122	44656	47514
124	44354	46789
126	43726	46292
128	43843	46302
130	43365	45414
132	43690	45381
134	43702	45462
136	43452	45512
138	43609	45354
140	43679	45306
142	45431	44956
144	45291	45370
146	45288	45221
148	45401	45357
150	45328	45122
152	45361	45499
154	45248	45219
156	45410	45544
158	45538	45175

Figure 7.3 Raw fluorescence data from Figure 5.15

Fluorescence measurements (arbitrary units) taken from standard reaction (T+V) and control reaction where t-SNARE liposomes are pre-incubated with cytosolic $Snc2p_{1-88}$, every 2 minutes for 160 minutes. After the 2 hour time point, 10 µl n-dodecylmaltoside was added before final 40 minutes of measurements were recorded. The maximal fluorescence measured after addition of detergent was used to normalise data as a percentage of this maximum.

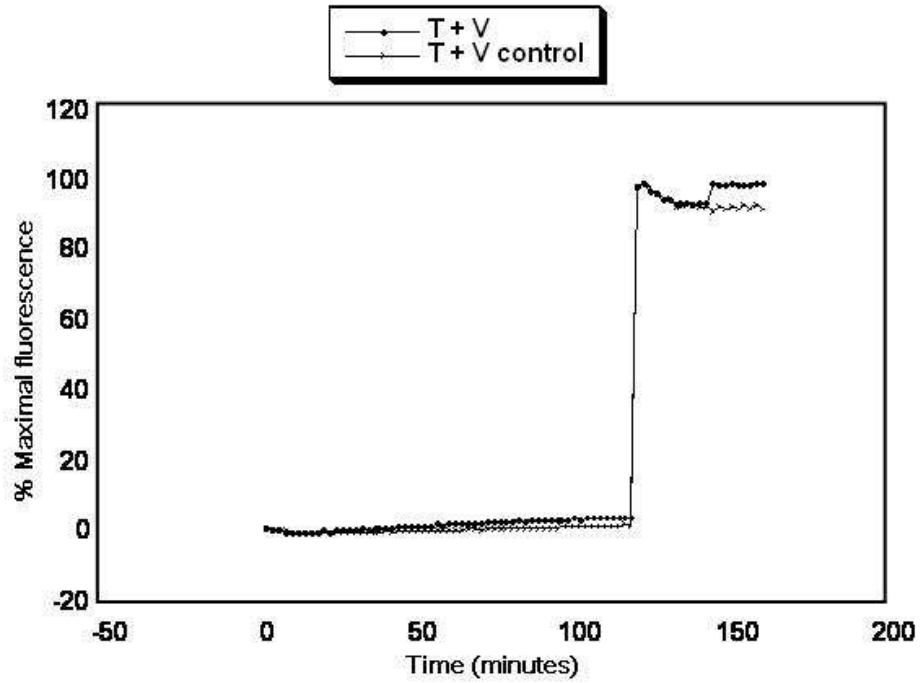

Figure 7.4 Normalisation of data from Figure 5.15

Data from Figure 7.3 presented as a graph after normalisation to the maximal fluorescence determined by addition of detergent.

Time	Raw Fluorescence				Time	Raw Fluorescence			
(minutes)	T (Tlg1p) + V	T (Tlg1p) + V control	T (Sx8/Tlg1p) + V	T (Sx8/Tlg1p) + V control	(minutes)	T (Tlg1p) + V	T (Tlg1p) + V control	T (Sx8/Tlg1p) + V	T (Sx8/Tlg1p) + V control
0	16878	16299	17169	16186	82	16047	15571	18160	16193
2	16341	15770	16990	16061	84	16091	15547	18162	16282
4	16003	15272	16888	15891	86	16123	15504	18205	16333
6	15629	15048	16761	15771	88	16139	15507	18291	16268
8	15529	14847	16753	15701	90	16118	15522	18251	16364
10	15460	14730	16689	15588	92	16069	15630	18199	16323
12	15345	14722	16586	15640	94	16114	15635	18414	16386
14	15314	14778	16564	15563	96	16155	15649	18410	16348
16	15319	14733	16611	15539	98	16240	15604	18499	16330
18	15306	14788	16780	15525	100	16210	15613	18515	16418
20	15265	14747	16698	15502	102	16190	15696	18530	16401
22	15250	14836	16765	15670	104	16273	15642	18573	16381
24	15341	14958	16862	15672	106	16224	15629	18554	16533
26	15310	14983	16916	15742	108	16300	15651	18611	16511
28	15361	14945	16992	15802	110	16364	15646	18564	16388
30	15433	15074	17002	15788	112	16361	15816	18630	16407
32	15459	15095	17136	15829	114	16368	15731	18789	16436
34	15509	15090	17243	15853	116	16329	15806	18815	16479
36	15528	15110	17255	15881	118	59550	57205	59257	55465
38	15532	15147	17258	15982	120	57216	54765	58172	53949
40	15595	15100	17431	15910	122	54983	52513	56738	52528
42	15618	15224	17397	15955	124	53283	50729	55438	51250
44	15587	15189	17361	15995	126	51861	49631	54658	50360
46	15684	15147	17457	16018	128	50967	48806	54203	49508
48	15668	15145	17494	15921	130	50623	48282	53577	49521
50	15850	15296	17457	16043	132	50562	48174	53448	48972
52	15787	15160	17550	16061	134	50202	48075	53121	48860
54	15649	15147	17641	16016	136	50270	47565	52926	48591
56	15794	15292	17686	16049	138	50100	47574	52991	48579
58	15804	15265	17689	16088	140	50152	47572	52944	48387
60	15800	15304	17704	16112	142	49548	47474	52733	48287
62	15830	15323	17830	16133	144	50025	47757	52941	48760
64	15831	15329	17844	16131	146	49885	47498	52776	48526
66	15952	15402	17912	16137	148	50331	47636	52842	48582
68	15975	15344	17999	16206	150	50083	47516	52903	48566
70	15982	15428	17747	16149	152	49928	47767	52829	48293
72	15971	15421	18047	16206	154	49996	47641	52755	48531
74	15943	15488	17974	16202	156	50066	47707	53211	48575
76	15964	15364	17996	16206	158	50315	47682	53031	48622
78	16060	15465	18133	16211					
80	15998	15501	18123	16248					

Figure 7.5 Raw fluorescence data from Figure 5.16

Fluorescence measurements (arbitrary units) at 520 nm were measured for 2 hours for all reactions: reactions of Tlg1p or Sx8 / Tlg1p containing t-SNARE complexes with v-SNAREs, alongside a negative control for each where samples were pre-incubated in the presence of cytosolic $Snc2p_{1-88}$. After this, 10 µl of detergent n-dodecylmaltoside was added to each reaction and measurements were taken for a further 40 minutes. The maximal fluorescence measured after addition of detergent was used to normalise data as a percentage of this maximum.

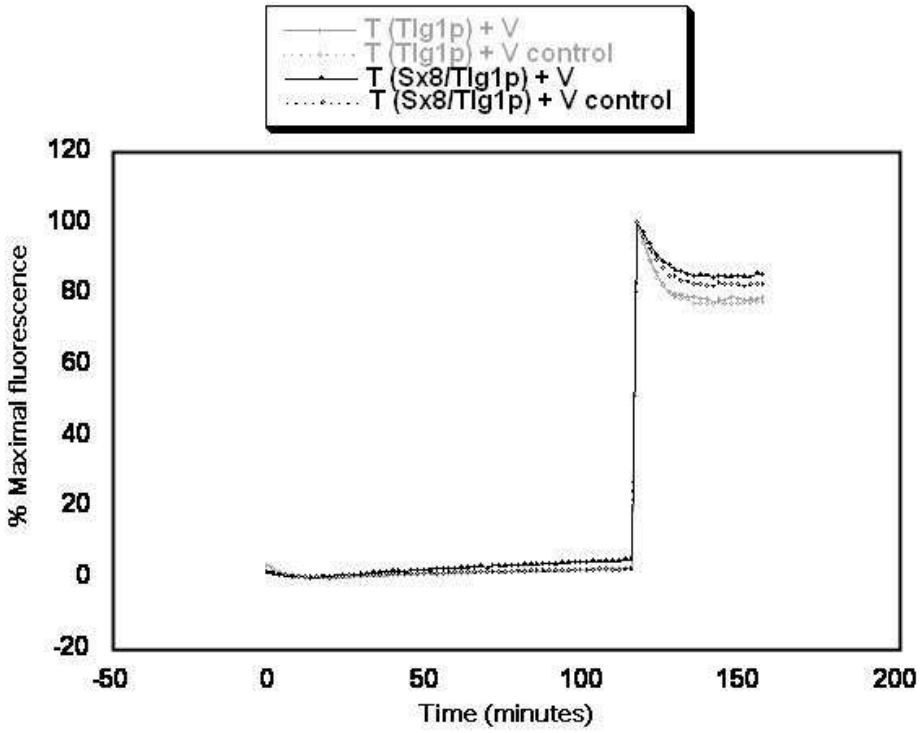

Figure 7.6 Normalisation of data from Figure 5.16

Data from figure 7.5 presented as a graph after normalisation to the maximal fluorescence determined by addition of detergent.

Time	Raw Fluorescence			Time	Raw Fluorescence		
(minutes)	1 µl cytosolic	10 µl cytosolic	V	(minutes)	1 µl cytosolic	10 µl cytosolic	V
0	15485	15428	10940	82	14889	15053	10444
2	15047	15020	10768	84	15023	14867	10411
4	14630	14669	10561	86	14971	14976	10438
6	14420	14339	10487	88	14928	14991	10419
8	14375	14271	10361	90	15052	15046	10410
10	14260	14244	10349	92	15108	15031	10435
12	14195	14041	10386	94	14989	15125	10473
14	14232	14137	10416	96	15145	15142	10393
16	14143	14061	10328	98	15117	15140	10426
18	14186	14058	10344	100	15202	15183	10419
20	14173	14177	10300	102	15189	15220	10465
22	14255	14200	10357	104	15189	15148	10402
24	14200	14193	10372	106	15179	15181	10459
26	14230	14248	10337	108	15213	15261	10469
28	14279	14282	10329	110	15208	15335	10433
30	14312	14262	10373	112	15385	15303	10488
32	14331	14297	10417	114	15245	15295	10437
34	14361	14344	10410	116	15303	15345	10518
36	14366	14329	10365	118	63778	63144	65000
38	14436	14376	10426	120	64806	64833	65000
40	14458	14375	10390	122	63785	64279	62423
42	14423	14469	10408	124	62336	62497	59053
44	14489	14446	10362	126	60379	60670	57037
46	14503	14510	10334	128	59104	59479	55610
48	14586	14492	10342	130	57912	58344	54631
50	14667	14507	10307	132	57195	57778	54091
52	14552	14512	10383	134	56811	57286	53549
54	14687	14588	10443	136	56424	56682	53108
56	14832	14632	10428	138	56132	56552	52933
58	14652	14685	10411	140	56301	56549	52712
60	14747	14761	10391	142	56243	56519	52978
62	14692	14748	10379	144	56001	56518	52710
64	14737	14730	10407	146	56054	56258	52653
66	14699	14770	10426	148	56065	56257	52802
68	14803	14824	10379	150	56001	56242	52728
70	14801	14812	10410	152	55932	56235	52739
72	14868	14795	10425	154	55799	56263	52651
74	14823	14851	10446	156	56178	56357	52600
76	14852	14896	10387	158	56478	56192	52658
78	14916	14946	10377				
80	15021	14909	10416				

Figure 7.7 Raw fluorescence data from Figure 5.17

Fluorescence measurements (arbitrary units) from various control reactions were taken every 2 minutes for 160 minutes. The first two reactions incubated t-SNARE liposomes with either 1 µl or 10 µl cytosolic $Snc2p_{1\text{-}88}$, before addition of v-SNARE liposomes. The final control reaction contained only donor v-SNARE liposomes. After the 2 hour time point, 10 µl n-dodecylmaltoside was added before final 40 minutes of measurements were recorded. The maximal fluorescence measured after addition of detergent was used to normalise data as a percentage of this maximum.

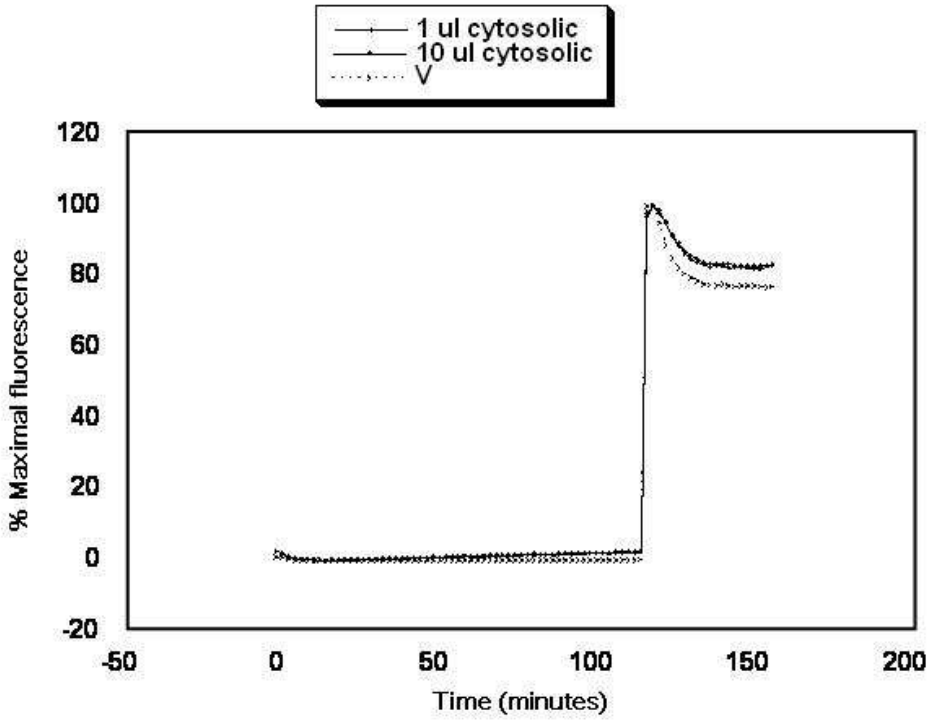

Figure 7.8 Normalisation of data from Figure 5.17

Data from Figure 7.7 presented as a graph after normalisation to the maximal fluorescence determined by addition of detergent.

Time	Raw Fluorescence			Time	Raw Fluorescence		
(minutes)	T + V Control	T + V*	T* + V	(minutes)	T + V Control	T + V*	T* + V
0	17818	13589	17715	82	16591	13073	16748
2	17322	13272	17297	84	16690	13058	16773
4	16754	12919	16827	86	16732	13057	16744
6	16329	12757	16616	88	16636	13104	16768
8	16173	12565	16375	90	16745	13118	16829
10	16142	12606	16264	92	16836	13215	16705
12	16078	12447	16180	94	16706	13191	16812
14	16001	12423	16107	96	16703	13121	16870
16	15902	12469	16147	98	16800	13153	16827
18	15928	12447	16200	100	16762	13155	16832
20	15958	12400	16099	102	16780	13237	16672
22	15968	12442	16265	104	16773	13277	16808
24	15892	12423	16085	106	16823	13217	16700
26	16019	12416	16095	108	16781	13112	16914
28	16048	12490	16271	110	16859	13224	16814
30	16088	12456	16264	112	16898	13336	16822
32	16106	12541	16272	114	16872	13288	16798
34	16165	12629	16344	116	16899	13222	16805
36	16267	12648	16369	118	65000	65000	65000
38	16260	12640	16300	120	64953	65000	65000
40	16233	12586	16378	122	64269	64535	64897
42	16251	12657	16367	124	62837	62959	64194
44	16225	12640	16559	126	61564	62579	63072
46	16259	12691	16431	128	60888	61841	62259
48	16331	12708	16375	130	60288	61113	61745
50	16277	12742	16615	132	59855	60606	61404
52	16334	12749	16554	134	59320	60295	60984
54	16439	12765	16533	136	59656	60251	60776
56	16437	12785	16496	138	59344	60294	60565
58	16459	12926	16632	140	59169	60010	60552
60	16489	12874	16687	142	59556	59952	60605
62	16497	12864	16592	144	59265	59849	60629
64	16538	12935	16578	146	59438	59642	60555
66	16400	12953	16719	148	59332	60248	60814
68	16547	13012	16585	150	59574	59991	60773
70	16602	12965	16779	152	59459	60213	60456
72	16497	12998	16752	154	59383	59993	60797
74	16626	13017	16760	156	59677	60343	60863
76	16565	12978	16742	158	59777	59865	60840
78	16555	13022	16677				
80	16610	13066	16675				

Figure 7.9 Raw fluorescence data from Figure 5.18

Fluorescence measurements (arbitrary units) from control reactions were taken every 2 minutes for 160 minutes. The first reaction is the standard control where 10 µl cytosolic $Snc2p_{1-88}$ is added to t-SNAREs prior to incubation with v-SNARE liposomes. The next two control reactions contained either t- or v-SNARE liposomes incubated with empty donor (V*) and acceptor liposomes (T*) respectively. The final control reaction contained only donor v-SNARE liposomes. After the 2 hour time point, 10 µl n-dodecylmaltoside was added before final 40 minutes of measurements were recorded. The maximal fluorescence measured after addition of detergent was used to normalise data as a percentage of this maximum.

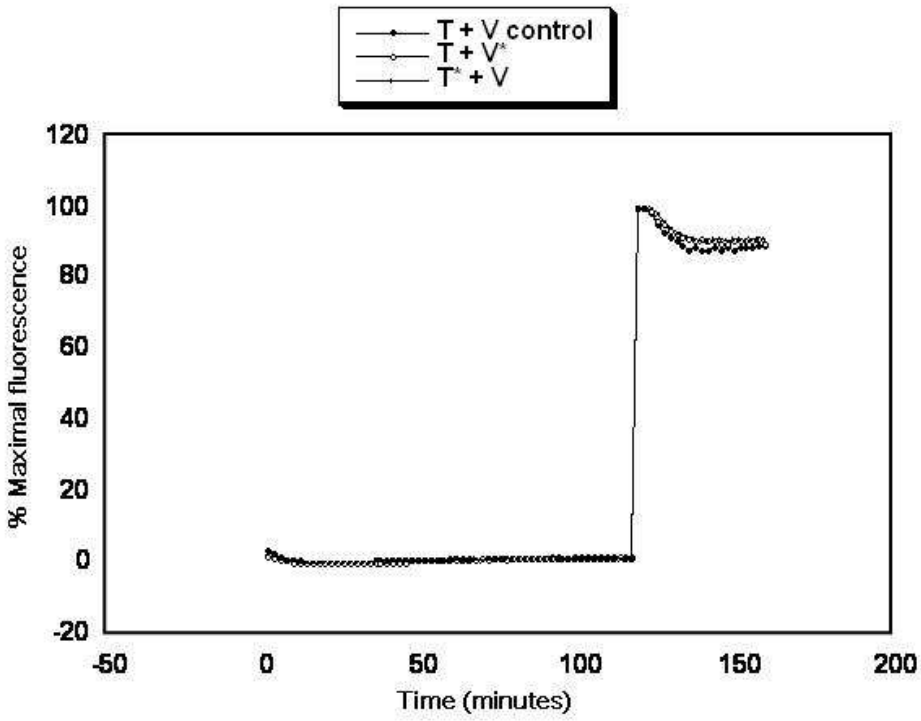

Figure 7.10 Normalisation of data from Figure 5.18

Data from Figure 7.9 presented as a graph after normalisation to the maximal fluorescence determined by addition of detergent.

Time	Raw Fluorescence				Time	Raw Fluorescence			
(minutes)	T + V	T + V control	T + V + Vps45p	T + V + Vps45p control	(minutes)	T + V	T + V control	T + V + Vps45p	T + V + Vps45p control
0	12786	12592	8093	9251	82	12869	12654	8434	9418
2	12704	12468	7999	9248	84	12916	12666	8424	9457
4	12551	12295	7928	9160	86	12924	12583	8402	9425
6	12551	12347	7868	9072	88	12996	12710	8462	9369
8	12538	12289	7838	9066	90	12926	12704	8471	9379
10	12514	12349	7855	9032	92	13015	12639	8468	9415
12	12510	12288	7809	9046	94	13000	12789	8528	9484
14	12571	12254	7901	9007	96	13005	12781	8529	9479
16	12472	12285	7873	9006	98	13054	12761	8578	9490
18	12458	12291	7880	9083	100	13132	12837	8565	9474
20	12570	12268	7871	9037	102	13112	12792	8581	9441
22	12565	12271	7886	9104	104	13106	12807	8621	9482
24	12591	12313	7923	9082	106	13023	12834	8603	9450
26	12592	12331	7893	9131	108	13091	12837	8640	9428
28	12644	12375	7958	9157	110	13075	12853	8625	9394
30	12558	12313	7966	9111	112	13091	12901	8614	9466
32	12620	12340	7999	9126	114	13100	12798	8640	9454
34	12560	12400	8029	9138	116	13136	12796	8670	9503
36	12675	12279	8000	9167	118	63820	61259	35979	42577
38	12554	12367	8006	9224	120	62354	60834	34387	41185
40	12601	12363	8091	9262	122	60580	58370	32591	39246
42	12653	12414	8123	9277	124	58275	56542	31255	38049
44	12664	12414	8083	9268	126	56309	55131	30228	36821
46	12763	12435	8069	9294	128	54700	53820	29332	35949
48	12748	12471	8142	9333	130	53897	52650	28859	35371
50	12734	12414	8203	9293	132	52763	52045	28431	34579
52	12660	12494	8180	9342	134	52325	51317	28077	33942
54	12626	12469	8177	9279	136	51998	50755	27871	33920
56	12701	12373	8234	9295	138	51549	50264	27674	33445
58	12749	12425	8267	9348	140	51316	50021	27421	33485
60	12824	12566	8282	9313	142	51219	50219	27411	33562
62	12879	12551	8308	9348	144	51183	50188	27383	33347
64	12880	12530	8282	9336	146	50960	49741	27543	33022
66	12727	12546	8253	9380	148	50889	49660	27427	33142
68	12867	12553	8294	9386	150	50890	49581	27630	33100
70	12805	12607	8309	9345	152	50719	49770	27482	33148
72	12816	12581	8298	9376	154	50838	49657	27762	33332
74	12768	12570	8404	9340	156	50861	49923	27666	33324
76	12939	12531	8387	9385	158	51205	49819	27733	33326
78	12859	12686	8341	9342					
80	12907	12619	8406	9426					

Figure 7.11 Raw fluorescence data from Figure 5.19

Fluorescence measurements (arbitrary units) from all fusion reactions were taken every 2 minutes for 160 minutes. Reactions containing t- and v-SNARE liposomes alone or incubated in the presence of Vps45p were carried out; each with a negative control previously incubated with cytosolic $Snc2p_{1-88}$ to inhibit fusion. After the 2 hour time point, 10 µl n-dodecylmaltoside was added before final 40 minutes of measurements were recorded. The maximal fluorescence measured after addition of detergent was used to normalise data as a percentage of this maximum.

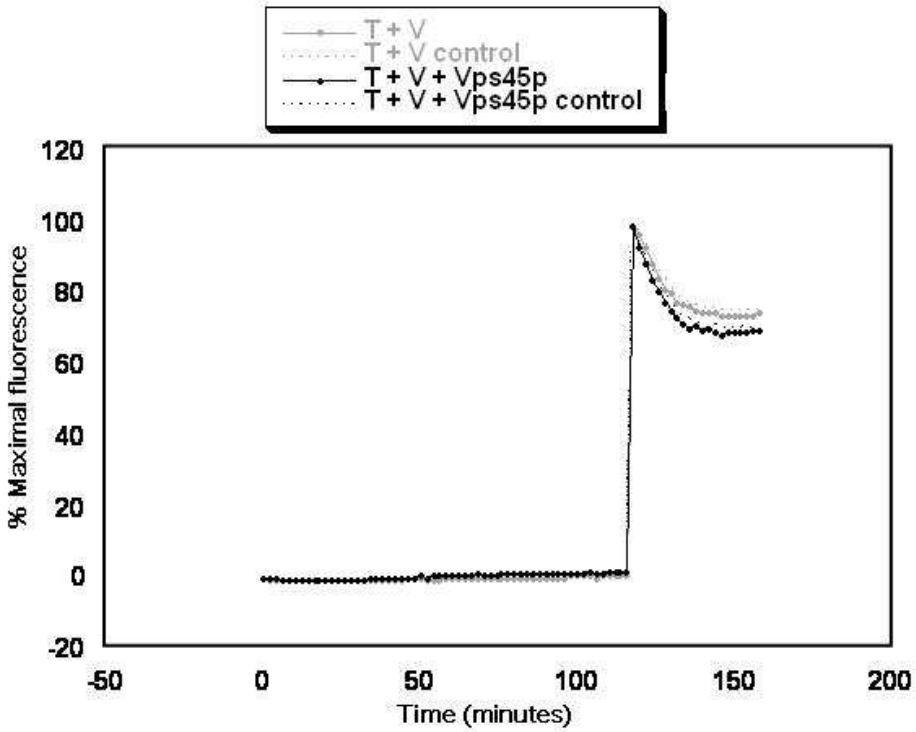

Figure 7.12 Normalisation of data from Figure 5.19

Data from Figure 7.11 presented as a graph after normalisation to the maximal fluorescence determined by addition of detergent.

Time	Raw Fluorescence				Time	Raw Fluorescence			
(minutes)	T+V	T+V control	T+V + Vps45p	T+V + Munc18c	(minutes)	T+V	T+V control	T+V + Vps45p	T+V + Munc18c
0	16426	15551	15319	15698	82	17489	15926	16287	16519
2	16130	15291	15091	15495	84	17616	16033	16316	16684
4	16043	15244	15108	15332	86	17386	15889	16301	16598
6	15909	15154	14922	15357	88	17700	15981	16398	16692
8	15997	15147	14935	15186	90	17706	15976	16523	16688
10	15786	14964	14801	15176	92	17721	16076	16475	16766
12	15976	14975	14916	15160	94	17791	16009	16488	16913
14	16011	15121	14870	15311	96	17771	16041	16532	16801
16	15994	15059	15019	15285	98	17898	16094	16557	16758
18	16019	15083	15051	15374	100	18028	16209	16762	16918
20	16075	15132	14975	15375	102	18018	16163	16639	16947
22	16239	15180	15127	15399	104	17986	16253	16708	16887
24	16297	15140	14981	15370	106	18033	16307	16671	17007
26	16325	15316	15181	15437	108	18057	16139	16789	17088
28	16396	15286	15264	15417	110	18257	16125	16688	17115
30	16343	15369	15331	15524	112	18235	16143	16849	17187
32	16507	15296	15331	15696	114	18103	16208	16888	17110
34	16498	15293	15271	15684	116	18240	16115	17028	17142
36	16628	15400	15388	15799	118	54627	54206	50883	54968
38	16635	15412	15502	15742	120	55504	54064	50937	54957
40	16643	15442	15544	15765	122	54819	53416	50106	54030
42	16803	15429	15449	15944	124	54670	52722	50318	52985
44	16624	15448	15565	15821	126	54390	52241	50255	52505
46	16731	15640	15620	15902	128	54339	51865	50395	51984
48	16901	15537	15722	15886	130	53983	51555	50535	51763
50	16946	15612	15703	16014	132	54203	51745	50861	51266
52	16867	15507	15669	16056	134	53891	51436	50653	51207
54	17051	15717	15818	16153	136	53715	51609	50314	51139
56	17047	15660	15731	16082	138	53605	51734	50274	50987
58	17024	15763	15931	16210	140	53760	51740	50116	51069
60	17130	15768	15974	16107	142	53562	51745	50391	50663
62	17294	15751	15951	16213	144	53858	52241	50291	50960
64	17169	15698	15961	16218	146	53808	52278	50426	50819
66	17280	15861	16040	16334	148	53578	52381	50395	50820
68	17369	15753	16092	16351	150	53664	52704	50224	50943
70	17437	15772	16099	16471	152	53721	53004	50268	50817
72	17309	15723	16089	16439	154	53830	53126	50444	50573
74	17405	15891	16304	16479	156	53783	53388	50236	51166
76	17404	16015	16141	16314	158	53503	53334	50260	51055
78	17500	15974	16263	16529					
80	17591	15825	16258	16599					

Figure 7.13 Raw fluorescence data from Figure 5.20

Fluorescence measurements (arbitrary units) from all fusion reactions were taken every 2 minutes for 160 minutes. Reactions containing t- and v-SNARE liposomes alone or incubated with either Vps45p or Munc18c were carried out. A control reaction where t-SNARE liposomes were previously incubated with cytosolic $Snc2p_{1-88}$ was included. After the 2 hour time point, 10 µl n-dodecylmaltoside was added before final 40 minutes of measurements were recorded. The maximal fluorescence measured after addition of detergent was used to normalise data as a percentage of this maximum

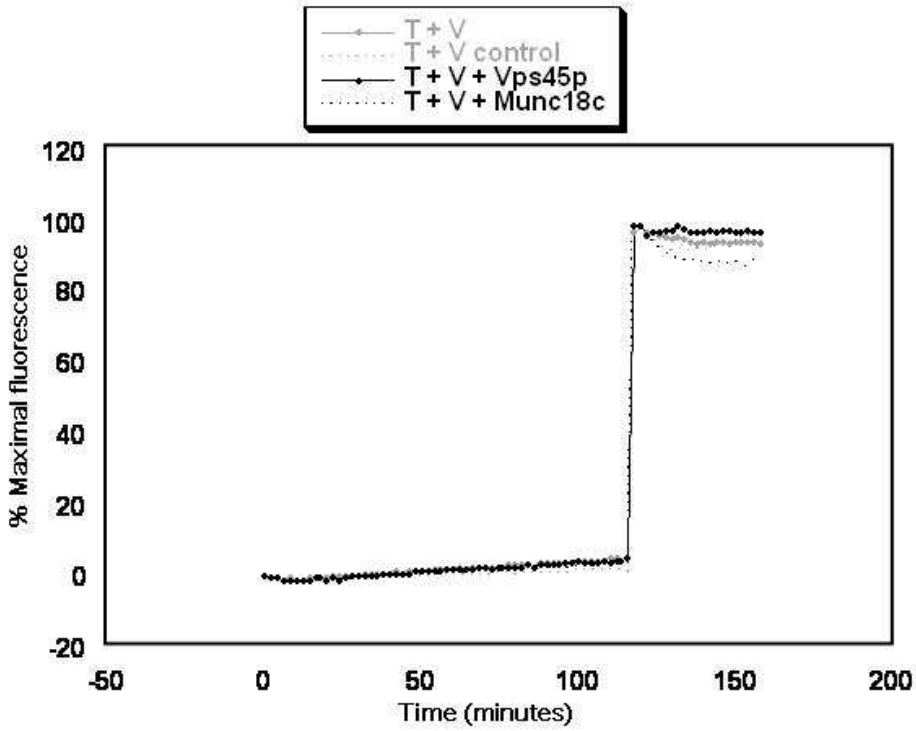

Figure 7.14 Normalisation of data from Figure 5.20

Data from Figure 7.13 presented as a graph after normalisation to the maximal fluorescence determined by addition of detergent.

7.3 Appendix III: Publications related to this work

Struthers M, Shanks SG, **MacDonald C**, Carpp LN, Drozdowska A, Kioumourtzoglou D, Furgason ML, Munson M and Bryant NJ. (2009) Functional homology of mammalian syntaxin16 and yeast Tlg2p reveals a conserved regulatory mechanism. *J. Cell Sci.* **122**:*2292-9*.

Furgason ML, **MacDonald C**, Shanks SG, Ryder SP, Bryant NJ, Munson M. (2009) The N-terminal peptide of the syntaxin Tlg2p modulates binding of its closed conformation to Vps45p. *Proc. Natl. Acad. Sci.* **103**: *14303-8*.

MacDonald C, Munson M and Bryant NJ. (2010) Auto-inhibition of SNARE complex assembly by a conformational switch represents a conserved feature of syntaxins. *Biochem. Soc. Trans. (in press; due to be published February 2010)*

Bibliography

AALTO, M. K., KERANEN, S. & RONNE, H. (1992) A family of proteins involved in intracellular transport. *Cell,* 68**,** 181-2.

ABELIOVICH, H., DARSOW, T. & EMR, S. D. (1999) Cytoplasm to vacuole trafficking of aminopeptidase I requires a t-SNARE-Sec1p complex composed of Tlg2p and Vps45p. *Embo J,* 18**,** 6005-16.

ABELIOVICH, H., GROTE, E., NOVICK, P. & FERRO-NOVICK, S. (1998) Tlg2p, a yeast syntaxin homolog that resides on the Golgi and endocytic structures. *J Biol Chem,* 273**,** 11719-27.

ADVANI, R. J., BAE, H. R., BOCK, J. B., CHAO, D. S., DOUNG, Y. C., PREKERIS, R., YOO, J. S. & SCHELLER, R. H. (1998) Seven novel mammalian SNARE proteins localize to distinct membrane compartments. *J Biol Chem,* 273**,** 10317-24.

ANDAG, U., NEUMANN, T. & SCHMITT, H. D. (2001) The coatomer-interacting protein Dsl1p is required for Golgi-to-endoplasmic reticulum retrieval in yeast. *J Biol Chem,* 276**,** 39150-60.

ANTONIN, W., DULUBOVA, I., ARAC, D., PABST, S., PLITZNER, J., RIZO, J. & JAHN, R. (2002a) The N-terminal domains of syntaxin 7 and vti1b form three-helix bundles that differ in their ability to regulate SNARE complex assembly. *J Biol Chem,* 277**,** 36449-56.

ANTONIN, W., FASSHAUER, D., BECKER, S., JAHN, R. & SCHNEIDER, T. R. (2002b) Crystal structure of the endosomal SNARE complex reveals common structural principles of all SNAREs. *Nat Struct Biol,* 9**,** 107-11.

ARAI, S., NODA, Y., KAINUMA, S., WADA, I. & YODA, K. (2008) Ypt11 functions in bud-directed transport of the Golgi by linking Myo2 to the coatomer subunit Ret2. *Curr Biol,* 18**,** 987-91.

ARAN, V., BRANDIE, F. M., BOYD, A. R., KANTIDAKIS, T., RIDEOUT, E. J., KELLY, S. M., GOULD, G. W. & BRYANT, N. (2009) Characterisation of two distinct binding modes between Syntaxin 4 and Munc18c. *Biochem J.*

AVERY, J., JAHN, R. & EDWARDSON, J. M. (1999) Reconstitution of regulated exocytosis in cell-free systems: a critical appraisal. *Annu Rev Physiol,* 61**,** 777-807.

AZEM, A., KESSEL, M. & GOLOUBINOFF, P. (1994) Characterization of a functional GroEL14(GroES7)2 chaperonin hetero-oligomer. *Science,* 265**,** 653-6.

BANFIELD, D. K., LEWIS, M. J. & PELHAM, H. R. (1995) A SNARE-like protein required for traffic through the Golgi complex. *Nature,* 375**,** 806-9.

BANKAITIS, V. A., JOHNSON, L. M. & EMR, S. D. (1986) Isolation of yeast mutants defective in protein targeting to the vacuole. *Proc Natl Acad Sci U S A,* 83**,** 9075-9.

BANTA, L. M., VIDA, T. A., HERMAN, P. K. & EMR, S. D. (1990) Characterization of yeast Vps33p, a protein required for vacuolar protein sorting and vacuole biogenesis. *Mol Cell Biol,* 10**,** 4638-49.

BARK, I. C. & WILSON, M. C. (1994) Human cDNA clones encoding two different isoforms of the nerve terminal protein SNAP-25. *Gene,* 139**,** 291-2.

BARLOWE, C. (1997) Coupled ER to Golgi transport reconstituted with purified cytosolic proteins. *J Cell Biol,* 139**,** 1097-108.

BARRICK, D. & HUGHSON, F. M. (2002) Irreversible assembly of membrane fusion machines. *Nat Struct Biol,* 9**,** 78-80.

BECHERER, K. A., RIEDER, S. E., EMR, S. D. & JONES, E. W. (1996) Novel syntaxin homologue, Pep12p, required for the sorting of lumenal hydrolases to the lysosome-like vacuole in yeast. *Mol Biol Cell,* 7**,** 579-94.

BENNETT, M. K., CALAKOS, N. & SCHELLER, R. H. (1992) Syntaxin: a synaptic protein implicated in docking of synaptic vesicles at presynaptic active zones. *Science,* 257**,** 255-9.

BENNETT, M. K. & SCHELLER, R. H. (1993) The molecular machinery for secretion is conserved from yeast to neurons. *Proc Natl Acad Sci U S A,* 90**,** 2559-63.

BENTZ, J. & MITTAL, A. (2000) Deployment of membrane fusion protein domains during fusion. *Cell Biol Int,* 24**,** 819-38.

BOCK, J. B., MATERN, H. T., PEDEN, A. A. & SCHELLER, R. H. (2001) A genomic perspective on membrane compartment organization. *Nature,* 409**,** 839-41.

BOEKE, J. D., TRUEHEART, J., NATSOULIS, G. & FINK, G. R. (1987) 5-Fluoroorotic acid as a selective agent in yeast molecular genetics. *Methods Enzymol,* 154**,** 164-75.

BONANGELINO, C. J., CHAVEZ, E. M. & BONIFACINO, J. S. (2002) Genomic screen for vacuolar protein sorting genes in Saccharomyces cerevisiae. *Mol Biol Cell,* 13**,** 2486-501.

BONIFACINO, J. S. & GLICK, B. S. (2004) The mechanisms of vesicle budding and fusion. *Cell,* 116**,** 153-66.

BOWERS, K. & STEVENS, T. H. (2005) Protein transport from the late Golgi to the vacuole in the yeast Saccharomyces cerevisiae. *Biochim Biophys Acta,* 1744**,** 438-54.

BRACHER, A., KADLEC, J., BETZ, H. & WEISSENHORN, W. (2002) X-ray structure of a neuronal complexin-SNARE complex from squid. *J Biol Chem,* 277**,** 26517-23.

BRACHER, A., PERRAKIS, A., DRESBACH, T., BETZ, H. & WEISSENHORN, W. (2000) The X-ray crystal structure of neuronal Sec1 from squid sheds new light on the role of this protein in exocytosis. *Structure,* 8**,** 685-94.

BRACHER, A. & WEISSENHORN, W. (2002) Structural basis for the Golgi membrane recruitment of Sly1p by Sed5p. *Embo J,* 21**,** 6114-24.

BRACHER, A. & WEISSENHORN, W. (2004) Crystal structure of the Habc domain of neuronal syntaxin from the squid Loligo pealei reveals conformational plasticity at its C-terminus. *BMC Struct Biol,* 4**,** 6.

BRADFORD, M. M. (1976) A rapid and sensitive method for the quantitation of microgram quantities of protein utilizing the principle of protein-dye binding. *Anal Biochem,* 72**,** 248-54.

BRANDIE, F. M., ARAN, V., VERMA, A., MCNEW, J. A., BRYANT, N. J. & GOULD, G. W. (2008) Negative regulation of syntaxin4/SNAP-23/VAMP2-mediated membrane fusion by Munc18c in vitro. *PLoS ONE,* 3**,** e4074.

BRENNER, S. (1974) The genetics of Caenorhabditis elegans. *Genetics,* 77**,** 71-94.

BRENNWALD, P., KEARNS, B., CHAMPION, K., KERANEN, S., BANKAITIS, V. & NOVICK, P. (1994) Sec9 is a SNAP-25-like component of a yeast SNARE complex that may be the effector of Sec4 function in exocytosis. *Cell,* 79**,** 245-58.

BRUNGER, A. T. (2005) Structure and function of SNARE and SNARE-interacting proteins. *Q Rev Biophys,* 38**,** 1-47.

BRYANT, N. J. & JAMES, D. E. (2001) Vps45p stabilizes the syntaxin homologue Tlg2p and positively regulates SNARE complex formation. *Embo J,* 20**,** 3380-8.

BRYANT, N. J. & JAMES, D. E. (2003) The Sec1p/Munc18 (SM) protein, Vps45p, cycles on and off membranes during vesicle transport. *J Cell Biol,* 161**,** 691-6.

BRYANT, N. J. & STEVENS, T. H. (1998) Vacuole biogenesis in Saccharomyces cerevisiae: protein transport pathways to the yeast vacuole. *Microbiol Mol Biol Rev,* 62**,** 230-47.

BUCCI, C., PARTON, R. G., MATHER, I. H., STUNNENBERG, H., SIMONS, K., HOFLACK, B. & ZERIAL, M. (1992) The small GTPase rab5 functions as a regulatory factor in the early endocytic pathway. *Cell,* 70**,** 715-28.

BULLOUGH, P. A., HUGHSON, F. M., SKEHEL, J. J. & WILEY, D. C. (1994) Structure of influenza haemagglutinin at the pH of membrane fusion. *Nature,* 371**,** 37-43.

BURD, C. G., PETERSON, M., COWLES, C. R. & EMR, S. D. (1997) A novel Sec18p/NSF-dependent complex required for Golgi-to-endosome transport in yeast. *Mol Biol Cell,* 8**,** 1089-104.

BURGOYNE, R. D. & MORGAN, A. (2007) Membrane trafficking: three steps to fusion. *Curr Biol,* 17**,** R255-8.

BURKHARDT, P., HATTENDORF, D. A., WEIS, W. I. & FASSHAUER, D. (2008) Munc18a controls SNARE assembly through its interaction with the syntaxin N-peptide. *Embo J,* 27**,** 923-33.

CALAKOS, N., BENNETT, M. K., PETERSON, K. E. & SCHELLER, R. H. (1994) Protein-protein interactions contributing to the specificity of intracellular vesicular trafficking. *Science,* 263**,** 1146-9.

CANAVES, J. M. & MONTAL, M. (1998) Assembly of a ternary complex by the predicted minimal coiled-coil-forming domains of syntaxin, SNAP-25, and synaptobrevin. A circular dichroism study. *J Biol Chem,* 273**,** 34214-21.

CARPP, L. N., CIUFO, L. F., SHANKS, S. G., BOYD, A. & BRYANT, N. J. (2006) The Sec1p/Munc18 protein Vps45p binds its cognate SNARE proteins via two distinct modes. *J Cell Biol,* 173**,** 927-36.

CARPP, L. N., SHANKS, S. G., STRUTHERS, M. S. & BRYANT, N. J. (2007) Cellular levels of the syntaxin Tlg2p are regulated by a single mode of binding to Vps45p. *Biochem Biophys Res Commun,* 363**,** 857-60.

CARR, C. M., GROTE, E., MUNSON, M., HUGHSON, F. M. & NOVICK, P. J. (1999) Sec1p binds to SNARE complexes and concentrates at sites of secretion. *J Cell Biol,* 146**,** 333-44.

CHALFIE, M., TU, Y., EUSKIRCHEN, G., WARD, W. W. & PRASHER, D. C. (1994) Green fluorescent protein as a marker for gene expression. *Science,* 263**,** 802-5.

CHANDRASEKHAR, G. N., TILLY, K., WOOLFORD, C., HENDRIX, R. & GEORGOPOULOS, C. (1986) Purification and properties of the groES morphogenetic protein of Escherichia coli. *J Biol Chem,* 261**,** 12414-9.

CHANG, J. Y. (1985) Thrombin specificity. Requirement for apolar amino acids adjacent to the thrombin cleavage site of polypeptide substrate. *Eur J Biochem,* 151**,** 217-24.

CHAPMAN, E. R., AN, S., BARTON, N. & JAHN, R. (1994) SNAP-25, a t-SNARE which binds to both syntaxin and synaptobrevin via domains that may form coiled coils. *J Biol Chem,* 269**,** 27427-32.

CHAVRIER, P., PARTON, R. G., HAURI, H. P., SIMONS, K. & ZERIAL, M. (1990) Localization of low molecular weight GTP binding proteins to exocytic and endocytic compartments. *Cell,* 62**,** 317-29.

CHEN, J., WHARTON, S. A., WEISSENHORN, W., CALDER, L. J., HUGHSON, F. M., SKEHEL, J. J. & WILEY, D. C. (1995) A soluble domain of the membrane-anchoring chain of influenza virus hemagglutinin (HA2) folds in Escherichia coli into the low-pH-induced conformation. *Proc Natl Acad Sci U S A,* 92**,** 12205-9.

CHEN, X., LU, J., DULUBOVA, I. & RIZO, J. (2008) NMR analysis of the closed conformation of syntaxin-1. *J Biomol NMR,* 41**,** 43-54.

CHEN, Y. A. & SCHELLER, R. H. (2001) SNARE-mediated membrane fusion. *Nat Rev Mol Cell Biol,* 2**,** 98-106.

CHERNOMORDIK, L. V. & KOZLOV, M. M. (2003) Protein-lipid interplay in fusion and fission of biological membranes. *Annu Rev Biochem,* 72**,** 175-207.

CHERNOMORDIK, L. V. & KOZLOV, M. M. (2005) Membrane hemifusion: crossing a chasm in two leaps. *Cell,* 123**,** 375-82.

CHERNOMORDIK, L. V. & KOZLOV, M. M. (2008) Mechanics of membrane fusion. *Nat Struct Mol Biol,* 15**,** 675-83.

CHERNOMORDIK, L. V. & MELIKOV, K. (2006) Are there too many or too few SNAREs in proteoliposomes? *Biophys J,* 90**,** 2657-8.

CHIEN, C. T., BARTEL, P. L., STERNGLANZ, R. & FIELDS, S. (1991) The two-hybrid system: a method to identify and clone genes for proteins that interact with a protein of interest. *Proc Natl Acad Sci U S A,* 88**,** 9578-82.

CHRISTOFORIDIS, S., MCBRIDE, H. M., BURGOYNE, R. D. & ZERIAL, M. (1999) The Rab5 effector EEA1 is a core component of endosome docking. *Nature,* 397**,** 621-5.

CLARY, D. O., GRIFF, I. C. & ROTHMAN, J. E. (1990) SNAPs, a family of NSF attachment proteins involved in intracellular membrane fusion in animals and yeast. *Cell,* 61**,** 709-21.

COE, J. G., LIM, A. C., XU, J. & HONG, W. (1999) A role for Tlg1p in the transport of proteins within the Golgi apparatus of Saccharomyces cerevisiae. *Mol Biol Cell,* 10**,** 2407-23.

CONIBEAR, E. & STEVENS, T. H. (2000) Vps52p, Vps53p, and Vps54p form a novel multisubunit complex required for protein sorting at the yeast late Golgi. *Mol Biol Cell,* 11**,** 305-23.

CONNELL, E., DARIOS, F., BROERSEN, K., GATSBY, N., PEAK-CHEW, S. Y., RICKMAN, C. & DAVLETOV, B. (2007) Mechanism of arachidonic acid action on syntaxin-Munc18. *EMBO Rep,* 8**,** 414-9.

COWLES, C. R., EMR, S. D. & HORAZDOVSKY, B. F. (1994) Mutations in the VPS45 gene, a SEC1 homologue, result in vacuolar protein sorting defects and accumulation of membrane vesicles. *J Cell Sci,* 107 (Pt 12)**,** 3449-59.

D'ANDREA-MERRINS, M., CHANG, L., LAM, A. D., ERNST, S. A. & STUENKEL, E. L. (2007) Munc18c interaction with syntaxin 4 monomers and SNARE complex intermediates in GLUT4 vesicle trafficking. *J Biol Chem,* 282**,** 16553-66.

DARSOW, T., ODORIZZI, G. & EMR, S. D. (2000) Invertase fusion proteins for analysis of protein trafficking in yeast. *Methods Enzymol,* 327**,** 95-106.

DARSOW, T., RIEDER, S. E. & EMR, S. D. (1997) A multispecificity syntaxin homologue, Vam3p, essential for autophagic and biosynthetic protein transport to the vacuole. *J Cell Biol,* 138**,** 517-29.

DENNISON, S. M., BOWEN, M. E., BRUNGER, A. T. & LENTZ, B. R. (2006) Neuronal SNAREs do not trigger fusion between synthetic membranes but do promote PEG-mediated membrane fusion. *Biophys J,* 90**,** 1661-75.

DULUBOVA, I., KHVOTCHEV, M., LIU, S., HURYEVA, I., SUDHOF, T. C. & RIZO, J. (2007) Munc18-1 binds directly to the neuronal SNARE complex. *Proc Natl Acad Sci U S A,* 104**,** 2697-702.

DULUBOVA, I., SUGITA, S., HILL, S., HOSAKA, M., FERNANDEZ, I., SUDHOF, T. C. & RIZO, J. (1999) A conformational switch in syntaxin during exocytosis: role of munc18. *Embo J,* 18**,** 4372-82.

DULUBOVA, I., YAMAGUCHI, T., GAO, Y., MIN, S. W., HURYEVA, I., SUDHOF, T. C. & RIZO, J. (2002) How Tlg2p/syntaxin 16 'snares' Vps45. *Embo J,* 21**,** 3620-31.

DULUBOVA, I., YAMAGUCHI, T., WANG, Y., SUDHOF, T. C. & RIZO, J. (2001) Vam3p structure reveals conserved and divergent properties of syntaxins. *Nat Struct Biol,* 8**,** 258-64.

FASSHAUER, D., ANTONIN, W., MARGITTAI, M., PABST, S. & JAHN, R. (1999) Mixed and non-cognate SNARE complexes. Characterization of assembly and biophysical properties. *J Biol Chem,* 274**,** 15440-6.

FASSHAUER, D., BRUNS, D., SHEN, B., JAHN, R. & BRUNGER, A. T. (1997a) A structural change occurs upon binding of syntaxin to SNAP-25. *J Biol Chem,* 272**,** 4582-90.

FASSHAUER, D. & MARGITTAI, M. (2004) A transient N-terminal interaction of SNAP-25 and syntaxin nucleates SNARE assembly. *J Biol Chem,* 279**,** 7613-21.

FASSHAUER, D., OTTO, H., ELIASON, W. K., JAHN, R. & BRUNGER, A. T. (1997b) Structural changes are associated with soluble N-ethylmaleimide-sensitive fusion protein attachment protein receptor complex formation. *J Biol Chem,* 272**,** 28036-41.

FASSHAUER, D., SUTTON, R. B., BRUNGER, A. T. & JAHN, R. (1998) Conserved structural features of the synaptic fusion complex: SNARE proteins reclassified as Q- and R-SNAREs. *Proc Natl Acad Sci U S A,* 95**,** 15781-6.

FERNANDEZ, I., UBACH, J., DULUBOVA, I., ZHANG, X., SUDHOF, T. C. & RIZO, J. (1998) Three-dimensional structure of an evolutionarily conserved N-terminal domain of syntaxin 1A. *Cell,* 94**,** 841-9.

FIEBIG, K. M., RICE, L. M., POLLOCK, E. & BRUNGER, A. T. (1999) Folding intermediates of SNARE complex assembly. *Nat Struct Biol,* 6**,** 117-23.

FIELDS, S. & SONG, O. (1989) A novel genetic system to detect protein-protein interactions. *Nature,* 340**,** 245-6.

FIVASH, M., TOWLER, E. M. & FISHER, R. J. (1998) BIAcore for macromolecular interaction. *Curr Opin Biotechnol,* 9**,** 97-101.

FRIED, M. & CROTHERS, D. M. (1981) Equilibria and kinetics of lac repressor-operator interactions by polyacrylamide gel electrophoresis. *Nucleic Acids Res,* 9**,** 6505-25.

FUKUDA, R., MCNEW, J. A., WEBER, T., PARLATI, F., ENGEL, T., NICKEL, W., ROTHMAN, J. E. & SOLLNER, T. H. (2000) Functional architecture of an intracellular membrane t-SNARE. *Nature,* 407**,** 198-202.

FUNG, B. K. & STRYER, L. (1978) Surface density determination in membranes by fluorescence energy transfer. *Biochemistry,* 17**,** 5241-8.

FURGASON, M. L., MACDONALD, C., SHANKS, S. G., RYDER, S. P., BRYANT, N. J. & MUNSON, M. (2009) The N-terminal peptide of the syntaxin Tlg2p modulates binding of its closed conformation to Vps45p. *Proc Natl Acad Sci U S A.*

GARNER, M. M. & REVZIN, A. (1981) A gel electrophoresis method for quantifying the binding of proteins to specific DNA regions: application to components of the Escherichia coli lactose operon regulatory system. *Nucleic Acids Res,* 9**,** 3047-60.

GENGYO-ANDO, K., KAMIYA, Y., YAMAKAWA, A., KODAIRA, K., NISHIWAKI, K., MIWA, J., HORI, I. & HOSONO, R. (1993) The C. elegans unc-18 gene encodes a protein expressed in motor neurons. *Neuron,* 11**,** 703-11.

GETHING, M. J. & SAMBROOK, J. (1992) Protein folding in the cell. *Nature,* 355**,** 33-45.

GETZ, E. B., XIAO, M., CHAKRABARTY, T., COOKE, R. & SELVIN, P. R. (1999) A comparison between the sulfhydryl reductants tris(2-carboxyethyl)phosphine and dithiothreitol for use in protein biochemistry. *Anal Biochem,* 273**,** 73-80.

GILLINGHAM, A. K. & MUNRO, S. (2003) Long coiled-coil proteins and membrane traffic. *Biochim Biophys Acta,* 1641**,** 71-85.

GISSEN, P., JOHNSON, C. A., GENTLE, D., HURST, L. D., DOHERTY, A. J., O'KANE, C. J., KELLY, D. A. & MAHER, E. R. (2005) Comparative evolutionary analysis of VPS33 homologues: genetic and functional insights. *Hum Mol Genet,* 14**,** 1261-70.

GLICK, B. S. & ROTHMAN, J. E. (1987) Possible role for fatty acyl-coenzyme A in intracellular protein transport. *Nature,* 326**,** 309-12.

GRABOWSKI, R. & GALLWITZ, D. (1997) High-affinity binding of the yeast cis-Golgi t-SNARE, Sed5p, to wild-type and mutant Sly1p, a modulator of transport vesicle docking. *FEBS Lett,* 411**,** 169-72.

GROTE, E., CARR, C. M. & NOVICK, P. J. (2000) Ordering the final events in yeast exocytosis. *J Cell Biol,* 151**,** 439-52.

GUO, W., ROTH, D., WALCH-SOLIMENA, C. & NOVICK, P. (1999) The exocyst is an effector for Sec4p, targeting secretory vesicles to sites of exocytosis. *Embo J,* 18**,** 1071-80.

GUO, W., SACHER, M., BARROWMAN, J., FERRO-NOVICK, S. & NOVICK, P. (2000) Protein complexes in transport vesicle targeting. *Trends Cell Biol,* 10**,** 251-5.

GURUNATHAN, S., MARASH, M., WEINBERGER, A. & GERST, J. E. (2002) t-SNARE phosphorylation regulates endocytosis in yeast. *Mol Biol Cell,* 13**,** 1594-607.

HALACHMI, N. & LEV, Z. (1996) The Sec1 family: a novel family of proteins involved in synaptic transmission and general secretion. *J Neurochem,* 66**,** 889-97.

HARDWICK, K. G. & PELHAM, H. R. (1992) SED5 encodes a 39-kD integral membrane protein required for vesicular transport between the ER and the Golgi complex. *J Cell Biol,* 119**,** 513-21.

HARRISON, S. C. (2008) Viral membrane fusion. *Nat Struct Mol Biol,* 15**,** 690-8.

HARRISON, S. D., BROADIE, K., VAN DE GOOR, J. & RUBIN, G. M. (1994) Mutations in the Drosophila Rop gene suggest a function in general secretion and synaptic transmission. *Neuron,* 13**,** 555-66.

HASILIK, A. & TANNER, W. (1978) Biosynthesis of the vacuolar yeast glycoprotein carboxypeptidase Y. Conversion of precursor into the enzyme. *Eur J Biochem,* 85**,** 599-608.

HATA, Y., SLAUGHTER, C. A. & SUDHOF, T. C. (1993) Synaptic vesicle fusion complex contains unc-18 homologue bound to syntaxin. *Nature,* 366**,** 347-51.

HAYASHI, T., MCMAHON, H., YAMASAKI, S., BINZ, T., HATA, Y., SUDHOF, T. C. & NIEMANN, H. (1994) Synaptic vesicle membrane fusion complex: action of clostridial neurotoxins on assembly. *Embo J,* 13**,** 5051-61.

HEDMAN, J. M., EGGLESTON, M. D., ATTRYDE, A. L. & MARSHALL, P. A. (2007) Prevacuolar compartment morphology in vps mutants of Saccharomyces cerevisiae. *Cell Biol Int,* 31**,** 1237-44.

HEIM, R., CUBITT, A. B. & TSIEN, R. Y. (1995) Improved green fluorescence. *Nature,* 373**,** 663-4.

HESS, D. T., SLATER, T. M., WILSON, M. C. & SKENE, J. H. (1992) The 25 kDa synaptosomal-associated protein SNAP-25 is the major methionine-rich polypeptide in rapid axonal transport and a major substrate for palmitoylation in adult CNS. *J Neurosci,* 12**,** 4634-41.

HEYDUK, T., MA, Y., TANG, H. & EBRIGHT, R. H. (1996) Fluorescence anisotropy: rapid, quantitative assay for protein-DNA and protein-protein interaction. *Methods Enzymol,* 274**,** 492-503.

HOLTHUIS, J. C., NICHOLS, B. J., DHRUVAKUMAR, S. & PELHAM, H. R. (1998) Two syntaxin homologues in the TGN/endosomal system of yeast. *Embo J,* 17**,** 113-26.

HONG, W. (2005) SNAREs and traffic. *Biochim Biophys Acta,* 1744**,** 120-44.

HORAZDOVSKY, B. F., BUSCH, G. R. & EMR, S. D. (1994) VPS21 encodes a rab5-like GTP binding protein that is required for the sorting of yeast vacuolar proteins. *Embo J,* 13**,** 1297-309.

HOSONO, R., HEKIMI, S., KAMIYA, Y., SASSA, T., MURAKAMI, S., NISHIWAKI, K., MIWA, J., TAKETO, A. & KODAIRA, K. I. (1992) The unc-18 gene encodes a novel protein affecting the kinetics of acetylcholine metabolism in the nematode Caenorhabditis elegans. *J Neurochem,* 58**,** 1517-25.

HU, S. H., LATHAM, C. F., GEE, C. L., JAMES, D. E. & MARTIN, J. L. (2007) Structure of the Munc18c/Syntaxin4 N-peptide complex defines universal features of the N-peptide binding mode of Sec1/Munc18 proteins. *Proc Natl Acad Sci U S A,* 104**,** 8773-8.

INOUE, A., OBATA, K. & AKAGAWA, K. (1992) Cloning and sequence analysis of cDNA for a neuronal cell membrane antigen, HPC-1. *J Biol Chem,* 267**,** 10613-9.

JAHN, R. (2000) Sec1/Munc18 proteins: mediators of membrane fusion moving to center stage. *Neuron,* 27**,** 201-4.

JAHN, R., LANG, T. & SUDHOF, T. C. (2003) Membrane fusion. *Cell,* 112**,** 519-33.

JAHN, R. & SCHELLER, R. H. (2006) SNAREs--engines for membrane fusion. *Nat Rev Mol Cell Biol,* 7**,** 631-43.

JAHN, R. & SUDHOF, T. C. (1999) Membrane fusion and exocytosis. *Annu Rev Biochem,* 68**,** 863-911.

JAMES, P., HALLADAY, J. & CRAIG, E. A. (1996) Genomic libraries and a host strain designed for highly efficient two-hybrid selection in yeast. *Genetics,* 144**,** 1425-36.

JOHNSON, J. R., FERDEK, P., LIAN, L. Y., BARCLAY, J. W., BURGOYNE, R. D. & MORGAN, A. (2009) Binding of UNC-18 to the N-terminus of syntaxin is essential for neurotransmission in Caenorhabditis elegans. *Biochem J,* 418**,** 73-80.

JOHNSON, L. M., BANKAITIS, V. A. & EMR, S. D. (1987) Distinct sequence determinants direct intracellular sorting and modification of a yeast vacuolar protease. *Cell,* 48**,** 875-85.

JOHNSTON, M. (1987) A model fungal gene regulatory mechanism: the GAL genes of Saccharomyces cerevisiae. *Microbiol Rev,* 51**,** 458-76.

JONES, E. W. (1977) Proteinase mutants of Saccharomyces cerevisiae. *Genetics,* 85**,** 23-33.

KAPLAN, R. S. & PEDERSEN, P. L. (1989) Sensitive protein assay in presence of high levels of lipid. *Methods Enzymol,* 172**,** 393-9.

KATAGIRI, H., TERASAKI, J., MURATA, T., ISHIHARA, H., OGIHARA, T., INUKAI, K., FUKUSHIMA, Y., ANAI, M., KIKUCHI, M., MIYAZAKI, J. & ET AL. (1995) A novel isoform of syntaxin-binding protein homologous to yeast Sec1 expressed ubiquitously in mammalian cells. *J Biol Chem,* 270**,** 4963-6.

KEEGAN, L., GILL, G. & PTASHNE, M. (1986) Separation of DNA binding from the transcription-activating function of a eukaryotic regulatory protein. *Science,* 231**,** 699-704.

KHVOTCHEV, M., DULUBOVA, I., SUN, J., DAI, H., RIZO, J. & SUDHOF, T. C. (2007) Dual modes of Munc18-1/SNARE interactions are coupled by functionally critical binding to syntaxin-1 N terminus. *J Neurosci,* 27**,** 12147-55.

KIM, D. W., SACHER, M., SCARPA, A., QUINN, A. M. & FERRO-NOVICK, S. (1999) High-copy suppressor analysis reveals a physical interaction between Sec34p and Sec35p, a protein implicated in vesicle docking. *Mol Biol Cell,* 10**,** 3317-29.

KINUTA, M. & TAKEI, K. (2002) Utilization of liposomes in vesicular transport studies. *Cell Struct Funct,* 27**,** 63-9.

KOSODO, Y., NODA, Y., ADACHI, H. & YODA, K. (2002) Binding of Sly1 to Sed5 enhances formation of the yeast early Golgi SNARE complex. *J Cell Sci,* 115**,** 3683-91.

KOSODO, Y., NODA, Y., ADACHI, H. & YODA, K. (2003) Cooperation of Sly1/SM-family protein and sec18/NSF of Saccharomyces cerevisiae in disassembly of cis-SNARE membrane-protein complexes. *Biosci Biotechnol Biochem,* 67**,** 448-50.

KWEON, Y., ROTHE, A., CONIBEAR, E. & STEVENS, T. H. (2003) Ykt6p is a multifunctional yeast R-SNARE that is required for multiple membrane transport pathways to the vacuole. *Mol Biol Cell,* 14**,** 1868-81.

LAEMMLI, U. K. (1970) Cleavage of structural proteins during the assembly of the head of bacteriophage T4. *Nature,* 227**,** 680-5.

LANE, S. R. & LIU, Y. (1997) Characterization of the palmitoylation domain of SNAP-25. *J Neurochem,* 69**,** 1864-9.

LATHAM, C. F., LOPEZ, J. A., HU, S. H., GEE, C. L., WESTBURY, E., BLAIR, D. H., ARMISHAW, C. J., ALEWOOD, P. F., BRYANT, N. J., JAMES, D. E. & MARTIN, J. L. (2006) Molecular dissection of the Munc18c/syntaxin4 interaction: implications for regulation of membrane trafficking. *Traffic,* 7**,** 1408-19.

LATHAM, C. F. & MEUNIER, F. A. (2007) Munc18a: Munc-y business in mediating exocytosis. *Int J Biochem Cell Biol,* 39**,** 1576-81.

LATHAM, C. F., OSBORNE, S. L., CRYLE, M. J. & MEUNIER, F. A. (2007) Arachidonic acid potentiates exocytosis and allows neuronal SNARE complex to interact with Munc18a. *J Neurochem,* 100**,** 1543-54.

LAUFMAN, O., KEDAN, A., HONG, W. & LEV, S. (2009) Direct interaction between the COG complex and the SM protein, Sly1, is required for Golgi SNARE pairing. *Embo J,* 28**,** 2006-17.

LAUGHON, A. & GESTELAND, R. F. (1984) Primary structure of the Saccharomyces cerevisiae GAL4 gene. *Mol Cell Biol,* 4**,** 260-7.

LE MAIRE, M., CHAMPEIL, P. & MOLLER, J. V. (2000) Interaction of membrane proteins and lipids with solubilizing detergents. *Biochim Biophys Acta,* 1508**,** 86-111.

LERMAN, J. C., ROBBLEE, J., FAIRMAN, R. & HUGHSON, F. M. (2000) Structural analysis of the neuronal SNARE protein syntaxin-1A. *Biochemistry,* 39**,** 8470-9.

LI, B. & FIELDS, S. (1993) Identification of mutations in p53 that affect its binding to SV40 large T antigen by using the yeast two-hybrid system. *Faseb J,* 7**,** 957-63.

LI, L., ELLEDGE, S. J., PETERSON, C. A., BALES, E. S. & LEGERSKI, R. J. (1994) Specific association between the human DNA repair proteins XPA and ERCC1. *Proc Natl Acad Sci U S A,* 91**,** 5012-6.

LIPSCHUTZ, J. H. & MOSTOV, K. E. (2002) Exocytosis: the many masters of the exocyst. *Curr Biol,* 12**,** R212-4.

LIU, S., WILSON, K. A., RICE-STITT, T., NEIMAN, A. M. & MCNEW, J. A. (2007) In vitro fusion catalyzed by the sporulation-specific t-SNARE light-chain Spo20p is stimulated by phosphatidic acid. *Traffic,* 8**,** 1630-43.

MA, J. & PTASHNE, M. (1987) Deletion analysis of GAL4 defines two transcriptional activating segments. *Cell,* 48**,** 847-53.

MANOLSON, M. F., PROTEAU, D., PRESTON, R. A., STENBIT, A., ROBERTS, B. T., HOYT, M. A., PREUSS, D., MULHOLLAND, J., BOTSTEIN, D. & JONES, E.

W. (1992) The VPH1 gene encodes a 95-kDa integral membrane polypeptide required for in vivo assembly and activity of the yeast vacuolar H(+)-ATPase. *J Biol Chem,* 267**,** 14294-303.

MARGITTAI, M., FASSHAUER, D., JAHN, R. & LANGEN, R. (2003) The Habc domain and the SNARE core complex are connected by a highly flexible linker. *Biochemistry,* 42**,** 4009-14.

MARTIN, J., MAYHEW, M., LANGER, T. & HARTL, F. U. (1993) The reaction cycle of GroEL and GroES in chaperonin-assisted protein folding. *Nature,* 366**,** 228-33.

MCALISTER-HENN, L., GIBSON, N. & PANISKO, E. (1999) Applications of the yeast two-hybrid system. *Methods,* 19**,** 330-7.

MCBRIDE, H. M., RYBIN, V., MURPHY, C., GINER, A., TEASDALE, R. & ZERIAL, M. (1999) Oligomeric complexes link Rab5 effectors with NSF and drive membrane fusion via interactions between EEA1 and syntaxin 13. *Cell,* 98**,** 377-86.

MCLAUCHLAN, H., NEWELL, J., MORRICE, N., OSBORNE, A., WEST, M. & SMYTHE, E. (1998) A novel role for Rab5-GDI in ligand sequestration into clathrin-coated pits. *Curr Biol,* 8**,** 34-45.

MCNEW, J. A. (2008) Regulation of SNARE-mediated membrane fusion during exocytosis. *Chem Rev,* 108**,** 1669-86.

MCNEW, J. A., PARLATI, F., FUKUDA, R., JOHNSTON, R. J., PAZ, K., PAUMET, F., SOLLNER, T. H. & ROTHMAN, J. E. (2000) Compartmental specificity of cellular membrane fusion encoded in SNARE proteins. *Nature,* 407**,** 153-9.

MCNEW, J. A., SOGAARD, M., LAMPEN, N. M., MACHIDA, S., YE, R. R., LACOMIS, L., TEMPST, P., ROTHMAN, J. E. & SOLLNER, T. H. (1997) Ykt6p, a prenylated SNARE essential for endoplasmic reticulum-Golgi transport. *J Biol Chem,* 272**,** 17776-83.

MCNEW, J. A., WEBER, T., ENGELMAN, D. M., SOLLNER, T. H. & ROTHMAN, J. E. (1999) The length of the flexible SNAREpin juxtamembrane region is a critical determinant of SNARE-dependent fusion. *Mol Cell,* 4**,** 415-21.

MELIA, T. J., WEBER, T., MCNEW, J. A., FISHER, L. E., JOHNSTON, R. J., PARLATI, F., MAHAL, L. K., SOLLNER, T. H. & ROTHMAN, J. E. (2002) Regulation of membrane fusion by the membrane-proximal coil of the t-SNARE during zippering of SNAREpins. *J Cell Biol,* 158**,** 929-40.

MISURA, K. M., BOCK, J. B., GONZALEZ, L. C., JR., SCHELLER, R. H. & WEIS, W. I. (2002) Three-dimensional structure of the amino-terminal domain of syntaxin 6, a SNAP-25 C homolog. *Proc Natl Acad Sci U S A,* 99**,** 9184-9.

MISURA, K. M., SCHELLER, R. H. & WEIS, W. I. (2000) Three-dimensional structure of the neuronal-Sec1-syntaxin 1a complex. *Nature,* 404**,** 355-62.

MORRISON, H. A., DIONNE, H., RUSTEN, T. E., BRECH, A., FISHER, W. W., PFEIFFER, B. D., CELNIKER, S. E., STENMARK, H. & BILDER, D. (2008) Regulation of early endosomal entry by the Drosophila tumor suppressors Rabenosyn and Vps45. *Mol Biol Cell,* 19**,** 4167-76.

MUNSON, M. (2009) Tip20p reaches out to Dsl1p to tether membranes. *Nat Struct Mol Biol,* 16**,** 100-2.

MUNSON, M., CHEN, X., COCINA, A. E., SCHULTZ, S. M. & HUGHSON, F. M. (2000) Interactions within the yeast t-SNARE Sso1p that control SNARE complex assembly. *Nat Struct Biol,* 7**,** 894-902.

MUNSON, M. & HUGHSON, F. M. (2002) Conformational regulation of SNARE assembly and disassembly in vivo. *J Biol Chem,* 277**,** 9375-81.

NEWMAN, A. P., GROESCH, M. E. & FERRO-NOVICK, S. (1992) Bos1p, a membrane protein required for ER to Golgi transport in yeast, co-purifies with the carrier vesicles and with Bet1p and the ER membrane. *Embo J,* 11**,** 3609-17.

NICHOLS, B. J., HOLTHUIS, J. C. & PELHAM, H. R. (1998) The Sec1p homologue Vps45p binds to the syntaxin Tlg2p. *Eur J Cell Biol,* 77**,** 263-8.

NICHOLSON, K. L., MUNSON, M., MILLER, R. B., FILIP, T. J., FAIRMAN, R. & HUGHSON, F. M. (1998) Regulation of SNARE complex assembly by an N-terminal domain of the t-SNARE Sso1p. *Nat Struct Biol,* 5**,** 793-802.

NIELSEN, E., CHRISTOFORIDIS, S., UTTENWEILER-JOSEPH, S., MIACZYNSKA, M., DEWITTE, F., WILM, M., HOFLACK, B. & ZERIAL, M. (2000) Rabenosyn-5, a novel Rab5 effector, is complexed with hVPS45 and recruited to endosomes through a FYVE finger domain. *J Cell Biol,* 151**,** 601-12.

NOTHWEHR, S. F., BRYANT, N. J. & STEVENS, T. H. (1996) The newly identified yeast GRD genes are required for retention of late-Golgi membrane proteins. *Mol Cell Biol,* 16**,** 2700-7.

NOVICK, P., FIELD, C. & SCHEKMAN, R. (1980) Identification of 23 complementation groups required for post-translational events in the yeast secretory pathway. *Cell,* 21**,** 205-15.

O'SHANNESSY, D. J., BRIGHAM-BURKE, M. & PECK, K. (1992) Immobilization chemistries suitable for use in the BIAcore surface plasmon resonance detector. *Anal Biochem,* 205**,** 132-6.

ODORIZZI, G., KATZMANN, D. J., BABST, M., AUDHYA, A. & EMR, S. D. (2003) Bro1 is an endosome-associated protein that functions in the MVB pathway in Saccharomyces cerevisiae. *J Cell Sci,* 116**,** 1893-903.

OHYA, T., MIACZYNSKA, M., COSKUN, U., LOMMER, B., RUNGE, A., DRECHSEL, D., KALAIDZIDIS, Y. & ZERIAL, M. (2009) Reconstitution of Rab- and SNARE-dependent membrane fusion by synthetic endosomes. *Nature,* 459**,** 1091-7.

OKA, T. & KRIEGER, M. (2005) Multi-component protein complexes and Golgi membrane trafficking. *J Biochem,* 137**,** 109-14.

OKAMOTO, M. & SUDHOF, T. C. (1997) Mints, Munc18-interacting proteins in synaptic vesicle exocytosis. *J Biol Chem,* 272**,** 31459-64.

OSSIG, R., DASCHER, C., TREPTE, H. H., SCHMITT, H. D. & GALLWITZ, D. (1991) The yeast SLY gene products, suppressors of defects in the essential GTP-binding

Ypt1 protein, may act in endoplasmic reticulum-to-Golgi transport. *Mol Cell Biol,* 11**,** 2980-93.

OSTROWICZ, C. W., MEIRINGER, C. T. & UNGERMANN, C. (2008) Yeast vacuole fusion: a model system for eukaryotic endomembrane dynamics. *Autophagy,* 4**,** 5-19.

OYLER, G. A., HIGGINS, G. A., HART, R. A., BATTENBERG, E., BILLINGSLEY, M., BLOOM, F. E. & WILSON, M. C. (1989) The identification of a novel synaptosomal-associated protein, SNAP-25, differentially expressed by neuronal subpopulations. *J Cell Biol,* 109**,** 3039-52.

PALADE, G. (1975) Intracellular aspects of the process of protein synthesis. *Science,* 189**,** 347-58.

PARK, S. H. & RAINES, R. T. (1997) Green fluorescent protein as a signal for protein-protein interactions. *Protein Sci,* 6**,** 2344-9.

PARK, S. H. & RAINES, R. T. (2004) Fluorescence polarization assay to quantify protein-protein interactions. *Methods Mol Biol,* 261**,** 161-6.

PARLATI, F., MCNEW, J. A., FUKUDA, R., MILLER, R., SOLLNER, T. H. & ROTHMAN, J. E. (2000) Topological restriction of SNARE-dependent membrane fusion. *Nature,* 407**,** 194-8.

PARLATI, F., VARLAMOV, O., PAZ, K., MCNEW, J. A., HURTADO, D., SOLLNER, T. H. & ROTHMAN, J. E. (2002) Distinct SNARE complexes mediating membrane fusion in Golgi transport based on combinatorial specificity. *Proc Natl Acad Sci U S A,* 99**,** 5424-9.

PARLATI, F., WEBER, T., MCNEW, J. A., WESTERMANN, B., SOLLNER, T. H. & ROTHMAN, J. E. (1999) Rapid and efficient fusion of phospholipid vesicles by the alpha-helical core of a SNARE complex in the absence of an N-terminal regulatory domain. *Proc Natl Acad Sci U S A,* 96**,** 12565-70.

PATZER, E. J., WAGNER, R. R. & DUBOVI, E. J. (1979) Viral membranes: model systems for studying biological membranes. *CRC Crit Rev Biochem,* 6**,** 165-217.

PAUMET, F., BRUGGER, B., PARLATI, F., MCNEW, J. A., SOLLNER, T. H. & ROTHMAN, J. E. (2001) A t-SNARE of the endocytic pathway must be activated for fusion. *J Cell Biol,* 155**,** 961-8.

PAUMET, F., RAHIMIAN, V., DI LIBERTO, M. & ROTHMAN, J. E. (2005) Concerted auto-regulation in yeast endosomal t-SNAREs. *J Biol Chem,* 280**,** 21137-43.

PAUMET, F., RAHIMIAN, V. & ROTHMAN, J. E. (2004) The specificity of SNARE-dependent fusion is encoded in the SNARE motif. *Proc Natl Acad Sci U S A,* 101**,** 3376-80.

PELHAM, H. R. (1999) SNAREs and the secretory pathway-lessons from yeast. *Exp Cell Res,* 247**,** 1-8.

PELHAM, H. R. (2001) SNAREs and the specificity of membrane fusion. *Trends Cell Biol,* 11**,** 99-101.

PENG, R. & GALLWITZ, D. (2002) Sly1 protein bound to Golgi syntaxin Sed5p allows assembly and contributes to specificity of SNARE fusion complexes. *J Cell Biol,* 157**,** 645-55.

PENG, R. & GALLWITZ, D. (2004) Multiple SNARE interactions of an SM protein: Sed5p/Sly1p binding is dispensable for transport. *Embo J,* 23**,** 3939-49.

PENG, R. W. (2005) Decoding the interactions of SM proteins with SNAREs. *ScientificWorldJournal,* 5**,** 471-7.

PEREIRA-LEAL, J. B. & SEABRA, M. C. (2001) Evolution of the Rab family of small GTP-binding proteins. *J Mol Biol,* 313**,** 889-901.

PFEFFER, S. R. (1999) Transport-vesicle targeting: tethers before SNAREs. *Nat Cell Biol,* 1**,** E17-22.

PIPER, R. C., WHITTERS, E. A. & STEVENS, T. H. (1994) Yeast Vps45p is a Sec1p-like protein required for the consumption of vacuole-targeted, post-Golgi transport vesicles. *Eur J Cell Biol,* 65**,** 305-18.

POIRIER, M. A., HAO, J. C., MALKUS, P. N., CHAN, C., MOORE, M. F., KING, D. S. & BENNETT, M. K. (1998a) Protease resistance of syntaxin.SNAP-25.VAMP complexes. Implications for assembly and structure. *J Biol Chem,* 273**,** 11370-7.

POIRIER, M. A., XIAO, W., MACOSKO, J. C., CHAN, C., SHIN, Y. K. & BENNETT, M. K. (1998b) The synaptic SNARE complex is a parallel four-stranded helical bundle. *Nat Struct Biol,* 5**,** 765-9.

PRASHER, D. C., ECKENRODE, V. K., WARD, W. W., PRENDERGAST, F. G. & CORMIER, M. J. (1992) Primary structure of the Aequorea victoria green-fluorescent protein. *Gene,* 111**,** 229-33.

PREKERIS, R., KLUMPERMAN, J. & SCHELLER, R. H. (2000) Syntaxin 11 is an atypical SNARE abundant in the immune system. *Eur J Cell Biol,* 79**,** 771-80.

PRESTON, R. A., MANOLSON, M. F., BECHERER, K., WEIDENHAMMER, E., KIRKPATRICK, D., WRIGHT, R. & JONES, E. W. (1991) Isolation and characterization of PEP3, a gene required for vacuolar biogenesis in Saccharomyces cerevisiae. *Mol Cell Biol,* 11**,** 5801-12.

PRICE, A., SEALS, D., WICKNER, W. & UNGERMANN, C. (2000) The docking stage of yeast vacuole fusion requires the transfer of proteins from a cis-SNARE complex to a Rab/Ypt protein. *J Cell Biol,* 148**,** 1231-8.

PROTOPOPOV, V., GOVINDAN, B., NOVICK, P. & GERST, J. E. (1993) Homologs of the synaptobrevin/VAMP family of synaptic vesicle proteins function on the late secretory pathway in S. cerevisiae. *Cell,* 74**,** 855-61.

RAND, R. P. (1981) Interacting phospholipid bilayers: measured forces and induced structural changes. *Annu Rev Biophys Bioeng,* 10**,** 277-314.

RAVICHANDRAN, V., CHAWLA, A. & ROCHE, P. A. (1996) Identification of a novel syntaxin- and synaptobrevin/VAMP-binding protein, SNAP-23, expressed in non-neuronal tissues. *J Biol Chem,* 271**,** 13300-3.

RAYMOND, C. K., HOWALD-STEVENSON, I., VATER, C. A. & STEVENS, T. H. (1992) Morphological classification of the yeast vacuolar protein sorting mutants: evidence for a prevacuolar compartment in class E vps mutants. *Mol Biol Cell,* 3**,** 1389-402.

RICE, L. M., BRENNWALD, P. & BRUNGER, A. T. (1997) Formation of a yeast SNARE complex is accompanied by significant structural changes. *FEBS Lett,* 415**,** 49-55.

RICHMOND, J. E., WEIMER, R. M. & JORGENSEN, E. M. (2001) An open form of syntaxin bypasses the requirement for UNC-13 in vesicle priming. *Nature,* 412**,** 338-41.

RICKMAN, C., MEDINE, C. N., BERGMANN, A. & DUNCAN, R. R. (2007) Functionally and spatially distinct modes of munc18-syntaxin 1 interaction. *J Biol Chem,* 282**,** 12097-103.

RIENTO, K., JANTTI, J., JANSSON, S., HIELM, S., LEHTONEN, E., EHNHOLM, C., KERANEN, S. & OLKKONEN, V. M. (1996) A sec1-related vesicle-transport protein that is expressed predominantly in epithelial cells. *Eur J Biochem,* 239**,** 638-46.

RIZO, J. & SUDHOF, T. C. (2002) Snares and Munc18 in synaptic vesicle fusion. *Nat Rev Neurosci,* 3**,** 641-53.

ROBINSON, J. S., KLIONSKY, D. J., BANTA, L. M. & EMR, S. D. (1988) Protein sorting in Saccharomyces cerevisiae: isolation of mutants defective in the delivery and processing of multiple vacuolar hydrolases. *Mol Cell Biol,* 8**,** 4936-48.

ROHMAN, M. & HARRISON-LAVOIE, K. J. (2000) Separation of copurifying GroEL from glutathione-S-transferase fusion proteins. *Protein Expr Purif,* 20**,** 45-7.

ROSEN, H. (1957) A modified ninhydrin colorimetric analysis for amino acids. *Arch Biochem Biophys,* 67**,** 10-5.

ROSSANESE, O. W., REINKE, C. A., BEVIS, B. J., HAMMOND, A. T., SEARS, I. B., O'CONNOR, J. & GLICK, B. S. (2001) A role for actin, Cdc1p, and Myo2p in the inheritance of late Golgi elements in Saccharomyces cerevisiae. *J Cell Biol,* 153**,** 47-62.

ROTHMAN, J. E. (1994) Mechanisms of intracellular protein transport. *Nature,* 372**,** 55-63.

ROTHMAN, J. H., HOWALD, I. & STEVENS, T. H. (1989) Characterization of genes required for protein sorting and vacuolar function in the yeast Saccharomyces cerevisiae. *Embo J,* 8**,** 2057-65.

ROTHMAN, J. H. & STEVENS, T. H. (1986) Protein sorting in yeast: mutants defective in vacuole biogenesis mislocalize vacuolar proteins into the late secretory pathway. *Cell,* 47**,** 1041-51.

RYDER, S. P., RECHT, M. I. & WILLIAMSON, J. R. (2008) Quantitative analysis of protein-RNA interactions by gel mobility shift. *Methods Mol Biol,* 488**,** 99-115.

SACHER, M., KIM, Y. G., LAVIE, A., OH, B. H. & SEGEV, N. (2008) The TRAPP complex: insights into its architecture and function. *Traffic,* 9**,** 2032-42.

SALMINEN, A. & NOVICK, P. J. (1987) A ras-like protein is required for a post-Golgi event in yeast secretion. *Cell,* 49**,** 527-38.

SAPPERSTEIN, S. K., LUPASHIN, V. V., SCHMITT, H. D. & WATERS, M. G. (1996) Assembly of the ER to Golgi SNARE complex requires Uso1p. *J Cell Biol,* 132**,** 755-67.

SATO, T. K., DARSOW, T. & EMR, S. D. (1998) Vam7p, a SNAP-25-like molecule, and Vam3p, a syntaxin homolog, function together in yeast vacuolar protein trafficking. *Mol Cell Biol,* 18**,** 5308-19.

SATO, T. K., REHLING, P., PETERSON, M. R. & EMR, S. D. (2000) Class C Vps protein complex regulates vacuolar SNARE pairing and is required for vesicle docking/fusion. *Mol Cell,* 6**,** 661-71.

SCALES, S. J., CHEN, Y. A., YOO, B. Y., PATEL, S. M., DOUNG, Y. C. & SCHELLER, R. H. (2000) SNAREs contribute to the specificity of membrane fusion. *Neuron,* 26**,** 457-64.

SCHAFFNER, W. & WEISSMANN, C. (1973) A rapid, sensitive, and specific method for the determination of protein in dilute solution. *Anal Biochem,* 56**,** 502-14.

SCOTT, B. L., VAN KOMEN, J. S., IRSHAD, H., LIU, S., WILSON, K. A. & MCNEW, J. A. (2004) Sec1p directly stimulates SNARE-mediated membrane fusion in vitro. *J Cell Biol,* 167**,** 75-85.

SCOTT, B. L., VAN KOMEN, J. S., LIU, S., WEBER, T., MELIA, T. J. & MCNEW, J. A. (2003) Liposome fusion assay to monitor intracellular membrane fusion machines. *Methods Enzymol,* 372**,** 274-300.

SEALS, D. F., EITZEN, G., MARGOLIS, N., WICKNER, W. T. & PRICE, A. (2000) A Ypt/Rab effector complex containing the Sec1 homolog Vps33p is required for homotypic vacuole fusion. *Proc Natl Acad Sci U S A,* 97**,** 9402-7.

SERON, K., TIEAHO, V., PRESCIANOTTO-BASCHONG, C., AUST, T., BLONDEL, M. O., GUILLAUD, P., DEVILLIERS, G., ROSSANESE, O. W., GLICK, B. S., RIEZMAN, H., KERANEN, S. & HAGUENAUER-TSAPIS, R. (1998) A yeast t-SNARE involved in endocytosis. *Mol Biol Cell,* 9**,** 2873-89.

SEVRIOUKOV, E. A., HE, J. P., MOGHRABI, N., SUNIO, A. & KRAMER, H. (1999) A role for the deep orange and carnation eye color genes in lysosomal delivery in Drosophila. *Mol Cell,* 4**,** 479-86.

SHEN, J., TARESTE, D. C., PAUMET, F., ROTHMAN, J. E. & MELIA, T. J. (2007) Selective activation of cognate SNAREpins by Sec1/Munc18 proteins. *Cell,* 128**,** 183-95.

SHESTAKOVA, A., SUVOROVA, E., PAVLIV, O., KHAIDAKOVA, G. & LUPASHIN, V. (2007) Interaction of the conserved oligomeric Golgi complex with t-SNARE Syntaxin5a/Sed5 enhances intra-Golgi SNARE complex stability. *J Cell Biol,* 179**,** 1179-92.

SINIOSSOGLOU, S. & PELHAM, H. R. (2002) Vps51p links the VFT complex to the SNARE Tlg1p. *J Biol Chem,* 277**,** 48318-24.

SMITH, D. B. & JOHNSON, K. S. (1988) Single-step purification of polypeptides expressed in Escherichia coli as fusions with glutathione S-transferase. *Gene,* 67**,** 31-40.

SOLLNER, T., BENNETT, M. K., WHITEHEART, S. W., SCHELLER, R. H. & ROTHMAN, J. E. (1993a) A protein assembly-disassembly pathway in vitro that may correspond to sequential steps of synaptic vesicle docking, activation, and fusion. *Cell,* 75**,** 409-18.

SOLLNER, T., WHITEHEART, S. W., BRUNNER, M., ERDJUMENT-BROMAGE, H., GEROMANOS, S., TEMPST, P. & ROTHMAN, J. E. (1993b) SNAP receptors implicated in vesicle targeting and fusion. *Nature,* 362**,** 318-24.

SOLLNER, T. H. (2004) Intracellular and viral membrane fusion: a uniting mechanism. *Curr Opin Cell Biol,* 16**,** 429-35.

SRIVASTAVA, A. & JONES, E. W. (1998) Pth1/Vam3p is the syntaxin homolog at the vacuolar membrane of Saccharomyces cerevisiae required for the delivery of vacuolar hydrolases. *Genetics,* 148**,** 85-98.

STEIN, A., WEBER, G., WAHL, M. C. & JAHN, R. (2009) Helical extension of the neuronal SNARE complex into the membrane. *Nature.*

STENMARK, H. (2009) Rab GTPases as coordinators of vesicle traffic. *Nat Rev Mol Cell Biol,* 10**,** 513-25.

STEVENS, T., ESMON, B. & SCHEKMAN, R. (1982) Early stages in the yeast secretory pathway are required for transport of carboxypeptidase Y to the vacuole. *Cell,* 30**,** 439-48.

STROP, P., KAISER, S. E., VRLJIC, M. & BRUNGER, A. T. (2008) The structure of the yeast plasma membrane SNARE complex reveals destabilizing water-filled cavities. *J Biol Chem,* 283**,** 1113-9.

STRUCK, D. K., HOEKSTRA, D. & PAGANO, R. E. (1981) Use of resonance energy transfer to monitor membrane fusion. *Biochemistry,* 20**,** 4093-9.

STRUTHERS, M. S., SHANKS, S. G., MACDONALD, C., CARPP, L. N., DROZDOWSKA, A. M., KIOUMOURTZOGLOU, D., FURGASON, M. L., MUNSON, M. & BRYANT, N. J. (2009) Functional homology of mammalian syntaxin 16 and yeast Tlg2p reveals a conserved regulatory mechanism. *J Cell Sci,* 122**,** 2292-9.

SUBRAMANIAN, S., WOOLFORD, C. A. & JONES, E. W. (2004) The Sec1/Munc18 protein, Vps33p, functions at the endosome and the vacuole of Saccharomyces cerevisiae. *Mol Biol Cell,* 15**,** 2593-605.

SUDHOF, T. C., BAUMERT, M., PERIN, M. S. & JAHN, R. (1989) A synaptic vesicle membrane protein is conserved from mammals to Drosophila. *Neuron,* 2**,** 1475-81.

SUDHOF, T. C. & ROTHMAN, J. E. (2009) Membrane fusion: grappling with SNARE and SM proteins. *Science,* 323**,** 474-7.

SUTTON, R. B., FASSHAUER, D., JAHN, R. & BRUNGER, A. T. (1998) Crystal structure of a SNARE complex involved in synaptic exocytosis at 2.4 A resolution. *Nature,* 395**,** 347-53.

TANG, B. L., LOW, D. Y. & HONG, W. (1998) Syntaxin 11: a member of the syntaxin family without a carboxyl terminal transmembrane domain. *Biochem Biophys Res Commun,* 245**,** 627-32.

TELLAM, J. T., MCINTOSH, S. & JAMES, D. E. (1995) Molecular identification of two novel Munc-18 isoforms expressed in non-neuronal tissues. *J Biol Chem,* 270**,** 5857-63.

TENG, F. Y., WANG, Y. & TANG, B. L. (2001) The syntaxins. *Genome Biol,* 2**,** REVIEWS3012.

TERBUSH, D. R., MAURICE, T., ROTH, D. & NOVICK, P. (1996) The Exocyst is a multiprotein complex required for exocytosis in Saccharomyces cerevisiae. *Embo J,* 15**,** 6483-94.

TERBUSH, D. R. & NOVICK, P. (1995) Sec6, Sec8, and Sec15 are components of a multisubunit complex which localizes to small bud tips in Saccharomyces cerevisiae. *J Cell Biol,* 130**,** 299-312.

THAIN, A., GASTON, K., JENKINS, O. & CLARKE, A. R. (1996) A method for the separation of GST fusion proteins from co-purifying GroEL. *Trends Genet,* 12**,** 209-10.

TOGNERI, J., CHENG, Y. S., MUNSON, M., HUGHSON, F. M. & CARR, C. M. (2006) Specific SNARE complex binding mode of the Sec1/Munc-18 protein, Sec1p. *Proc Natl Acad Sci U S A,* 103**,** 17730-5.

TOONEN, R. F. (2003) Role of Munc18-1 in synaptic vesicle and large dense-core vesicle secretion. *Biochem Soc Trans,* 31**,** 848-50.

TOONEN, R. F. & VERHAGE, M. (2003) Vesicle trafficking: pleasure and pain from SM genes. *Trends Cell Biol,* 13**,** 177-86.

TRIMBLE, R. B., MALEY, F. & CHU, F. K. (1983) GlycoProtein biosynthesis in yeast. protein conformation affects processing of high mannose oligosaccharides on carboxypeptidase Y and invertase. *J Biol Chem,* 258**,** 2562-7.

TRIMBLE, W. S., COWAN, D. M. & SCHELLER, R. H. (1988) VAMP-1: a synaptic vesicle-associated integral membrane protein. *Proc Natl Acad Sci U S A,* 85**,** 4538-42.

TRIPATHI, A., REN, Y., JEFFREY, P. D. & HUGHSON, F. M. (2009) Structural characterization of Tip20p and Dsl1p, subunits of the Dsl1p vesicle tethering complex. *Nat Struct Mol Biol,* 16**,** 114-23.

TSUI, M. M. & BANFIELD, D. K. (2000) Yeast Golgi SNARE interactions are promiscuous. *J Cell Sci,* 113 (Pt 1)**,** 145-52.

UNGAR, D. & HUGHSON, F. M. (2003) SNARE protein structure and function. *Annu Rev Cell Dev Biol,* 19**,** 493-517.

UNGAR, D., OKA, T., BRITTLE, E. E., VASILE, E., LUPASHIN, V. V., CHATTERTON, J. E., HEUSER, J. E., KRIEGER, M. & WATERS, M. G. (2002) Characterization of a mammalian Golgi-localized protein complex, COG, that is required for normal Golgi morphology and function. *J Cell Biol,* 157**,** 405-15.

VANRHEENEN, S. M., CAO, X., SAPPERSTEIN, S. K., CHIANG, E. C., LUPASHIN, V. V., BARLOWE, C. & WATERS, M. G. (1999) Sec34p, a protein required for vesicle tethering to the yeast Golgi apparatus, is in a complex with Sec35p. *J Cell Biol,* 147**,** 729-42.

VERHAGE, M., MAIA, A. S., PLOMP, J. J., BRUSSAARD, A. B., HEEROMA, J. H., VERMEER, H., TOONEN, R. F., HAMMER, R. E., VAN DEN BERG, T. K., MISSLER, M., GEUZE, H. J. & SUDHOF, T. C. (2000) Synaptic assembly of the brain in the absence of neurotransmitter secretion. *Science,* 287**,** 864-9.

VERHAGE, M. & TOONEN, R. F. (2007) Regulated exocytosis: merging ideas on fusing membranes. *Curr Opin Cell Biol,* 19**,** 402-8.

VICOGNE, J. & PESSIN, J. E. (2008) SNARE-mediated fusion of liposomes. *Methods Mol Biol,* 457**,** 241-51.

VIDAL, M., BRACHMANN, R. K., FATTAEY, A., HARLOW, E. & BOEKE, J. D. (1996a) Reverse two-hybrid and one-hybrid systems to detect dissociation of protein-protein and DNA-protein interactions. *Proc Natl Acad Sci U S A,* 93**,** 10315-20.

VIDAL, M., BRAUN, P., CHEN, E., BOEKE, J. D. & HARLOW, E. (1996b) Genetic characterization of a mammalian protein-protein interaction domain by using a yeast reverse two-hybrid system. *Proc Natl Acad Sci U S A,* 93**,** 10321-6.

VOGEL, K. & ROCHE, P. A. (1999) SNAP-23 and SNAP-25 are palmitoylated in vivo. *Biochem Biophys Res Commun,* 258**,** 407-10.

VON MOLLARD, G. F., NOTHWEHR, S. F. & STEVENS, T. H. (1997) The yeast v-SNARE Vti1p mediates two vesicle transport pathways through interactions with the t-SNAREs Sed5p and Pep12p. *J Cell Biol,* 137**,** 1511-24.

WADA, Y., KITAMOTO, K., KANBE, T., TANAKA, K. & ANRAKU, Y. (1990) The SLP1 gene of Saccharomyces cerevisiae is essential for vacuolar morphogenesis and function. *Mol Cell Biol,* 10**,** 2214-23.

WADA, Y., NAKAMURA, N., OHSUMI, Y. & HIRATA, A. (1997) Vam3p, a new member of syntaxin related protein, is required for vacuolar assembly in the yeast Saccharomyces cerevisiae. *J Cell Sci,* 110 (Pt 11)**,** 1299-306.

WADA, Y., OHSUMI, Y. & ANRAKU, Y. (1992) Genes for directing vacuolar morphogenesis in Saccharomyces cerevisiae. I. Isolation and characterization of two classes of vam mutants. *J Biol Chem,* 267**,** 18665-70.

WALHOUT, A. J. & VIDAL, M. (2001) High-throughput yeast two-hybrid assays for large-scale protein interaction mapping. *Methods,* 24**,** 297-306.

WALKER, P. A., LEONG, L. E., NG, P. W., TAN, S. H., WALLER, S., MURPHY, D. & PORTER, A. G. (1994) Efficient and rapid affinity purification of proteins using recombinant fusion proteases. *Biotechnology (N Y),* 12**,** 601-5.

WATSON, H. C., WALKER, N. P., SHAW, P. J., BRYANT, T. N., WENDELL, P. L., FOTHERGILL, L. A., PERKINS, R. E., CONROY, S. C., DOBSON, M. J., TUITE, M. F. & ET AL. (1982) Sequence and structure of yeast phosphoglycerate kinase. *Embo J,* 1**,** 1635-40.

WEBB, G. C., HOEDT, M., POOLE, L. J. & JONES, E. W. (1997) Genetic interactions between a pep7 mutation and the PEP12 and VPS45 genes: evidence for a novel SNARE component in transport between the Saccharomyces cerevisiae Golgi complex and endosome. *Genetics,* 147**,** 467-78.

WEBER, T., ZEMELMAN, B. V., MCNEW, J. A., WESTERMANN, B., GMACHL, M., PARLATI, F., SOLLNER, T. H. & ROTHMAN, J. E. (1998) SNAREpins: minimal machinery for membrane fusion. *Cell,* 92**,** 759-72.

WEIMBS, T., LOW, S. H., CHAPIN, S. J., MOSTOV, K. E., BUCHER, P. & HOFMANN, K. (1997) A conserved domain is present in different families of vesicular fusion proteins: a new superfamily. *Proc Natl Acad Sci U S A,* 94**,** 3046-51.

WEIMBS, T., MOSTOV, K., LOW, S. H. & HOFMANN, K. (1998) A model for structural similarity between different SNARE complexes based on sequence relationships. *Trends Cell Biol,* 8**,** 260-2.

WEIMER, R. M., RICHMOND, J. E., DAVIS, W. S., HADWIGER, G., NONET, M. L. & JORGENSEN, E. M. (2003) Defects in synaptic vesicle docking in unc-18 mutants. *Nat Neurosci,* 6**,** 1023-30.

WEISMAN, L. S., EMR, S. D. & WICKNER, W. T. (1990) Mutants of Saccharomyces cerevisiae that block intervacuole vesicular traffic and vacuole division and segregation. *Proc Natl Acad Sci U S A,* 87**,** 1076-80.

WEISSMAN, J. S., KASHI, Y., FENTON, W. A. & HORWICH, A. L. (1994) GroEL-mediated protein folding proceeds by multiple rounds of binding and release of nonnative forms. *Cell,* 78**,** 693-702.

WENDLAND, B., EMR, S. D. & RIEZMAN, H. (1998) Protein traffic in the yeast endocytic and vacuolar protein sorting pathways. *Curr Opin Cell Biol,* 10**,** 513-22.

WHITE, J., HELENIUS, A. & GETHING, M. J. (1982a) Haemagglutinin of influenza virus expressed from a cloned gene promotes membrane fusion. *Nature,* 300**,** 658-9.

WHITE, J., KARTENBECK, J. & HELENIUS, A. (1982b) Membrane fusion activity of influenza virus. *Embo J,* 1**,** 217-22.

WHITE, J., KIELIAN, M. & HELENIUS, A. (1983) Membrane fusion proteins of enveloped animal viruses. *Q Rev Biophys,* 16**,** 151-95.

WHYTE, J. R. & MUNRO, S. (2001) The Sec34/35 Golgi transport complex is related to the exocyst, defining a family of complexes involved in multiple steps of membrane traffic. *Dev Cell,* 1**,** 527-37.

WHYTE, J. R. & MUNRO, S. (2002) Vesicle tethering complexes in membrane traffic. *J Cell Sci,* 115**,** 2627-37.

WICKNER, W. (2002) Yeast vacuoles and membrane fusion pathways. *Embo J,* 21**,** 1241-7.

WILSON, I. A., SKEHEL, J. J. & WILEY, D. C. (1981) Structure of the haemagglutinin membrane glycoprotein of influenza virus at 3 A resolution. *Nature,* 289**,** 366-73.

WILSON, M. C., MEHTA, P. P. & HESS, E. J. (1996) SNAP-25, enSNAREd in neurotransmission and regulation of behaviour. *Biochem Soc Trans,* 24**,** 670-76.

WU, M. N., FERGESTAD, T., LLOYD, T. E., HE, Y., BROADIE, K. & BELLEN, H. J. (1999) Syntaxin 1A interacts with multiple exocytic proteins to regulate neurotransmitter release in vivo. *Neuron,* 23**,** 593-605.

YAFFE, M. P. (1991) Organelle inheritance in the yeast cell cycle. *Trends Cell Biol,* 1**,** 160-4.

YAMAGUCHI, T., DULUBOVA, I., MIN, S. W., CHEN, X., RIZO, J. & SUDHOF, T. C. (2002) Sly1 binds to Golgi and ER syntaxins via a conserved N-terminal peptide motif. *Dev Cell,* 2**,** 295-305.

YAMAKAWA, H., SEOG, D. H., YODA, K., YAMASAKI, M. & WAKABAYASHI, T. (1996) Uso1 protein is a dimer with two globular heads and a long coiled-coil tail. *J Struct Biol,* 116**,** 356-65.

YANG, B., GONZALEZ, L., JR., PREKERIS, R., STEEGMAIER, M., ADVANI, R. J. & SCHELLER, R. H. (1999) SNARE interactions are not selective. Implications for membrane fusion specificity. *J Biol Chem,* 274**,** 5649-53.

YANG, B., STEEGMAIER, M., GONZALEZ, L. C., JR. & SCHELLER, R. H. (2000) nSec1 binds a closed conformation of syntaxin1A. *J Cell Biol,* 148**,** 247-52.

YASUKAWA, T., KANEI-ISHII, C., MAEKAWA, T., FUJIMOTO, J., YAMAMOTO, T. & ISHII, S. (1995) Increase of solubility of foreign proteins in Escherichia coli by coproduction of the bacterial thioredoxin. *J Biol Chem,* 270**,** 25328-31.

YOUNG, K., LIN, S., SUN, L., LEE, E., MODI, M., HELLINGS, S., HUSBANDS, M., OZENBERGER, B. & FRANCO, R. (1998) Identification of a calcium channel modulator using a high throughput yeast two-hybrid screen. *Nat Biotechnol,* 16**,** 946-50.

ZERIAL, M. & MCBRIDE, H. (2001) Rab proteins as membrane organizers. *Nat Rev Mol Cell Biol,* 2**,** 107-17.

ZIMMERBERG, J., VOGEL, S. S. & CHERNOMORDIK, L. V. (1993) Mechanisms of membrane fusion. *Annu Rev Biophys Biomol Struct,* 22**,** 433-66.

ZWILLING, D., CYPIONKA, A., POHL, W. H., FASSHAUER, D., WALLA, P. J., WAHL, M. C. & JAHN, R. (2007) Early endosomal SNAREs form a structurally conserved SNARE complex and fuse liposomes with multiple topologies. *Embo J,* 26**,** 9-18.